

กำลังต้านทานการเกิดสภาวะลึควีไฟต์ชันของชั้นดินทรายในภาคเหนือของประเทศไทย



นายพิชัย ภัทรรัตนกุล

# สถาบันวิทยบริการ จุฬาลงกรณ์มหาวิทยาลัย

วิทยานิพนธ์นี้เป็นส่วนหนึ่งของการศึกษาตามหลักสูตรปริญญาวิทยาศาสตรดุษฎีบัณฑิต

สาขาวิชาวิศวกรรมโยธา ภาควิชาวิศวกรรมโยธา

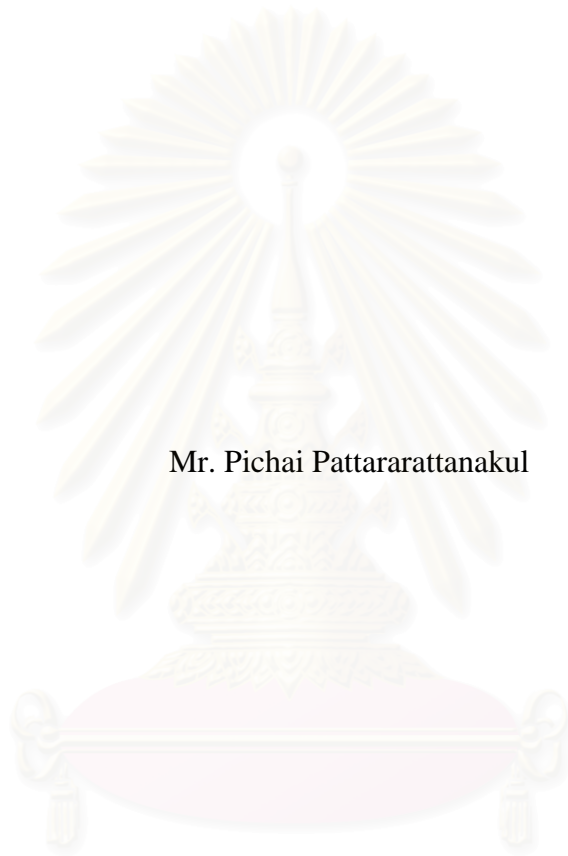
คณะวิศวกรรมศาสตร์ จุฬาลงกรณ์มหาวิทยาลัย

ปีการศึกษา 2546

ISBN: 974-17-4074-3

ลิขสิทธิ์ของจุฬาลงกรณ์มหาวิทยาลัย

LIQUEFACTION RESISTANCE OF SANDS IN THE NORTHERN  
PART OF THAILAND



Mr. Pichai Pattararattanakul

สถาบันวิทยบริการ  
จุฬาลงกรณ์มหาวิทยาลัย

A Dissertation Submitted in Partial Fulfillment of the Requirements

for the Degree of Doctor of Philosophy in Civil Engineering

Department of Civil Engineering

Chulalongkorn University

Academic Year 2003

ISBN 974-17-4074-3

Thesis Title	Liquefaction Resistance of Sands in the Northern Part of Thailand
By	Mr. Pichai Pattararattanakul
Field of Study	Civil Engineering
Thesis Advisor	Assistant Professor Supot Teachavorasinskun

---

Accepted by the Faculty of Civil Engineering, Chulalongkorn University in Partial Fulfillment of the Requirements for the Doctor's Degree

..... Dean of Faculty of Engineering  
(Professor Somsak Panyakeow, D.Eng.)

#### THESIS COMMITTEE

..... Chairman  
(Assistant Professor Thavee Thanacharoengit, Dr.Eng.)

..... Thesis Advisor  
(Assistant Professor Supot Teachavorasinskun, D.Eng.)

..... Member  
(Associate Professor Chitchai Anantasech, Ph.D.)

..... Member  
(Assistant Professor Surachat Sambhandharaksa, Sc.D.)

..... Member  
(Assistant Professor Boonchai Ukritchon, Sc.D.)

..... Member  
(Dr. Tirawat Boonyatee, D.Eng.)

พิชัย ภัทรรัตนกุล: กำลังต้านทานการเกิดสภาวะลิกวิแฟคชันของชั้นดินทรายในภาคเหนือของประเทศไทย (LIQUEFACTION RESISTANCE OF SANDS IN THE NORTHERN PART OF THAILAND) อ. ที่ปรึกษา: ผู้ช่วยศาสตราจารย์ ดร. สุพจน์ เตชวรสินสกุล, 286 หน้า. ISBN 974-17-4074-3.

เป็นที่ยอมรับกันว่าพื้นที่ในแถบจังหวัดทางภาคเหนือของประเทศไทย เป็นบริเวณที่มีความเสี่ยงภัยต่อแผ่นดินไหวในระดับปานกลาง และจากการสำรวจทางธรณีวิทยา พบว่ารอยเลื่อนหลาย ๆ รอยเลื่อน ในบริเวณภาคเหนือและภาคตะวันตกของประเทศ เป็นรอยเลื่อนที่มีพลัง ซึ่งเป็นไปได้ว่ารอยเลื่อนที่พบเหล่านี้ จะสามารถทำให้เกิดแผ่นดินไหวขนาด 5.5 ถึง 6.5 ริคเตอร์ แม้ว่าจะได้มีการประกาศให้อาคารหรือสิ่งก่อสร้าง ในพื้นที่ทางภาคเหนือและภาคตะวันตก ต้องทำการออกแบบต้านแรงแผ่นดินไหวตั้งแต่ปี ค.ศ. 1980 แต่ไม่ค่อยได้รับความสนใจ เนื่องจากวิศวกรส่วนใหญ่ยังขาดพื้นฐานความรู้ทางด้านพลศาสตร์ โดยเฉพาะพลศาสตร์ของดิน จากข้อมูลการเจาะสำรวจชั้นดินที่รวบรวมได้ในจังหวัดเชียงใหม่และเชียงราย พบว่าชั้นดินส่วนใหญ่ประกอบด้วยชั้นทรายหลวมถึงแน่นปานกลางกระจายอยู่ในระดับที่มีความลึกไม่มาก และมี SPT N-value ที่ปรับแก้แล้วประมาณ 5-20 ครั้งต่อฟุต ข้อมูลการเจาะสำรวจชั้นดินดังกล่าว และแบบจำลองทางสถิติซึ่งได้จากการวิเคราะห์ข้อมูลการเกิดลิกวิแฟคชันที่รวบรวมจากทั่วโลก จะถูกนำมาใช้ในการวิเคราะห์เพื่อหาแรงดันน้ำส่วนเกินที่เกิดจากแรงแผ่นดินไหวโดยวิธีหน่วยแรงประสิทธิผล ซึ่งผลการวิเคราะห์ที่ได้ จะถูกเสนอในรูปแบบของความสัมพันธ์ระหว่างความน่าจะเป็นของการเกิดลิกวิแฟคชัน แรงดันน้ำส่วนเกิน และความเร่งสูงสุดที่ผิวดิน เพื่อใช้ประเมินความเสี่ยงและกำลังต้านทานการเกิดสภาวะลิกวิแฟคชันของชั้นดินทรายในจังหวัดเชียงใหม่และเชียงราย

สถาบันวิทยบริการ  
จุฬาลงกรณ์มหาวิทยาลัย

ภาควิชา..... วิศวกรรมโยธา.....ลายมือชื่อนิสิต.....  
สาขาวิชา..... วิศวกรรมโยธา.....ลายมือชื่ออาจารย์ที่ปรึกษา.....  
ปีการศึกษา..... 2546.....

## 4271811621: MAJOR CIVIL ENGINEERING

KEYWORD: AMPLIFICATION / EARTHQUAKES / LIQUEFACTION / SEISMIC RISK

PICHAJ PATTARARATTANAKUL: LIQUEFACTION RESISTANCE OF SANDS IN THE NORTHERN PART OF THAILAND. THESIS ADVISOR: ASST. PROF. SUPOT TEACHAVORASINSKUN, D.Eng., 286 pp. ISBN 974-17-4074-3.

The northern part of Thailand is located in low to medium seismic risk zones. There are a few active faults recently found in the western and northern parts of the country. These could possibly induce earthquakes of magnitude ( $M_L$ ) of 5.5-6.5. Although seismic design code has been enforced in the area since 1980, the fundamental knowledge on dynamic soil behavior has not been extensively attained. Literature reviews of the existing boreholes from the two largest provinces in the north, including Chiang Mai and Chiang Rai, revealed that the areas are underlain by loose to medium dense sand layers found at shallow depths. The corrected SPT  $N$ -value of those sand layers varies in the range of 5-20 blows/ft. These borehole information, together with the result obtained from the logistic regression based on worldwide liquefaction database are used to conduct the effective stress analysis. A simple tool correlating the liquefaction probability, estimated excess pore water pressure and peak ground acceleration is proposed. Preliminary risk zones in these two provinces were identified.

สถาบันวิทยบริการ  
จุฬาลงกรณ์มหาวิทยาลัย

Department..... Civil Engineering ..... Student's signature.....

Field of study..... Civil Engineering ..... Advisor's signature.....

Academic year..... 2003.....

## ACKNOWLEDGEMENTS

First and foremost, I would like to express my sincere gratitude to my thesis advisor Dr. Supot Teachavorasinskun, who made it possible for me to study in the area of earthquake geotechnical engineering at Chulalongkorn University. He has played a major role in guiding the direction of this study. In addition, he has provided support and guidance in many other ways. Without his vision, effort and encouragement, this thesis could never reached completion.

Prof. Satoshi Morio of Maizuru National College of Technology, Japan for giving me an excellence computer program FLIP and his advice during the analytical phase of this study. At the same time, I also wish to express my appreciation to the members of the thesis committees, including Dr. Thavee Thanacharoengit, Dr. Surachat Sambhandharaksa, Dr. Boonchai Ukritchon, Dr. Tirawat Boonyatee, and especially Dr. Chitchai Anantasech of Chiang Mai University, for their constructive criticism and suggestions to this study.

Krungthep Engineering Consultants (KEC) Co., Ltd. and Worman and Associates Consultants (WAC) Co., Ltd. for providing borehole data in Chiang Mai and Chiang Rai.

I would like to thank my best younger friend Yuttana Kurojjanawong, who has made my life in geotechnical engineering division very enjoyable and has always provided me great suggestions for studying in the geotechnical engineering area.

Most of all, I would like to express my special appreciation to Piyawan Yimanan, my sweetest friend who always stood beside me and traveling with me in past few years. Her love, strength, and wisdom have inspired me to be the best I can be through many difficult times.

Finally, I owe my deepest gratitude to my parents, Arthorn and Pikun Pattararattanakul; their love is the greatest power in the world and has driven me to succeed in every destination I have dreamed of. I respectfully dedicate this thesis to my loving parents.

# TABLE OF CONTENTS

	<b>PAGE</b>
ABSTRACT (THAI).....	iv
ABSTRACT (ENGLISH) .....	v
ACKNOWLEDGEMENTS .....	vi
TABLE OF CONTENTS .....	vii
LIST OF TABLES .....	xi
LIST OF FIGURES.....	xii
<b>CHAPTER</b>	
<b>1. INTRODUCTION.....</b>	<b>1</b>
1.1 OVERVIEW.....	1
1.2 OBJECTIVE AND SCOPE.....	3
<b>2. LITERATURE REVIEW.....</b>	<b>6</b>
2.1 INTRODUCTION.....	6
2.2 BASIC SEISMOLOGY.....	6
2.2.1 THE NATURE OF EARTHQUAKES.....	6
2.2.2 EARTHQUAKE TERMINOLOGY.....	7
2.2.3 SEISMIC WAVES.....	7
2.3 EARTHQUAKE CHARACTERISTICS.....	8
2.3.1 INTENSITY SCALE.....	8
2.3.2 RICHTER MAGNITUDE SCALE .....	9
2.3.3 RICHTER MAGNITUDE CALCULATION.....	10
2.3.4 PEAK GROUND ACCELERATION .....	11
2.3.5 SEISMOMETER AND ACCELEROMETER.....	12
2.3.6 PREDOMINANT PERIOD AND DURATION .....	13
2.3.7 SITE PERIOD.....	13
2.4 DYNAMIC SOIL PROPERTIES.....	14
2.4.1 SHEAR WAVE VELOCITY OR SHEAR MODULUS .....	15
2.4.1.1 CORRELATIONS BASED ON LABORATORY MEASUREMENT.....	15
2.4.1.2 CORRELATIONS BASED ON FIELD MEASUREMENT.....	19
(a) CORRELATIONS BASED ON DEPTH .....	19
(b) CORRELATIONS BASED ON SPT N-VALUE.....	20
2.4.2 MODULUS REDUCTION .....	22
2.4.3 DAMPING RATIO .....	25

## TABLE OF CONTENTS (CONT.)

<b>CHAPTER</b>	<b>PAGE</b>
2.5 GROUND RESPONSE ANALYSIS .....	26
2.5.1 ONE-DIMENSIONAL GROUND RESPONSE.....	26
2.5.2 EQUIVALENT LINEAR METHOD .....	27
2.6 AMPLIFICATION OF EARTHQUAKE GROUND MOTIONS.....	30
2.6.1 AMPLIFICATION FACTOR .....	30
2.6.2 EFFECTS OF LOCAL SITE CONDITIONS ON GROUND MOTION.....	32
2.7 LIQUEFACTION .....	33
2.7.1 GENERAL .....	33
2.7.2 CAUSES OF SOIL LIQUEFACTION.....	35
2.7.3 FAILURE MECHANISMS FOR SLOPE GROUND.....	38
2.7.3.1 LATERAL SPREADS.....	38
2.7.3.2 FLOW FAILURES.....	38
2.7.4 FAILURE MECHANISMS FOR HORIZONTAL GROUND .....	39
2.7.4.1 SAND BOILS.....	39
2.7.4.2 GROUND OSCILLATION.....	40
2.7.4.3 LOSS OF BEARING STRENGTH.....	40
2.7.4.4 SUBSIDENCE AND SETTLEMENT .....	40
2.8 EVALUATION OF LIQUEFACTION RESISTANCE OF SOILS.....	41
2.8.1 DETERMINISTIC APPROACH OR CYCLIC STRESS APPROACH.....	41
2.8.1.1 CYCLIC STRESS RATIO (CSR) AND CYCLIC RESISTANCE RATIO (CRR).....	42
2.8.1.2 EVALUATION OF CYCLIC STRESS RATIO (CSR) .....	42
2.8.1.3 EVALUATION OF LIQUEFACTION RESISTANCE (CRR) .....	45
2.8.1.4 MAGNITUDE SCALING FACTORS (MSF) .....	47
2.8.1.5 EFFECTS OF INITIAL STATIC SHEAR STRESSES AND HIGH OVERBURDEN STRESSES ON LIQUEFACTION RESISTANCE .....	48
2.8.1.6 FACTOR OF SAFETY AGAINST LIQUEFACTION.....	49
2.8.2 PROBABILISTIC APPROACH .....	50
<b>3. PROFILE OF THE STUDY AREA .....</b>	<b>52</b>
3.1 LOCATION AND TOPOGRAPHY .....	52
3.2 SEISMICITY.....	53
3.3 SOIL PROFILE.....	54
3.4 INPUT MOTIONS FOR ANALYSIS.....	54
3.5 ESTIMATION OF SHEAR WAVE VELOCITY.....	55



## TABLE OF CONTENTS (CONT.)

<b>CHAPTER</b>	<b>PAGE</b>
3.5.1 FORMULA FOR CLAY .....	55
3.5.2 FORMULA FOR SAND .....	56
3.6 SUMMARY .....	56
<b>4. AMPLIFICATION OF EARTHQUAKE GROUND MOTIONS .....</b>	<b>58</b>
4.1 INTRODUCTION .....	58
4.2 COMPUTER PROGRAM SHAKE .....	58
4.3 MODULUS REDUCTION AND DAMPING RATIO .....	60
4.4 RESULTS OF ANALYSES .....	61
4.5 SUMMARY .....	62
<b>5. EVALUATION OF LIQUEFACTION RESISTANCE BY PROBABILISTIC APPROACH.....</b>	<b>64</b>
5.1 INTRODUCTION .....	64
5.2 LIQUEFACTION DATA CATALOG .....	65
5.3 REGRESSION METHOD FOR LIQUEFACTION DATA ANALYSIS .....	69
5.4 LOGISTIC MODELS OF LIQUEFACTION BEHAVIOR .....	70
5.5 SUMMARY .....	72
<b>6. FINITE ELEMENT ANALYSIS OF PORE WATER PRESSURE IN SAND DEPOSITES DURING EARTHQUAKES .....</b>	<b>73</b>
6.1 INTRODUCTION .....	73
6.2 CONSTITUTIVE MODEL OF SOILS .....	74
6.2.1 BASIC CONSTITUTIVE EQUATIONS .....	74
6.2.2 PHYSICAL BACKGROUND OF THE MODEL .....	77
6.2.3 SHEAR MECHANISM .....	78
6.2.4 VOLUMETRIC MECHANISM .....	80
6.3 COMPUTER PROGRAM FLIP .....	81
6.4 LIQUEFACTION TESTS ON SANDS USING A CYCLIC TRIAXIAL APPARATUS .....	82
6.5 DETERMINATION OF MODEL PARAMETERS .....	82
6.6 RESULTS OF ANALYSES .....	84
6.7 SUMMARY .....	85

## TABLE OF CONTENTS (CONT.)

<b>CHAPTER</b>	<b>PAGE</b>
<b>7. CONCLUSIONS AND RECOMMENDATIONS .....</b>	<b>87</b>
7.1 CONCLUSIONS .....	87
7.2 RECOMMENDATIONS FOR FUTURE RESEARCH.....	89
<b>REFERENCES.....</b>	<b>91</b>
<b>TABLES.....</b>	<b>104</b>
<b>FIGURES.....</b>	<b>114</b>
<b>APPENDICES.....</b>	<b>172</b>
APPENDIX A. LIQUEFACTION DATA CATALOG .....	173
APPENDIX B. BOREHOLE DATA USED IN THIS STUDY .....	186
B.1 CHIANG MAI .....	187
B.2 CHIANG RAI .....	247
<b>VITAE.....</b>	<b>286</b>

สถาบันวิทยบริการ  
จุฬาลงกรณ์มหาวิทยาลัย

## LIST OF TABLES

<b>TABLE</b>	<b>PAGE</b>
1.1 Examples of recent earthquakes felt in Thailand.....	105
2.1 Modified Mercalli intensity scale (Kramer, 1996) .....	106
2.2 Richter magnitude scale ( $M_L$ ).....	106
2.3 Parameters affecting shear modulus and damping of soils subjected to dynamic loading (Hardin and Drnevich, 1972a) .....	107
2.4 Values of $G_{max} / S_u$ (Weiler, 1988).....	107
2.5 Parameters for Ohsaki and Iwasaki (1973) relationship between SPT N-value and $V_s$ (Sykora, 1987).....	107
2.6 Ohta and Goto (1976) relationships between SPT N-value and $V_s$ (Sykora, 1987).....	108
2.7 Imai and Tonouchi (1982) relationships between SPT N-value and $V_s$ (Sykora, 1987).....	109
2.8 Effect of environmental and loading conditions on modulus ratio (at given strain level) of normally consolidated and moderately overconsolidated soils (modified from Dobry and Vucetic, 1987) .....	109
2.9 Effect of environmental and loading conditions on damping ratio of normally consolidated and moderately overconsolidated soils (modified from Dobry and Vucetic, 1987).....	110
2.10 Magnitude scaling factor (Seed and Idriss, 1982) .....	110
3.1 Maximum estimated $M_L$ for seismic source zones in Thailand region (after Nutalaya et al., 1985 and modified by Warnitchai and Lisantono, 1996).....	111
3.2 Summary of input motions used in analyses .....	111
6.1 Physical properties of sand used in cyclic triaxial test (Gauchan, 1984) .....	112
6.2 Model parameters (Iai et al., 1993).....	112
6.3 Model parameters for dilatancy .....	112
6.4 Summary of the estimated values of factor of safety based on the procedure proposed by Seed et al. (1983).....	113

## LIST OF FIGURES

FIGURE	PAGE
1.1 Evidence indicating the occurrence of liquefaction in the northern area of Thailand.....	115
1.2 General study methodology adopted .....	116
1.3 Example of deterministic method of liquefaction evaluation derived from empirical data for soils with $D_{50} > 0.25$ mm (Seed et al., 1983) .....	117
2.1 Earthquake terminology (Lindeburg, 1998) .....	118
2.2 Types of seismic waves: (a) P-wave; (b) S-wave; (c) R-wave; (d) L-wave (Kramer, 1996) .....	118
2.3 Typical seismometer amplitude trace (Lindeburg, 1998).....	119
2.4 Richter magnitude correction nomograph (Lindeburg, 1998).....	119
2.5 Two hypothetical Fourier amplitude spectra with the same predominant period but very different frequency contents. The upper curve describes a wideband motion and the lower a narrowband motion.....	120
2.6 Variation of k-coefficient with plasticity index (Dickenson, 1994).....	120
2.7 Backbone curve showing typical variation of $G_{sec}$ with shear strain.....	121
2.8 Variation of the modulus ratio with shear strain .....	121
2.9 Modulus reduction curves for fine-grained soils of different plasticity (Vucetic and Dobry, 1991) .....	122
2.10 Influence of mean effective confining pressure on modulus reduction curves for (a) nonplastic ( $PI = 0$ ) soil, and (b) plastic ( $PI = 50$ ) soil (Ishibashi, 1992) .....	122
2.11 Variation of damping ratio of fine-grained soil with cyclic shear strain amplitude and plasticity index (Vucetic and Dobry, 1991).....	123
2.12 Ground response nomenclature: (a) soil overlying bedrock; (b) no soil overlying bedrock.....	123
2.13 Relationship between hysteresis loop and: (a) shear modulus; (b) damping ratio .....	124
2.14 Iteration toward strain-compatible shear modulus and damping ratio in equivalent linear analysis.....	124
2.15 Kanai's amplification factor for soft ground (Kanai, 1957).....	125

## LIST OF FIGURES (CONT.)

FIGURE	PAGE
2.16	Approximate relationships between peak accelerations on rock and other local site conditions (Seed et al., 1976)..... 125
2.17	Approximate relationship between peak accelerations on rock and soft soil sites (Idriss, 1990)..... 126
2.18	Average normalized response spectra (5% damping) for different local site conditions (Seed et al., 1976) ..... 126
2.19	Relationship between limiting epicentral distance of sites at which liquefaction has been observed and moment magnitude for shallow earthquakes. Deep earthquakes (focal depths > 50 km) have produced liquefaction at greater distances. (Ambraseys, 1988)..... 127
2.20	Cyclic shear stresses on soil element during ground shaking: (a) idealized field loading conditions; (b) shear stress variation determined by response analysis ..... 128
2.21	Lateral spreading adjacent to a river channel: (a) before earthquake; (b) after earthquake (Youd, 1984) ..... 129
2.22	Examples of flow failure caused by liquefaction and loss of strength of soils lying on a steep slope ..... 129
2.23	Formation of water interlayers in shaking table tests of Liu and Qiao, (1984)..... 130
2.24	Ground oscillation: (a) before earthquake; (b) after earthquake (Youd, 1984)..... 130
2.25	Example of structure tilted due to loss of bearing strength. Liquefaction weakens the soil reducing foundation support which allows heavy structures to settle and tip ..... 131
2.26	Tilting of apartment buildings, Niigata (1964)..... 131
2.27	Procedure for determining maximum shear stress, $(\tau_{\max})_r$ (Seed and Idriss, 1982) ..... 132
2.28	$r_d$ versus depth curves developed by Seed and Idriss (1971) with add mean-value lines plotted from Eq. (2.34) (Youd and Idriss, 2001) ..... 132
2.29	Time history of shear stresses during earthquake (Seed and Idriss, 1982)... 133

## LIST OF FIGURES (CONT.)

FIGURE	PAGE
2.30	Plot used to determine the cyclic resistance ratio for clean and silty sands for $M = 7.5$ earthquakes (Seed et al., 1985)..... 133
2.31	Approximate relationships between the moment magnitude scale $M_w$ and other magnitude scales. Shown are the short-period body wave magnitude scale $m_b$ , the local magnitude scale $M_L$ , the long-period body wave magnitude scale $m_B$ , the Japan Meteorological Agency magnitude scale $M_{JMA}$ , and the surface-wave magnitude scale $M_S$ (reproduced from Day, 2002) ..... 134
2.32	Variation of correction factor, $K_\alpha$ , with initial shear/normal stress ratio (Seed and Harder, 1990)..... 135
2.33	Variation of correction factor, $K_\sigma$ , with effective overburden pressure (Seed and Harder, 1990)..... 135
3.1	Location of the study area..... 136
3.2	Seismic source zones in Thailand and vicinity (Nutalaya et al., 1985)..... 137
3.3	Map showing contours of peak ground acceleration (in units of acceleration of gravity) with 10% chance of being exceeded in a 50-year exposure time, and seismic zones for earthquake-resistant design (Wanitchai and Lisantono, 1996) ..... 138
3.4	Typical subsoil section in Chiang Mai Province (modified from Anantasech and Thanadpipat, 1985)..... 139
3.5	Typical subsoil profile in Chiang Rai province..... 140
3.6	Examples of the soil profiles and soil properties collected from Chiang Mai ..... 141
3.7	Examples of the soil profiles and soil properties collected from Chiang Rai ..... 142
3.8	Grain size distribution of sands: (a) Chiang Mai; (b) Chiang Rai..... 143
3.9	Acceleration time history of input motions ..... 144
3.10	Acceleration response spectra of input motions used in this study ..... 145
4.1	One-dimensional idealization of a horizontally layered soil deposit over a uniform half-space (Idriss and Sun, 1992)..... 146

## LIST OF FIGURES (CONT.)

FIGURE	PAGE
4.2	Shear modulus and damping variation with shear strain for clays of varying plasticity (Vucetic and Dobry, 1991) ..... 147
4.3	Shear modulus and damping variation with shear strain for sands (Seed et al., 1984) ..... 148
4.4	Variations of amplification factors with base rock acceleration in Chiang Mai ..... 149
4.5	Variations of amplification factors with base rock acceleration in Chiang Rai ..... 150
4.6	Comparison between peak ground accelerations of Chiang Mai and observed results from 1985 Mexico and 1989 Loma Preita earthquakes (modified from Idriss, 1991) ..... 151
4.7	Comparison between peak ground accelerations of Chiang Rai and observed results from 1985 Mexico and 1989 Loma Preita earthquakes (modified from Idriss, 1991) ..... 152
5.1	Example of deterministic method of liquefaction evaluation derived from empirical data for soils with $D_{50} > 0.25$ mm (Seed et al., 1983) ..... 153
5.2	Example of liquefaction data catalog (Liao and Whitman, 1986a) ..... 154
5.3	Contours of equal probability of liquefaction ( $P_L$ ) for magnitude, $M = 7.5$ with deterministic line by Seed et al. (1985) ..... 155
5.4	Contours of equal probability of liquefaction ( $P_L$ ) for magnitude, $M = 5.5$ with deterministic line modified from Seed et al. (1985) ..... 155
6.1	Flow diagram for evaluation of pore water pressure generation ..... 156
6.2	Schematic figure for multiple simple shear mechanisms (pairs of circles indicate mobilized virtual shear strain in positive and negative modes of compression shear and simple shear) (Iai et al., 1992) ..... 156
6.3	Schematic figure of contact normal $n_k$ , tangential direction $t_k$ and contact force increment $dP_k$ (Iai et al., 1993) ..... 157
6.4	Schematic figure of liquefaction front, state variable $S$ and shear stress ratio $r$ (Iai et al., 1992) ..... 157

## LIST OF FIGURES (CONT.)

FIGURE	PAGE
6.5	Relationship between normalized plastic shear work $w$ and liquefaction front parameter $S_0$ (Iai et al., 1992)..... 158
6.6	Grain size distribution of sands: (a) Chiang Mai; (b) Chiang Rai..... 159
6.7	Liquefaction resistance curves from undrained cyclic triaxial test (Gauchan, 1984) ..... 160
6.8	Test and computed liquefaction resistance curves..... 161
6.9	Relationship between amplification factor and maximum pore water pressure ratio for Chiang Mai ..... 162
6.10	Relationship between amplification factor and maximum pore water pressure ratio for Chiang Rai..... 164
6.11	Relationship between cyclic stress ratio for earthquake magnitude of 5.5 and maximum pore water pressure ratio for Chiang Mai ..... 166
6.12	Relationship between cyclic stress ratio for earthquake magnitude of 5.5 and maximum pore water pressure ratio for Chiang Rai..... 167
6.13	Relationship between maximum ground acceleration and maximum pore water pressure ratio for Chiang Mai ..... 168
6.14	Relationship between maximum ground acceleration and maximum pore water pressure ratio for Chiang Rai ..... 169
6.15	Relationship between maximum ground acceleration and maximum pore water pressure ratio at GL -2.5 m for Chiang Mai ..... 170
6.16	Relationship between maximum ground acceleration and maximum pore water pressure ratio at GL -2.5 m for Chiang Rai ..... 171



# CHAPTER 1

## INTRODUCTION

### 1.1 OVERVIEW

Thai people were not concerned about earthquake until recent occurrence of several moderate earthquakes. On April 22, 1983, an earthquake of magnitude 5.9 on the Richter scale occurred near a dam site in Kanchanaburi, about 200 kilometers from Bangkok, the capital city of Thailand. The main tremor of this earthquake was felt all over the western part and most of the central part of the country. Five years later (November 6, 1988), an earthquake of magnitude 7.3 hit the southern part of China near the Burmese border. This earthquake was felt in Bangkok even though the epicenter was at a distance of more than 1,000 kilometers; this is a consequence of Bangkok's deep, soft-alluvial soil which tends to amplify the motion of incoming seismic waves. On September 29 and October 1 of the following year, several moderate earthquakes (5.3-5.4 on the Richter scale) hit the northern part of Thailand along the Burmese border. In the city of Chiang Mai, about 180 kilometers from the epicenter, the intensity of ground shaking was rated as VI on the Modified Mercalli Intensity (MMI) scale. Fortunately, the strong ground shaking in the vicinity of these earthquake epicenters have never coincided with any town or city, hence neither buildings have been destroyed nor people have been killed so far. However, damage from the 11 September 1994 Phan earthquake in northern Thailand being quickly followed by the 17 January 1995 Kobe earthquake served as a wake up call to the people of Thailand. Examples of recent earthquakes felt in Thailand are summarized in Table 1.1.

Among the northern provinces of Thailand, Chiang Mai and Chiang Rai were selected as the studied area because of the following reasons:

1. They are located close to some of the recently found active faults.
2. They are the most densely populated areas in the north.
3. They are underlain by layers of soft to medium clay and/or loose to medium dense sand at shallow depths as illustrated by Anantasech and Thanadpipat (1985). The existence of the loose to medium dense sand layer at shallow depths (2 – 8 m from ground surface) implies a certain liquefaction risk of those two provinces.
4. From the metropolitan records of both provinces, more than 80% of housings (1 – 2 stories building) in the center of the cities were built on shallow foundation. These are the structures most prone to damages due to liquefaction and/or partially increase in excess pore water pressure.
5. Figure 1.1 shows evidences indicating the occurrence of liquefaction in a suburban area in Chiang Mai. Trace of sand extruding into the upper gravel layer clearly indicates past liquefaction of the lower sand layer.

Therefore, in the present study, the soil amplification and the liquefaction potential of subsoil induced by medium earthquakes in both provinces are investigated. Although full initialization of liquefaction may not be the case, partial development of excess pore water pressure might cause damages to 1 – 2 stories housing which is usually built on ground or short piles. A preliminary study is therefore needed to survey the liquefaction susceptibility of the areas. Integration among field parameters, probabilistic study, and dynamic analytical results is used as a primary tool for further detail evaluation.

Figure 1.2 shows the general methodology adopted. There are three main information required in the procedure, including:

- (a) Subsurface information. Around 50 existing boring logs were collected from each province. The sub soils in both provinces are subject to wide variation. Nevertheless, layers of loose to medium dense sand are found at depths of 2 – 8 m in most of the area.
- (b) Laboratory determination of liquefaction resistance. Existing cyclic triaxial tests determining the liquefaction resistance of sand were used to obtain some effective stress parameters required in the effective stress analysis (Iai et al., 1992).
- (c) Existing liquefaction database (Liao and Whitman, 1986a). Since there is no liquefaction database existing for Thailand, the worldwide liquefaction database is used as a reference for determination of other related parameters.

Those three components shall be integrated to obtain a specific tool or guideline for indicating earthquake liquefaction potential in the studied area.

## **1.2 OBJECTIVE AND SCOPE**

The major objectives of this thesis are:

- 1) To quantify the potential amplification of earthquake ground motions in the city of Chiang Mai and Chiang Rai due to soil effects. The scope of the study is the selection of a range of peak rock outcrop accelerations and appropriate acceleration time histories to be used based on the seismicity of the region.
- 2) To develop simple and practical procedures for evaluating liquefaction risk. Charts similar to a semi-empirical chart such as that shown in Figure 1.3 are developed, but with lines corresponding to various liquefaction probability values.
- 3) To evaluate the liquefaction potential and susceptibility of sands in the city of Chiang Mai and Chiang Rai due to medium earthquakes ( $M = 5.5$ ) based on probabilistic approach.

- 4) To develop guidelines and charts for analysis and evaluation of the generation of pore water pressure of sands in the city of Chiang Mai and Chiang Rai due to medium earthquakes corresponding to various probability values using finite element analysis. The parameters used in the analysis are obtained by back-fitting the calculated results with experimental data from undrained cyclic triaxial tests.

Scope and outline of the thesis are as follows:

The thesis mainly focuses on the evaluation of the potential amplification of earthquake ground motions, the liquefaction potential and susceptibility of sands, and the generation of pore water pressure due to medium earthquakes ( $M = 5.5$ ) in the city of Chiang Mai and Chiang Rai. The evaluations were based on subsoil data, geology of the area, and the seismicity of Chiang Mai and Chiang Rai. Subsoil data were collected in the form of boring logs through standard penetration tests (SPT) from the consulting/engineering firms.

Chapter 2 of this thesis presents a review of the theoretical background about basic seismology, earthquake characteristics, Seismic response analysis, dynamic soil properties for seismic response analysis, soil amplification in earthquake engineering, and the methods for evaluation of liquefaction resistance of soils.

Chapter 3 describes the profile of the studied area.

Chapter 4 shows the evaluation of the amplification of earthquake ground motions in the city of Chiang Mai and Chiang Rai. Subsequently, the analysis results and discussion are presented.

Chapter 5 describes the catalog of liquefaction case studies which is used to develop liquefaction probability charts in this research. A description of the logistic regression method for evaluating the liquefaction resistance is presented and logistic models of liquefaction occurrence are then formulated.

In Chapter 6, the laboratory test results on undrained cyclic triaxial of sands were used to obtain some effective stress parameters required in the effective stress model. After the model parameters have been completely obtained, the finite element

method is used to estimate pore water pressure. Finally, charts and guidelines for analysis and evaluation of the generation of pore water pressure of sands due to medium earthquakes corresponding to various probability values are presented.

A summary of the thesis, the conclusions drawn from the research, and suggestions for future work, are presented in Chapter 7.



สถาบันวิทยบริการ  
จุฬาลงกรณ์มหาวิทยาลัย

## CHAPTER 2

### LITERATURE REVIEW

#### 2.1 INTRODUCTION

In this chapter, the theoretical background and a review of the previous work about basic seismology, earthquake characteristics, seismic response analysis, dynamic soil properties for seismic response analysis, soil amplification in earthquake engineering, and evaluation of liquefaction resistance of soils are presented.

#### 2.2 BASIC SEISMOLOGY

##### 2.2.1 THE NATURE OF EARTHQUAKES

An earthquake is an oscillatory, sometimes violent movement of the Earth's surface that follows a release of energy in the Earth's crust. This energy can be generated by a sudden dislocation of segments of the crust, a volcanic eruption, or man-made explosion. Most of the destructive earthquakes, however, are caused by dislocations of the crust. When subjected to geologic forces from plate tectonics, the crust initially strains (i.e., bends and shears) elastically. For pure axial loading, Hooke's law gives the stress that accompanies this strain.

$$\sigma = E\varepsilon \quad (\text{Axial Loading}) \quad (2.1)$$

As rock is stressed, it stores strain energy,  $U$ . The elastic strain energy per unit volume for pure axial loading is:

$$U = \frac{\sigma\varepsilon}{2} \quad (\text{Axial Loading}) \quad (2.2)$$

When the stress exceeds the ultimate strength of the rocks, the rocks break and quickly move or snap into new positions. In the process of breaking, the strain energy is released and seismic waves are generated. This is the basic description of the elastic rebound theory of earthquake generation. These waves travel from the source of the earthquake (known as the epicenter or focus) to more distant location along the surface of and through the Earth. Some of the vibrations are of high enough frequency to be audible, while others are of very low frequency with periods of many seconds and thus are inaudible.

### **2.2.2 EARTHQUAKE TERMINOLOGY**

The epicenter of an earthquake is the point on the Earth's surface directly above the focus (also known as the hypocenter). The location of an earthquake is commonly described by the geographic position of its epicenter and its focal depth. The focal depth of an earthquake is the depth from the Earth's surface to the focus. These terms are illustrated in Figure 2.1. Earthquakes with focal depths of less than approximately 60 kilometers are classified as shallow earthquakes. Very shallow earthquakes are caused by the fracturing of brittle rock in the crust or by internal strain energy that overcomes the friction locking opposite sides of a fault. Intermediate earthquakes, whose causes are not fully understood, have focal depths ranging from 60 to 300 kilometers. Deep earthquakes may have focal depths of up to 700 kilometers.

### **2.2.3 SEISMIC WAVES**

Seismic waves are of three types: compression, shear, and surface waves. Compression and shear waves travel from the hypocenter through the Earth's interior

to distant points on the surface. Only compression waves, however, can pass through the Earth's molten core. Because compression waves (also known as longitudinal waves) travel at great speeds (5800 m/s in granite) and ordinarily reach the surface first, they are known as P-waves (for "primary waves").

Shear waves (also known as transverse waves) do not travel as rapidly (3000 m/s in granite) through the Earth's crust and mantle as do compression waves. Because they ordinarily reach the surface later, they are known as S-waves (for "secondary waves"). Instead of affecting material directly behind or ahead of their lines of travel, shear waves displace material at right angles to their path. While S-waves travel more slowly than P-waves, they transmit more energy and cause the majority of damage to structures. The speed at which P-waves and S-waves travel varies with the stiffness of materials they travel through.

Surface waves, also known as R-waves (for "Rayleigh waves") or L-waves (for "Love waves"), may or may not form. They arrive after the primary and secondary waves. In granite, R-waves move at approximately 2700 m/s. The types of seismic waves are shown in Figure 2.2.

## **2.3 EARTHQUAKE CHARACTERISTICS**

### **2.3.1 INTENSITY SCALE**

The intensity of an earthquake is based on the damage and other observed effects on people, buildings, and other features. Intensity varies from place to place within the disturbed region. An intensity scale consists of a series of responses, such as people awakening, and movement of furniture. Although numerous intensity scales have been developed, the scale encountered most often in the world is the Modified Mercalli Intensity (MMI) scale, originally developed in 1902 by the Italian seismologist Mercalli and modified in 1931 by the American seismologists Harry Wood and Frank Neumann.



The Modified Mercalli scale consists of 12 increasing levels of intensity (expressed as Roman numerals following the initials MM) that range from imperceptible shaking to catastrophic destruction. The lower numbers of the intensity scale generally are based on the manner in which the earthquake is felt by people. The higher numbers are based on observed structural damage. The numerals do not have a mathematical basis and therefore are more meaningful to nontechnical people than to those in technical fields. The Modified Mercalli intensity scale is shown in Table 2.1.

### **2.3.2 RICHTER MAGNITUDE SCALE**

In 1935, Charles F. Richter of the California Institute of Technology developed the Richter magnitude scale to measure earthquake strength. The magnitude,  $M_L$ , of an earthquake is determined from the logarithm of the amplitude recorded by a seismometer. Adjustments are included in the magnitude to compensate for the variation in the distance between the various seismometers and the epicenter. Because the Richter magnitude is a logarithmic scale, each whole number increase in magnitude represents a ten-fold increase in measured amplitude.

Richter magnitude is expressed in whole numbers and decimal fractions. For example, a magnitude of 5.3 might correspond to a moderate earthquake. A strong earthquake might be rated at 7.3. Great earthquakes have magnitudes above 7.5. Earthquakes with magnitudes of 2.0 or less are known as micro-earthquakes and are rarely felt by people. Several thousand seismic events with magnitudes of approximately 4.5 or greater occur each year and are strong enough to be recorded by seismometers all over the world. Earthquakes of this size and below have little potential to cause structural damage. The magnitude of an earthquake depends on the length and breadth of the fault slip, as well as on the amount of slip.

### 2.3.3 RICHTER MAGNITUDE CALCULATION

The Richter magnitude,  $M_L$ , is calculated from the maximum amplitude,  $A$ , of the seismometer trace, as illustrated in Figure 2.3.  $A_0$  is the seismometer reading produced by an earthquake of standard size (i.e., a calculation earthquake). Generally,  $A_0$  is 0.001 mm.

$$M_L = \log_{10} \left( \frac{A}{A_0} \right) \quad (2.3)$$

Equation (2.3) assumes that a distance of 100 kilometers separates the seismometer and epicenter. For other distances, the nomograph of Figure 2.4 and the following procedure can be used to calculate the magnitude. Due to the lack of reliable information on the nature of the Earth between the observation point and the earthquake epicenter, an error of 10 to 40 kilometers in locating the epicenter is not unrealistic.

- Step 1: Determine the time between the arrival of the P- and S-waves.
- Step 2: Determine the maximum amplitude of oscillation.
- Step 3: Connect the arrival time difference on the left scale and the amplitude on the right scale with a straight line.
- Step 4: Read the Richter magnitude on the center scale.
- Step 5: Read the distance separating the seismometer and the epicenter from the left scale.

Whereas one seismometer can determine the approximate distance to the epicenter, it takes three seismometers to determine and verify the location of the epicenter. The Richter scale ranges from zero to 8.9 (the largest recorded, Chile 1960). Because it is a logarithmic scale, an earthquake of 6.0 is 10 times more severe

than one of 5.0 and similarly, one of 7.0 is 100 times more severe. The Richter magnitude scale is shown in Table 2.2.

### 2.3.4 PEAK GROUND ACCELERATION

The peak (maximum) ground acceleration, PGA, is easily measure by a seismometer or accelerometer and is one of the most important characteristics of an earthquake. PGA can be given in various units, including  $\text{ft}/\text{sec}^2$ ,  $\text{in}/\text{sec}^2$ , or  $\text{m}/\text{s}^2$ . However, it is most common to specify PGA in “g’s” (i.e., as a fraction or percent of gravitational acceleration).

$$PGA = \left( \frac{a_{\text{ft}/\text{sec}^2}}{32.2} \right) \times 100 \% \quad (2.4)$$

$$= \left( \frac{a_{\text{in}/\text{sec}^2}}{386} \right) \times 100 \% \quad (2.5)$$

$$= \left( \frac{a_{\text{m}/\text{s}^2}}{9.81} \right) \times 100 \% \quad (2.6)$$

Equation (2.7) (as determined by Gutenberg and Richter in 1956) is one of many approximate relationships between the Richter magnitude,  $M_L$ , and the PGA at the epicenter. The ground acceleration (in rock) will decrease as the distance from the epicenter increases, and for this reason, equations of this type are called attenuation equations.

$$\log_{10} PGA = -2.1 + 0.81M_L - 0.027M_L^2 \quad (2.7)$$

Attenuation equations are very site dependent. Since Equation (2.7) was developed, newer studies have resulted in better correlations in different formats and

for many different locations, but they are based on limited data. Such studies are regularly incorporated into revisions of the seismic provisions of building codes.

### **2.3.5 SEISMOMETER AND ACCELEROMETER**

Seismic waves travel through the Earth and are recorded on seismometers. A seismometer is the detecting and recording parts of a larger apparatus known as seismograph. Seismometers are pendulum type devices that are mounted on the ground and measure the displacement of the ground with respect to a stationary reference point. Since a seismometer usually records motion in only one orthogonal direction, three seismometers are needed to record all components of ground motion. Figure 2.3 illustrates a typical seismometer trace, known as a seismogram.

Note that while seismic activity usually continues for some time after the start of the earthquake, the major movement occurs in a concentrated period known as the strong phase. The longer the earthquake shakes, the more seismic energy is absorbed by buildings; thus, the duration of strong phase shaking greatly affects the damage inflicted. The peak acceleration is a spike that imparts no energy. The effective peak ground acceleration causes structures to move.

Seismometers record the varying amplitude of ground oscillations beneath the instrument. Sensitive seismometers greatly magnify these ground motions and can detect strong earthquakes occurring anywhere in the world. The time, location, and magnitude of an earthquake can be determined from the data recorded by seismometer stations. Since a seismometer is a spring-mass-dashpot device, it will magnify or distort earthquakes with frequencies in certain ranges. The ratio of actual damping to critical damping can be changed to minimize such distortion. Good seismometer design calls for a damping ratio of between 0.6 and 0.7 with a natural period of vibration smaller than the smallest period to be measured.

An accelerometer (accelerograph) is seismometer mounted in buildings for the purpose of recording large accelerations. For this reason, they are also known as

strong motion seismometers. The large swings accelerometers record typically exceed the scale limits of most seismometers. An accelerometer located in a building does not run continually. It triggered by a P-wave and runs for a fixed period of time.

### **2.3.6 PREDOMINANT PERIOD AND DURATION**

A single parameter that provides a useful, although somewhat crude representation of the frequency content of a ground motion is the predominant period,  $T_p$ . The predominant period is defined as the period of vibration corresponding to the maximum value of the Fourier amplitude spectrum. To avoid improper influence of individual spikes of the Fourier amplitude spectrum, the predominant period is often obtained from a smoothed spectrum. While the predominant period provides some information regarding the frequency content, it is easy to see from Figure 2.5 that motions with radically different frequency contents can have the same predominant period.

The duration of strong ground motion can have a strong influence on earthquake damage. Many physical processes, such as the degradation of stiffness and strength of certain types of structures and build up of pore water pressures in loose, saturated sands, are sensitive to number of load or stress reversals that occur during an earthquake. A motion of short duration may not produce enough load reversals for damaging response to build up in a structure, even if the amplitude of the motion is high. On the other hand, a motion with moderate amplitude but long duration can produce enough load reversals to cause substantial damage.

### **2.3.7 SITE PERIOD**

The site (soil) period is now recognized as a significant factor contributing to structural damage. When a site has a natural frequency of vibration that corresponds to the predominant earthquake frequency, site movement can be greatly magnified.

This is known as resonance. Thus the buildings can experience ground motion much greater than would be predicted from only the seismic energy release.

Determining the actual site period is no easy matter. Since the site period can be computed precisely from widely available formulas and still be grossly inaccurate.

## **2.4 DYNAMIC SOIL PROPERTIES**

The nature and distribution of earthquake damage is strongly influenced by the response of soils to cyclic loading. This response is controlled in large part by the mechanical properties of the soil. Geotechnical earthquake engineering encompasses a wide range of problems involving many types of loading and many potential mechanisms of failure, and different soil properties influence the behavior of the soil for different problems. For many important problems, particularly those dominated by wave propagation effects, only low levels of strain are induced in the soil. For other important problems, such as those involving the stability of masses of soil, large strains are induced in the soil. The behavior of soils subjected to dynamic loading is governed by what have come to be popularly known as dynamic soil properties.

Soil properties that influence wave propagation and other low strain phenomena include stiffness, damping, poisson's ratio, and density. Of these, stiffness and damping are the most important; the others have less influence and tend to fall within relatively narrow ranges. The stiffness and damping characteristics of cyclically loaded soil are critical to the evaluation of many geotechnical earthquake engineering problems. Not only at low strains but because soils are nonlinear materials, also at intermediate and high strains. At high levels of strain, the influence of the rate and number of cycles of loading on shear strength may also be important. Volume change characteristics are also important at high strain levels.

## 2.4.1 SHEAR WAVE VELOCITY OR SHEAR MODULUS

In geotechnical earthquake engineering analysis such as a seismic site response analysis using the equivalent linear method and liquefaction analysis using finite element method, which will be explained later, one of the key input parameters is the shear modulus ( $G$ ) at low strain ( $\gamma \cong 5 \times 10^{-4} \%$ ), generally represented as  $G_{\max}$ . Though  $G_{\max}$  is difficult to accurately measure in the laboratory due to the effects of sample disturbance, it can be readily determined from the shear wave velocity ( $V_s$ ) and the mass density ( $\rho$ ) from the relationship  $G = \rho \times V_s^2$ . With the need to estimate values of  $G_{\max}$  or  $V_s$  for the soil profiles for the northern part of Thailand, particularly Chiang Mai and Chiang Rai, several empirical correlations based on available field and laboratory measurements were reviewed.

Researchers have been attempting to formulate correlations between shear modulus or shear wave velocity and various geotechnical parameters for at least thirty years. These formulas have evolved from measurements made in both the field and laboratory, even though the accuracy of such correlations varies considerably.

In the following review, due to the difficulty in finding some of the original papers, most of the correlations were obtained from the excellent summary report by Sykora (1987). The correlations are presented in the units of the original paper when available, or in the units as presented by Sykora (1987), which are often U.S. Customary units. When any of the correlations are actually used as part of this research in subsequent sections, they are converted to the appropriate metric units.

### 2.4.1.1 CORRELATIONS BASED ON LABORATORY

#### MEASUREMENT

Hardin and Richart (1963) conducted one of the first investigations of variables affecting  $V_s$  in soils. A resonant column testing device was utilized to load cyclically samples of Ottawa sands, crushed quartz sand, and crushed quartz silt. The

considered variables were effective confining pressure ( $\sigma'_0$ ), void ratio ( $e$ ), moisture content, grain size distribution, and grain characteristic. The shear strain amplitude, however, was not examined and was kept constantly at  $10^{-5}$  in/in for all tests. The confining pressure and void ratio were shown to apparently have the most influence on  $V_s$ . Based on the results of their study, Hardin and Richart developed empirical equations relating shear wave velocity to void ratio and effective confining with a reported accuracy within  $\pm 10\%$ , and the equations are:

$$\sigma'_0 < 2000 \text{ psf}; \quad V_s = (119 - 56.0e)(\sigma'_0)^{0.30} \quad (\text{ft/sec}) \quad (2.8)$$

$$\sigma'_0 > 2000 \text{ psf}; \quad V_s = (170 - 78.2e)(\sigma'_0)^{0.25} \quad (\text{ft/sec}) \quad (2.9)$$

Seed and Idriss (1970) developed one of the initial simple relationships relating small shear strain modulus to undrained shear strength ( $S_u$ ) based on an empirical study of 21 clays involving predominantly laboratory data. They proposed a linear relationship between  $G_{\max}$  and  $S_u$  as follows:

$$G_{\max} = 2200 \cdot S_u \quad (2.10)$$

However, subsequent researchers (Trudeau et al., 1973; Koutsoftas and Fischer, 1980; and Egan and Ebeling, 1985) have shown that the ratio  $G_{\max}/S_u$ , called normalized modulus, is not constant, but depends on undrained shear strength  $S_u$ , overconsolidation ratio (OCR), plasticity index (PI), and effective confining stress ( $\sigma'_0$ ).

Hardin and Drnevich (1972a, 1972b) examined the effect of various parameters affecting the stress-strain relations in soils in the strain range of 1% and less using results of the resonant column and cyclic simple shear testing. They concluded that strain amplitude, effective mean principal stress, and void ratio are very important factors, for both clean sands and clays. Furthermore, degree of



saturation is very significant for clays. The parameters examined by Hardin and Dnervich (1972a) and the effect of these parameters on  $G_{\max}$  are presented in Table 2.3.

Using the results of their earlier study, Hardin and Drnevich (1972b) subsequently developed a relationship for  $G_{\max}$  as a function of void ratio, OCR, plasticity index, and mean effective stress, as shown in Equation (2.11).

$$G_{\max} = 1230 \cdot \frac{(2.973 - e)^2}{1 + e} \cdot OCR^k \cdot \sigma_m'^{0.5} \quad (\text{psi}) \quad (2.11)$$

where  $\sigma_m'$  is the mean effective stress in pounds per square inch (psi), and  $k$  is a dimensionless parameter that varies with plasticity index as shown in Figure 2.6.

Kokusho (1980) tested saturated samples of Toyoura sand using cyclic triaxial apparatus. From the test data, he proposed a relationship for  $G_{\max}$  as a function of void ratio and effective confining stress ( $\sigma_0'$ ). The relationship is:

$$G_{\max} = 8400 \cdot \frac{(2.17 - e)^2}{1 + e} \cdot \sigma_0'^{0.5} \quad (\text{kPa}) \quad (2.12)$$

Kokusho, Yoshida, and Esashi (1982) tested undisturbed samples of soft clay with plasticity index ranges from 40 to 85 using cyclic triaxial apparatus. They then presented the following equation as function of void ratio and effective confining stress ( $\sigma_0'$ ):

$$G_{\max} = 141 \cdot \frac{(7.32 - e)^2}{1 + e} \cdot \sigma_0'^{0.6} \quad (\text{kPa}) \quad (2.13)$$

Knox, Stokoe, and Kopperman (1982) tested a 7-ft-cube sample of dry sand in a steel frame structure (true triaxial device) and concluded that, for shear wave propagating in a principal stress direction, shear wave velocity only depended on the

stress in the direction of particle motion and that in the direction of wave propagation. Shear wave velocity was found to be independent of the state of stress in the third orthogonal direction. Sykora (1987) substituted equation by Knox, et. al. (1982) to equation by Hardin and Drnevich (1972b), Equation (2.11), then the result is:

$$G_{\max} = 1230 \cdot \frac{(2.973 - e)^2}{1 + e} \cdot OCR^k \cdot \sigma_a'^{0.25} \cdot \sigma_b'^{0.25} \cdot \sigma_c'^{0.0} \quad (\text{psi}) \quad (2.14)$$

where  $\sigma_a'$  is the effective stress in direction of shear wave propagation,  $\sigma_b'$  is the effective stress in direction of shear wave particle motion, and  $\sigma_c'$  is the effective stress in third (remaining) orthogonal direction, with all stresses being in units of psi.

Weiler (1988) developed the empirical relationship between  $G_{\max}$  and undrained shear strength ( $S_u$ ) of clay, measured in CU triaxial compression test, as shown in Table 2.4.

Dickenson (1994) presented the results of a study of the dynamic response of soft and deep cohesive soils during the 1989 Loma Prieta earthquake. He developed a nonlinear relationship between shear wave velocity determined from field testing and undrained shear strength for four cohesive soil units in the San Francisco Bay area: San Francisco Bay Mud, Yerba Buena Mud, Alameda Formation (marine), and Alameda Formation (oxidized). The relationship includes both the soft San Francisco Bay Mud as well as the deeper and stiffer old bay clays of the Alameda Formation. His proposed relationship is:

$$V_s = 18 \cdot S_u^{0.475} \quad (\text{ft/sec}) \quad (2.15)$$

where  $S_u$ , the undrained shear strength, has unit of psf. It should be noted that  $S_u$  determined from unconfined compression, unconsolidated undrained triaxial (TX), and consolidated undrained triaxial tests were used directly in Dickenson's equation. Field vane strengths were corrected using Bjerrum's plasticity-based correlation

(Bjerrum, 1972), and the direct simple shear (DSS) strengths were modified using an assumed relationship of  $(S_u)_{TX} \cong 1.35(S_u)_{DSS}$ . The relationship showed good agreement with the data, but Dickenson suggested that all such relationships be verified for specific soils by field testing.

#### **2.4.1.2 CORRELATIONS BASED ON FIELD MEASUREMENT**

The disturbance inherent in obtaining soil samples for subsequent laboratory testing makes it extremely difficult to measure values of low strain shear modulus representative of the in situ conditions, particularly for cohesionless soils. Therefore, in situ soil testing, such as the Standard Penetration Test (SPT) and the Cone Penetration Test (CPT) have become the primary methods of estimating  $V_s$  of soil in situ, with the exception of direct measurement. Schmertmann et al. (1978) concluded that a properly standardized SPT has a reasonable potential to evaluate shear waves velocity. The correlations based on field measurement have developed over the past twenty years in soil dynamic toward the estimation of the dynamic behavior of soil and the determination of representative constitutive relationships. The following suites of correlations represent part of that development.

##### **(a) CORRELATIONS BASED ON DEPTH**

The most generally reported shear wave velocity formulas are those that are a function of depth, however, these formula usually are presented for specific soils and locations (e.g., San Francisco Bay Mud). An example of such a relation is that proposed by Fumal (1978) for soil in the San Francisco Bay area. He collected and analyzed downhole seismic data from 59 sites throughout the San Francisco Bay region and determined a correlation for the variation of  $V_s$  with depth:

$$V_s = 471 \cdot Z^{0.20} \quad (\text{ft/sec}) \quad (2.16)$$

where  $Z$  is depth in feet. Fumal's relationship applied not only to San Francisco Bay Mud, but to sand, stiff clay, and gravelly soil as well.

### (b) CORRELATIONS BASED ON SPT N-VALUE

Sakai (1968) postulated soil to be an elastic material, and used both SPT and plate bearing test results to evaluate Young's modulus ( $E$ ). He then converted the Young's modulus to shear wave velocity by Equation (2.17).

$$V_s = \sqrt{\frac{E}{\rho} \cdot \frac{1}{2(1 + \nu)}} \quad (2.17)$$

where  $\rho$  is mass density and  $\nu$  is Poisson's ratio. Sakai then substituted the values of Poisson's ratio ranging from 0.2 to 0.5 and the average strains that were developed during the plate bearing test to develop the following equation for sand:

$$V_s = (49 \text{ to } 110)N^{0.5} \quad (\text{ft/sec}) \quad (2.18)$$

where  $N$  is the N-value obtained from the SPT. A similar relationship was developed by Kanai (1966) based on the results of over 70 microtremor measurements, almost entirely sands, to create the equation:

$$V_s = 62 \cdot N^{0.62} \quad (\text{ft/sec}) \quad (2.19)$$

Ohsaki and Iwasaki (1973) analyzed over 200 sets of  $V_s$  data, collected by predominantly the downhole method, throughout Japan. They developed correlations between shear modulus and uncorrected N-value, geologic age and soil type. Ohsaki and Iwasaki then presented the following equation for all soil types:

$$G_{\max} = 124 \cdot N^{0.78} \quad (\text{tsf}) \quad (2.20)$$

By assuming a constant unit weight of 112.4 pcf ( $\cong 1.80 \text{ t/m}^3$ ), they presented the following relationship between  $V_s$  and uncorrected N-value:

$$V_s = 267 \cdot N^{0.39} \quad (\text{ft/sec}) \quad (2.21)$$

Ohsaki and Iwasaki (1973) also presented their analysis by classifying to geologic age, soil type. The parameters and correlation coefficients are compared and shown in Table 2.5, with the form of the equation as:

$$G_{\max} = a \cdot N^b \quad (\text{tsf}) \quad (2.22)$$

Ohta and Goto (1978) accumulated and analyzed almost 300 sets data from soil in Japan. The data analysis was carefully thought out regarding shear wave velocity, geologic age, depth, N-value, and soil types. They developed 15 empirical formulas, with only the 8 best-fit equations shown in Table 2.6, which involve N-value.

Imai and Tonuchi (1982) synthesized data from 400 sites throughout Japan, 1654 sets of data in all, and developed the following equation:

$$V_s = 318 \cdot N^{0.314} \quad (\text{ft/sec}) \quad (2.23)$$

Imai and Touchi also showed relations for shear wave velocity and shear modulus from SPT N-value for various soil categories as shown in Table 2.7.

Seed, Idriss, and Arango (1983) suggested using the following equation for sand and silty sand to access shear modulus,  $G_{\max}$ , and shear wave velocity,  $V_s$ , using N-value:

$$G_{\max} = 65 \cdot N \quad (\text{tsf}) \quad (2.24)$$

$$V_s = 185 \cdot N^{0.5} \quad (\text{ft/sec}) \quad (2.25)$$

Sykora and Strokoe (1983) published correlations between the shear wave velocity and SPT N-value for cohesionless soils, and the relationship is:

$$V_s = 100.584 \cdot N^{0.29} \quad (\text{m/s}) \quad (2.26)$$

According to Dickenson (1994), the proposed formula by Ohta and Goto (1978) can be reasonably be used for sandy soils in the San Francisco Bay area. Dickenson (1994) then presented the following formula for cohesionless soil in the San Francisco Bay area:

$$V_s = 290 \cdot (N + 1)^{0.30} \quad (\text{ft/sec}) \quad (2.27)$$

Based on the results of the above review of correlations, several were selected as appropriate for the northern area soils. These are presented in the later section.

## 2.4.2 MODULUS REDUCTION

Laboratory tests have shown that soil stiffness is influenced by cyclic strain amplitude, void ratio, mean principal effective stress, plasticity index, overconsolidation ratio, and number of loading cycles. The secant shear modulus, which will be described in Section 2.5.2, of an element soil varies with cyclic shear strain amplitude. At low strain amplitudes, the secant shear modulus is high, but it decreases as the strain amplitude increases. The locus of points corresponding to the tips of hysteresis loops of various cyclic strain amplitudes is called a backbone (or skeleton) curve, as shown in Figure 2.7; its slope at the origin (zero cyclic strain

amplitude) represents the largest value of the shear modulus,  $G_{\max}$ . At greater cyclic strain amplitudes, the modulus ratio  $G_{\text{sec}}/G_{\max}$  drops to value of less than 1. Characterization of the stiffness of an element of soil therefore requires consideration of both  $G_{\max}$  and the manner in which the modulus ratio  $G/G_{\max}$  varies with cyclic strain amplitude and other parameters. The variation of the modulus ratio with shear strain is described graphically by a modulus reduction curve, as shown in Figure 2.8.

In early years of geotechnical earthquake engineering, the modulus reduction behaviors of coarse- and fine-grained soils were treated separately (e.g., Seed and Idriss, 1970). Recent research, however, has revealed a gradual transition between the modulus reduction behavior of nonplastic coarse-grained soil and plastic fine-grained soils.

Zen et al. (1978) and Kokushu et al. (1982) first noted the influence of soil plasticity on the shape of the modulus reduction curve; the shear modulus of highly plastic soils was observed to degrade more slowly with shear strain than did low-plasticity soils. After reviewing experimental results from a broad range of materials, Dobry and Vucetic (1987) and Sun et al. (1988) concluded that the shape of the modulus reduction curve is influenced more by the plasticity index than by the void ratio and presented curves of the type shown in Figure 2.9. These curves show that the linear cyclic threshold shear strain is greater for highly plastic soils than for soils of low plasticity. This characteristic is extremely important, it can strongly influence the manner in which a soil deposit will amplify or attenuate earthquake motions. The  $PI = 0$  modulus reduction curve from Figure 2.9 is very similar to the average modulus reduction curve that was commonly used for sands (Seed and Idriss, 1970) when coarse- and fine-grained soil were treated separately. This similarity suggests that the modulus reduction curves of Figure 2.9 may be applicable to both fine- and coarse-grained soils. The difficulty of testing very large specimens has precluded the widespread testing of gravelly soils in the laboratory, but available test data indicate that the average reduction curve for gravel is similar to, though slightly flatter than, that of sand (Seed et al., 1986; Yasuda and Matsumoto, 1993).

Modulus reduction behavior is also influenced by effective confining pressure, particularly for soils of low plasticity (Iiwasaki et al., 1978; Kokushu, 1980). The linear threshold shear strain is greater at high effective confining pressure than at low effective confining pressures. The effects of effective confining pressure and plasticity index on modulus reduction behavior were combined by Ishibashi and Zhang (1993) in the form:

$$\frac{G}{G_{\max}} = K(\gamma, PI) \cdot (\sigma'_m)^{m(\gamma, PI) - m_0} \quad (2.28)$$

where

$$K(\gamma, PI) = 0.5 \left\{ 1 + \tanh \left[ \ln \left( \frac{0.000102 + n(PI)}{\gamma} \right)^{0.492} \right] \right\}$$

$$m(\gamma, PI) - m_0 = 0.272 \left\{ 1 - \tanh \left[ \ln \left( \frac{0.000556}{\gamma} \right)^{0.4} \right] \right\} \exp(-0.0145 PI^{1.3})$$

$$n(PI) = \begin{cases} 0.0 & \text{for } PI = 0 \\ 3.37 \times 10^{-6} PI^{1.404} & \text{for } 0 < PI \leq 15 \\ 7.0 \times 10^{-7} PI^{1.976} & \text{for } 15 < PI \leq 70 \\ 2.7 \times 10^{-5} PI^{1.115} & \text{for } PI > 70 \end{cases}$$

The effect of confining pressure on modulus reduction behavior of low- and high-plasticity soils is illustrated in Figure 2.10. The influence of various environmental and loading conditions on the modulus ratio of normally consolidated and moderately overconsolidated clays is described in Table 2.8.



### 2.4.3 DAMPING RATIO

Theoretically, no hysteretic dissipation of energy takes place at strains below the linear cyclic threshold shear strain. Experimental evidence, however, shows that some energy is dissipated even at very low strain levels, so the damping ratio is never zero. Above the threshold strain, the breadth of the hysteresis loops exhibited by a cyclically loaded soil increase with increasing cyclic strain amplitude, which indicates that the damping ratio increases with increasing strain amplitude.

Just as modulus reduction behavior is influenced by plasticity characteristics, so is damping behavior (Kokushu et al., 1982; Dobry and Vucetic, 1987; Sun et al., 1988). Damping ratios of highly plastic soils are lower than those of low plasticity soils at the same cyclic strain amplitude, as shown in Figure 2.11. The  $PI = 0$  damping curve from Figure 2.11 is nearly identical to the average damping curve that was used for coarse-grained soils when they were treated separately from fine-grained soils. This similarity suggests that the damping curves of Figure 2.11 can be applied to both fine- and coarse-grained soils. The damping behavior of gravel is very similar to that of sand (Seed et al., 1984a).

Damping behavior is also influenced by effective confining pressure, particularly for soils of low plasticity. Ishibashi and Zhang (1993) developed an empirical expression for the damping ratio of plastic and nonplastic soils. Using Equation (2.28) to compute the modulus reduction factor,  $G/G_{\max}$ , the damping ratio is given by:

$$\xi = 0.333 \cdot \frac{1 + \exp(-0.0145 PI^{1.3})}{2} \left[ 0.586 \left( \frac{G}{G_{\max}} \right)^2 - 1.547 \frac{G}{G_{\max}} + 1 \right] \quad (2.29)$$

The influence of various environmental and loading conditions on the damping ratio of normally consolidated and moderately overconsolidated soils is described in Table 2.9.

## 2.5 GROUND RESPONSE ANALYSIS

### 2.5.1 ONE-DIMENSIONAL GROUND RESPONSE

Geotechnical earthquake engineers are usually confronted with problems of determining the spatial and temporal variation of seismic motions in soil profile from a motion specified at a single point. Solutions to such problems, which are called as ground response problem, are crucial for liquefaction and soil-structure interaction analyses. Engineering analyses of ground response usually accept three assumptions: (1) ground motions developed near the surface of a soil deposit may be attributed merely to the vertical propagation of shear waves, (2) the ground surface, the interface between each layer, and the bed rock are essentially horizontal, (3) the material in each layer is homogeneous viscoelastic, but nonlinear. From these three assumptions, many researchers have developed computer programs to model one-dimensional wave propagation through soil (e.g. Schnabel et al., 1972). For one-dimensional ground response analysis, the soils and bedrock surface are assumed to extend infinitely in the horizontal direction.

Before describing of the ground response analysis, it is necessary to define several terms that are commonly used to describe ground motions. From Figure 2.12a, the motion at the surface of a soil deposit is the free surface motion. The motion at the base of the soil deposit (also the top of bedrock) is called a bedrock motion. The motion at a location where bedrock is exposed at the ground surface is called a rock outcropping motion. If the soil deposit was not present, as shown in Figure 2.12b, the motion at the top of bedrock would be the bedrock outcropping motion.

The nonlinear behavior of soil can be practically approximated by the equivalent linear method, as will be described below.

## 2.5.2 EQUIVALENT LINEAR METHOD

A typical soil subjected to symmetric cyclic loading as would be expected beneath a level ground surface far from adjacent structures, might exhibit a hysteresis loop of the type shown in Figure 2.13. This hysteresis loop can be described in two ways: first, by the actual path of the loop itself, and second, by parameters that describe its general shape. In general terms, two important characteristics of the shape of a hysteresis loop are its inclination and its breadth. The inclination of the loop depends on the stiffness of the soil, which can be described at any point during the load process by the tangent shear modulus,  $G_{\tan}$ . Obviously,  $G_{\tan}$  varies throughout a cycle of loading, but its average value over the entire loop can be approximated by the secant shear modulus:

$$G_{\text{sec}} = \frac{\tau_c}{\gamma_c} \quad (2.30)$$

where  $\tau_c$  and  $\gamma_c$  are the shear stress and shear strain amplitude, respectively. Thus  $G_{\text{sec}}$  describes the general inclination of the hysteresis loop. The breadth of the hysteresis loop is related to the area, which as a measure of energy dissipation, can conveniently be described by the damping ratio:

$$\xi = \frac{W_D}{4\pi W_S} = \frac{1}{2\pi} \cdot \frac{A_{\text{loop}}}{G_{\text{sec}} \gamma_c^2} \quad (2.31)$$

where  $W_D$  is the dissipated energy,  $W_S$  the maximum strain energy, and  $A_{\text{loop}}$  the area of the hysteresis loop. The parameters  $G_{\text{sec}}$  and  $\xi$  are often referred to as equivalent linear material parameters. For ground response analysis, they are used directly to describe the soil behavior.

Because some of the most commonly used methods of ground response analysis are based on the use of equivalent linear properties, considerable attention has been given to the characterization of  $G_{\text{sec}}$  and  $\xi$  for different soils. It is important to recognize, however, that the equivalent linear model is only an approximation of the actual nonlinear behavior of the soil. The assumption of linearity embedded in its use has important implications when it is used for ground response analysis. It also means that it cannot be used directly for problems involving permanent deformation or failure; equivalent linear models imply that the strain will always return to zero after cyclic loading, and since a linear material has no limiting strength, failure cannot occur.

The dynamic behavior of soil cannot be analyzed by constant elastic modulus and constant damping because these parameters depend on strain level. Nevertheless, we can solve the intricate problem by applying the equivalent linear method (Seed and Idriss, 1970). A good approximation of the effects of soil nonlinearity on the response is modeled by the use of strain compatible shear modulus and damping ratio in a sequence of linear analysis through an iterative process.

In any ground response analysis, the equivalent linear method begins with a linear analysis using estimated soil properties, shear modulus ( $G$ ) and damping ratio ( $\xi$ ), in each layer of the soil profile. This analysis yields complete time histories of shear strain, from which the effective shear strain amplitude is determined for each layer. The effective shear strain amplitude, which is function of the magnitude of earthquake, is typically taken as 65% of the maximum shear strain. Substituting in the calculated effective strain amplitudes, an improved set of shear modulus and damping ratio are obtained from suitable soil data curve, as described in Section 2.4.2 and 2.4.3. A new linear analysis is performed with these properties. The iterative process is terminated when the properties from two consecutive analysis, shear modulus and damping ratio, differ from each other by less than a specified tolerance (usually 5 to 10%). This process will usually converge in less than 5 iterations. The output of the

last iteration is taken as the final solution to approximate a nonlinear solution. Referring to Figure 2.14, the iterative procedure operates as follows:

Step 1: Initial estimates of  $G$  and  $\xi$  are made for each layer. The initially estimated values usually correspond to the same strain level; the low-strain values (0.001%) are often used for the initial estimate.

Step 2: The estimated  $G$  and  $\xi$  values are used to compute the ground response, including time histories of shear strain for each layer.

Step 3: The effective shear strain in each layer is determined from the maximum shear strain in the computed shear strain time history. For layer  $j$ :

$$\gamma_{eff\ j}^{(i)} = R_{\gamma} \cdot \gamma_{max\ j}^{(i)}$$

where the superscript refers to the iteration number and  $R_{\gamma}$  is the ratio of the effective shear strain to maximum shear strain.  $R_{\gamma}$  depends on earthquake magnitude (Idriss and Sun, 1992) and can be estimated from:

$$R_{\gamma} = \frac{M - 1}{10}$$

Step 4: From this effective shear strain, new equivalent linear value,  $G^{(i+1)}$  and  $\xi^{(i+1)}$  are chosen for the next iteration.

Step 5: Steps 2 to 4 are repeated until differences between the computed shear modulus and damping ratio values in two successive iterations fall below some predetermined value in all layers. Although convergence is not absolutely guaranteed, differences of less than 5 to 10% are usually achieved in three or five iterations (Schnabel et al., 1972).

The equivalent linear approach to one-dimensional ground response analysis of layered sites has been coded into a widely used computer program called SHAKE (Schnabel et al., 1972).

## **2.6 AMPLIFICATION OF EARTHQUAKE GROUND MOTIONS**

Earthquake produces seismic waves that travel in every direction from the seismic source. A train of these seismic waves, when recorded by an instrument, is manifested as a record of earthquake ground motions. Basic characteristics of strong ground motions are influenced by the source, travel path, and modified by local soil conditions. In some cases, local soil conditions play a predominant role to the ground motion features. Therefore, the concept of soil amplification is defined as modification of the input bedrock ground motion by the overlying unconsolidated materials.

The phenomena were initially derived from the great differences in the degree of earthquake damage at places about the same distance from the epicenter. Early example can be come back to 1923 Kanto earthquake, Japan. Still further, it was shown by the strong earthquake in Caracas in 1967. The most notable example was 1985 Mexico earthquake in which there were the enormous differences in intensities of shaking and associated building damage in the different parts of the city. More recent two cases are the 1988 Armenia earthquake, Russia and the 1989 Loma Prieta earthquake, California, USA.

### **2.6.1 AMPLIFICATION FACTOR**

Amplification factor is defined as the ratio between earthquake ground motion intensity on soil surface and that on rock surface. In soft surface layers, vibrations are amplified due to multi-reflection phenomena. In order to express the degree of magnification quantitatively, it will suffice the corresponding component

vibrations of the earthquake wave in the base ground and the waveform at the ground surface and obtain the magnification of the latter over the former. In this regard, the formula proposed by Kanai (1957) is presented. Kanai (1957) has arrived at the formula below by combining the results of the actual measurements with the theoretical calculations:

$$A = 1 + \frac{1}{\sqrt{\left[ \frac{1+k}{1-k} \cdot \left( 1 - \left( \frac{T}{T_G} \right)^2 \right) \right]^2 + \left( \frac{0.3}{\sqrt{T_G}} \cdot \frac{T}{T_G} \right)^2}} \quad (2.31)$$

where A = soil amplification factor (i.e., ratio of amplitude of response wave at the ground surface and that of incident wave)

T = period of component vibration of seismic wave

$T_G$  = predominant period of surface layer

$k = (\rho_1 \beta_1) / (\rho_2 \beta_2)$

$\rho_1$  = density of soft surface layer

$\rho_2$  = density of base layer

$\beta_1$  = velocity of seismic wave in surface layer

$\beta_2$  = velocity of seismic wave in base layer

The graphical form of this formula is shown in Figure 2.15 in which the following properties are recognized in the multiplication of the surface layer:

1. The amplification factor is largest when the period of the input wave coincides with the predominant period of the ground.
2. The ground whose predominant period is longer has a larger ratio of magnification.
3. The amplification factor of ground having very long predominant period becomes a constant value  $2/(1+k)$  independent of the period of the input wave.

4. The soil amplification factor is more conspicuous for ground having a smaller value  $k$  than for ground having a larger one.

In fact, the amplitude of the amplification ground motion is a function of the shear wave velocity, the density and material damping, the thickness, water content, the geometry of the unconsolidated deposits and underlying rock, and where the surface of bedrock topography is irregular.

## **2.6.2 EFFECTS OF LOCAL SITE CONDITIONS ON GROUND MOTION**

Case histories of ground response in Mexico City (i.e., 1985 Mexico earthquake), the San Francisco Bay area (i.e., 1989 Loma Prieta earthquake), and many other locations have clearly shown that local site conditions strongly influence peak acceleration amplitudes.

Comparisons of peak acceleration attenuation relationships for sites underlain by different types of soil profiles show distinct trends in amplification behavior (Seed et al., 1976b). Although attenuation data are scattered, overall trends suggest that peak accelerations at the surfaces of soil deposits are slightly greater than on rock when peak accelerations are small and somewhat smaller at higher acceleration level, as shown in Figure 2.16. Based on data from Mexico City and the San Francisco Bay area, and on additional ground response analyses, Idriss (1990) related peak accelerations on soft soil sites to those on rock sites, as shown in Figure 2.17. At low to moderate acceleration levels (i.e., less than about 0.4g), peak accelerations at soft sites are likely to be greater than on rock sites. In some cases, such as Mexico City in 1985 and the San Francisco Bay area in 1989, relatively small rock accelerations may cause high accelerations at the surface of soft soil deposits. At higher acceleration levels, however, the low stiffness and nonlinearity of soft soils often prevent them from developing peak accelerations as large as those observed on rock.



Local site conditions also influence the frequency content of surface motions and hence the response spectra (i.e., the variation of peak dynamic response of a single-degree-of-freedom system, for different values of its natural frequency or period, given a specified input transient motion) they produce. Seed et al. (1976) computed response spectra from ground motions recorded at sites underlain by four categories of site conditions: rock sites, stiff soil sites (less than 200 ft (61 m) deep), deep cohesionless soil sites (greater than 250 ft (76 m) deep), and sites underlain by soft to medium-stiff clays and sands. Normalizing the computed spectra (by dividing spectral accelerations by the peak ground acceleration) illustrates the effects of local soil conditions on the shape of the spectra, as shown in Figure 2.18. The effects are apparent: at periods above about 0.5 sec, spectral amplifications are much higher for soil sites than for rock sites. At longer periods, the spectral amplification increases with decreasing subsurface profile stiffness. Figure 2.18 clearly shows that deep and soft soil deposits produce greater proportions of long-period (low-frequency) motion. This effect can be very significant, particularly when long-period structures such as bridges and tall buildings are founded on such deposits (i.e., the dynamic response of long-period structures is increased if the local ground conditions are soft).

## **2.7 LIQUEFACTION**

### **2.7.1 GENERAL**

Liquefaction describes a phenomenon in which cyclic stresses produced by ground shaking induce excess pore water pressure in cohesionless soils of sufficient magnitude to cause partial or complete loss of shear strength of the deposits. These soils may thereby acquire a high degree of mobility, leading to damaging deformations. This phenomenon only occurs below the water table, but after liquefaction has developed, it can propagate upward into overlying non-saturated soil as excess pore water escapes.

Liquefaction susceptibility under a given earthquake is related to the gradation and relative density characteristics of the soil, the in situ stresses prior to ground motion, and the depth of the water table as well as other factors.

It has long been known that the intensity of ground shaking during earthquake and its associated damage to buildings and other properties are affected by the geologic and ground conditions. The phenomenon of liquefaction has been reported in numerous earthquakes to cause landslides and damage to buildings, but it was more dramatically illustrated by widespread building damage and large landslides in the Niigata, Japan earthquake of 1964 and the Alaska, USA earthquake the same year.

Ambraseys (1988) compiled worldwide data from shallow earthquakes to estimate a limiting epicentral distance beyond which liquefaction has not been observed in earthquakes of different magnitudes (Figure 2.19). The distance to which liquefaction can be expected increases dramatically with increasing magnitude. While relationships of the type shown in Figure 2.19 offer no guarantee that liquefaction cannot occur at greater distances, they are helpful for estimation of regional liquefaction hazard scenarios.

Soil deposits that are susceptible to liquefaction are formed within a relatively narrow range of geological environments (Youd, 1991). The depositional environment, hydrological environment, and age of a soil deposit all contribute to its liquefaction susceptibility.

Since liquefaction requires the development of excess pore water pressure, liquefaction susceptibility is influenced by the compositional characteristics that influence volume change behavior. Compositional characteristics associated with high volume change potential tend to be associated with high liquefaction susceptibility. These characteristics include particle size, shape, and gradation.

For many years, liquefaction-related phenomena were thought to be limited to sands. Finer-grained soils were considered incapable of generating the high pore pressures commonly associated with liquefaction, and coarser-grained soils were considered too permeable to sustain any generated pore water pressure long enough for liquefaction to develop.

Liquefaction of nonplastic silts has been observed (Ishihara, 1984, 1985) in the laboratory and the field, indicating that plasticity characteristics rather than grain size alone influence the liquefaction susceptibility of fine-grained soils. Coarse silts with bulky particle shape, which are nonplastic and cohesionless, are fully susceptible to liquefaction (Ishihara, 1993); finer silts with flaky or platelike particles generally exhibit sufficient cohesion to inhibit liquefaction. Clays remain nonsusceptible to liquefaction, although sensitive clays can exhibit strain-softening behavior (referred to as being contractive or flow) similar to that of liquefied soil.

Liquefaction susceptibility is influenced by gradation. Well-graded soils are generally less susceptible to liquefaction than poorly graded soils; the filling of voids between larger particles by smaller particles in a well-graded soil results in lower volume change potential under drained conditions and, consequently, lower excess pore water pressures under undrained conditions. Field evidence indicates that most liquefaction failures have involved uniformly graded soils.

## **2.7.2 CAUSES OF SOIL LIQUEFACTION**

The basic cause of liquefaction of sands has been understood, in a qualitative way, for many years. If a saturated sand is subjected to ground vibrations, it tends to compact and decrease in volume; if drainage is unable to occur, the tendency to decrease in volume results in an increase in pore water pressure, and if the pore water pressure builds up to the point at which it is equal to the overburden pressure, the effective stress becomes zero, the sand loses its strength completely, and it develops a liquefied state.

In more quantitative terms, it is now generally believed that the basic cause of liquefaction in saturated cohesionless soils during earthquakes is the buildup of excess hydrostatic pressure due to the application of cyclic shear stresses induced by the ground motions. These stresses are generally considered to be due primarily to upward propagation of shear waves in a soil deposit, although other forms of wave

motions are also expected to occur. Thus, soil elements can be considered to undergo a series of cyclic stress conditions as illustrated in Figure 2.20, the stress series being somewhat random in pattern but nevertheless cyclic in nature.

As a consequence of the applied cyclic stresses, the structure of the cohesionless soil tends to become more compact with a resulting transfer of stress to the pore water and a reduction in stress on the soil grains. As a result, the soil grain structure rebounds to the extent required to keep the volume constant, and this interplay of volume reduction and soil structure rebound determines the magnitude of the increase in pore water pressure in the soil (Martin et al., 1975).

As the pore water pressure approaches a value equal to the applied confining pressure, the sand begins to undergo deformations. If the sand is loose, the pore water pressure will increase suddenly to a value equal to the applied confining pressure, and the sand will rapidly begin to undergo large deformations with shear strains that may exceed  $\pm 20\%$  or more. If the sand will undergo virtually unlimited deformations without mobilizing significant resistance to deformation, it can be said to be liquefied. If, on the other hand, the sand is dense, it may develop a residual pore water pressure, on completion of a full stress cycle, which is equal to the confining pressure (a peak cyclic pore pressure ratio of 100%), but when the cyclic stress is reapplied on the next stress cycle, or if the sand is subjected to monotonic loading, the soil will tend to dilate, the pore pressure will drop if the sand is undrained, and the soil will ultimately develop enough resistance to withstand the applied stress. However, it will have to undergo some degree of deformation to develop the resistance, and as the cyclic loading continues, the amount of deformation required to produce a stable condition may increase. Ultimately, however, for any cyclic loading condition, there appears to be a cyclic strain level at which the soil will be able to resist any number of cycles of a given stress without further increase in maximum deformation (De alba et al., 1976). This type of behavior is termed “cyclic mobility” and it is considerably less serious than liquefaction, its significance depending on the magnitude of the limiting strain. It should be noted, however, that once the cyclic stress applications stop, if they return to a zero stress condition, there will be a residual pore water pressure in the soil equal

to the overburden pressure, and this will inevitably lead to an upward flow of water in the soil which could have deleterious consequences for overlying layers. Ishihara (1996) described the meaning of cyclic mobility as a state where zero effective stress or initial liquefaction occurs momentarily whenever there is no applied shear stress (a large amount of shear strain can occur after the onset of initial liquefaction) but the effective stress regains with the application of shear stress. Mori, Seed, and Chan (1978) defined the initial liquefaction with limited strain potential or cyclic mobility as a condition in which cyclic stress applications cause limited strains to develop either because of the remaining resistance of the soil to deformation or because the soil dilates, the pore pressure drops, and the soil stabilizes under the applied loads.

Liquefaction of sand in this way may develop in any zone of a deposit where the necessary combination of in situ conditions and vibratory deformations may occur. Such a zone may be at the surface or at some depth below the ground surface, depending only on the state of the sand and the induced motions.

However, liquefaction of the upper layers of a deposit may also occur, not as a direct result of the ground motion to which they are subjected, but because of the development of liquefaction in an underlying zone of the deposit. Once liquefaction develops at a some depth in a mass of sand, the excess hydrostatic pressures in the liquefied zone will dissipate by flow of water in an upward direction. If the hydraulic gradient becomes sufficient large, the upward flow of water will induce a quick or liquefied condition in the surface layers of the deposit. Liquefaction of this type will depend on the extent to which the necessary hydraulic gradient can be developed and maintained; this, in turn, will be determined by the compaction characteristics of the sand, the nature of ground deformations, the permeability of the sand, the boundary drainage conditions, the geometry of the particular situation, and the duration of the induced vibrations.

## **2.7.3 FAILURE MECHANISMS FOR SLOPE GROUND**

### **2.7.3.1 LATERAL SPREADS**

Lateral spreads involve lateral displacement of large, surficial block of soil as a result of liquefaction of a subsurface layer (Figure 2.21). Displacement occurs in response to the combination of gravitational forces and inertial forces generated by an earthquake. Lateral spreads generally develop on gentle slopes (most commonly less than 3 degrees) and move toward a free face such as an incised river channel. Horizontal displacements commonly range up to several meters. The displaced ground usually breaks up internally, causing fissures, scarps, horsts, and grabens to form on the failure surface. Lateral spreads commonly disrupt foundations of buildings built on or across the failure, sever pipelines and other utilities in the failure mass, and compress or buckle engineering structures, such a bridges, founded on the toe of the failure.

### **2.7.3.2 FLOW FAILURES**

Flow failures are the most catastrophic ground failures caused by liquefaction. These failures commonly displace large masses of soil laterally tens of meters and in a few instances, large masses of soil have traveled tens of kilometers down long slopes at velocities ranging up to tens of kilometers per hour. Flows may be comprised of completely liquefied soil or blocks of intact material riding on a layer of liquefied soil. Flows develop in loose saturated sands or silts on relatively steep slopes, usually greater than 3 degrees, as shown in Figure 2.22.

## 2.7.4 FAILURE MECHANISMS FOR HORIZONTAL GROUND

### 2.7.4.1 SAND BOILS

Liquefaction is often accompanied by the development of sand boils. During and following earthquake shaking, seismically induced excess pore pressures are dissipated predominantly by the upward flow of pore water. This flow produces upward-acting forces on soil particles, these forces can loosen the upper portion of the deposit and leave it in a state susceptible to liquefaction in future earthquake (Youd, 1984). If the hydraulic gradient driving the flow reaches a critical value, the vertical effective stress will drop to zero and the soil will be in a quick condition. In such cases, the water velocities may be sufficient to carry soil particles to the surface. In the field, soil conditions are rarely uniform so the escaping pore water tends to flow at high velocity through localized cracks or channels. Sand particles can be carried through these channels and ejected at the ground surface to form sand boils.

Sand boils are of little engineering significance by themselves, but they are useful indicators of high excess pore pressure generation. Shaking table (Liu and Qiao, 1984) and centrifuge (Fiegel and Kutter, 1992) tests have shown that pore water draining from the voids of the loose layers can accumulate beneath the less previous layers and form water interlayers, as shown in Figure 2.23. Sand boils can develop when the water interlayers break through to the ground surface. Some redistribution of soil grains is also likely to accompany the formation of water interlayers; specifically the sand immediately beneath the water interlayer may be loosened by the upward flow of water toward the interlayer. If such conditions develop beneath an inclined ground surface, the presence of the water interlayer and the reduced steady state strength of the loosened sand immediately beneath it can contribute to large flow deformations.

#### **2.7.4.2 GROUND OSCILLATION**

The occurrence of liquefaction at depth beneath a flat ground surface can decouple the liquefied soils from the surficial soils and produce large, transient ground oscillations. The surficial soils are often broken into blocks (Figure 2.24) separately by fissures that can open and close during the earthquake. Ground waves with amplitudes of up to several meters have been observed during ground oscillation, but permanent displacements are usually small. Prediction of the amplitude of ground oscillation at a particular site is very difficult; even detailed nonlinear ground response analyses can provide only crude estimates.

#### **2.7.4.3 LOSS OF BEARING STRENGTH**

When the soil supporting a building or other structure liquefies and loses strength, large deformations can occur within the soil which may allow the structure to settle and tip, as shown in Figure 2.25. Conversely, buried tanks and piles may rise buoyantly through the liquefied soil. For example, many buildings settled and tipped during the 1964 Niigata, Japan, earthquake. The most spectacular bearing failures during that event were in the Kawangishicho apartment complex where several four-story buildings tipped as much as 60 degrees, as shown in Figure 2.26. Apparently, liquefaction first developed in a sand layer several meters below ground surface and then propagated upward through overlying sand layers. The rising wave of liquefaction weakened the soil supporting the buildings and allowed the structures to slowly settle and tip.

#### **2.7.4.4 SUBSIDENCE AND SETTLEMENT**

In many cases, the weight of a structure will not be great enough to cause the large settlements associated with soil bearing capacity failure described above.



However, smaller settlements may occur as soil pore water pressures dissipate and the soil consolidates after the earthquake. These settlements may be damaging, although they would tend to be much less so than the large movements accompanying flow failures, lateral spreading, and bearing capacity failures. The eruption of sand boils is a common manifestation of liquefaction that can also lead to localized differential settlements.

## **2.8 EVALUATION OF LIQUEFACTION RESISTANCE OF SOILS**

A number of approaches to evaluation of the potential for initial of liquefaction or liquefaction resistance have developed over the years. In the following sections, the most common of these approaches will be reviewed.

### **2.8.1 DETERMINISTIC APPROACH OR CYCLIC STRESS**

#### **APPROACH**

In the 1960s and 1970s, many advances in the state of knowledge of liquefaction phenomena resulted from the pioneering work of H.B. Seed and his colleagues at the University of California at Berkley. This research was directed largely toward evaluation of the loading conditions required to trigger liquefaction. This loading was described in terms of cyclic shear stresses, and liquefaction potential was evaluated on the basis of the amplitude and number of cycles of earthquake-induced shear stress. The general approach has come to be known as the cyclic stress approach.

Seed and Lee (1966) defined initial liquefaction as the point at which the increase in pore pressure is equal to the initial effective confining pressure (i.e., when  $u_{excess} = \sigma'_{3c}$  or when pore pressure ratio,  $r_u = 100\%$ ). Because most of the early laboratory testing investigations were based on cyclic triaxial tests on isotropically

consolidated specimens (consequently, with complete stress reversal), initial liquefaction could be produced in both loose and dense specimens.

The cyclic stress approach is conceptually quite simple: the earthquake-induced loading, expressed in terms of cyclic shear stresses, is compared with the liquefaction resistance of the soil, also expressed in terms of cyclic shear stresses. Application of the cyclic stress approach, however, requires careful attention to the manner in which the loading conditions and liquefaction resistance are characterized.

### **2.8.1.1 CYCLIC STRESS RATIO (CSR) AND CYCLIC RESISTANCE RATIO (CRR)**

Calculation, or estimation, of two variables is required for evaluation of liquefaction resistance of soils: (1) the seismic demand on a soil layer, expressed in terms of CSR; and (2) the capacity of the soil to resist liquefaction, expressed in terms of CRR. The latter variable has been termed the cyclic stress ratio or the cyclic stress ratio required to generate liquefaction, and has been given different symbols by different writers. For example, Seed and Harder (1990) used the symbol  $CSR_{\ell}$ , Youd (1993) used the symbol CSRL, and Kramer (1996) used the symbol  $CSR_L$  to denote this ratio. To reduce confusion and to better distinguish induced cyclic shear stresses from mobilized liquefaction resistance, the capacity of soil to resist liquefaction is termed the CRR in this research.

### **2.8.1.2 EVALUATION OF CYCLIC STRESS RATIO (CSR)**

The shear stresses developed at any point in a soil deposit during an earthquake appear to be due primarily to the vertical propagation of shear waves in the deposit. This leads to a simplified procedure for evaluating the induced shear stresses (Seed and Idriss, 1971). If the soil column above a soil element at depth  $h$  behaved as rigid body, the maximum shear stress on the soil element would be

$$(\tau_{\max})_r = \frac{\gamma h}{g} \cdot a_{\max} \quad (2.32)$$

where  $a_{\max}$  is the maximum horizontal ground surface acceleration,  $g$  is the acceleration of gravity, and  $\gamma$  is the unit weight of the soil; see Figure 2.27(a). Because the soil column behaves as a deformable body, the actual shear stress at depth  $h$ ,  $(\tau_{\max})_d$ , as determined by a ground response analysis will be less than  $(\tau_{\max})_r$  and might be expressed by

$$(\tau_{\max})_d = r_d \cdot (\tau_{\max})_r \quad (2.33)$$

where  $r_d$  is a stress reduction coefficient with a value less than 1. The variations of  $(\tau_{\max})_r$  and  $(\tau_{\max})_d$  will typically have the form shown in Figure 2.27(b) and, in any given deposit, the value of  $r_d$  will decrease from a value 1 at the ground surface to much lower values at large depths, as shown in Figure 2.27(c).

Computations of the value of  $r_d$  for a wide variety of earthquake motions and soil conditions having sand in the upper 15 m. have shown that  $r_d$  generally falls within the range of values shown in Figure 2.28. It may be seen that in the upper 9 or 12 m., the scatter of the results is not great and, for any of the deposits, the error involved in using the average values shown by the dashed line would generally be less than about 5%. For routine practice, the following equations may be used to estimate average values of  $r_d$  (Liao and Whitman, 1986a):

$$r_d = 1.0 - 0.00765 z \quad \text{for } z \leq 9.15 \text{ m} \quad (2.34a)$$

$$r_d = 1.174 - 0.0267 z \quad \text{for } 9.15 < z \leq 23 \text{ m} \quad (2.34b)$$

where  $z$  is depth below ground surface in meters.

Thus the assessment of the maximum shear stress developed during an earthquake can be made from the relationship

$$\tau_{\max} = \frac{\gamma h}{g} \cdot a_{\max} \cdot r_d \quad (2.35)$$

where  $r_d$  are taken from the dashed line in Figure 2.28 or Equation (2.34). The critical depth for development of liquefaction, if it is going to occur, will normally be in the depth covered by this relationship.

The actual time history of shear stress at any point in a soil deposit during an earthquake will have an irregular form such as that shown in Figure 2.29. From such relationships it is necessary appropriate to determine the equivalent uniform average shear stress. By appropriate weighting of the individual stress cycles, based on laboratory test data, this determination can readily be made. However, after making these determinations for a number of different cases it has been found that with a reasonable degree of accuracy, the average equivalent uniform shear stress,  $\tau_{av}$ , is about 65% of the maximum shear stress,  $\tau_{\max}$ . Combining this result with the above expression for  $\tau_{\max}$  it follows that for practical purposes, the average cyclic shear stress may be determined by:

$$\tau_{av} = 0.65 \cdot \frac{\gamma h}{g} \cdot a_{\max} \cdot r_d \quad (2.36)$$

or equivalently:

$$CSR = \frac{\tau_{av}}{\sigma'_{vo}} = 0.65 \cdot \frac{\sigma'_{vo}}{\sigma'_{vo}} \cdot \frac{a_{\max}}{g} \cdot r_d \quad (2.37)$$

where CSR = cyclic stress ratio caused by the earthquake,  $\sigma_{vo}$  = total overburden pressure on sand layer under consideration, and  $\sigma'_{vo}$  = initial effective overburden pressure on sand layer under consideration

### **2.8.1.3 EVALUATION OF LIQUEFACTION RESISTANCE (CRR)**

A plausible method for evaluating cyclic resistance ratio, CRR, is to retrieve and test undisturbed soil specimen in the laboratory. Unfortunately, in situ stress states generally cannot be reestablished in the laboratory, and granular soils are extremely difficult to sample without disturbance. Hence, methods to characterize the soil in the ground rely heavily on in situ tests. Several field tests have gained common usage for evaluation of liquefaction resistance, including the standard penetration test (SPT), the cone penetration test (CPT), and field measurements of shear wave velocity ( $V_s$ ). But the most commonly used method for determining the liquefaction resistance is to use the data obtained from the standard penetration test because it is relatively easy to use, the test is economical compared to other types of field testing, and the SPT equipment can be quickly adapted and included as part of almost any type of drilling rig.

Seed and his colleagues developed correlations between the SPT N-value and the cyclic stress ratio to cause liquefaction or cyclic resistance ratio during earthquakes of magnitude  $M = 7.5$ . The correlations, which are presented in Figure 2.30, were based on the observed response of sites during earthquake loading. Sites were considered to have liquefied based on observed surface features, such as sand boils. Lower bound curves separating liquefied from non-liquefied sites are shown in Figure 2.30 corresponding to various fines contents of the sands. It should be noted that the CRR curves in Figure 2.30 are valid only for magnitude 7.5 earthquakes. Scaling factors to adjust CRR curves to other magnitudes are addressed in the next section of this chapter.

To compare the ground conditions at one site with those of another, it is necessary to standardize the measured penetration values to the standard driving energy level of 60% of the theoretical free-fall energy of the hammer, the rate at which the blows are applied, the borehole diameter, the rod lengths, and the effective overburden pressure of 100 kPa (1 tsf). Hence, the CRR curves presented in Figure 2.30 show the normalized SPT N-value,  $(N_1)_{60}$ . Corrections can be applied to the penetration test results to compensate for the testing procedures by using the following equation:

$$(N_1)_{60} = N_m C_N \frac{E_m}{0.60 E_{ff}} C_B C_R C_S \quad (2.38)$$

where  $N_m$  = the measured penetration resistance, Blows/ft

$C_N$  = correction factor to normalize  $N_m$  to an effective overburden pressure  $\sigma'_{vo}$  of 100 kPa (100 kPa = 1 tsf = 10 t/m<sup>2</sup> = 1 atm)

$$= \sqrt{\frac{10}{\sigma'_{vo}}} \leq 1.7 \text{ for } \sigma'_{vo} \leq 20 \text{ t/m}^2 \text{ (Liao and Whitman, 1986b)}$$

$$= \frac{2.2}{\left(1.2 + \frac{\sigma'_{vo}}{10}\right)} \leq 1.7 \text{ for } 20 < \sigma'_{vo} \leq 30 \text{ t/m}^2 \text{ (Kayen et al., 1992)}$$

$E_m$  = the actual hammer energy which is the percent of the theoretical free-fall hammer energy; the value of  $E_m$  depends on the type of hammer used and on the standards of practice in different parts of the world such as anvil lifting mechanism and the method of hammer release ( $E_m$  is 0.6 for a safety hammer and 0.45 to 0.6 for donut hammer, Seed et al. (1985))

$E_{ff}$  = the theoretical free-fall hammer energy

$C_B$  = correction factor for borehole diameter ( $C_B = 1.0$  for boreholes of 65 to 115 mm diameter, 1.05 for 150 mm diameter, and 1.15 for 200 mm diameter)

$C_R$  = correction factor for rod length ( $C_R = 0.75$  for up to 3 m of drill rods, 0.8 for 3 to 4 m of drill rods, 0.85 for 4 to 6 m of drill rods, 0.95 for 6 to 10 m of drill rods, and 1.0 for drill rods in excess of 10 m)

$C_S$  = correction for samplers with or without liners ( $C_S = 1.0$  for standard sampler and 1.1 to 1.3 for sampler without liner)

Although application of rod length correction factors mentioned above will give more precise  $(N_1)_{60}$  values, these corrections may be neglected for liquefaction resistance calculation for rod lengths between 3 and 10 m because rod length corrections were not applied to SPT test data from these depths in compiling the original liquefaction case history databases. Thus rod length corrections are implicitly incorporated into the empirical SPT procedure.

#### **2.8.1.4 MAGNITUDE SCALING FACTOR (MSF)**

The liquefaction resistance or CRR curves in Figure 2.30 apply only to magnitude 7.5 earthquakes. To adjust the CRR curves to magnitude smaller or larger than 7.5, one has to use correction factor termed “magnitude scaling factor (MSF).” Several MSF values have been proposed by various investigators (i.e., Seed and Idriss (1982), Ambraseys (1988), Arango (1996), Andrus and Stokoe (1997), and Youd and Noble (1997)). The MSF in Table 2.10 (Seed and Idriss, 1982) is the routinely used values in engineering practice. In addition, the 1996 NCEER workshop (Youd and Idriss, 1997) recommended that the lower bound for MSF values can be defined by the following equation:

$$\text{MSF} = (M_w / 7.5)^{-2.56} \quad (2.39)$$

where  $M_w$  is the moment magnitude. It should be noted that the local magnitude  $M_L$ , the surface wave magnitude  $M_S$ , and moment magnitude  $M_w$  scales are reasonably close to one another below a value of about 7, as shown in Figure 2.31. Thus for a magnitude of 7 or below, any one of these magnitude scales can be used to determine the MSF. At high magnitude values, the moment magnitude  $M_w$  tends to significantly deviate from the other magnitude scales, and the moment magnitude  $M_w$  should be used to determine the MSF from Table 2.10 or Equation (2.39).

### **2.8.1.5 EFFECTS OF INITIAL STATIC SHEAR STRESSES AND HIGH OVERBURDEN STRESSES ON LIQUEFACTION RESISTANCE**

There are two important limitations associated with Figure 2.30. The field data correspond to level ground conditions with no initial static shear stresses on horizontal planes and to effective overburden pressures less than  $15 \text{ t/m}^2$  (150 kPa). Seed (1983) outlined procedures for making corrections when these conditions are violated.

The first estimate of the liquefaction resistance of a soil element in a dam or slope is determined using the in situ  $(N_1)_{60}$  penetration resistance and the appropriate curve for critical conditions in Seed's liquefaction assessment chart (Figure 2.30). This resistance must then be corrected for deviations from the standard conditions of the database underlying the chart. A typical element in a slope, for example, will carry a static shear stress,  $\tau_{st}$ , on the horizontal plane and therefore has an initial shear stress ratio  $\tau_{st} / \sigma'_{vo} = \alpha$ . A correction factor,  $K_\alpha$ , is established for various values of  $\alpha$  by laboratory tests. Note that, as is commonly assumed in practice, initial static shear increases liquefaction resistance substantially. However, this increase applies to



resistance to cyclic mobility rather than to liquefaction, that is to non-contractive materials. The liquefaction resistance of dilative soils (moderately dense to dense granular materials under low confining stress) increases with increased static shear stress. Conversely, the liquefaction resistance of contractive soils (loose soils and moderately dense soils under high confining stress) decreases with increased static shear stress. Seed and Harder (1990) proposed a chart (Figure 2.32) for a variation of correction factor,  $K_\alpha$ , with initial shear stress ratio,  $\alpha$ . The values of  $K_\alpha$  vary for different soils and should be evaluated on a site-specific basis whenever possible. In addition, the 1996 NCEER workshop (Youd and Idriss, 1997) recommended that the proposed chart for  $K_\alpha$  should not be used by non-specialists in geotechnical earthquake engineering or in routine engineering practice.

For effective overburden pressures other than in the range 10-15 t/m<sup>2</sup> (100-150 kPa) and for sites that support heavy structures, a correction factor  $K_\sigma$  is used. Cyclically loaded laboratory test data indicate that liquefaction resistance increases with increasing confining stress. The rate of increase, however, is nonlinear. To account for the nonlinearity between liquefaction resistance or CRR and effective overburden pressure, Seed and Harder (1990) introduced the values of  $K_\sigma$  for many soils as shown in Figure 2.33. Increasing confining pressure can lead to a substantial reduction in resistance to cyclic loading. The values of  $K_\sigma$  vary for different soils and should be evaluated on a site-specific basis whenever possible.

#### **2.8.1.6 FACTOR OF SAFETY AGAINST LIQUEFACTION**

Once the cyclic stress ratio caused by the anticipated earthquake (Equation (2.37)) and the liquefaction resistance of the soils corresponding to earthquake of magnitude 7.5 (Figure 2.30) has been characterized, liquefaction potential can be evaluated. The factor of safety against liquefaction (FS) is defined as follows:

$$FS = \left( \frac{CRR_{7.5}}{CSR} \right) \cdot MSF \cdot K_{\alpha} \cdot K_{\sigma} \quad (2.40)$$

where  $CSR$  = calculated cyclic stress ratio generated by the earthquake shaking, Equation (2.37);  $CRR_{7.5}$  = cyclic resistance ratio for magnitude 7.5 earthquakes determined from Figure 2.30;  $MSF$  = magnitude scaling factor determined from Table 2.10 or Equation (2.39);  $K_{\alpha}$  = correction factor for sloping ground or for initial static shear stress determined from Figure 2.32; and  $K_{\sigma}$  = correction factor for effective overburden pressure determined from Figure 2.33.

If the factor of safety in Equation (2.40) is equal or less than 1.0, liquefaction is said to take place. Otherwise, liquefaction does not occur. In addition, it should be noted that the higher the factor of safety, the more resistant the soil is to liquefaction.

## 2.8.2 PROBABILISTIC APPROACH

There are many potential sources of uncertainty in both the loading and resistance aspects of liquefaction problems, and probabilistic approaches have been developed to deal with them. Uncertainties in cyclic loading can be evaluated using the standard probabilistic seismic hazard analyses (Cornell, 1968; Algermissen et al., 1982; Reiter, 1990). Uncertainties in liquefaction resistance can be treated in one of two general ways.

One group of methods is based on probabilistic characterization of the parameters shown by laboratory tests to influence pore pressure generation. Haldar and Tang (1979) characterized uncertainty in the parameters of the simplified cyclic stress approach or deterministic approach described in Section 2.8.1. Fardis and Veneziano (1982) used a similar approach with total stress and effective stress models. Chameau and Clough (1983) described pore pressure generation probabilistically using experimental data and an effective stress model. Each of these methods can compute the probability of liquefaction due to a particular set of loading

conditions. Their accuracy depends on the accuracy of the underlying liquefaction / pore pressure model and on how accurately the uncertainty of the model parameters can be determined.

An alternative method is based on in situ test-based characterization of liquefaction resistance (Christian and Swiger, 1975; Yegian and Whitman, 1978; Veneziano and Liao, 1984). This method, which will be presented in Chapter 5, use various statistical classification and regression analyses to assign probabilities of liquefaction to different combinations of loading and resistance parameters.



สถาบันวิทยบริการ  
จุฬาลงกรณ์มหาวิทยาลัย

## CHAPTER 3

### PROFILE OF THE STUDY AREA

#### 3.1 LOCATION AND TOPOGRAPHY

Chiang Mai, Thailand's second largest city with an area of 22,800 square kilometers and capital of the northern region, located about 700 kilometers north of Bangkok at latitude  $18.80^{\circ}$  N and longitude  $98.98^{\circ}$  E. A large part (69.31 %) of Chiang Mai's land is covered by mountains and forests. These generally run in a north-south pattern through the province and give birth to several streams and tributaries (such as the Mae Jam, Mae Ngud, and Mae Klang) which in turn feed important rivers and irrigation canals (such as the Muang and Faay) which provide the water necessary to Chiang Mai's agriculture. Chiang Mai's largest and most important river is the Ping, which originates in the mountains of Chiang Dao and flows southward for 540 kilometers. It is along the banks of this river that Chiang Mai's flat, fertile valley area lies.

Chiang Rai, the northernmost province of Thailand with an area of 11,678 square kilometers, is approximately 785 kilometers from Bangkok at latitude  $19.91^{\circ}$  N and longitude  $99.83^{\circ}$  E. The province is situated on the Kok River basin. The average elevation is about 580 meters above sea level. Mostly mountainous, it reaches the Mae Khong River to the north and borders on both Myanmar and Laos. North Chiang Rai falls within the region known as the Golden Triangle, the area where the borders of Thailand, Myanmar and Laos converge.

The areas of investigation are shown in Figure 3.1.

### 3.2 SEISMICITY

Thailand lies in the interior of the Eurasian plate, with the boundary of the Burma microplate and Indian plate occurring to the west in the Andaman sea. Nutalaya et al. (1985) collected the database containing instrumental data of earthquakes from 1910 to 1989 within the region bounded by latitudes  $5^{\circ}$  N to  $25^{\circ}$  N and longitudes  $90^{\circ}$  E to  $110^{\circ}$  E, which includes Thailand, Indochina, and parts of Burma and China. These data were collected from several agencies which include the U.S. Geological Survey (USGS), the International Seismological Center (ISC) in U.K., and the Thai Meteorological Department (TMD). In addition, 12 seismic source zones within the region (zones A to L in Figure 3.2) have been identified on the basis of the spatial distribution of seismicity and regional seismotectonic structure. The maximum observed local magnitude (Richter scale,  $M_L$ ) earthquake to occur within the eleven closest zones is shown in Table 3.1. As seen from Table 3.1, the maximum estimate  $M_L$  occurring within these zones ranges from 6.5 for the Northern Thailand Zone to 7.9 for the Tenasserim Range Zone.

Wanitchai and Lisantono (1996) proposed a seismic hazard map of Thailand as shown in Figure 3.3. As seen from Figure 3.3, Thailand is divided into various seismic zones according to the following criteria: zone 0 for  $PGA_0 < 0.025g$ , where  $PGA_0$  is the peak ground acceleration (PGA) with a 10% probability of being exceeded in a 50-year period at any given site and  $g$  is the acceleration of gravity; zone 1 for  $0.025g < PGA_0 < 0.075g$ ; zone 2A for  $0.075g < PGA_0 < 0.15g$ ; zone 2B for  $0.15g < PGA_0 < 0.20g$ ; zone 3 for  $0.20g < PGA_0 < 0.30g$ ; and zone 4 for  $PGA_0 > 0.30g$ . These criteria are similar to those used in the 1988, 1991, and 1994 U.S. Uniform Building Code (UBC) zoning maps except that in the UBC, effective peak acceleration (EPA) is used instead of PGA. By its definition, EPA is the peak ground acceleration after the ground motion record has been filtered to remove the very high frequencies that have little influence upon structural response. However, it appeared that for  $PGA < 0.3g$  there is no significant different between PGA and EPA. The

zoning map in Figure 3.3 shows that some parts of the northern and western Thailand can be considered as moderate risk and moderately high risk zones equivalent to the UBC zone 2B and 3, respectively.

### **3.3 SOIL PROFILE**

The soil underlying Chiang Mai and Chiang Rai consist of alternating layers of silty sand, clayey sand, sandy silt, and silty clay. Anantasech and Thanadpipat (1985) collected geotechnical investigation data of Chiang Mai City and proposed soil profiles of the city from north to south, and from east to west as shown in Figure 3.4. For Chiang Rai City, the general soil profile is shown in Figure 3.5. Examples of boring information in Chiang Mai and Chiang Rai are depicted in Figure 3.6 and 3.7, respectively. The sub soils in both provinces are subject to wide variation. Layers of loose to medium dense sand are found in most of the investigated boreholes. Those layers are distributed throughout the cities. Figure 3.8 summarizes the gradation of sands found in both provinces. Great variation of grain size distribution can be observed. The average diameter,  $D_{50}$ , of sands varies in the range of 0.2 to 1.5 mm.

### **3.4 INPUT MOTIONS FOR ANALYSIS**

Due to the lack of strong motion records in Thailand, it is necessary to use the records from elsewhere. Three strong motions with different predominant periods used as input motions to the analyses are shown in Figure 3.9. These acceleration time histories are actual strong motion records recorded at rock sites; and selected from California earthquakes including the 1940 El Centro, 1989 Loma Prieta, and 1994 Northridge earthquakes. The recording station and estimated predominant period of the input motions are summarized in Table 3.2. The response spectra for 5 percent damping of the input motions are shown in Figure 3.10.

### 3.5 ESTIMATION OF SHEAR WAVE VELOCITY

Due to the lack of data of the shear wave velocity measured in the field, the empirical correlations based on available field and laboratory measurements were used in this study. There are many researchers proposed the empirical correlations of the shear wave velocity (or maximum shear modulus) based on SPT N-value and the undrained shear strength ( $S_u$ ) from laboratory tests such as: Kanai (1966); Sakai (1968); Seed and Idriss (1970); Ohsaki and Iwasaki (1973); Ohta and Goto (1978); Imai and Tonouchi (1982); Seed et al. (1983); Sykora and Stokoe (1983); and Dickenson (1994). Even any empirical correlations inherently are site dependent. They, however, give very useful and reasonable guidelines for field engineers to evaluate the shear wave velocity of the in situ soil.

#### 3.5.1 FORMULA FOR CLAY

The formula proposed by Dickenson (1994) was used to compute shear wave velocity of soft clay deposit in Chiang Mai and Chiang Rai. Dickenson (1994) presented the results of a study of the dynamic response of soft and deep cohesive soils during the 1989 Loma Prieta earthquake and developed a nonlinear relationship between shear wave velocity determined from field testing and undrained shear strength for cohesive soil. The proposed relationship is:

$$V_s = 68.7 \cdot S_u^{0.475} \quad (\text{m/sec}) \quad (3.1)$$

where  $S_u$ , the undrained shear strength, has unit of  $t/m^2$ . It should be noted that  $S_u$  determined from unconfined compression, unconsolidated undrained triaxial (TX), and consolidated undrained triaxial tests were used directly in Dickenson's equation.

For the estimation of the shear wave velocity for medium to stiff clay layer, the relationship, developed by Imai and Tonouchi (1982), for any soil type based on uncorrected N-value was used. The relationship is:

$$V_s = 96.926 \cdot N^{0.314} \quad (\text{m/sec}) \quad (3.2)$$

### 3.5.2 FORMULA FOR SAND

There are two relationships used to estimate shear wave velocity for sand layer in the study area. For silty sand layer, the relationship proposed by Seed et al. (1983) was used. Seed et al. (1983) suggested using the following equation for sand and silty sand to assess shear wave velocity by using SPT N-value:

$$V_s = 56.388 \cdot N^{0.5} \quad (\text{m/sec}) \quad (3.3)$$

For sandy soils, the correlation between shear wave velocity and SPT N-value developed by Sykora and Stokoe (1983) was used, and the relationship is:

$$V_s = 100.584 \cdot N^{0.29} \quad (\text{m/sec}) \quad (3.4)$$

The SPT N-value used in Equation (3.3) and (3.4) is the corrected N-value,  $(N_1)_{60}$ , which is normalized to an overburden pressure of approximately 100 kPa (1 t/ft<sup>2</sup>) and a hammer energy ratio or hammer efficiency of 60%.

### 3.6 SUMMARY

In this chapter, location, topography, seismicity, and soil profile of Chiang Mai and Chiang Rai, were briefly presented. Subsequently, the strong motions with different predominant periods recorded at rock sites were described. Shear wave



velocity or shear modulus of subsoil in both provinces can be estimated using the empirical correlations based on available field and laboratory measurements (SPT N-value and undrained shear strength). The strong motions and the shear wave velocity described in this chapter are used as input to the analyses of soil amplification and generation of pore water pressure which is described in Chapter 4 and 6, respectively.



สถาบันวิทยบริการ  
จุฬาลงกรณ์มหาวิทยาลัย

## **CHAPTER 4**

### **AMPLIFICATION OF EARTHQUAKE GROUND MOTIONS**

#### **4.1 INTRODUCTION**

Since the provinces in the northern and western parts of Thailand have been classified as a moderate seismic risk regions by the ministerial regulations on seismic resistant design, and there are several moderate earthquakes (5.2-5.5 on the Richter scale) have occurred in the northern part of the country during the past decades. In consequence, the Thai people are becoming increasingly concerned about seismic risk. Therefore, in order to describe some effects of earthquake ground motions in the mentioned areas, particularly Chiang Mai and Chiang Rai; one-dimensional ground response analysis using the equivalent linear approach is conducted.

#### **4.2 COMPUTER PROGRAM SHAKE**

The computer program SHAKE was written in 1970-71 by Dr. Per Schnabel and Prof. John Lysmer and was published in December 1972 by Dr. Per Schnabel and Prof. John Lysmer and H. Bolton Seed in report no. UCB/EERC 72/12, issued by the Earthquake Engineering Research Center at the University of California in Berkeley.

The soil profile is idealized as a system of homogeneous, visco-elastic sublayers of infinite horizontal extent; the idealized soil profile is shown in Figure 4.1. The response of this system is calculated considering vertically propagating shear waves. The algorithm on the program SHAKE (Schnabel et al., 1972) is based on the continuous solution to the wave equation (Kanai, 1951; Matthiesen et al., 1964; Roesset and Whitman, 1969; Lysmer et al., 1971), which was adapted for transient motions using the Fast Fourier Transform techniques of Cooley and Tukey (1965).

As described in the Section 2.5 of Chapter 2, an equivalent linear procedure (Idriss and Seed, 1968; Seed and Idriss, 1970) is used to account for the nonlinearity of the soil using an iterative procedure to obtain values for modulus and damping that are compatible with the equivalent uniform strain induced in each sublayer. Thus, at the outset, a set of properties (shear modulus, damping, and total unit weight) is assigned to each sublayer of the soil deposit. The analysis is conducted using these properties and the shear strains induced in each sublayer is calculated. The shear modulus and the damping ratio for each sublayer are then modified based on the applicable relationship relating these two properties to shear strain. The analysis is repeated until strain-compatible modulus and damping values are arrived at. Starting with the maximum shear modulus for each sublayer and a low value of damping, essentially strain-compatible properties are obtained in 3 to 5 iterations for most soil profiles.

The following assumptions are incorporated in the analysis (Schnabel et al., 1972):

- Each sublayer,  $j$ , is completely defined by its shear modulus,  $G_j$ ; damping ratio,  $\xi_j$ ; total unit weight,  $\gamma_{ij}$ ; and thickness,  $h_j$ , these properties are independent of frequency. It is noted that the initially estimated values of  $G$  and  $\xi$  usually correspond to the same strain level; the low-strain values (0.001%) are often used for the initial estimate. In this study, the initial values of  $G$  were determined from the shear wave velocity ( $V_s$ ) and the mass density ( $\rho$ ) from the relationship  $G = \rho \times V_s^2$ . The shear wave velocity can be calculated from the empirical correlations based on available field and laboratory measurements as previously described in Section 3.5 of Chapter 3.
- The responses in the soil profile are caused by the upward propagation of shear waves from the underlying rock half-space.
- The strain dependence of the shear modulus and damping in each sublayer is accounted for by an equivalent linear procedure based on an equivalent uniform strain computed in that sublayer. According to Idriss and Sun (1992), the ratio of

this equivalent uniform shear strain divided by the calculated maximum strain which is typically used from 0.4 to 0.75 based on magnitude earthquake ( $M$ ) is evaluated by:

$$\text{Ratio} = \frac{M - 1}{10} \quad (4.1)$$

The same value of this ratio is used for all sublayers.

### 4.3 MODULUS REDUCTION AND DAMPING RATIO

It has long been known that soil exhibits nonlinear behavior. This is particularly true when subjected to dynamic loading. Pioneering studies by Hardin and Drnevich (1972b) and Seed and Idriss (1970) using laboratory tests on soil such as the resonant column, cyclic simple shear, and cyclic triaxial, as well as shaking table tests and back calculated results, indicate that shear strain is the single most important parameter when looking at the variation of shear modulus and fraction of critical damping for the seismic response of different soil types. Seed and Idriss (1970) proposed that the variation of shear modulus with shear strain could be normalized by plotting the ratio of  $G/G_{\max}$  (i.e., the ratio of shear modulus at a given strain,  $G$ , over the low strain shear modulus,  $G_{\max}$ ) versus shear strain, for different soil types (e.g., sand, clay, and gravel). The advantage to these normalized relationships for seismic site response analyses is that in many cases, only the  $G_{\max}$  would need to be determined in the field from  $V_s$  testing; the variation of  $G$  with shear strain could be estimated based on soil type from the normalized relationships.

However, since laboratory testing to determine the variation of  $G$  with shear strain,  $\gamma$ , for soils in Chiang Mai and Chiang Rai was beyond the scope of this study, it was decided to use the latest normalized relationships available. For clays, Vucetic and Dobry (1991) combined the results of many previous studies to develop normalized relationships of  $G$  and  $\gamma$  as a function of plasticity index. Their

relationships for both variation of  $G$  and damping ratio ( $\lambda$ ) as a function of  $\gamma$  are shown in Figure 4.2. For sands, the relationships proposed by Seed et al. (1984a) were used. Their relationships for  $G/G_{\max}$  and damping as a function of  $\gamma$  are presented in Figure 4.3. Both the relationships by Vucetic and Dobry (1991) and by Seed et al. (1984) are in wide use for estimating shear modulus and damping variation with shear strain of soil for purpose of site response analysis.

#### 4.4 RESULTS OF ANALYSES

One-dimensional dynamic ground response analyses were performed on eighteen sites within Chiang Mai City and fourteen sites within Chiang Rai City using the computer program SHAKE (Schnabel et al., 1972) for equivalent linear response. The examples of soil profiles of Chiang Mai and Chiang Rai are presented in Figure 3.6 and 3.7. Soil properties are defined by borings made for foundation design at the site and geologic references for the area. Soil type is indicated by Unified Soil Classification System group symbols.

Since one of unknown in the analyses is the depth to bedrock and no data was available to make a reasonable estimate of its shear wave velocity. However, for the purposes of seismic ground response analyses, the depth to bedrock itself is not as important as the depth to rock-like material that behaved essentially as bedrock (Lysmer et al., 1970), that is, material having a shear wave velocity on the order of 800 to 1200 m/sec. Lysmer et al. (1970) also found that the response at the ground surface was relatively independent of the shear wave velocity of the assumed rock-like material. Some effect was observed, however, on the assumed depth to rock-like material, and whether or not an intermediate rock-like layer was modeled between the bottom of the soil profile and the surface of the bedrock. This effect was mainly on the frequency content of the motion at the ground surface; the peak ground acceleration was relatively unaffected. Thus the depth to rock-like material in the

analyses was assumed at the bottom of the soil profile which has the SPT N-value of more than 50 blows/ft with a shear wave velocity of 900 m/sec.

The seismic ground response analyses were conducted using the three seismograms described in Chapter 3 with bedrock accelerations scaled to 0.02, 0.05, 0.07, 0.10, and 0.30g. The results for the amplification of Chiang Mai and Chiang Rai are presented in Figure 4.4 and 4.5, respectively. It can be seen from the results that the amplification, which is defined as the ratio between the acceleration at ground surface and the acceleration at rock surface, decreases with increasing bedrock acceleration. It should be noted that for long duration and high strain ground motions, the amplification level would decrease because of the nonlinear behavior of soil. In addition, it is also apparent from Figure 4.4 and 4.5 that the amount of amplification is dependent on the predominant period of the input motion.

The variation of peak ground acceleration with the applied peak rock acceleration is shown in Figure 4.6 and 4.7 for Chiang Mai and Chiang Rai, respectively. They show that the peak ground acceleration increases with increasing amplitude of the base motion. Furthermore, the peak ground accelerations presented in Figure 4.6 and 4.7 are also plotted against peak rock acceleration along with observed values from the 1985 Mexico earthquake and the 1989 Loma Prieta earthquake; the results show that the range of calculated accelerations tends to be lower than observed in previous earthquakes, particularly for the Mexico earthquake which most of subsoil consist of soft soil deposits.

#### **4.5 SUMMARY**

In this chapter, the results of a study on the amplification of earthquake ground motion in the city of Chiang Mai and Chiang Rai, were illustrated. Three input motions with different predominant periods were used. Soil properties used as input to the analysis, specifically shear wave velocity, were estimated using existing correlations with field and laboratory data. Seismic ground response analyses were,

then, conducted using the computer program SHAKE based on the equivalent linear method. Concerning amplification of the peak ground acceleration, it is apparent from the results in the study that the soils underlying the city of Chiang Mai and Chiang Rai have ability to amplify earthquake ground motions on the order of 1.5 to 3 times. The amount of this amplification depends on the actual soil properties and profiles or local site conditions, the level of acceleration in the underlying rock-like material, and the predominant periods of the input rock motion. In addition, it is also found that the amount of this amplification decreases with increasing bedrock acceleration because of nonlinearity of soils.



สถาบันวิทยบริการ  
จุฬาลงกรณ์มหาวิทยาลัย

## CHAPTER 5

# EVALUATION OF LIQUEFACTION RESISTANCE BY PROBABILISTIC APPROACH

### 5.1 INTRODUCTION

Liquefaction occurs primarily in loose saturated sands. As seismic waves propagate through the soil, the structure of the soil is altered with a corresponding increase in the pore water pressure. As the pore water pressure increases, the effective stress decreases. If the effective stress is reduced to a point in which it is equal to zero, the soil loses its strength and liquefaction develops. Liquefaction is a function of soil type, relative density, age, fines content, and intensity and duration of the earthquake motion (Seed and Idriss 1971).

Several methods have been proposed to evaluate earthquake liquefaction potential. These methods range from purely empirical to highly analytical and require various degrees of laboratory and/or in situ testing. A common approach of the deterministic type is to use charts such as that shown in Figure 5.1. The horizontal axis measures the strength of the soil in terms of the corrected standard penetration resistance ( $N_1$ ), and the vertical axis measures the intensity of ground motion through the cyclic stress ratio ( $CSR$ ). Points are drawn to represent cases of liquefaction (solid dots) and non-liquefaction (open circles), and a line is subjectively drawn to separate events of the two types. The line is then used as a deterministic classification criterion.

It is evident that there is no sharp demarcation between the two sets of observations in Figure 5.1, and that the probability of liquefaction actually varies in a continuous fashion as a function of soil strength and the intensity of ground motion. This conditional probability can be evaluated by using appropriate statistical procedures to analyze field data of the type in Figure 5.1.



The objective of this chapter is to use methods of statistical regression to quantify the probability of liquefaction by using the data catalog compiled by Liao and Whitman (1986a). In the context of the data catalog, the term “liquefaction” is defined as the surface manifestation of any phenomenon associated with a significant loss of shearing resistance in saturated cohesionless soils due to earthquake loading. No attempt is made to distinguish between liquefaction shear failure and cyclic mobility (Castro, 1969, 1975). Also, even though liquefaction or cyclic mobility may occur at depth without exhibiting effects at the ground surface (Ishihara, 1985), such instances are classified here as cases of nonliquefaction. Note also that the results of this study are primarily applicable to sites with level ground conditions and are generally not valid for the evaluation of liquefaction of embankments or for sloping grounds.

## 5.2 LIQUEFACTION DATA CATALOG

The data catalog used in the statistical analysis comprise 278 case studies, with 114 cases representing sites that liquefied during earthquakes and 164 cases representing sites that did not liquefy. The catalog was compiled by Liao and Whitman (1986a) through the synthesis of eight previously published “source catalogs”. The source catalogs are those of Whitman (1971), Seed et al. (1975), Yegian (1976), Yegian and Vitelli (1981), Xie (1979), Davis and Berrill (1981), Tokimatsu and Yoshimi (1983), and Seed et al. (1984b).

The catalog is based on 40 earthquakes, of which the earliest is the historical 1802 Niigata earthquake and the most recent is the 1981 Westmorland, California earthquake. Of the 278 cases, 120 are from Japan, 100 from California, 20 from China, and 38 from other locations in the world. The example of the data catalog is shown in Figure 5.2.

The variables, notations, and abbreviations of the various column headings in the data catalog (Figure 5.2) are described as follows:

- Entries of (-1) under any of the table headings indicate missing data.
- CASE (Case Code): Consists of two parts. The first two digits identify the earthquake. The last two digits identify the case associated with that earthquake.
- ECAT (Source Catalog Code): Indicates data source catalog.
  - 0 = data not reported in previous catalogs
  - 1 = Whitman (1971)
  - 2 = Seed, Idriss, and Arango (1975)
  - 3 = Yegian (1976)
  - 4 = Yegian and Vitelli (1981)
  - 5 = Xie (1979)
  - 6 = Davis and Berrill (1981)
  - 7 = Tokimatsu and Yoshimi (1983)
  - 8 = Seed, Tokimatsu, Harder, and Chung (1984)
  - 9 = Liao (1986)
- LIQ1 (Liquefaction Code 1)
  - 0. = no liquefaction.
  - 1. = liquefaction.
- LIQ2 (Liquefaction Code 2): Based on Tokimatsu and Yoshimi (1983).
  - .0 = no liquefaction.
  - .5 = marginal site, defined as a site located just outside the boundary of liquefaction zone.
  - .7 = moderate liquefaction, indicated by appearance of sand boils, but with minor ground or foundation movements.
  - 1.0 = extensive liquefaction, indicated by sand boils and/or major ground or foundation movements.
- M (Richter Magnitude)
- H (Focal Depth): Units of kilometers.
- EP (Epicentral Distance to Site): Units of kilometers.

- DER (Distance to Energy Release): Unit in kilometers. Closest distance to fault rupture or to the zone of major energy release. A distance measure that is largely judgmental in many cases. If a measure of DER is not available, DER is set to EP.
- DUR (Duration of Shaking): Units in seconds.
- A (Peak Ground Acceleration at Site): Units of fraction of gravitational acceleration, g.
- CSR (Cyclic Stress Ratio): This quantity is calculated using the Seed and Idriss (1971) procedure, as described in Section 2.8.1.2 of Chapter 2.
- CSRN (Cyclic Stress Ratio for Magnitude 7.5 Earthquakes)
- ZW (Depth to Water Table): Units of meters.
- ZL (Critical Depth of Liquefaction): Units of meters.
- SIGT (Total Vertical Stress): Units of  $\text{kg}/\text{cm}^2$ .
- SIGE (Effective Vertical Stress): Units of  $\text{kg}/\text{cm}^2$ .
- N (SPT N-Value)
- N1 (SPT N-Value Corrected for Overburden Pressure): All of the values of N1 are calculated based on the Liao and Whitman (1986) correction factor.
- CE (Correction Factor for Sampling Equipment and Practices): See Equation (2.38) in Section 2.8.1.3 of Chapter 2 for details.
- N160 (Corrected SPT N-Value Normalized to the Overburden Pressure; and Sampling Equipment and Practices): See Equation (2.38) in Section 2.8.1.3 of Chapter 2 for details.
- FC (Fines Content): Units of percent. Fines defined as material passing No. 200 sieve.

For calculated CSR values in the catalog, it is noted that the primary variable affecting the value of CSR is the peak ground acceleration ( $a_{\max}$ ), which can be obtained in several ways. In 127 out of 278 catalog entries, the peak acceleration is obtained from measurement at a nearby station that can mean a strong motion recorder located several kilometers away. In a few cases, a strong motion recorder is

actually close enough to be considered on site, which is indicated that the acceleration measurement is considered to be very accurate in representing the ground motion at the site. Other methods of estimating acceleration include performing a site response analysis with the input from a ground motion record some distance away, scaled to reflect inferred bedrock motion at the site of interest. In many cases, accelerations are calculated from earthquake attenuation relationships and/or correlations to an intensity damage scale (e.g., Modified Mercalli scale).

However, in many of the historical cases of liquefaction/non-liquefaction from California and Japan where the acceleration was not reported, or where the reported acceleration was suspected, accelerations were estimated from one of two attenuation relationships. For cases in California, the Joyner and Boore (1981) equation was used:

$$\log_{10}(a/g) = -1.02 - 0.249M - \log r - 0.00255r \quad (5.1a)$$

or

$$\frac{a}{g} = \frac{0.0955 \cdot 10^{0.249M}}{r \cdot 10^{0.00225r}} \quad (5.1b)$$

where  $M$  is the moment magnitude, and  $r = (d^2 + 7.3^2)^{1/2}$ , in which  $d$  is defined as the closest distance (in kilometers) to surface projection of the fault rupture. For Japanese earthquakes, the relationship used is that due to Kawashima et al. (1984) for soft alluvium or reclaimed ground:

$$\frac{a}{g} = \frac{0.4109 \cdot 10^{0.262M}}{(R_{EP} + 30)^{1.208}} \quad (5.2)$$

where  $M$  is the Japanese Meteorological Association (JMA) magnitude and  $R_{EP}$  is the epicentral distance in kilometers.

### 5.3 REGRESSION METHOD FOR LIQUEFACTION DATA ANALYSIS

Each case study in the database can be represented through a binary variable  $Y$  which indicates whether liquefaction occurred ( $Y = 1$ ) or did not occur ( $Y = 0$ ) and a vector of explanatory variables  $X = [X_1, X_2, \dots, X_m]^T$ , which includes ground motion and soil deposit characteristics. The problem is to use the available  $n$  observations  $(X_1, Y_1), \dots, (X_n, Y_n)$  to express the probability of liquefaction  $P_L$  as a function of  $X$ . Therefore, the regression technique called “the binary logistic regression” will be used for analyzing the database and can be written in the form:

$$\ln\left(\frac{P_L}{1 - P_L}\right) = \beta_0 + \beta_1 X_1 + \dots + \beta_m X_m \quad (5.3)$$

where  $P_L$  is defined as the probability that liquefaction will occur,  $1 - P_L$  is the probability that liquefaction will not occur,  $X_k$ 's ( $k = 1, 2, \dots, m$ ) are various “explanatory variables” such as cyclic stress ratio and corrected SPT resistance, and  $\beta_k$ 's ( $k = 1, 2, \dots, m$ ) are regression coefficients to be obtained by fitting Equation (5.1) to data. Solving Equation (5.3) for  $P_L$  gives the following expression for the probability of liquefaction in terms of the variables  $X_1, \dots, X_m$ :

$$P_L = \frac{\exp(\beta_0 + \beta_1 X_1 + \dots + \beta_m X_m)}{1 + \exp(\beta_0 + \beta_1 X_1 + \dots + \beta_m X_m)} \quad (5.4a)$$

or equivalently:

$$P_L = \frac{1}{1 + \exp[-(\beta_0 + \beta_1 X_1 + \dots + \beta_m X_m)]} \quad (5.4b)$$

Flexibility of the model is greatly enhanced if one allows  $X_1, \dots, X_m$  in Equation (5.3) and (5.4) to be functions of the original explanatory variables rather than the variables themselves. For example,  $X_1$  might be the logarithm of the cyclic stress ratio ( $CSR$ ) instead of  $CSR$  itself. This option will be used in the analysis of liquefaction data.

Since procedures and details of the regression method to determine the regression coefficients ( $\beta_k$ 's) are beyond the scope of this study. However, they can be seen from other standard statistical textbooks such as: Dillon and Goldstein (1984); Johnson and Wichern (1988); Morrison (1990); Kleinbaum (1994); and Johnson (1998). The regression coefficients ( $\beta_k$ 's) in the study are obtained by using a well-known statistical computer program SPSS (SPSS, 1999).

## 5.4 LOGISTIC MODELS OF LIQUEFACTION BEHAVIOR

Models of the type in Equation (5.4b) may be used to quantify the probability of liquefaction once the variables  $X_1, \dots, X_m$  have been selected. The term “variable selection” refers here to the choice of both the physical factors that influence liquefaction and the functions of such factors that should enter the regression model as variables  $X_1, \dots, X_m$ . For example, it may be important to decide not only whether a variable such as the cyclic stress ratio ( $CSR$ ) should be among the explanatory variables, but also whether it should appear in Equation (5.4b) as  $X_1 = CSR$ ,  $X_1 = \ln(CSR)$ , or in some other form. However, the models are limited to the use of variables recorded in the data catalog. Thus, potentially important parameters that are not reported or are difficult to quantify cannot at present be considered in variable

selection. Performing a logistic regression analysis of the database yields the following probability equations:

For earthquake magnitude of 7.5:

$$\ln\left(\frac{P_L}{1-P_L}\right) = 9.119 - 0.243(N_1)_{60} + 3.458 \ln(CSR_{7.5}) \quad (5.5)$$

For earthquake magnitude of 5.5:

$$\ln\left(\frac{P_L}{1-P_L}\right) = 6.354 - 0.242(N_1)_{60} + 3.450 \ln(CSR_{5.5}) \quad (5.6)$$

where  $(N_1)_{60}$  = the corrected SPT resistance which is normalized to an overburden pressure of approximately 100 kPa (1 t/ft<sup>2</sup>), a hammer energy ratio or a hammer efficiency of 60%, the borehole diameter, and the rod lengths;  $CSR_{7.5}$  = the cyclic stress ratio generated at the site normalized to a magnitude of 7.5; and  $CSR_{5.5}$  = the cyclic stress ratio generated at the site normalized to a magnitude of 5.5. The magnitude scaling factors published by Seed and Idriss (1982), which have been conventionally used in liquefaction hazard analyses, were used in this study.

Figure 5.3 and 5.4 show a set of probability curves defined by Equation (5.5) and (5.6), respectively. Also shown in Figure 5.3 and 5.4 is the deterministic criteria defined by Seed et al. (1985). The correlation of regression (equivalent to  $R^2$ ) for Equation (5.5) and (5.6) is 0.637. The success rate in classification of liquefaction from both equations is greater than 80% for both liquefied and non-liquefied cases. Note that the probabilistic line at  $P_L = 30\%$  well traces the deterministic criteria proposed by Seed et al. (1985) as shown in the figures. This result generally agrees with the findings of Youd and Noble (1997), and Toprak et al. (1999). The success rate is therefore determined based on  $P_L = 30\%$  line.

## 5.5 SUMMARY

A statistical regression procedure has been used to derive models for calculating the probability of liquefaction as a function of earthquake load and soil resistance parameters. The data to which the models are fitted consist of 278 cases of liquefaction and non-liquefaction, obtained from worldwide liquefaction database.

Based on goodness-of-fit statistics and on considerations of usefulness in application, two models [Equation (5.5) and (5.6)] are recommended for the calculation of liquefaction probability. The models are based on the Seed and Idriss (1971) parameterization and employ the magnitude cyclic stress ratio  $CSR$  as a measure of earthquake load; and use the corrected/normalized SPT value  $(N_1)_{60}$  as a measure of soil-liquefaction resistance.

As mentioned earlier, Chiang Mai and Chiang Rai are located in the seismic zone G (see Figure 3.2) which probable causes earthquake magnitude ( $M_L$ ) of 5 to 6. Thus, Equation (5.6), which was developed for earthquake magnitude of 5.5, shall be used to study the generation of pore water pressure of sand layer in the areas. This subject is described in Chapter 6.



## CHAPTER 6

### FINITE ELEMENT ANALYSIS OF PORE WATER PRESSURE IN SAND DEPOSITES DURING EARTHQUAKES

#### 6.1 INTRODUCTION

The response of a saturated sand deposit to earthquake motions is very important and difficult problem of soil dynamics; and a completely satisfactory generalized solution is not yet available. The dynamic response, at least for loose to medium dense sands, is dominated by the effects of the progressive pore water pressure increases that develop during an earthquake. The resistance to deformation at any point in the sand deposit is a function of effective stress which in turn depends on the simultaneous rates of generation and dissipation of pore water pressure.

The purpose of this chapter is to illustrate the application of a numerical finite element scheme for development of guidelines and charts for analysis and evaluation of the generation of pore water pressure due to medium earthquakes ( $M = 5.5$ ) corresponding to various probability values. The analytical procedure employed to quantify the pore water pressure is outlined in Figure 6.1. For each site, the minimum SPT N-value of sand at certain depth (from the ground surface to about 15 m) was selected in order to determine the value of cyclic stress ratio ( $CSR$ ) from the probability curve (Figure 5.4). The maximum ground surface acceleration ( $a_{max}$ ) for the specific probability values ( $P_L$ ) of that site was then computed from the simplified equation [Equation (2.37)] proposed by Seed et al. (1983) as mentioned in Section 2.8.1.2 of Chapter 2. The pore water pressure was evaluated by performing trial and error of the scaled base acceleration. This was continued until the computed maximum ground acceleration was similar to the prescribed value given by the simplified equation. Note that the probability values ( $P_L$ ) used in this study are 0.05,

0.10, 0.30, and 0.50. The computer program used for evaluating the pore water pressure is called “FLIP”.

The parameters used in the analysis are obtained by back-fitting the calculated results with experimental data from undrained cyclic triaxial tests. The finite element method presented here is based on the effective stress analysis of a horizontally layered saturated sand deposit shaken by horizontal shear waves propagating vertically. The computer program and the model parameters of soils used in the analyses have been described in the following sections.

## **6.2 CONSTITUTIVE MODEL OF SOILS**

### **6.2.1 BASIC CONSTITUTIVE EQUATIONS**

As mentioned earlier, liquefaction of cohesionless soils has contributed to the failure of soil structure systems during earthquakes. The mechanisms of liquefaction have been studied extensively, and many soil liquefaction models have been proposed.

Available soil liquefaction models are based on either: (1) experimentally observed undrained stress paths during pore water pressure build up (Ishihara et al., 1975; Ishihara et al., 1976); (2) a correlation between pore water pressure response and volume change tendency of dry soils (Martin et al., 1975; Finn et al., 1977); (3) the formulation of pore water pressure response directly from observed data (Shibata et al., 1972; Seed et al. 1976a; Ishibashi et al., 1977; Sherif et al. 1978); (4) a plasticity theory in which the plastic volume change is related to pore water pressure build up (Mroz et al., 1978; Zienkiewicz et al., 1978); or (5) treatment of the soil as a two-phase medium (Liou et al., 1977; Blazquez et al., 1980). The soil model used in this study is an effective stress model proposed by Iai et al. (1992); and can be briefly described as follows:

The model is constructed within the framework of plasticity theory but it is quite different from the conventional type of plasticity models. First of all, the model is defined in strain space. Secondly, the concept of multiple shear mechanism is introduced for taking the effect of principal stress axes rotation into account. Thirdly, the dilatancy is treated as an additional volumetric strain component in such a manner as strains due to creep and temperature are treated in the constitutive equation. The behavior of soil under the plane strain condition is basically represented as a relation between effective stress and strain defined in terms of such vectors as

$$\{\sigma'\}^T = \{\sigma'_x \quad \sigma'_y \quad \tau_{xy}\} \quad (6.1)$$

$$\{\varepsilon\}^T = \{\varepsilon_x \quad \varepsilon_y \quad \varepsilon_{xy}\} \quad (6.2)$$

in which compressive stress and contractive strain will be assumed negative and the strain components will be given from displacements  $u$  and  $v$  in  $x$  and  $y$  directions by

$$\varepsilon_x = \frac{\partial u}{\partial x}, \quad \varepsilon_y = \frac{\partial v}{\partial y}, \quad \gamma_{xy} = \frac{\partial u}{\partial y} + \frac{\partial v}{\partial x} \quad (6.3)$$

then the basic form of the constitutive relation is given by

$$\{d\sigma'\} = [D]\{(d\varepsilon) - \{d\varepsilon_p\}\} \quad (6.4)$$

in which

$$[D] = K \{n^{(0)}\} \{n^{(0)}\}^T + \sum_{i=1}^I R_{L/U}^{(i)} \{n^{(i)}\} \{n^{(i)}\}^T \quad (6.5)$$

In this relation, the term  $\{d\varepsilon_p\}$  in Equation (6.4) represents the additional strain increment vector to take the dilatancy into account and is given from the volumetric strain increment due to the dilatancy  $\varepsilon_p$  as

$$\{d\varepsilon_p\}^T = \{d\varepsilon_p / 2 \quad d\varepsilon_p / 2 \quad 0\} \quad (6.6)$$

and the first term in Equation (6.5) represents the volumetric mechanism with rebound modulus  $K$  and the direction vector is given by

$$\{n^{(0)}\}^T = \{1 \quad 1 \quad 0\} \quad (6.7)$$

The second term in Equation (6.5) represents the multiple shear mechanism. Each mechanism  $i = 1, \dots, I$  represents a virtual simple shear mechanism, with each simple shear plane oriented at an angle  $\theta_i / 2 + \pi / 4$  relative to the  $x$  axis. A schematic figure is shown in Figure 6.2. The tangential shear modulus  $R_{L/U}^{(i)}$  represents the hyperbolic stress strain relationship with hysteresis characteristics. The direction vectors for the multiple shear mechanism in Equation (6.5) are given by

$$\{n^{(i)}\}^T = \{\cos \theta_i \quad -\cos \theta_i \quad \sin \theta_i\} \quad (\text{for } i = 1, \dots, I) \quad (6.8)$$

in which

$$\theta_i = (i - 1)\Delta\theta \quad (\text{for } i = 1, \dots, I) \quad (6.9)$$

$$\Delta\theta = \pi / I \quad (6.10)$$

The loading and unloading for shear mechanism are separately defined for each virtual simple shear mechanism by the sign of  $\{n^{(i)}\}^T \{d\varepsilon\}$ .

## 6.2.2 PHYSICAL BACKGROUND OF THE MODEL

Physical meaning of the strain space multiple mechanism model can be found in the mechanics of assembly of sand particles (Iai et al., 1992). In the mechanics of assembly of sand particles, stress in sand as defined for continuum is given as a certain average of contact forces between the sand particles, which are assumed to be spheres. Before taking the average over all the contact forces in a representative volume element, the contact forces can be classified according to the directions. To define the directions, let us consider a plane of an arbitrary direction and find a class of pairs of contact forces and contact normals, both of which are parallel to the plane. (If the contact force is parallel to the contact normal, let us equally divide the contact force among all the relevant plane.) The average over this class of contact forces associated with the plane constitutes a partial stress contribution from “the virtual plane strain mechanism”.

The contact forces within each plane can be further classified according to the directions within the plane. To define this level of directions, let us think of a class of contact normals of which direction is at an angle  $\theta_i / 2$  relative to the reference axis appropriately defined within the plane. The contact forces can be further partitioned into its normal and tangential components as shown in Figure 6.3. Let us individually take an average of each component over the class of contacts to form a basic level of partial stress contribution.

To identify the nature of the basic level of partial stress contribution, let us consider a pair of those stress contributions associated with the contact normals being at right angle. Then it becomes evident that the pair of the normal components represents volumetric and compression shear stress contributions and the other pair of the tangential components represents a simple shear stress contribution. With the

rotation of the reference axis with an angle  $\pi / 4$ , the compression shear stress contribution associated with the contact normals at an angle  $\theta_i / 2$  becomes equivalent to the simple shear stress contribution associated with the contact normals at an angle  $\theta_i / 2 + \pi / 4$ . By summing up the simple shear stress contributions from the normal components at an angle  $\theta_i / 2$  and the tangential components at an angle  $\theta_i / 2 + \pi / 4$ , the basic level of shear stress contribution is defined for the  $i$ -th mechanism of “the virtual simple shear mechanism.”

To summarize, the stress is composed of the stress contributions from the virtual plane strain mechanisms, which are in turn composed of the basic stress contributions from the virtual volumetric and simple shear mechanisms. All of these contributions are due to the sand particle displacements, which are closely related to the average strain as defined for continuum.

The above-mentioned physical background of the soil model can be confirmed through a series of manipulations with the tensors representing the relevant quantities (Iai, 1993).

In what follows, some of the details of the model will be presented in order to explain the meaning of the model parameters.

### 6.2.3 SHEAR MECHANISM

As mentioned earlier, each virtual simple shear mechanism is assumed to follow a hyperbolic stress-strain relation with hysteresis given by a rule similar to Masing’s rule. Thus, the virtual tangent shear moduli are given for the initial loading by

$$R_L^{(i)} = \left[ 1 / \left( 1 + \left| \gamma^{(i)} / \gamma_v \right| \right)^2 \right] (Q_v / \gamma_v) \Delta \theta \quad (6.11)$$

in which  $Q_v$  = virtual shear strength and  $\gamma_v$  = virtual reference strain. The parameters  $Q_v$  and  $\gamma_v$  are not directly measurable but they can be readily determined from shear strength  $\tau_m$  and shear modulus of sand at small strain level  $G_m$  by

$$Q_v = \tau_m / \left( \sum_{i=1}^I \sin \theta_i \Delta \theta \right) \quad (6.12)$$

$$\gamma_v = (\tau_m / G_m) \left[ \left( \sum_{i=1}^I \sin^2 \theta_i \Delta \theta \right) / \left( \sum_{i=1}^I \sin \theta_i \Delta \theta \right) \right] \quad (6.13)$$

The derivation of Equation (6.12) and (6.13) are similar to that shown by Towhata and Ishihara (1985).

For incorporating the hysteresis, the Masing's rule is modified here in order to incorporate the ability to achieve realistic hysteresis loop instead of those given by Masing's rule. The approach for modifying the hysteresis loop is similar to that proposed by Ishihara et al. (1985).

From the above formulation, it becomes evident that the parameters necessary for specifying the hyperbolic relation are friction angle  $\phi_f'$  and elastic shear modulus  $G_{ma}$  measured at the reference confining pressure of  $\sigma_{ma}'$ . These parameters determine the constant of the hyperbolic relation under the initial effective confining pressure of  $\sigma_{mo}'$  as follows:

$$\tau_{mo} = (-\sigma_{mo}') \sin \phi_f' \quad (6.14)$$

$$G_{mo} = G_{ma} \left( \sigma_{mo}' / \sigma_{ma}' \right)^{0.5} \quad (6.15)$$

$$\gamma_{mo} = \tau_{mo} / G_{mo} \quad (6.16)$$

in which  $\tau_{mo}$  = shear strength,  $G_{mo}$  = elastic shear modulus, and  $\gamma_{mo}$  = reference shear strain.

#### 6.2.4 VOLUMETRIC MECHANISM

In order to define the volumetric mechanism, the rebound modulus  $K$  and the volumetric strain due to the dilatancy  $\varepsilon_p$  in Equation (6.4) through (6.6) should be specified. The rebound modulus  $K$  at the initial confining stress ( $-\sigma'_{mo}$ ) is given by

$$K_0 = K_a \left( \sigma'_{mo} / \sigma'_{ma} \right)^{0.5} \quad (6.17)$$

Excess pore water pressure, which is directly related to the volumetric strain due to the volumetric strain due to the dilatancy  $\varepsilon_p$  is generated by the following rule. First of all, a state variable  $S$  is defined as a variable which is equivalent to  $\sigma'_m / \sigma'_{mo}$  under the undrained condition with a constant total confining pressure. This state variable is determined from the shear stress ratio  $r = \tau / (-\sigma'_{mo})$  and the liquefaction front parameter  $S_0$ , to be defined as a measure of cyclic mobility, to simulate the stress path in  $p' - q$  space as follows (see Figure 6.4):

$$\begin{aligned} S &= S_0 && \text{(if } r < r_3 \text{)} \\ S &= S_2 + \sqrt{(S_0 - S_2)^2 + [(r - r_3) / m_1]^2} && \text{(if } r > r_3 \text{)} \end{aligned} \quad (6.18)$$

in which

$$\begin{aligned} \tau &= \sqrt{\tau_{xy}^2 + [(\sigma'_y - \sigma'_x) / 2]^2} \\ r_2 &= m_2 S_0 \end{aligned}$$



$$\begin{aligned}
r_3 &= m_3 S_0 \\
S_2 &= S_0 - (r_2 - r_3) / m_1 \\
m_1 &= \sin \phi_f \\
m_2 &= \sin \phi_p \quad (\phi_p \text{ is the phase transformation angle}) \\
m_3 &= 0.67 m_2
\end{aligned}$$

Secondly, the liquefaction front parameter  $S_0$  appearing in Equation (6.18) is defined as a function of the normalized plastic shear work  $w$  (i.e.,  $w = W_s / W_n$ , where  $W_s$  = plastic shear work, and  $W_n = \tau_{mo} \gamma_{mo} / 2$ ) as follows (see Figure 6.5):

$$\begin{aligned}
S_0 &= 1 - 0.6(w / w_1)^{p_1} && \text{(if } w < w_1 \text{)} \\
S_0 &= (0.4 - S_1)(w_1 / w)^{p_2} + S_1 && \text{(if } w > w_1 \text{)}
\end{aligned} \tag{6.19}$$

in which  $S_1$ ,  $w_1$ ,  $p_1$ , and  $p_2$  are the material parameters which characterize the cyclic mobility of sands. Additional parameter  $c_1$  is introduced for computing the plastic shear work; this parameter is introduced to explain the existence of the threshold limit in the shear stress or strain amplitude for generating excess pore water pressures. These parameters are determined by back-fitting to the test results obtained under the undrained cyclic loading condition.

When the effective stress analysis is conducted, the state variable  $S$ , given by Equation (6.18), is converted into the equivalent volumetric strain of plastic nature  $\varepsilon_p$  through the continuity condition, and then is substituted into Equation (6.4).

### 6.3 COMPUTER PROGRAM FLIP

The model presented in Section 6.2 is coded into the finite element computer program FLIP (**F**inite element analysis of **L**iquefaction **P**rogram) and is used in the

analysis of the generation of pore water pressure in this investigation. FLIP was developed by Iai et al. of Port and Harbour Research Institute, Japan. In the analysis, the equilibrium and mass balance equations for a porous saturated material are used with the undrained condition (Zienkiewicz and Bettess, 1982). For more details about FLIP, it can be seen from Iai et al. (1990, 1992).

#### **6.4 LIQUEFACTION TESTS ON SANDS USING A CYCLIC TRIAXIAL APPARATUS**

Laboratory testing of sands in the vicinity of the studied area were conducted by Gauchan (1984) at Asian Institute of technology, Thailand. The reconstituted samples were used and its physical properties are summarized in Table 6.1. Comparison of gradation between the samples and the sands in the studied area is shown in Figure 6.6. The samples were prepared into cylinder of 50 mm in diameter and 100 mm in height using dry deposition method and were classified into three groups (i.e., loose specimens ( $D_r = 45-50\%$ ), medium dense specimens ( $D_r = 55-65\%$ ), and dense specimens ( $D_r = 75-85\%$ )). The samples were then consolidated under isotropic condition. For each relative density, undrained cyclic triaxial tests were carried out employing three values of effective confining pressures, that is 50, 100, and 200 kPa. As the cyclic load sinusoidal wave of 1 Hz was used as the input wave, the application of the cyclic loading was continued until 10% axial strain in double amplitude was observed. The results, plotted as the liquefaction resistance curves, are shown in Figure 6.7.

#### **6.5 DETERMINATION OF MODEL PARAMETERS**

As seen in the preceding descriptions (Section 6.2), the model has ten parameters; two of which specify elastic properties of soil, other two specify plastic shear behavior, and the rest specify dilatancy as shown in Table 6.2. These parameters

were determined from the SPT N-values, which were corrected to the confining pressure of 100 kPa ( $1 \text{ tsf} = 10 \text{ t/m}^2 = 1 \text{ ksc} = 1 \text{ atm}$ ) as often done in the liquefaction potential evaluation (Seed et al., 1985), and the results of the undrained cyclic loading tests described earlier. The details in determining the soil parameters were as follows.

The elastic shear modulus  $G_{ma}$  at a reference confining pressure of  $(-\sigma'_{ma})$  was determined by referring to the correlation between SPT N-values and shear wave velocities as previously described in Section 3.5 of Chapter 3. The reference effective confining pressure of  $(-\sigma'_{ma})$ , which links elastic shear modulus to in situ confining pressure for each soil layer, was determined by referring to the  $K_0$  condition in which  $K_0 = 1 - \sin \phi'_f$  for normally consolidated coarse-grained soils (Jaky, 1944; Brooker and Ireland, 1965) and  $K_0 = 0.44 + 0.42 \left( \frac{PI(\%)}{100} \right)$  for normally consolidated fine-grained soils (Massarsch, 1979). For overconsolidated soils,  $K_0$  can be determined as a function of its value in the normally consolidated state using the relationship;  $K_{0,OC} = K_{0,NC} (OCR)^{0.5}$  (adapted from Schmidt, 1966; Alpan, 1967; Schmertmann, 1975; Ladd et al., 1977). The use of the reference effective confining pressure permits a gradual increase in the elastic shear modulus in accordance with a gradual increase in confining pressure within each soil layer. Shear resistance angle  $\phi'_f$  was estimated by referring to a correlation with SPT N-values proposed by Peck, Hanson, and Thornburn (1953). The relative density  $D_r$  was estimated based on the SPT N-value using a relationship proposed by Gibbs and Holz (1957). The hysteretic damping factor for an infinitely large shear strain  $H_m$  was determined to be 30% by referring to the typical laboratory results summarized by Ishihara (1982).

The rebound modulus or the elastic tangent bulk modulus of soil skeleton  $K_a$  was determined by assuming that Poisson's ratio is 0.33. The phase transformation angle  $\phi'_p$ , which separates dilative and contractive zones in  $p'-q$  space, was assumed to be 30 degrees for clean sand ( $FC < 5\%$ ) and 28 degrees for silty sand by referring to the typical value adopted for effective stress analyses of saturated sand (Ishihara et

al., 1989). The remaining five parameters  $p_1$ ,  $p_2$ ,  $w_1$ ,  $S_1$ , and  $c_1$ , which specify dilatancy of sand, were determined by the back-fitting to the liquefaction resistance curves of the sand as previously mentioned in Section 6.4. Figure 6.8 shows the comparison of shear stress ratio against number of cycle between laboratory test results and computed. The soil parameters determined in this manner are summarized in Table 6.3. More details in the back-fitting procedure as well as the definition of each parameter can be found in a paper by Iai et al. (1990).

## 6.6 RESULTS OF ANALYSES

Finite element analyses based on effective stress model were performed on twenty-nine sites within Chiang Mai City and seventeen sites within Chiang Rai City using the input parameters as mentioned above. From the analysis results, it can be found that the pore water pressure ratio in sand deposits increases with increasing probability of liquefaction ( $P_L$ ). It should be noted that the pore water pressure ratio for clay layer is not resulted by FLIP.

The relationship between soil amplification and maximum pore water pressure ratio is presented in Figure 6.9 and 6.10. From the figures, it is apparent that the maximum pore water pressure ratio of sand layer in sand sites is greater than that in clay sites. In contrast, the amplification factor in sand sites is less than that in clay sites. Note that a sand site is defined as a site that most of soil types are sand. Similarly, a clay site is defined as a site that most of soil types are clay.

Figure 6.11 and 6.12 show the analytical results by plotting the cyclic stress ratio ( $CSR$ ) for earthquake magnitude of 5.5 obtained from the logistic model as mentioned in Chapter 5 against the maximum pore water pressure ratio. The results show that the maximum pore water pressure ratio depends on the predominant periods of the input motion and tends to decrease with increase in the predominant period. This relationship can be used to evaluate the maximum excess pore water pressure of sand layer in the city of Chiang Mai and Chiang Rai.

Since Chiang Mai and Chiang Rai are located in the seismic zone G which probable causes earthquake magnitude ( $M_L$ ) of 5 to 6 with maximum ground acceleration ( $a_{\max}$ ) of 0.2g (Figure 3.2 and 3.3). Factor of safety computed following Seed et al. (1983) at various values of  $P_L$  is then obtained and summarized in Table 6.4. At  $P_L$  of 5%, there are more than 80% of the sandy sites subject to a certain level of liquefaction susceptibility.

Figure 6.13 and 6.14 show the typical analytical results by plotting the maximum pore water pressure ratio against the maximum ground acceleration. The vertical line crossed at  $a_{\max} = 0.2g$  is drawn for reference. The points located on the left of this line represent sites where factor of safety is less than 1.0 (corresponding to those shown in Table 6.4). The maximum pore water pressure ratio for cases when  $P_L = 5\%$  varies in the range of 0.1 - 0.8. Figure 6.15 and 6.16 show the maximum pore water pressure ratio at level of -2.5 m from ground surface. The pore water pressure ratio for cases when  $P_L = 5\%$  varies in the range of 0.1 - 0.5. Although near surface sand may not experience liquefaction, factor of safety of shallow foundation can be greatly reduced due to decrease in effective stress.

## 6.7 SUMMARY

This chapter illustrates the use of the finite element method to investigate the pore water pressure in sand deposits in the studied area. Several important findings from this investigation are summarized below:

- 1) The pore water pressure ratio in sand deposits increases with increasing probability of liquefaction ( $P_L$ ).
- 2) The maximum pore water pressure ratio of sand layer in sand sites is greater than that in clay sites. In contrast, the amplification factor in sand sites is less than that in clay sites.

- 3) The maximum pore water pressure ratio depends on the predominant periods of the input motion and tends to decrease with increase in the predominant period.
- 4) Although near surface sand in the studied area may not experience liquefaction, factor of safety of shallow foundation can be greatly reduced due to decrease in effective stress.



สถาบันวิทยบริการ  
จุฬาลงกรณ์มหาวิทยาลัย

## CHAPTER 7

### CONCLUSIONS AND RECOMMENDATIONS

#### 7.1 CONCLUSIONS

In this thesis, the amplification of earthquake ground motion, liquefaction probability, and the generation of pore water pressure due to medium earthquakes in the northern part of Thailand, particularly Chiang Mai and Chiang Rai, were studied. Due to the lack of strong motion record in Thailand, three input motions recorded from elsewhere with different predominant periods were adopted. Soil properties used as input to the analyses, specifically shear wave velocity, were estimated using existing correlations with field and laboratory data. Seismic site response analyses were conducted using the computer program SHAKE to quantify the potential amplification of earthquake ground motions in the cities due to soil effects.

The binary logistic regression technique using the worldwide liquefaction database was used to form the probabilistic base correlation between cyclic stress ratio and the SPT resistance for evaluating the liquefaction probability. Subsequently, the finite element program based on effective stress model called FLIP was used to evaluate the generation of pore water pressure in sand deposits corresponding to various probability values. The laboratory test results on undrained cyclic triaxial of sands were used to obtain some effective stress parameters required in the effective stress model. The following conclusions are drawn from the study:

- 1) The soil profile underlying the city of Chiang Mai and Chiang Rai has the ability to amplify earthquake ground motions 1.5 to 3 times. The amount of this amplification was found to decrease with increasing bedrock acceleration. This amplification depends on the local site conditions, the level of acceleration in the

underlying rock-like material, and the predominant periods and characteristics of the input motion.

- 2) The models obtained from the probabilistic method are based on the Seed and Idriss (1971) parameterization and employ the magnitude cyclic stress ratio  $CSR$  as a measure of earthquake load; and use the corrected/normalized SPT value  $(N_1)_{60}$  as a measure of soil-liquefaction resistance.
- 3) In the probability charts (Figure 5.3 and 5.4), the probabilistic line at  $P_L = 30\%$  well traces the deterministic criteria for clean sand base curve proposed by Seed et al. (1985). Therefore, the success rate line which is drawn to separate events of liquefaction and non-liquefaction is determined based on  $P_L = 30\%$  line.
- 4) The probabilistic procedure provides more statistical rigorous criteria for defining liquefaction resistance than was used in the original development of the deterministic or simplified procedure suggested by Seed and Idriss (1971). As with all empirical methods, however, the quality of the results are strongly dependent on the quantity and quality of the compiled input data.
- 5) With the proper input soil model parameters, the finite element method can be powerful and versatile analytical tool for studying the generation of pore water pressure in sand deposits due to earthquake shaking.
- 6) The pore water pressure ratio in sand deposits increases with increasing probability of liquefaction ( $P_L$ ).
- 7) The maximum pore water pressure ratio of sand layer in sand sites is greater than that in clay sites. In contrast, the amplification factor in sand sites is less than that in clay sites.
- 8) The maximum pore water pressure ratio depends on the predominant periods and characteristics of the input motion and tends to decrease with increase in the predominant period.
- 9) The charts correlating the liquefaction probability, estimated excess pore water pressure and peak ground acceleration proposed in this study can be used as a



simple tool for estimating excess pore water pressure in sand deposits due to earthquake shaking in the city of Chiang Mai and Chiang Rai.

- 10) Although near surface sand in the studied area may not experience liquefaction, factor of safety of shallow foundation can be greatly reduced due to decrease in effective stress.
- 11) The probabilistic procedure for evaluating liquefaction potential proposed in this study have the primary advantage for engineering applications is that the user can select an appropriate probability level of risk of occurrence for analyzing liquefaction hazard. Therefore, The developed method has the potential of becoming a practical tool for engineers involved in the assessment of liquefaction potential.

## **7.2 RECOMMENDATIONS FOR FUTURE RESEARCH**

Several other subjects related in this research have been identified that need further investigation. The needs are summarized below:

- 1) Additional strong motion records should be used as input motions to make the study more complete, including both actual seismograms from far-field sites and near-field sites; and synthetic seismograms with frequency contents or predominant periods matching the expected seismicity of the region.
- 2) The estimate of expected peak rock acceleration in Chiang Mai and Chiang Rai must be refined. This refinement would necessarily include definition and characterization of active faults that are likely to affect the cities.
- 3) The soil properties used in the analyses, particularly shear wave velocity and variation of shear modulus and damping with strain, must be better defined. This would include additional in situ testing for shear wave velocity and sophisticated laboratory testing for determining the variation of shear modulus and damping with shear strain. Although the published correlations and relationships used in

this study are often sufficient, it would seem prudent to develop relationships specifically for soil underlying Chiang Mai and Chiang Rai; the capital of the northern region of Thailand.

- 4) The depth to rock like material must be better determined through in situ testing to at least a depth of 160 m or more, in order to obtain the better analysis results.
- 5) The effects of several variables on the liquefaction probability, such as fines content (FC), gravel content (GC), and median grain size ( $D_{50}$ ), were not included in the proposed models due to limitations in the data. They should be included in the probability models once the complete database is obtained.
- 6) In this study, the soil liquefaction resistance was measured by the standard penetration test (SPT). Though this test is relatively crude, it is one of the few measurements that provide a direct link between actual observations of liquefaction and soil properties. However, measurements from other in situ tests, such as the cone penetration test (CPT), the shear wave velocity test ( $V_s$ ), and the Becker penetration test (BPT), are now being correlated to liquefaction performance. Logistic regression can also be applied to these measurements, once a significant database has been established.

## REFERENCES

- Algermissen, S. T., Perkins, D. M., Thenhaus, P. C., Hanson, S. L., and Bender, B. L. 1982. Probabilistic estimates of maximum acceleration and velocity in rock in the contiguous United States. Open-File Report 82-1033, U. S. Geological Survey, Washington, D. C.
- Alpan, I. 1967. The empirical evaluation of the coefficients  $K_o$  and  $K_{oR}$ . Soils and Foundations 7, 1: 31-40.
- Ambraseys, N. N. 1988. Engineering seismology. Earthquake Engineering and Structural Dynamics 17: 1-105.
- Anantasech, C., and Thanadpipat, C. 1985. Characteristics and engineering properties of subsoils in intermontane basin. Thailand Engineering Journal 38, 2: 101-106 (in Thai).
- Andrus, R. D., and Stokoe, K. H., II. 2000. Liquefaction resistance of soils from shear wave velocity. Journal of Geotechnical and Geoenvironmental Engineering ASCE 126, 11: 1015-1025.
- Arango, I. 1996. Magnitude scaling factors for soil liquefaction evaluations. Journal of Geotechnical Engineering ASCE 122, 11: 929-936.
- Bjerrum, L. 1972. Embankments on soft ground. Proceedings of the ASCE Specialty Conference on Performance of Earth and Earth-Supported Structures, II, pp. 1-54. Purdue University.
- Blazquez, R. M., Krizek, R. J., and Bazant, Z. P. 1980. Site factors controlling liquefaction. Journal of the Geotechnical Engineering Division ASCE 106, GT7: 785-801.
- Brooker, E. W., and Ireland, H. O. 1965. Earth pressure at rest related to stress history. Canadian Geotechnical Journal 2, 1: 1-15.
- Castro, G. 1969. Liquefaction of sands. Harvard Soil Mechanics Series 87, Harvard University, Cambridge, Massachusetts.

- Castro, G. 1975. Liquefaction and cyclic mobility of sands. Journal of the Geotechnical Engineering Division ASCE 101, GT6: 551-569.
- Chameau, J. L., and Clough, G. W. 1983. Probabilistic pore pressure analysis for seismic loading. Journal of Geotechnical Engineering ASCE 109, 4: 507-524.
- Christian, J. T., and Swiger, W. F. 1975. Statistic of liquefaction and SPT results. Journal of the Geotechnical Engineering Division ASCE 101, GT11: 1135-1150.
- Cooley, P. M., and Tukey, J. W. 1965. An algorithm for the machine computation of complex Fourier series. Mathematics of Computation 19, 4: 297-301.
- Cornell, C. A. 1968. Engineering seismic risk analysis. Bulletin of the Seismological Society of America 58: 1583-1606.
- Davis and Berrill, J. B. 1981. Assessment of liquefaction potential based on seismic energy dissipation. Proceedings of the International Conference on Recent Advances in Geotechnical Earthquake Engineering and Soil Dynamics, 1, pp. 197-190. St. Louis.
- Day, R. W. 2002. Geotechnical earthquake engineering handbook. New York: McGraw-Hill.
- De Alba, P., Seed, H. B., and Chan, C. K. 1976. Sand liquefaction in large-scale simple shear tests. Journal of Geotechnical Engineering Division ASCE 102, GT9: 909-927.
- Dickenson, S. E. 1994. Dynamic response of soft and deep cohesive soils during the Loma Prieta earthquake of October 17, 1989. Ph.D. Dissertation, Department of Civil Engineering, University of California, Berkeley, California.
- Dillon, W. R., and Goldstein, M. 1984. Multivariate analysis: Methods and applications. New York: John Wiley.
- Dobry, R., and Vucetic, M. 1987. Dynamic properties and seismic response of soft clay deposits. Proceedings of International Symposium on Geotechnical Engineering of Soft Soils, 2, pp. 51-87. Mexico City.

- Egan, J. A., and Ebeling, R. M. 1985. Variation of small-strain modulus with undrained shear strength of clay. Proceedings of 2<sup>nd</sup> International Conference on Soil Dynamics and Earthquake Engineering, 2, pp. 27-36.
- Fardis, M. N., and Veneziano, D. 1982. Probabilistic analysis of deposit liquefaction. Journal of the Geotechnical Engineering Division ASCE 108, GT3: 395-417.
- Fiegel, G. L., and Kutter, B. L. 1992. The mechanism of liquefaction in layered soils. Report CR92.009, Naval Civil Engineering Laboratory, Port Hueneme, California.
- Finn, W. D. L., Lee, K. W., and Martin, G. R. 1977. An effective stress model for liquefaction. Journal of the Geotechnical Engineering Division ASCE 103, GT6: 517-533.
- Fumal, T. E. 1978. Correlations between seismic wave velocities and physical properties of near-surface geologic materials in the southern San Francisco bay region, California. Open File Report 78-1067, U.S. Geological Survey, Menlo Park, California.
- Gauchan, J. 1984. Liquefaction tests on sand using a cyclic triaxial apparatus. Master's Thesis, Asian Institute of Technology, Bangkok, Thailand.
- Gibbs, H. J., and Holtz, W. G. 1957. Research on determining the density of sand by spoon penetration testing. Proceedings of the 4<sup>th</sup> International Conference on Soil Mechanics and Foundation Engineering, 1, pp. 35-39. London.
- Gutenberg, B., and Richter, C. F. 1956. Earthquake magnitude, intensity, energy and acceleration (Second Paper). Bulletin of the Seismology Society of America 46, 2: 143-145.
- Haldar, A., and Tang, W. H. 1979. Probabilistic evaluation of liquefaction potential. Journal of the Geotechnical Engineering Division ASCE 105, GT2: 145-163.
- Hardin, B. O., and Drnevich, V. P. 1972a. Shear modulus and damping in soils: Measurement and parameter effects. Journal of the Soil Mechanics and Foundations Division ASCE 98, SM6: 603-624.

- Hardin, B. O., and Drnevich, V. P. 1972b. Shear modulus and damping in soils: design equations and curves. Journal of the Soil Mechanics and Foundations Division ASCE 98, SM7: 667-692.
- Hardin, B. O., and Richart, F. 1963. Elastic wave velocities in granular soils. Journal of the Soil Mechanics and Foundations Division ASCE 89, 1: 33-65.
- Iai, S. 1993. Micromechanical background to a strain space multiple mechanism model for sand. Soils and Foundations 33, 1: 102-117.
- Iai, S., Kameoka, T., and Matsunaga, Y. 1993. Numerical (Class A) prediction of Model No.1. Verification of Numerical Procedures for the Analysis of Soil Liquefaction Problems (VELACS), pp. 109-127. Balkema, Rotterdam.
- Iai, S., Matsunaga, Y., and Kameoka, T. 1990. Parameter identification for a cyclic mobility model. Report of Port and Harbour Research Institute 29, 4: 57-83.
- Iai, S., Matsunaga, Y., and Kameoka, T. 1992. Strain space plasticity model for cyclic mobility. Soils and Foundations 32, 2: 1-15.
- Idriss, I. M. 1990. Response of soft soil sites during earthquakes. Proceedings of the H. Bolton Seed Memorial Symposium, 2, pp. 273-289. Vancouver, British Columbia.
- Idriss, I. M., and Seed, H. B. 1968. Seismic response of horizontal soil layers. Journal of the Soil Mechanics and Foundations Division ASCE 94, SM4.
- Idriss, I. M., and Sun, J. I. 1992. SHAKE91: a computer program for conducting equivalent linear seismic response analyses of horizontally layered soil deposits. User's Guide, University of California, Davis.
- Imai, T., and Tonuchi, K. 1982. Correlation of N-value with S-wave velocity and shear modulus. Proceedings of 2<sup>nd</sup> European Symposium on Penetration Testing, pp. 67-72. Amsterdam, Netherlands.
- Ishibashi, I., and Zhang, X. 1993. Unified dynamic shear moduli and damping ratios of sand and clay. Soils and Foundations 33, 1: 182-191.
- Ishibashi, I., Sherif, M. A., and Tsuchiya, C. 1977. Pore-pressure rise mechanism and soil liquefaction. Soils and Foundations 17, 2: 17-27.

- Ishihara, K. 1982. Evaluation of soil properties for use in earthquake response analysis. Proceedings of International Symposium on Numerical Models in Geomechanics, pp. 237-259. Zurich.
- Ishihara, K. 1984. Post-earthquake failure of a tailings dam due to liquefaction of the pond deposit. Proceedings of International Conference on Case Histories in Geotechnical Engineering, 3, pp. 1129-1143. University of Missouri, St. Louis.
- Ishihara, K. 1985. Stability of natural deposits during earthquakes. Proceedings of the 11<sup>th</sup> International Conference on Soil Mechanics and Foundation Engineering, 1, pp. 321-376.
- Ishihara, K. 1993. Liquefaction and flow failure during earthquakes. Geotechnique 43, 3: 351-415.
- Ishihara, K. 1996. Soil behaviour in earthquake geotechnics. Oxford: Clarendon Press.
- Ishihara, K., Tatsuoka, F., and Yasuda, S. 1975. Undrained deformation and liquefaction of sand under cyclic stresses. Soils and Foundations 15, 1: 29-44.
- Ishihara, K., Lysmer, J., Yasuda, S., and Hirao, H. 1976. Prediction of liquefaction in sand deposits during earthquakes. Soils and Foundations 16, 1: 1-16.
- Ishihara, K. Yoshida, N., and Tsujino, S. 1985. Modelling of stress-strain relations of soils in cyclic loading. Proceedings of the 5<sup>th</sup> International Conference on Numerical Methods in Geomechanics, 1, pp. 373-380.
- Ishihara et al. 1989. Effective stress analysis of ground and soil structures. Proceedings of Symposium on Seismic Performance of Ground and Soil Structures, pp. 50-63. Japanese Society of Soil Mechanics and Foundation Engineering.
- Iwasaki, T., Tatsuoka, F., and Takagi, Y. 1978. Shear modulus of sands under torsional shear loading. Soils and Foundations 18, 1: 39-56.
- Jaky, J. 1944. The coefficient of earth pressure at rest. Journal of the Society of Hungarian Architects and Engineers 78, 22: 355-358 (in Hungarian).
- Johnson, D. E. 1998. Applied multivariate methods for data analysis. Duxbury Press.

- Johnson, R. A., and Wichern, D. W. 1988. Applied multivariate statistical analysis. 4<sup>th</sup> ed. New Jersey: Prentice Hall.
- Joyner, W. B., and Boore, D. M. 1981. Peak horizontal acceleration and velocity from strong-motion records including records from the 1979 Imperial Valley, California, earthquake. Bulletin of the Seismological Society of America 71, 6: 2011-2038.
- Kanai, K. 1951. Relation between the nature of surface layer and the amplitude of earthquake motions. Bulletin of the Earthquake Research Institute Tokyo University 29.
- Kanai, K. 1957. Semi-empirical formula for the seismic characteristics of the ground. Bulletin of the Earthquake Research Institute Tokyo University 35: 308-325.
- Kanai, K. 1966. Observation of microtremors, XI, Matsushiro earthquake swarm areas. Bulletin of the Earthquake Research Institute Tokyo University 44: 315-337.
- Kawashima, K., Aizawa, K., and Takahashi, K. 1984. Attenuation of peak ground motion and absolute acceleration response spectra. Proceedings of the 8<sup>th</sup> World Conference on Earthquake Engineering, 2, pp. 257-264. San Francisco, California.
- Kayen, R. E., Mitchell, J. K., Seed, R. B., Lodge, A., Nishio, S., and Coutinho, R. 1992. Evaluation of SPT-, CPT-, and shear wave-based methods for liquefaction potential assessment using Loma Prieta data. Proceedings of the 4<sup>th</sup> Japan-U. S. Workshop on Earthquake Resistant Design of Lifeline Facilities and Countermeasures for Soil Liquefaction, 1, pp. 177-204. Buffalo, New York.
- Kleinbaum, D. A. 1994. Logistic regression. Springer-Verlag.
- Knox, D., Stokoe, K., and Kopperman, S. 1982. Effect of state of stress on shear wave velocity in dry sand. Geotechnical Engineering Report GR82-23, The University of Texas at Austin, Austin, Texas.
- Kokusho, T. 1980. Cyclic triaxial test of dynamic soil properties for wide strain range. Soils and Foundations 20, 2: 45-60.



- Kokusho, T., Yoshida, Y., and Esashi, Y. 1982. Dynamic properties of soft clay for wide range. Soils and Foundations 22, 4: 1-18.
- Koutsoftas, D., and Fischer, J. A. 1980. Dynamic properties of two marine clays. Journal of the Geotechnical Engineering Division ASCE 106, GT6: 645-657.
- Kramer, S. L. 1996. Geotechnical earthquake engineering. New Jersey: Prentice Hall.
- Ladd, C. C., Foott, R., Ishihara, K., Schlosser, F., and Poulos, H. G. 1977. Stress-deformation and strength characteristics. Proceedings of the 9<sup>th</sup> International Conference on Soil Mechanics and Foundation Engineering, 2, pp. 421-494. Japanese Society of Soil Mechanics and Foundation Engineering, Tokyo.
- Liao, S. S. C., and Whitman, R. V. 1986a. A catalog of liquefaction and non-liquefaction occurrences during earthquakes. Research Report, Department of Civil Engineering, Massachusetts Institute of Technology, Cambridge, Massachusetts.
- Liao, S. S. C., and Whitman, R. V. 1986b. Overburden correction factors for SPT in sand. Journal of Geotechnical Engineering ASCE 112, 3: 373-377.
- Lindeburg, M. R. 1998. Seismic design of building structures. 7<sup>th</sup> ed. Belmont, CA: Professional Publications, Inc.
- Liou, C. P., Streeter, V. L., and Richart, F. E., Jr. 1977. Numerical model for liquefaction. Journal of the Geotechnical Engineering Division ASCE 103, GT6: 589-606.
- Liu, H., and Qiao, T. 1984. Liquefaction potential of saturated sand deposits underlying foundation of structure. Proceedings of the 8<sup>th</sup> World Conference on Earthquake Engineering, 3, pp. 199-206. San Francisco.
- Lysmer, J., Seed, H. B., and Schnabel, P. B. 1970. Influence of base rock characteristics on ground response. Report No. EERC 70-7, Earthquake Engineering Research Center, University of California, Berkeley, California.
- Lysmer, J., Seed, H. B., and Schnabel, P. B. 1971. Influence of base-rock characteristics on ground response. Bulletin of the Seismological Society of America 61, 5: 1213-1232.

- Martin, G. R., Finn, W. D. L., and Seed, H. B. 1975. Fundamentals of liquefaction under loading. Journal of the Geotechnical Engineering Division ASCE 101, GT5: 423-429.
- Massarsch, K. R. 1979. Lateral earth pressure in normally consolidated clay. Proceedings of the 7<sup>th</sup> European Conference on Soil Mechanics and Foundation Engineering, 2, pp. 245-250. Brighton, England.
- Matthiesen, R. B., Duke, C. M., Leeds, D. J., and Fraser, J. C. 1964. Site characteristics of southern California strong-motion earthquake stations, part two. Report No. 64-15, Department of Civil Engineering, University of California, Los Angeles.
- Mori, K., Seed, H. B., and Chan, C. K. 1978. Influence of sample disturbance on sand response to cyclic loading. Journal of the Geotechnical Engineering Division ASCE 104, GT3: 323-339.
- Morrison, D. F. 1990. Multivariate statistical method, 3<sup>rd</sup> ed. New York: McGraw-Hill.
- Mroz, Z., Norris, V. A., and Zienkiewicz, O. C. 1978. An isotropic hardening model and analytical methods in geomechanics. International Journal for Numerical and Analytical Methods in Geomechanics 2: 203-221.
- Nuttalaya, P., Sodsri, S., and Arnold, E. P. 1985. Series on seismology volume II- Thailand. Southeast Asia Association of Seismology and Earthquake Engineering, Bangkok.
- Ohsaki, Y., and Iwasaki, R. 1973. On dynamic shear moduli and poisson's ratio of soil deposits. Soils and Foundations 13, 4: 61-73.
- Ohta, Y., and Goto, N. 1978. Empirical shear wave velocity equations in terms of characteristics soil indexes. Earthquake Engineering and Structural Dynamics 6: 167-187.
- Peck, R. B., Hanson, W. E., and Thornburn, T. H. 1953. Foundation Engineering. New York: John Wiley & Sons.
- Reiter, L. 1990. Earthquake hazard analysis—issues and insight. New York: Columbia University Press.

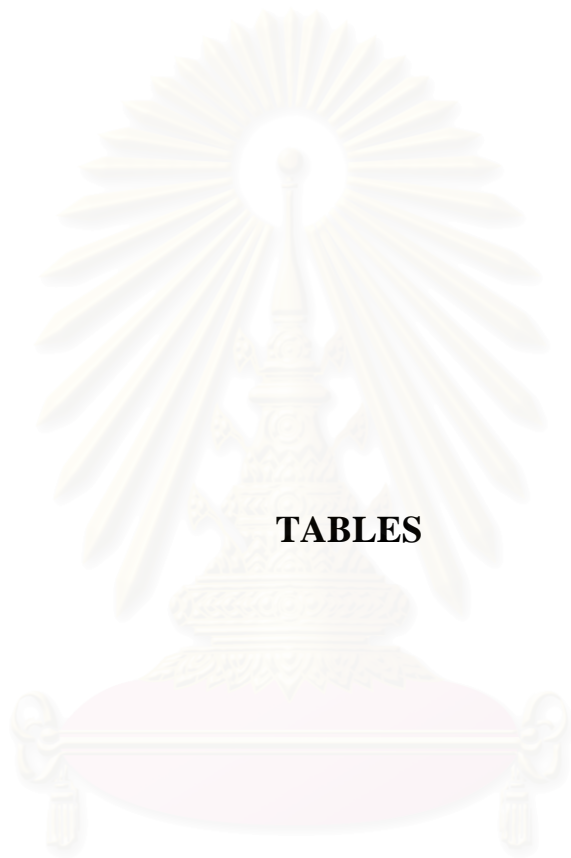
- Roesset, J. M., and Whitman, R. V. 1969. Theoretical background for amplification studies. Research Report No. R69-15, Soils Publication No. 231, Massachusetts Institute of Technology, Cambridge.
- Sakai, Y. 1968. A study on determination of S-wave velocity by soil penetrometer test.
- Schnabel, P. B., Lysmer, J., and Seed, H. B. 1972. SHAKE: A computer program for earthquake response analysis of horizontally layered sites. Report No. EERC 72-12, Earthquake Engineering Research Center, University of California, Berkeley, California.
- Seed, H. B. 1983. Earthquake-resistant design of earth dams. Proceeding, Symposium on Seismic Design of Earth Dams and Caverns, ASCE, pp. 41-64. New York.
- Seed, H. B., and Idriss, I. M. 1970. Soils moduli and damping factors for dynamic response analyses. Report No. EERC 70-10, Earthquake Engineering Research Center, University of California, Berkeley, California.
- Seed, H. B., and Idriss, I. M. 1971. Simplified procedure for evaluating soil liquefaction potential. Journal of the Soil Mechanics and Foundations Division ASCE Vol. 97, No. SM9: 1249-1273.
- Seed, H. B., and Idriss, I. M. 1982. Ground motions and soil liquefaction during earthquakes. California: Earthquake Engineering Research Institute.
- Seed, H. B., and Lee, K. L. 1966. Liquefaction of saturated sands during cyclic loading. Journal of Soil Mechanics and Foundations Division ASCE 92, SM6: 105-134.
- Seed, H. B., Arango, I., and Chan, C. K. 1975. Evaluation of soil liquefaction potential during earthquakes. Report No. EERC 75-28, Earthquake Engineering Research Center, University of California, Berkeley, California.
- Seed, H. B., Martin, P. P., and Lysmer, J. 1976a. Pore-water pressure changes during soil liquefaction. Journal of the Geotechnical Engineering Division ASCE 102, GT4: 323-346.
- Seed, H. B., Ugas, C., and Lysmer, J. 1976b. Site-dependent spectra for earthquake-resistant design. Bulletin of the Seismological Society of America 66: 221-243.

- Seed, H. B., Idriss, I. M., and Arango, I. 1983. Evaluation of liquefaction potential using field performance data. Journal of Geotechnical Engineering ASCE 109, 3: 458-482.
- Seed, H. B., Wong, R. T., Idriss, I. M., and Tokimatsu, K. 1984a. Moduli and damping factors for dynamic analyses of cohesionless soils. Report No. UCB/EERC-84/14, Earthquake Engineering Research Center, University of California, Berkeley, California.
- Seed, H. B., Tokimatsu, K., Harder, L. F., and Chung, R. M. 1984b. Influence of SPT procedures in soil liquefaction resistance evaluations. Report No. UBC/EERC 84-15, Earthquake Engineering Research Center, University of California, Berkeley, California.
- Seed, H. B., Tokimatsu, K., Harder, L. F., and Chung, R. M. 1985. Influence of SPT procedures in soil liquefaction resistance evaluations. Journal of Geotechnical Engineering ASCE 111, 12: 1425-1445.
- Seed, H. B., Wong, R. T., Idriss, I. M., and Tokimatsu, K. 1986. Moduli and damping factors for dynamic analyses of cohesionless soils. Journal of Geotechnical Engineering ASCE 112, GT11: 1016-1032.
- Seed, R. B., and Harder, L. F., Jr. 1990. SPT-based analysis of cyclic pore pressure generation and undrained residual strength. Proceedings of H. Bolton Seed Memorial Symposium, 2, pp. 351-376. University of California, Berkeley.
- Schmertmann, J. H. 1975. Measurement of in situ shear strength. Proceedings of the ASCE Specialty Conference on In Situ Measurement of Soil Properties, 2, pp. 57-138. Raleigh, N.C.
- Schmertmann, J. H., Smith, T. V., and Ho, R. 1978. Example of an energy calibration report on a standard penetration test (ASTM Standard D1586-67) drill rig. Geotechnical Testing Journal 1, 1: 57-61.
- Schmidt, B. 1966. Discussion on earth pressure at rest related to stress history. Canadian Geotechnical Journal Vol. 3, No. 4.
- Sherif, M. A., Ishibashi, I., and Tsuchiya, C. 1978. Pore-pressure prediction during earthquake loading. Soils and Foundations 18, 4: 19-30.

- Shibata, T., Yukitomo, H., and Miyoshi, M. 1972. Liquefaction process of sand during cyclic loading. Soils and Foundations 12, 1: 1-16.
- SPSS. 1999. SPSS base 9.0 for windows user's guide and applications guide. SPSS Inc.
- Sun, J. I., Golesorkhi, R., and Seed, H. B. 1988. Dynamic moduli and damping ratios for cohesive soils. Report No. EERC-88/15, Earthquake Engineering Research Center, University of California, Berkeley, California.
- Sykora, D. W. 1987. Examination of existing shear wave velocity and shear modulus correlations in soils. U.S. Army Engineering Waterways Experiment Station Misc. Paper GL-87-22.
- Sykora, D. W., and Stokoe, K. H. 1983. Correlations of in-situ measurements in sands with shear wave velocity. Geotechnical Engineering Report GR83-33, The University of Texas at Austin, Texas.
- Tokimatsu, K., and Yoshimi, Y. 1983. Empirical correlation of soil liquefaction based on SPT N-value and fines content. Soils and Foundations 23, 4: 56-74.
- Toprak, S., Holzer, T. L., Bennett, M. J., and Tinsley, J. C., III. 1999. CPT- and SPT-based probabilistic assessment of liquefaction. Proceedings of the U. S.-Japan Workshop on Earthquake Resistant Design of Lifeline Facilities and Countermeasures Against Liquefaction, pp. 69-86. Multidisciplinary Center for Earthquake Engineering Research, Buffalo, New York.
- Towhata, I., and Ishihara, K. 1985. Modelling soil behaviour under principal stress axes rotation. Proceedings of the 5<sup>th</sup> International Conference on Numerical Methods in Geomechanics, 1, pp. 523-530.
- Trudeau, P. J., Whitman, R. V., and Christian, J. T. 1973. Shear wave velocity and modulus of a marine clay. Boston Society of Civil Engineers 61, 1: 12-25.
- Veneziano, D., and Liao, S. 1984. Statistic analysis of liquefaction data. Proceedings of the 4<sup>th</sup> ASCE Specialty Conference on Probabilistic Mechanics and Structural Reliability, pp. 206-209.
- Vucetic, M., and Dobry, R. 1991. Effect of soil plasticity on cyclic response. Journal of Geotechnical Engineering ASCE 117, 1: 89-107.

- Warnitchai, P., and Lisantono, A. 1996. Probabilistic seismic risk mapping for Thailand. Proceedings of the 11<sup>th</sup> World Conference on Earthquake Engineering, Acapulco, Mexico.
- Weiler, W. A. 1988. Small strain shear modulus of clay. Proceedings of ASCE Conference on Earthquake Engineering and Soil Dynamics II: Recent Advances in Ground Motion Evaluation, Geotechnical Special Publication 20, ASCE, pp. 331-335. New York.
- Whitman, R. V. 1971. Resistance of soil to liquefaction and settlement. Soils and Foundations 11, No. 4: 59-68.
- Xie, J. 1979. Empirical criteria of sand liquefaction: the 1976 Tangshan China earthquake. Proceedings of the 2<sup>nd</sup> U. S. National Conference on Earthquake Engineering, Stanford University.
- Yasuda, N, and Matsumoto, N. 1993. Dynamic deformation characteristics of sands and rock-fill materials. Canadian Geotechnical Journal 30, 5: 747-757.
- Yegian, M. K. 1976. Risk analysis for earthquake-induced ground failure by liquefaction. Ph. D. Thesis, Massachusetts Institute of Technology, Cambridge, Massachusetts.
- Yegian, M. K., and Vitelli, B. M. 1981. Probabilistic analysis for liquefaction. Report No. CE-81-1, Northeastern University, Boston, Massachusetts.
- Yegian, M. K., and Whitman, R. V. 1978. Risk analysis for ground failure by liquefaction. Journal of the Geotechnical Engineering Division ASCE 104, GT7: 921-938.
- Youd, T. L. 1984. Recurrence of liquefaction at the same site. Proceedings of the 8<sup>th</sup> World Conference on Earthquake Engineering, 3, pp. 231-238. San Francisco.
- Youd, T. L. 1991. Mapping of earthquake-induced liquefaction for seismic zonation. Proceedings of the 4<sup>th</sup> International Conference on Seismic Zonation, Earthquake Engineering Research Institute, 1, pp. 111-147. Stanford University.
- Youd, T. L. 1993. Liquefaction-induced lateral spread displacement. NCEL Technical Note N-1862, U. S. Navy, Port Hueneme, California.

- Youd, T. L., and Idriss, I. M., eds. 1997. Proceedings of NCEER Workshop on Evaluation of Liquefaction Resistance of Soils, State University of New York at Buffalo.
- Youd, T. L., and Noble, S. K. 1997. Magnitude scaling factors. Proceedings of NCEER Workshop on Evaluation of Liquefaction Resistance of Soils, pp. 149-165. State University of New York at Buffalo.
- Zen, K., Umehara, Y., and Hamada, K. 1978. Laboratory tests and in-situ seismic survey on vibratory shear modulus of clayey soils with different plasticities. Proceedings of the 5<sup>th</sup> Japan Earthquake Engineering Symposium, pp. 721-728. Tokyo.
- Zienkiewicz, O. C., and Bettess, P. 1982. Soils and other saturated media under transient, dynamic conditions; general formulation and the validity of various simplifying assumption. In Pande, G. N., and Zienkiewicz, O. C. (eds.), Soil mechanics-transient and cyclic loads, pp. 1-16. (n.p.): John Wiley & Sons.
- Zienkiewicz, O. C., Chang, C. T., and Hinton, E. 1978. Non-linear seismic response and liquefaction. International Journal for Numerical and Analytical Methods in Geomechanics 2: 381-404.



**TABLES**

สถาบันวิทยบริการ  
จุฬาลงกรณ์มหาวิทยาลัย



**Table 1.1.** Examples of recent earthquakes felt in Thailand

<b>Date</b>	<b>Magnitude</b>	<b>Center</b>	<b>Were Felt at</b>
April 22, 1983	5.9	Kanchanaburi, Thailand	Bangkok, Western and northern parts
November 6, 1988	7.3	Southern of China (1,000 km from Bangkok)	Bangkok, Western and northern parts
September 29 – October 1, 1989	5.3 – 5.4 Several quakes	Western part	Bangkok, Western and northern parts
September 11, 1994	5.5	Phan District (Northern part)	Northern parts
January 22, 2003	7.5	Sumatra Island (1,000 km from Bangkok)	Bangkok
September 22, 2003	6.6	Burma (850 km from Bangkok)	Bangkok and Northern parts

สถาบันวิทยบริการ  
จุฬาลงกรณ์มหาวิทยาลัย

**Table 2.1.** Modified Mercalli intensity scale (Kramer, 1996)

<b>Intensity</b>	<b>Observed Effects of Earthquake</b>
I	Not felt except by very few under especially favorable conditions.
II	Felt only by a few persons at rest, especially by those on upper floors of buildings. Delicately suspended objects may swing.
III	Felt quite noticeably by persons indoors, especially in upper floors of buildings. Many people do not recognize it as an earthquake. Standing vehicles may rock slightly. Vibrations similar to the passing of a truck. Duration estimated.
IV	During the day, felt indoors by many, outdoors by a few. At night, some awakened. Dishes, windows, doors disturbed; walls make cracking sound. Sensation like heavy truck striking building. Standing vehicles rock noticeably.
V	Felt by nearly everyone; many awakened. Some dishes, windows broken. Unstable objects overturned. Pendulum clocks may stop.
VI	Felt by all, many frightened. Some heavy furniture moved. A few instances of fallen plaster. Damage slight.
VII	Damage negligible in buildings of good design and construction; slight to moderate in well-built ordinary structures; considerable damage in poorly built structures. Some chimney broken.
VIII	Damage slight in specially designed structures; considerable damage in ordinary substantial buildings, with partial collapse. Damage great in poorly built structures. Fallen chimneys, factory stacks, columns, monuments, walls. Heavy furniture overturned.
IX	Damage considerable in specially designed structures; well-designed frame structures thrown out of plumb. Damage great in substantial buildings, with partial collapse. Buildings shifted off foundations.
X	Some well-built wooden structures destroyed; most masonry and frame structures with foundations destroyed. Rails bent.
XI	Few, if any, masonry structures remain standing. Bridges destroyed. Rail bent greatly.
XII	Damage total. Lines of sight and level are destroyed. Objects thrown into air.

**Table 2.2.** Richter magnitude scale ( $M_L$ )

<b>Magnitude <math>M_L</math></b>	<b>Possible Effects</b>
0	Normally only detected by instruments
1	
2	
3	Faint tremor causing little damage
4	
5	Structural damage
6	Distinct shaking, less well-constructed building collapse
7	
8	Large buildings destroyed
9	Ground seems to shake

**Table 2.3.** Parameters affecting shear modulus and damping of soils subjected to dynamic loading (Hardin and Drnevich, 1972a)

Parameter (1)	IMPORTANCE TO <sup>a</sup>			
	Modulus		Damping	
	Clean sands (2)	Cohesive soils (3)	Clean sands (4)	Cohesive soils (5)
Strain Amplitude	V	V	V	V
Effective Mean Principal Stress	V	V	V	V
Void Ratio	V	V	V	V
Number of Cycles of Loading	R <sup>b</sup>	R	V	V
Degree of Saturation	R	V	L	U
Overconsolidation Ratio	R	L	R	L
Effective Strength Envelope	L	L	L	L
Octahedral Shear Stress	L	L	L	L
Frequency of Loading (above 0.1 Hz)	R	R	R	L
Other Time Effects (Thixotropy)	R	L	R	L
Grain Characteristics, Size, Shape, Gradation, Mineralogy	R	R	R	R
Soil Structure	R	R	R	R
Volume Change Due to Shear Strain (for strains less than 0.5 %)	U	R	U	R

<sup>a</sup> V means Very Important, L means Less Important, and R means Relatively Unimportant except as it may affect another parameter; U means relative importance is not clearly known at this time.

<sup>b</sup> Except for saturated clean sand where the number of cycles of loading is a Less Important Parameter.

**Table 2.4.** Values of  $G_{\max}/S_u$  (Weiler, 1988)

Plasticity Index	Overconsolidation Ratio, OCR		
	1	2	5
15-20	1100	900	600
20-25	700	600	500
35-45	450	380	300

**Table 2.5.** Parameters for Ohsaki and Iwasaki (1973) relationship between SPT N-value and  $V_s$  (Sykora, 1987)

Category	Groups	Parameter		Correlation Coefficient
		a	b	
All data	--	124	0.78	0.886
Geologic age	Tertiary (Pliocene)	57.3	0.97	0.821
	Diluvial (Pleistocene)	110	0.82	0.812
	Alluvial (Holocene)	149	0.64	0.786
Soil type	Cohesionless	66.3	0.94	0.852
	Intermediate	121	0.76	0.742
	Cohesive	143	0.71	0.921
$G/\sqrt{\sigma'_m}$	Sands	--	--	0.742

**Table 2.6.** Ohta and Goto (1976) relationships between SPT N-value and  $V_s$  (Sykora, 1987)

Equation No.	Combination of Correlative Parameters	Best-Fit Relation ( $V_s$ in fps)*	Correlation Coefficient
1	SPT N-value	$V_s = 280 N^{0.348}$	0.719
2	SPT N-value Soil Type	$V_s = 285 N^{0.333}$ $\left  \begin{array}{l} 1.000 \\ 1.018 \\ 1.086 \end{array} \right _S^{**}$	0.721
3	SPT N-value Geologic Age	$V_s = 302 N^{0.265}$ $\left  \begin{array}{l} 1.000 \\ 1.456 \end{array} \right _G^{**}$	0.784
4	SPT N-value Geologic Age Soil Type	$V_s = 306 N^{0.247}$ $\left  \begin{array}{l} 1.000 \\ 1.458 \end{array} \right _G \left  \begin{array}{l} 1.000 \\ 1.045 \\ 1.096 \end{array} \right _S$	0.786
5	SPT N-value Depth	$V_s = 155 N^{0.254} D^{0.222}$	0.820
6	SPT N-value Depth Soil Type	$V_s = 146 N^{0.218} D^{0.288}$ $\left  \begin{array}{l} 1.000 \\ 1.073 \\ 1.199 \end{array} \right _S$	0.826
7	SPT N-value Depth Geologic Age	$V_s = 180 N^{0.209} D^{0.188}$ $\left  \begin{array}{l} 1.000 \\ 1.308 \end{array} \right _S$	0.848
8	SPT N-value Depth Geologic Age Soil Type	$V_s = 179 N^{0.173} D^{0.195}$ $\left  \begin{array}{l} 1.000 \\ 1.306 \end{array} \right _G \left  \begin{array}{l} 1.000 \\ 1.085 \\ 1.189 \end{array} \right _S$	0.853

\* Depth in feet.

\*\* Ordinal numbers shall be interpreted as:

$\left  \begin{array}{l} Y_1 \\ Y_2 \end{array} \right _G$	$Y_1$ = factor corresponding to Holocene-age soil.
	$Y_2$ = factor corresponding to Pleistocene-age soils.

$\left  \begin{array}{l} Y_1 \\ Y_2 \\ Y_3 \end{array} \right _S$	$Y_1$ = factor corresponding to clays.
	$Y_2$ = factor corresponding to sands.
	$Y_3$ = factor corresponding to gravels.

**Table 2.7.** Imai and Tonouchi (1982) relationships between SPT N-value and  $V_s$  (Sykora, 1987)

Category	No. of Data	Shear Wave Velocity, fps		Shear Modulus, tsf	
		Best-Fit Relation	Correlation Coefficient	Best-Fit Relation	Correlation Coefficient
Clay fill	63	$V_s = 323 N^{0.248}$	0.574	$G = 158 N^{0.557}$	0.582
Loam	64	$V_s = 430 N^{0.153}$	0.314	$G = 229 N^{0.383}$	0.487
Sand fill	81	$V_s = 301 N^{0.257}$	0.647	$G = 145 N^{0.500}$	0.606
Tertiary clay and sand	108	$V_s = 358 N^{0.319}$	0.717	$G = 209 N^{0.686}$	0.682
Alluvial clay	325	$V_s = 351 N^{0.274}$	0.721	$G = 180 N^{0.607}$	0.715
Alluvial peat	17	$V_s = 209 N^{0.453}$	0.771	$G = 55.0 N^{1.08}$	0.769
Diluvial clay	222	$V_s = 420 N^{0.257}$	0.712	$G = 257 N^{0.555}$	0.712
Alluvial sand	294	$V_s = 288 N^{0.292}$	0.690	$G = 128 N^{0.611}$	0.871
Diluvial sand	338	$V_s = 361 N^{0.285}$	0.714	$G = 181 N^{0.631}$	0.729
Alluvial gravel	28	$V_s = 247 N^{0.351}$	0.791	$G = 84.5 N^{0.787}$	0.798
Diluvial gravel	114	$V_s = 446 N^{0.246}$	0.550	$G = 326 N^{0.528}$	0.552
All soils	1,654	$V_s = 318 N^{0.314}$	0.868	$G = 147 N^{0.680}$	0.867

\* Not adjusted for differences in energy efficiency between United States and Japanese SPT equipment and procedures.

**Table 2.8.** Effect of environmental and loading conditions on modulus ratio (at given strain level) of normally consolidated and moderately overconsolidated soils (modified from Dobry and Vucetic, 1987)

Increasing Factor	$G/G_{max}$
Confining pressure, $\sigma'_m$	Increase with $\sigma'_m$ ; effect decreases with increasing PI
Void ratio, $e$	Increases with $e$
Geologic age, $t_g$	May increase with $t_g$
Cementation, $c$	May increase with $c$
Overconsolidation ratio, OCR	Not affected
Plasticity index, PI	Increases with PI
Cyclic strain, $\gamma_c$	Decreases with $\gamma_c$
Strain rate, $\dot{\gamma}$	$G$ increases with $\dot{\gamma}$ , but $G/G_{max}$ probably not affected if $G$ and $G_{max}$ are measured at same $\dot{\gamma}$
Number of loading cycles, $N$	Decreases after $N$ cycles of large $\gamma_c$ ( $G_{max}$ measured before $N$ cycles) for clays; for sands, can increase (under drained conditions) or decrease (under undrained conditions)

**Table 2.9.** Effect of environmental and loading conditions on damping ratio of normally consolidated and moderately overconsolidated soils (modified from Dobry and Vucetic, 1987)

Increasing Factor	Damping ratio, $\xi$
Confining pressure, $\sigma'_m$	Decreases with $\sigma'_m$ ; effect decreases with increasing PI
Void ratio, $e$	Decreases with $e$
Geologic age, $t_g$	Decreases with $t_g$
Cementation, $c$	May decrease with $c$
Overconsolidation ratio, OCR	Not affected
Plasticity index, PI	Decreases with PI
Cyclic strain, $\gamma_c$	Increases with $\gamma_c$
Strain rate, $\dot{\gamma}$	Stays constant or may increase with $\dot{\gamma}$
Number of loading cycles, $N$	Not significant for moderate $\gamma_c$ and $N$

**Table 2.10.** Magnitude scaling factor (Seed and Idriss, 1982)

Anticipated Earthquake Magnitude	Magnitude Scaling Factor (MSF)
5.5	1.43
6.0	1.32
6.5	1.19
7.0	1.08
7.5	1.00
8.0	0.94
8.5	0.89

**Table 3.1.** Maximum estimated  $M_L$  for seismic source zones in Thailand region (after Nutalaya et al., 1985 and modified by Warnitchai and Lisantono, 1996)

Zone	Name	Maximum $M_L$
A	Arakan Coastal Area	6.75
B	West-Central Burma Basin	7.40
C	East-Central Burma Basin	7.75
D	Bhamo-Paoshan Area	5.96
E	Burma Eastern Highlands	7.30
F	Tenasserim Range	7.90
G	Northern Thailand	6.50
H	North Indochina	6.75
I	South Yunnan-Kwangsi	8.38
J	Andaman Arc	7.20
K	Andaman Basin	6.50

**Table 3.2.** Summary of input motions used in analyses

Earthquake	Year	Station	$a_{max}$ (g)	$T_p$ (sec)
Northridge	1994	Topanga	0.33	0.31
El Centro	1940	El Centro	0.34	0.68
Loma Prieta	1989	Yerba Buena Island	0.065	1.41

**Table 6.1.** Physical properties of sand used in cyclic triaxial test (Gauchan, 1984)

Gs	D <sub>50</sub> (mm)	Cu	e <sub>max</sub>	e <sub>min</sub>	γ <sub>max</sub> (t/m <sup>3</sup> )	γ <sub>min</sub> (t/m <sup>3</sup> )
2.64	0.72	3.52	0.88	0.54	1.71	1.40

**Table 6.2.** Model parameters (Iai et al., 1993)

Parameter	Type of Mechanism	Kind of the Parameter
$K_{ma}$	Elastic volumetric	Rebound modulus
$G_{ma}$	Elastic shear	Shear modulus
$\phi_f$	Plastic shear	Shear resistance angle
$\phi_p$	Plastic dilatancy	Phase transformation angle
$H_m$	Plastic shear	Hysteretic damping factor at large shear strain level
$p_1$	Plastic dilatancy	Initial phase of dilatancy
$p_2$	Plastic dilatancy	Final phase of dilatancy
$w_1$	Plastic dilatancy	Overall dilatancy
$S_1$	Plastic dilatancy	Ultimate limit of dilatancy
$c_1$	Plastic dilatancy	Threshold limit

**Table 6.3.** Model parameters for dilatancy

Dr (%)	$w_1$	$p_1$	$p_2$	$c_1$	$S_1$
45-50	38.5	0.7	0.4	1.0	0.005
55-65	9.5	0.6	0.5	1.0	0.005
75-85	18.8	0.6	0.8	1.0	0.005



**Table 6.4.** Summary of the estimated values of factor of safety based on the procedure proposed by Seed et al. (1983)

Chiang Mai				Chiang Rai			
Site no.	Factor of Safety			Site no.	Factor of Safety		
	$P_L = 5\%$	$P_L = 10\%$	$P_L = 30\%$		$P_L = 5\%$	$P_L = 10\%$	$P_L = 30\%$
1	0.51	0.64	0.95	1	2.74	3.40	5.03
2	0.51	0.63	0.94	2	1.39	1.72	2.55
3	0.66	0.82	1.21	3	2.01	2.50	3.70
4	1.26	1.56	2.31	4	0.84	1.03	1.53
5	1.68	2.08	3.08	5	0.36	0.45	0.67
6	0.57	0.70	1.03	6	0.60	0.74	1.10
7	1.23	1.52	2.25	7	1.00	1.24	1.83
8	0.83	1.02	1.51	8	0.99	1.23	1.82
9	0.64	0.79	1.17	9	1.26	1.57	2.32
10	0.89	1.10	1.63	10	0.77	0.96	1.42
11	1.23	1.52	2.25	11	0.49	0.61	0.90
12	1.80	2.23	3.30	12	1.05	1.30	1.92
13	1.66	2.06	3.06	13	0.86	1.06	1.57
14	0.69	0.87	1.27	14	0.50	0.63	0.93
15	0.87	1.08	1.60	15	1.05	1.30	1.93
16	0.50	0.62	0.92	16	10.24	12.72	18.81
17	0.52	0.65	0.96	17	0.78	0.98	1.44
18	0.58	0.71	1.06				
19	1.42	1.77	2.61				
20	0.81	1.00	1.48				
21	1.09	1.35	1.99				
22	1.03	1.29	1.91				
23	1.95	2.43	3.59				
24	0.85	1.05	1.55				
25	0.65	0.82	1.20				
26	2.04	2.53	3.74				
27	1.06	1.31	1.93				
28	0.45	0.56	0.83				
29	0.86	1.07	1.58				



**FIGURES**

สถาบันวิทยบริการ  
จุฬาลงกรณ์มหาวิทยาลัย

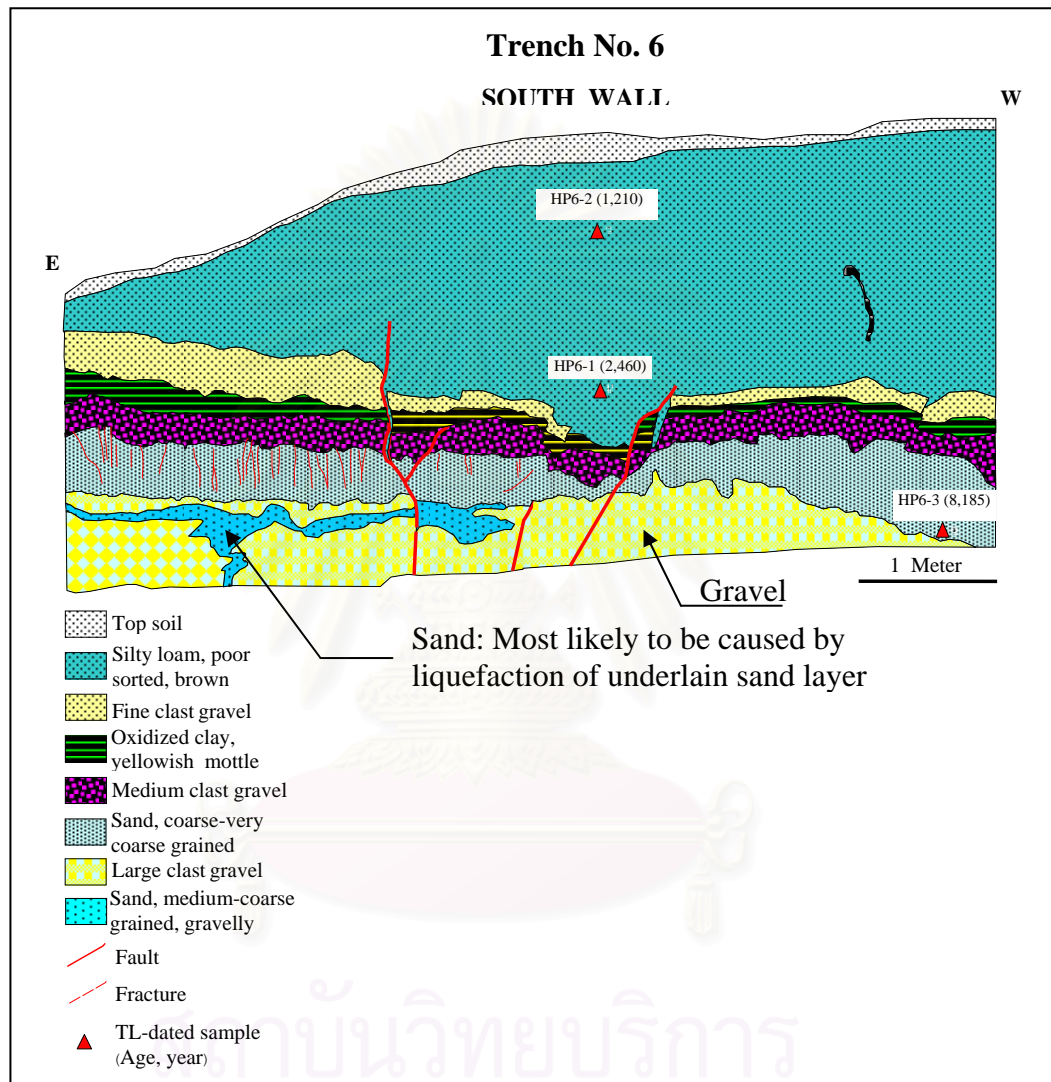


**Fig. 1.1.** Evidence indicating the occurrence of liquefaction in the northern area of Thailand

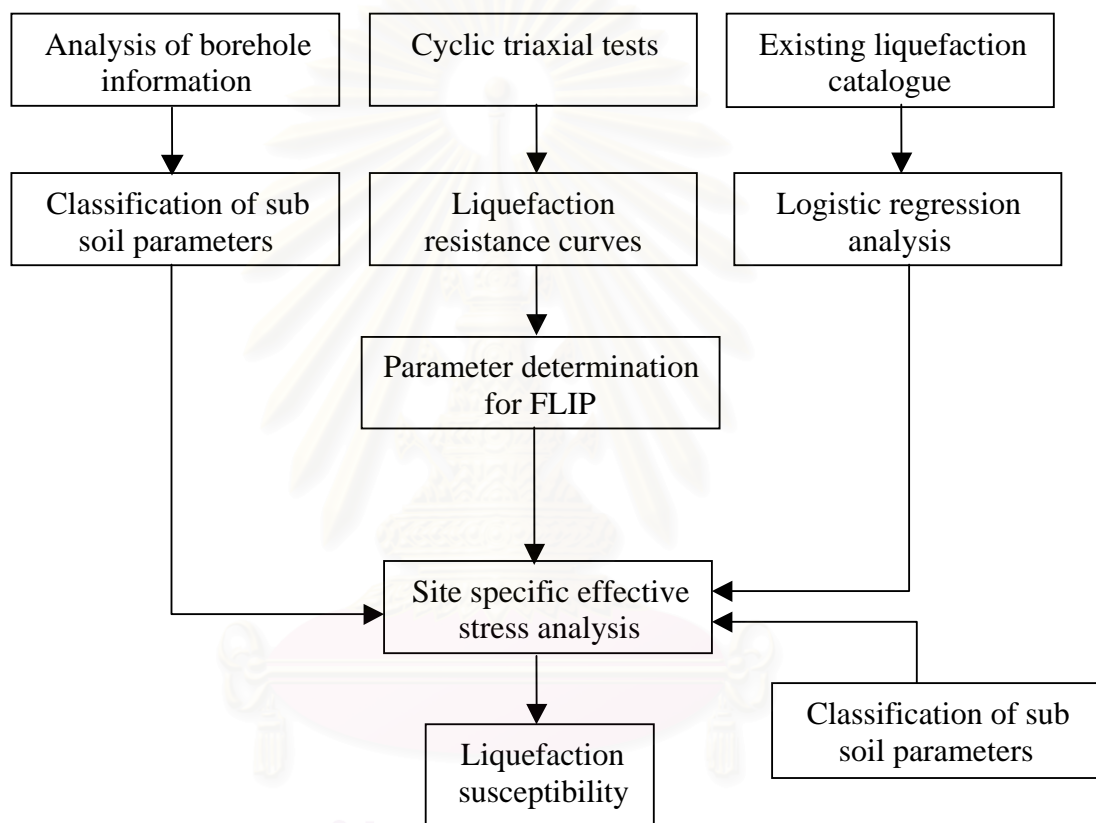


**Fig. 1.2.** General study methodology adopted

สถาบันวิทยบริการ  
จุฬาลงกรณ์มหาวิทยาลัย

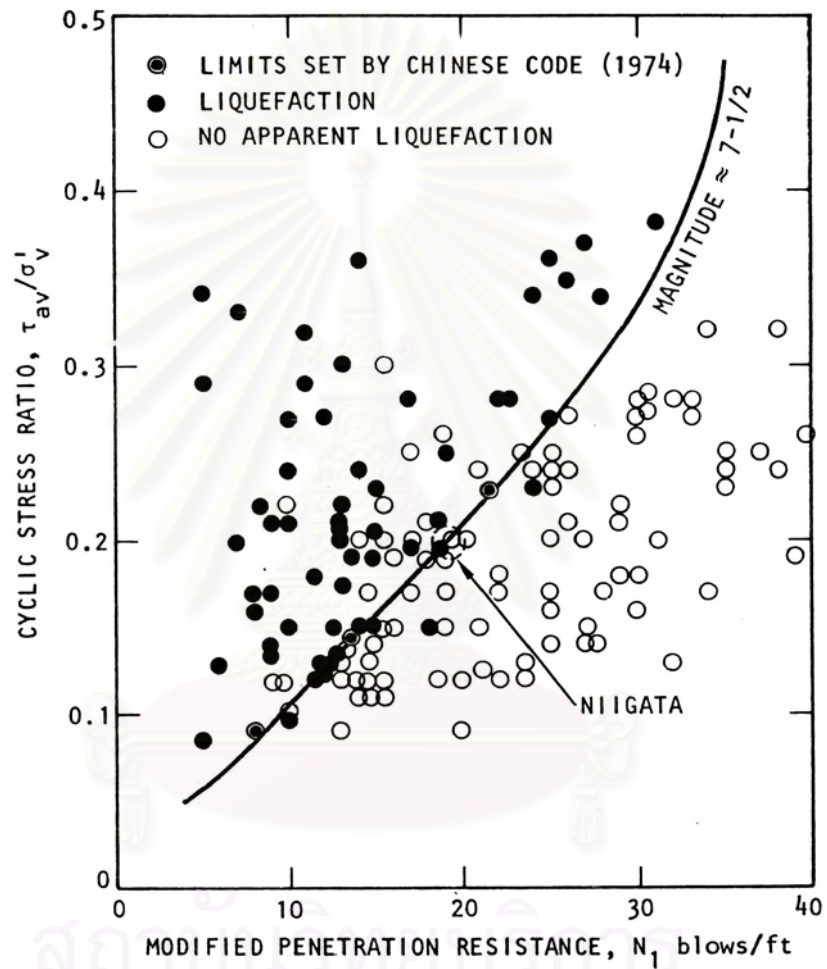


**Fig. 1.3.** Example of deterministic method of liquefaction evaluation derived from empirical data for soils with  $D_{50} > 0.25$  mm (Seed et al., 1983)

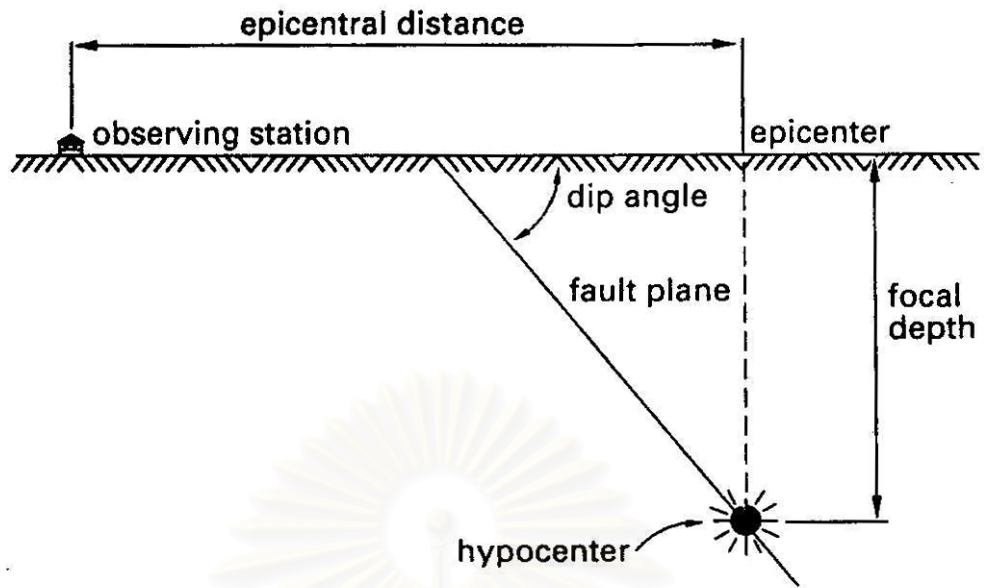


**Fig. 2.1.** Earthquake terminology (Lindeburg, 1998)

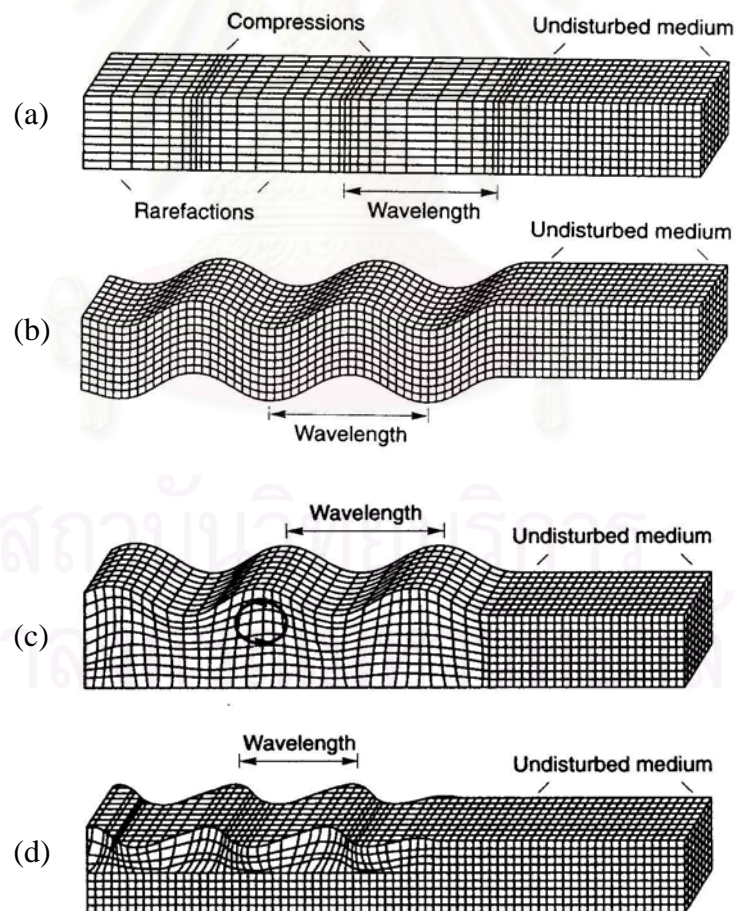


**Fig. 2.2.** Types of seismic waves: (a) P-wave; (b) S-wave; (c) R-wave; (d) L-wave (Kramer, 1996)

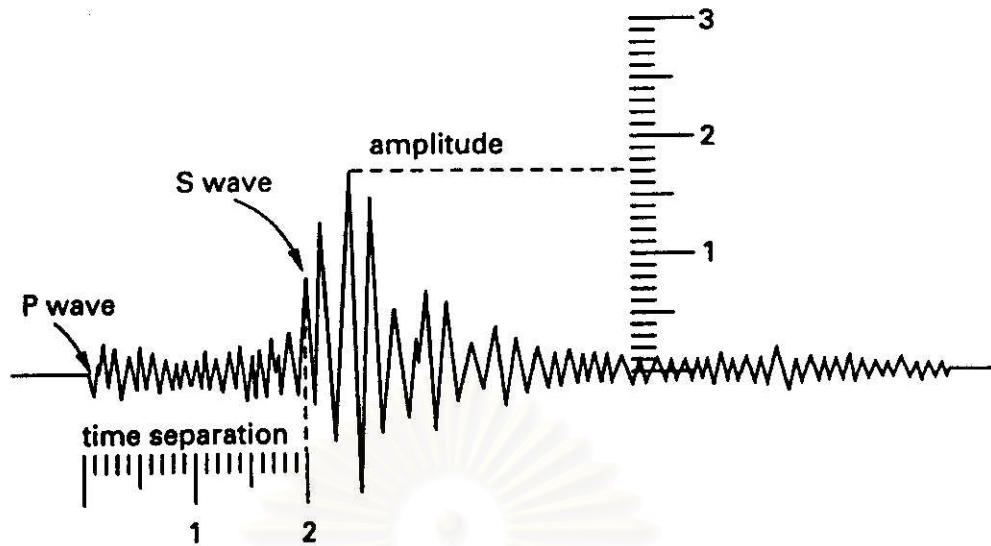


Fig. 2.3. Typical seismometer amplitude trace (Lindeburg, 1998)

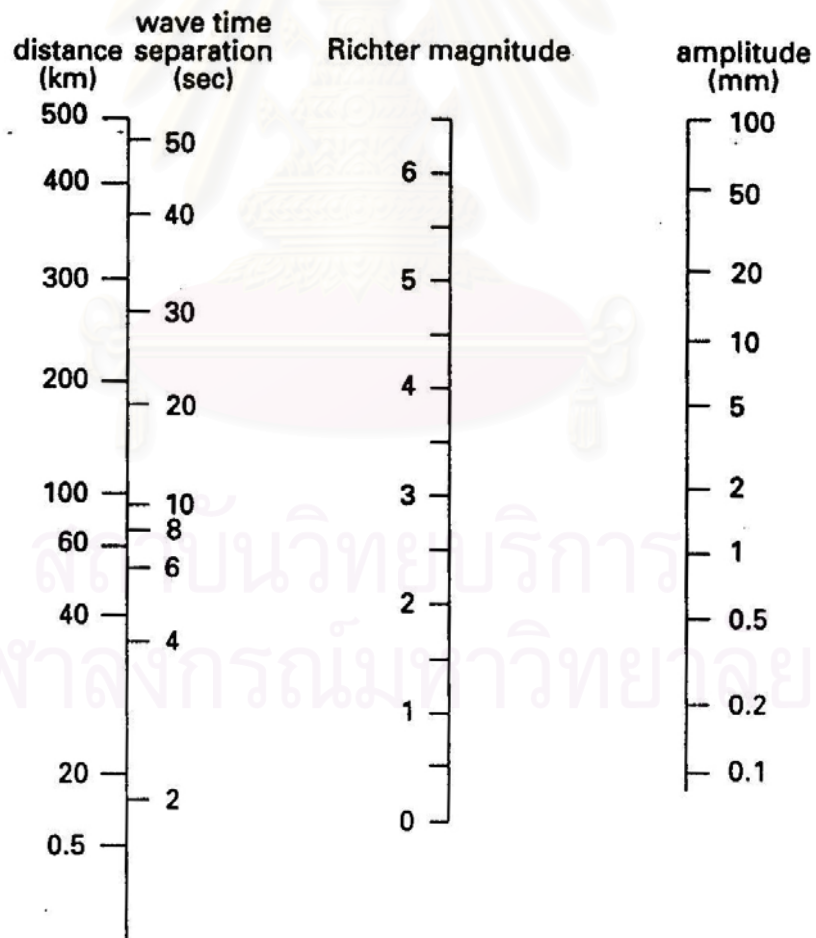
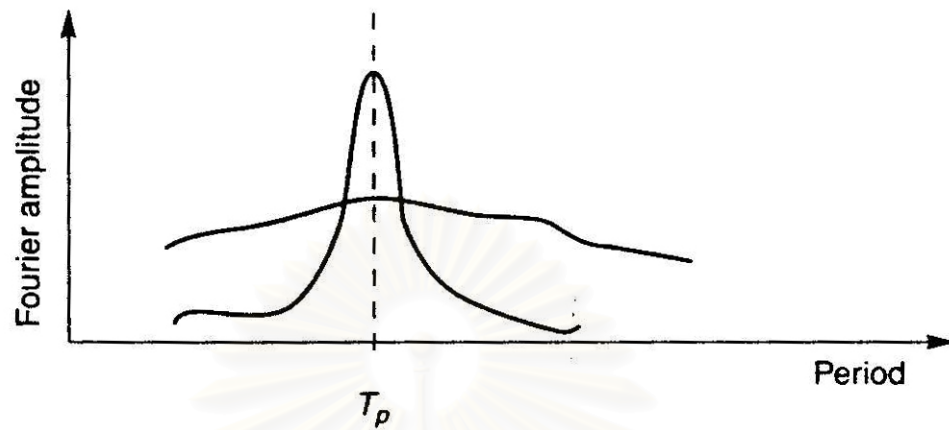
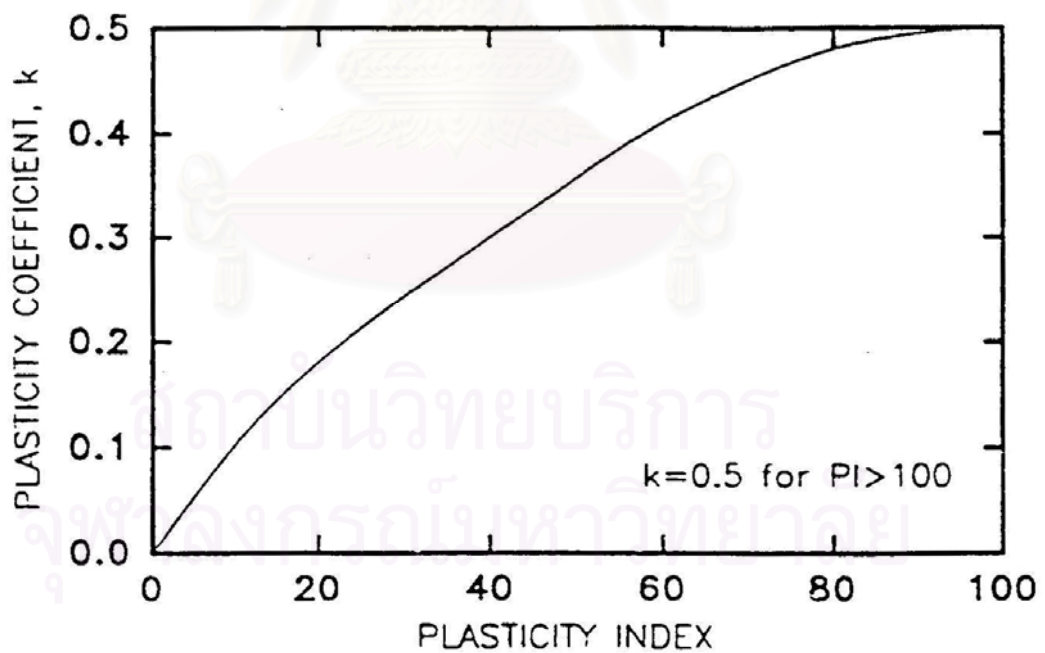


Fig. 2.4. Richter magnitude correction nomograph (Lindeburg, 1998)



**Fig. 2.5.** Two hypothetical Fourier amplitude spectra with the same predominant period but very different frequency contents. The upper curve describes a wideband motion and the lower a narrowband motion



**Fig. 2.6.** Variation of k-coefficient with plasticity index (Dickenson, 1994)



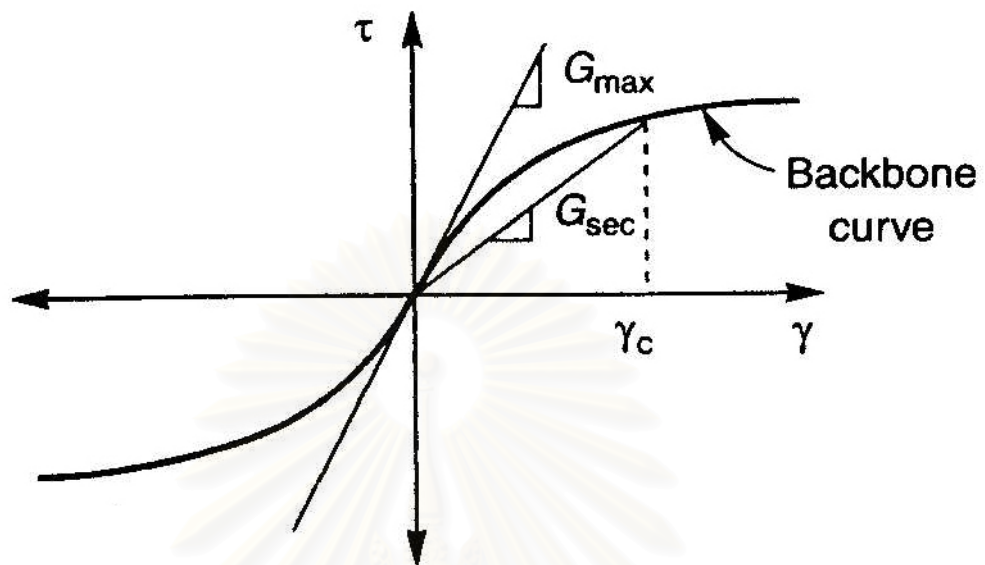


Fig. 2.7. Backbone curve showing typical variation of  $G_{\text{sec}}$  with shear strain

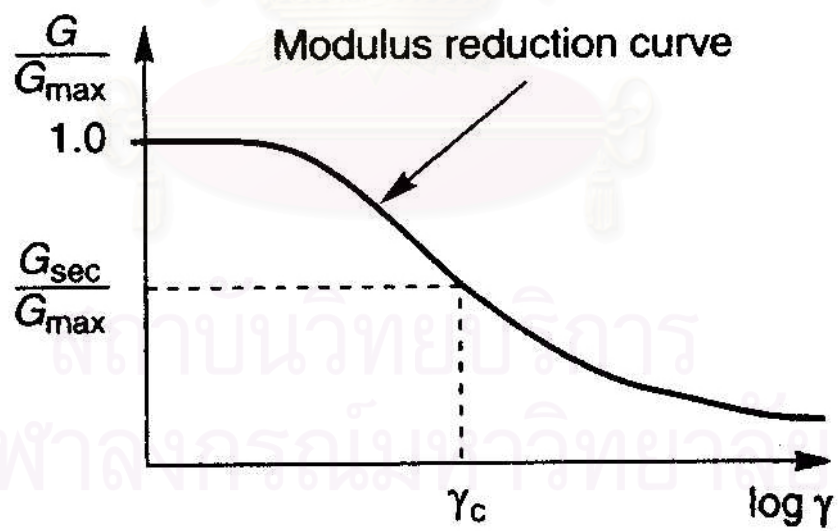
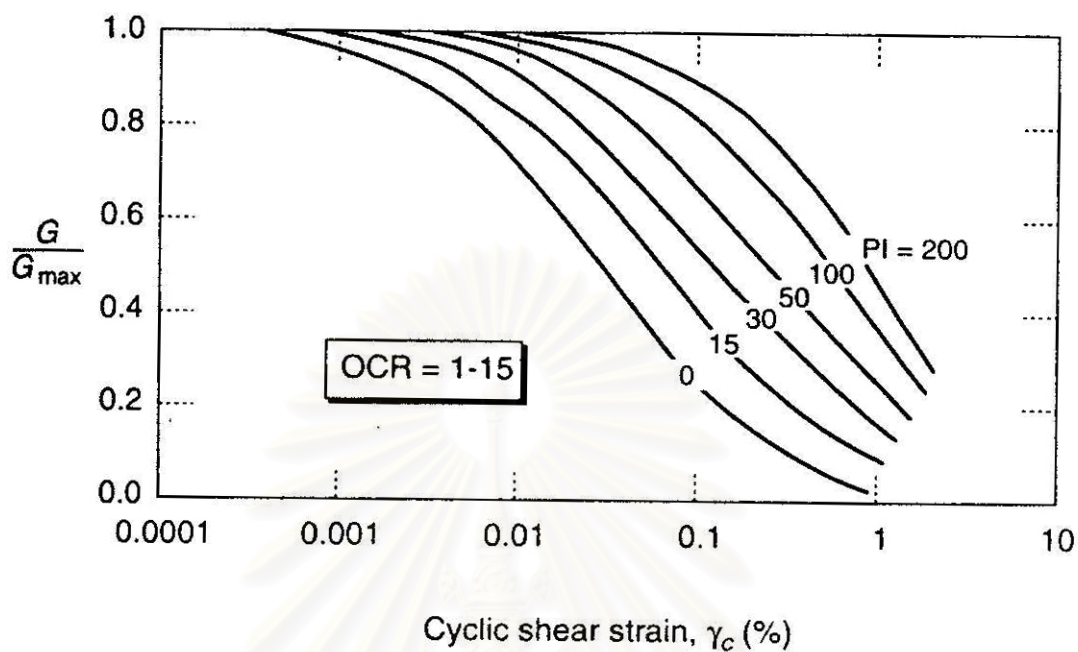
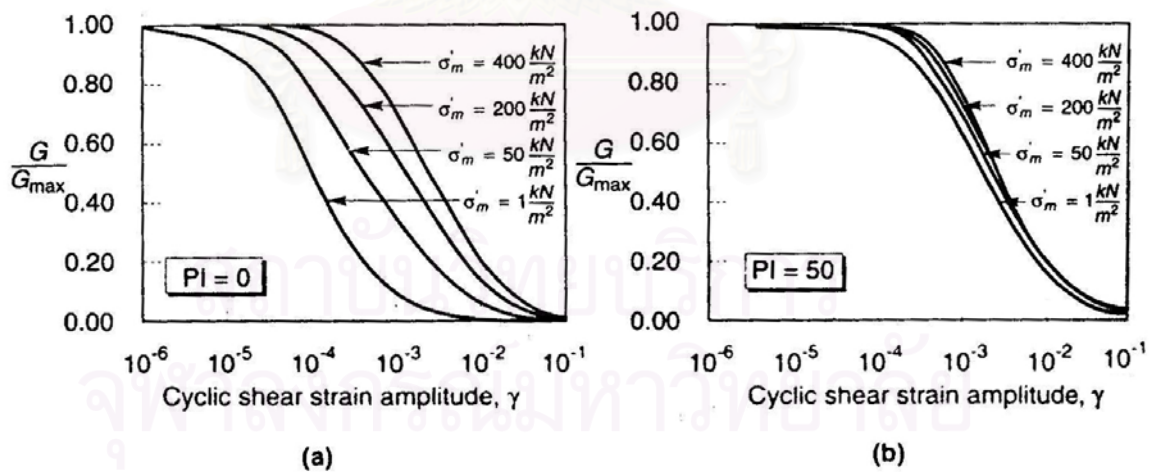


Fig. 2.8. Variation of the modulus ratio with shear strain



**Fig. 2.9.** Modulus reduction curves for fine-grained soils of different plasticity (Vucetic and Dobry, 1991)



**Fig. 2.10.** Influence of mean effective confining pressure on modulus reduction curves for (a) nonplastic ( $PI = 0$ ) soil, and (b) plastic ( $PI = 50$ ) soil (Ishibashi, 1992)

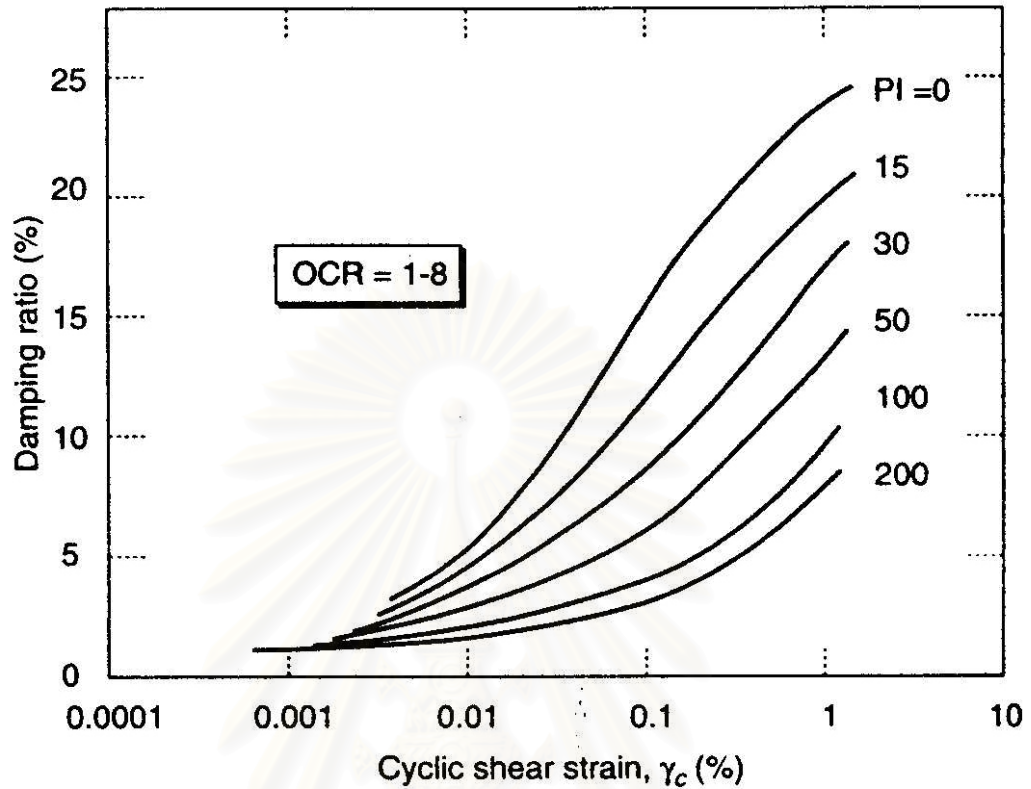


**Fig. 2.11.** Variation of damping ratio of fine-grained soil with cyclic shear strain amplitude and plasticity index (Vucetic and Dobry, 1991)

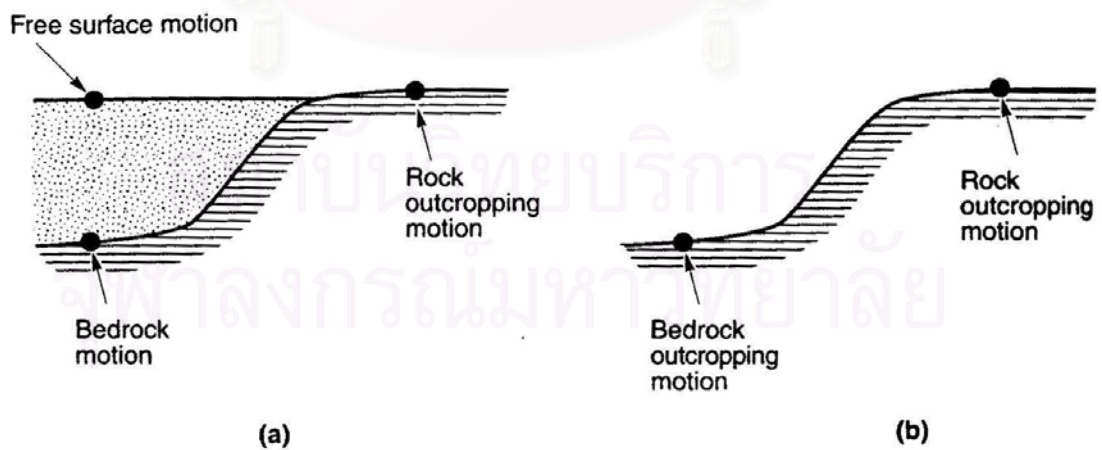


**Fig. 2.12.** Ground response nomenclature: (a) soil overlying bedrock; (b) no soil overlying bedrock

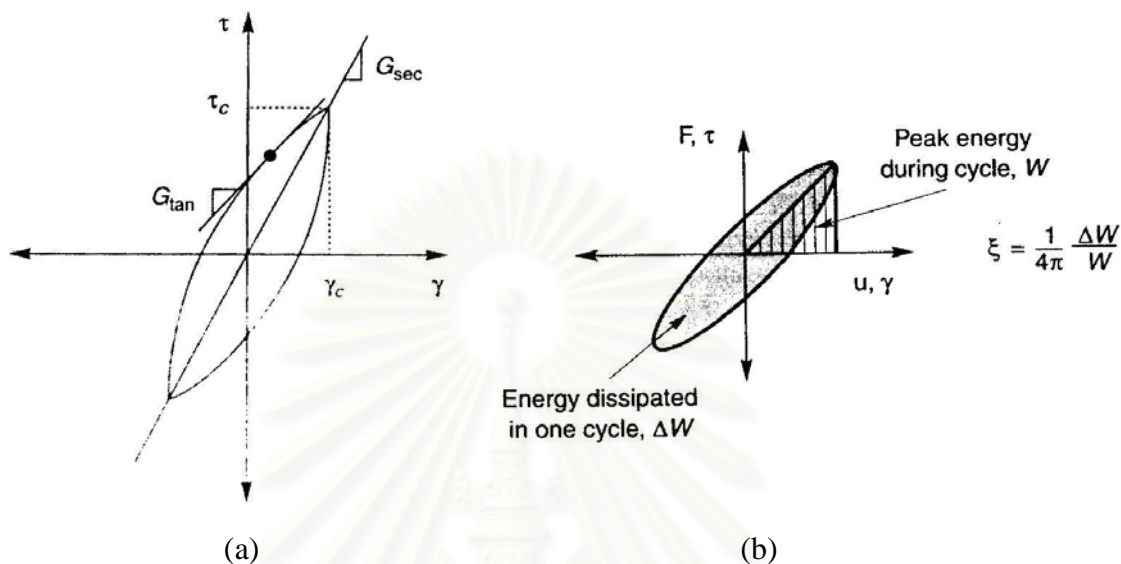


**Fig. 2.13.** Relationship between hysteresis loop and: (a) shear modulus; (b) damping ratio

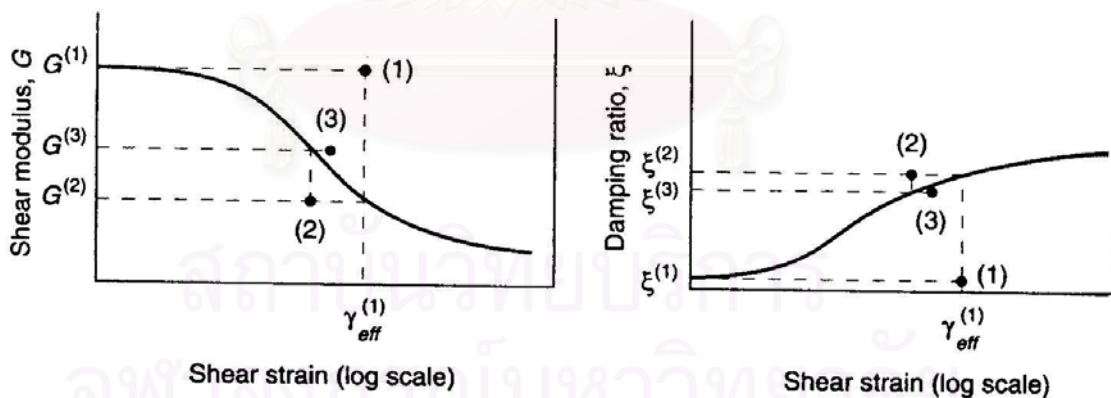


**Fig. 2.14.** Iteration toward strain-compatible shear modulus and damping ratio in equivalent linear analysis

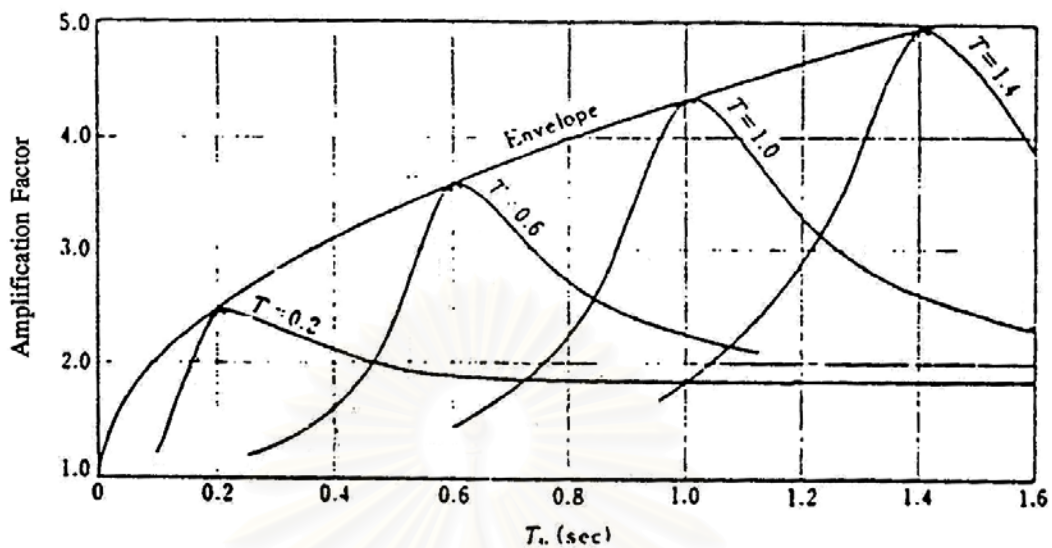


Fig. 2.15. Kanai's amplification factor for soft ground (Kanai, 1957)

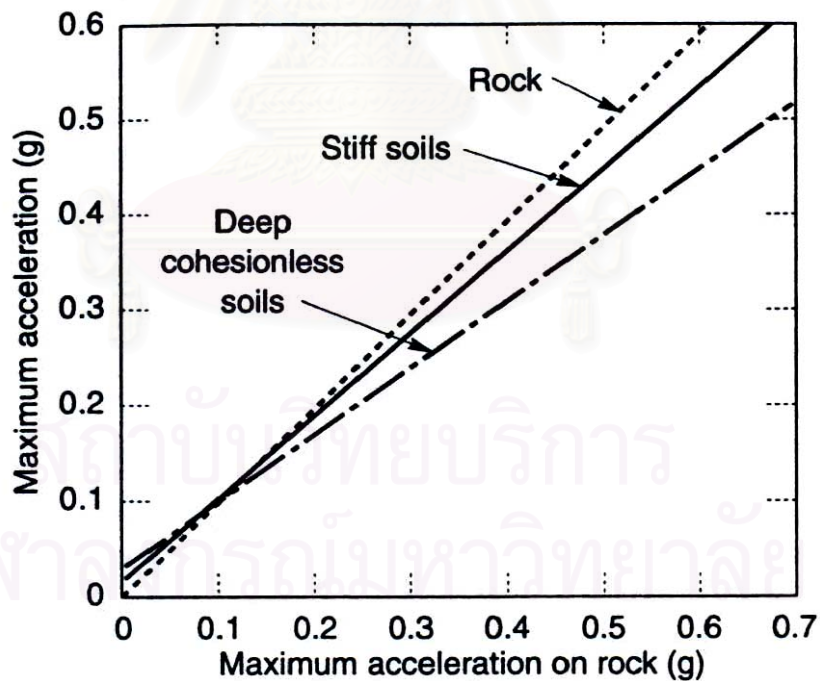
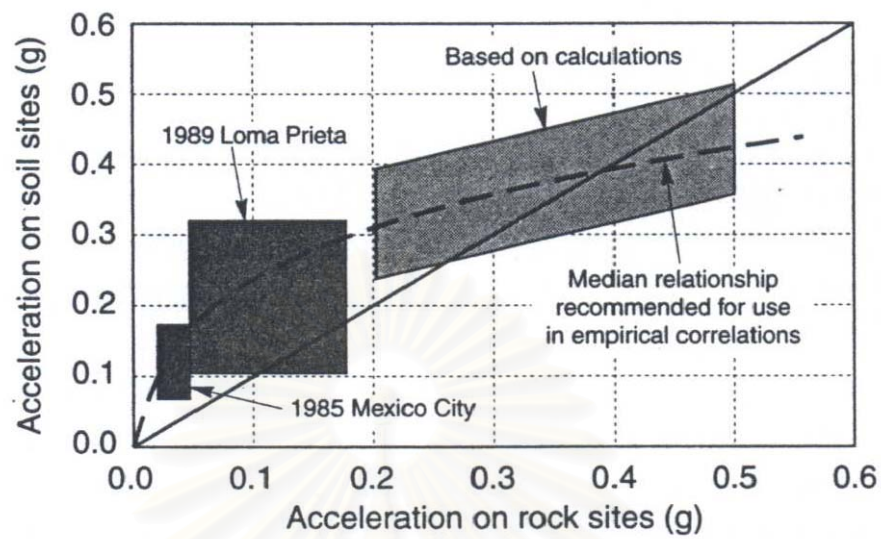
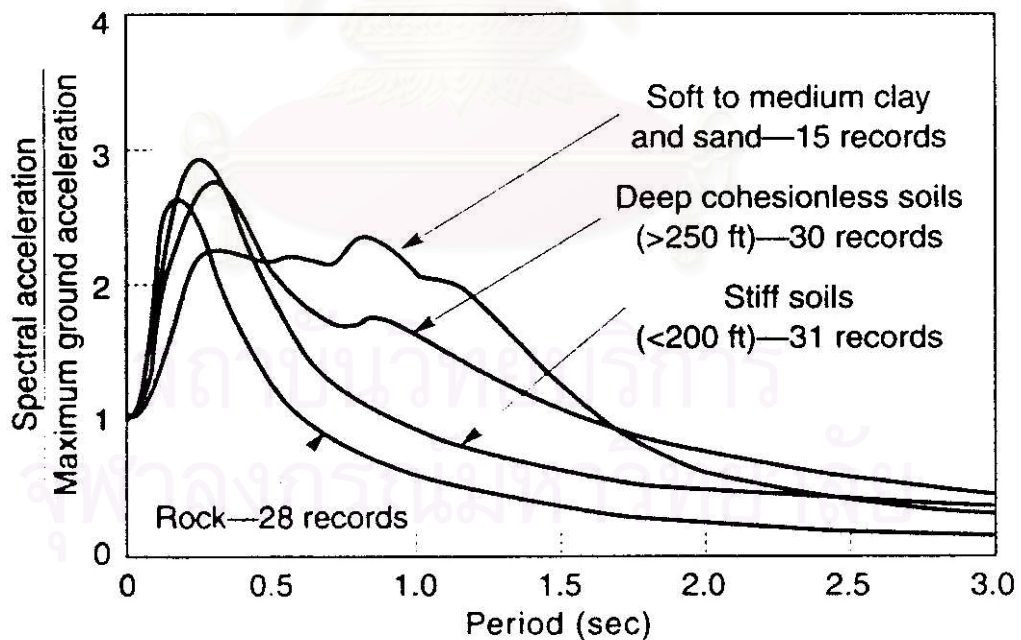


Fig. 2.16. Approximate relationships between peak accelerations on rock and other local site conditions (Seed et al., 1976)



**Fig. 2.17.** Approximate relationship between peak accelerations on rock and soft soil sites (Idriss, 1990)



**Fig. 2.18.** Average normalized response spectra (5% damping) for different local site conditions (Seed et al., 1976)

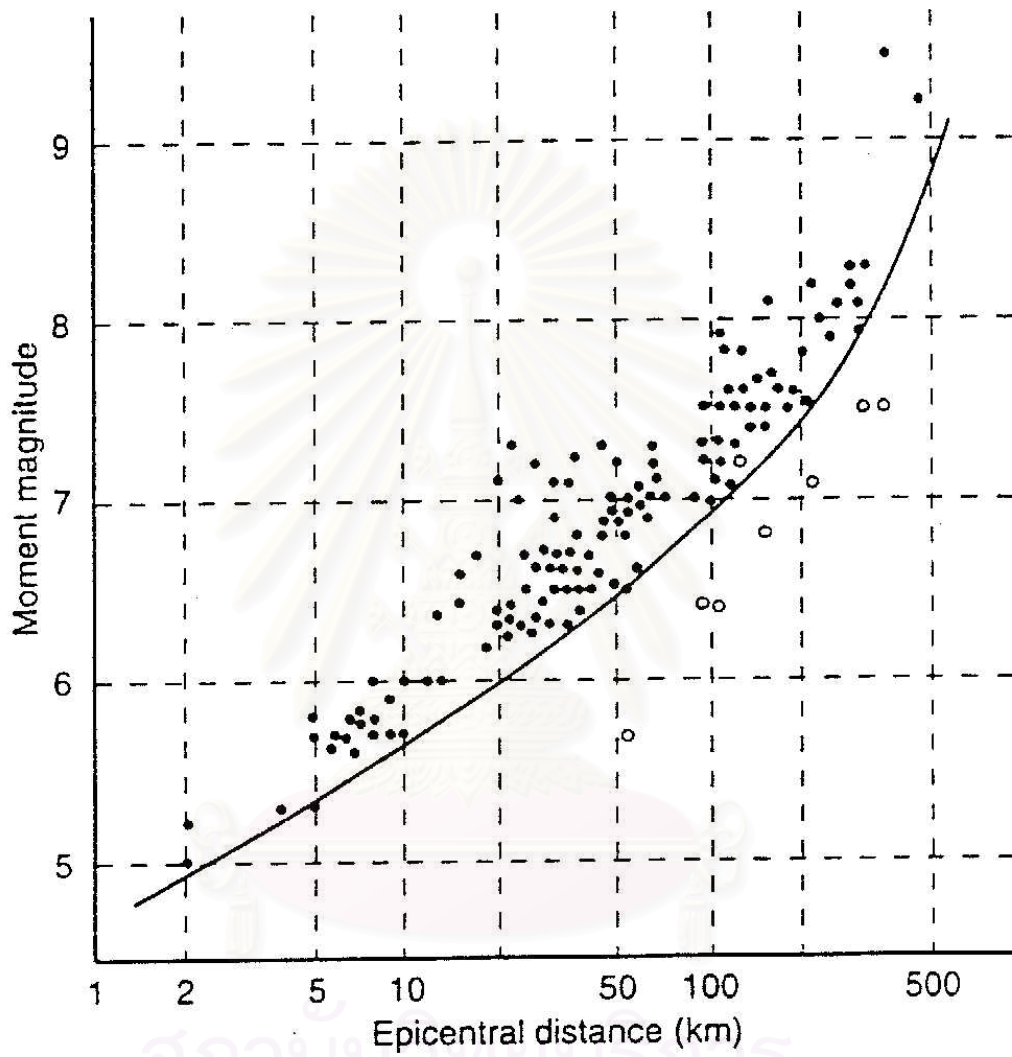


**Fig. 2.19.** Relationship between limiting epicentral distance of sites at which liquefaction has been observed and moment magnitude for shallow earthquakes. Deep earthquakes (focal depths  $> 50$  km) have produced liquefaction at greater distances. (Ambraseys, 1988)

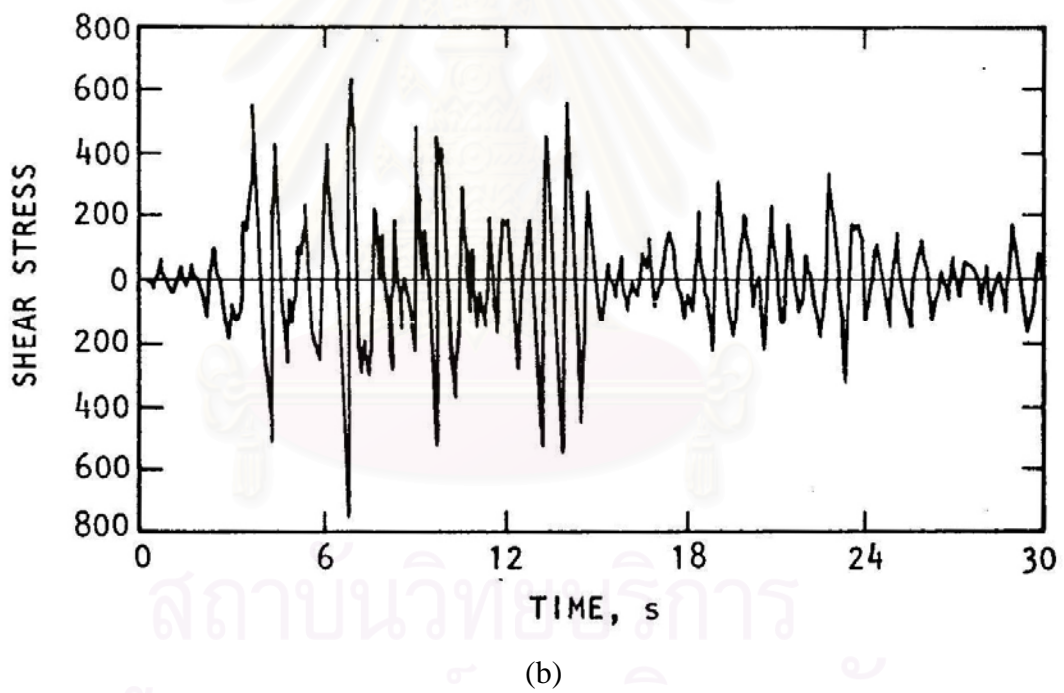
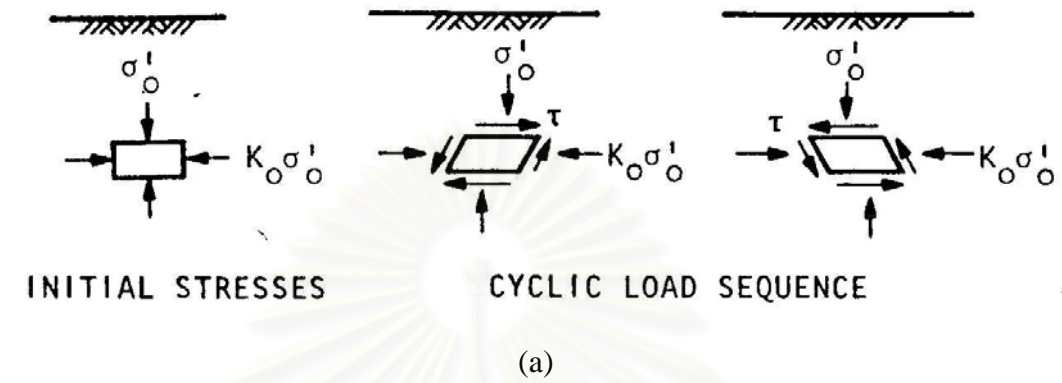


**Fig. 2.20.** Cyclic shear stresses on soil element during ground shaking: (a) idealized field loading conditions; (b) shear stress variation determined by response analysis



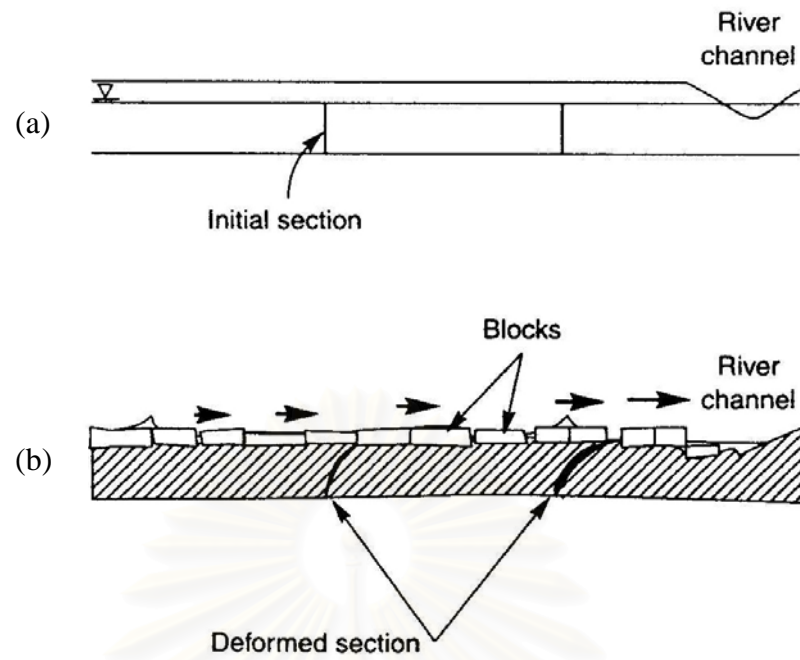


**Fig. 2.21.** Lateral spreading adjacent to a river channel: (a) before earthquake; (b) after earthquake (Youd, 1984)

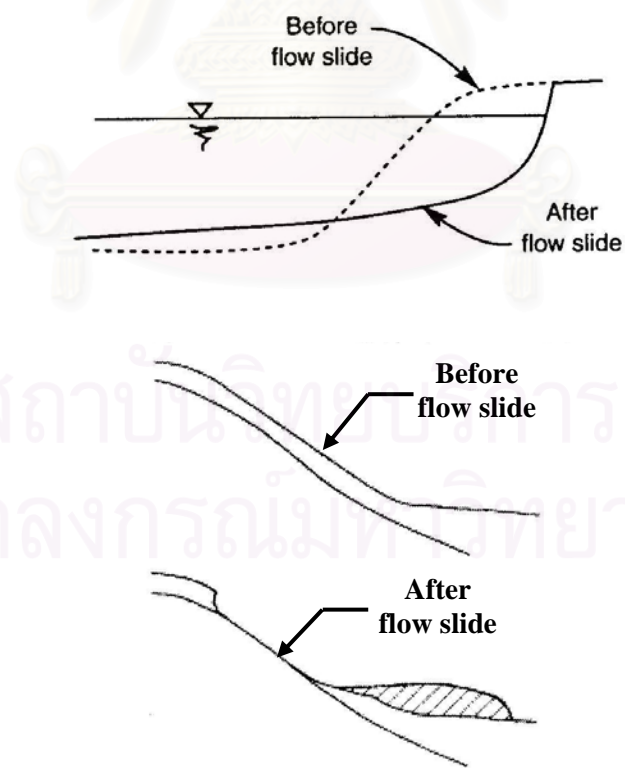


**Fig. 2.22.** Examples of flow failure caused by liquefaction and loss of strength of soils lying on a steep slope

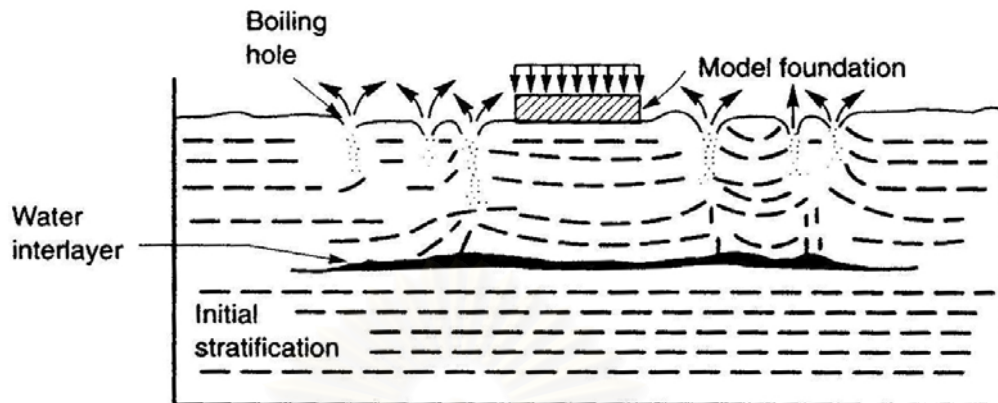


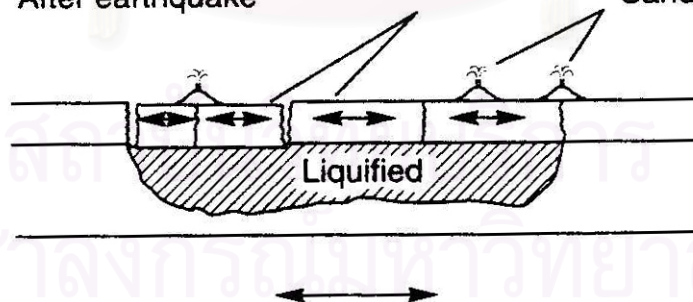
**Fig. 2.23.** Formation of water interlayers in shaking table tests of Liu and Qiao, (1984)

Before earthquake



(a)

After earthquake



(b)

**Fig. 2.24.** Ground oscillation: (a) before earthquake; (b) after earthquake (Youd, 1984)



**Fig. 2.25.** Example of structure tilted due to loss of bearing strength. Liquefaction weakens the soil reducing foundation support which allows heavy structures to settle and tip.



**Fig. 2.26.** Tilting of apartment buildings, Niigata (1964)

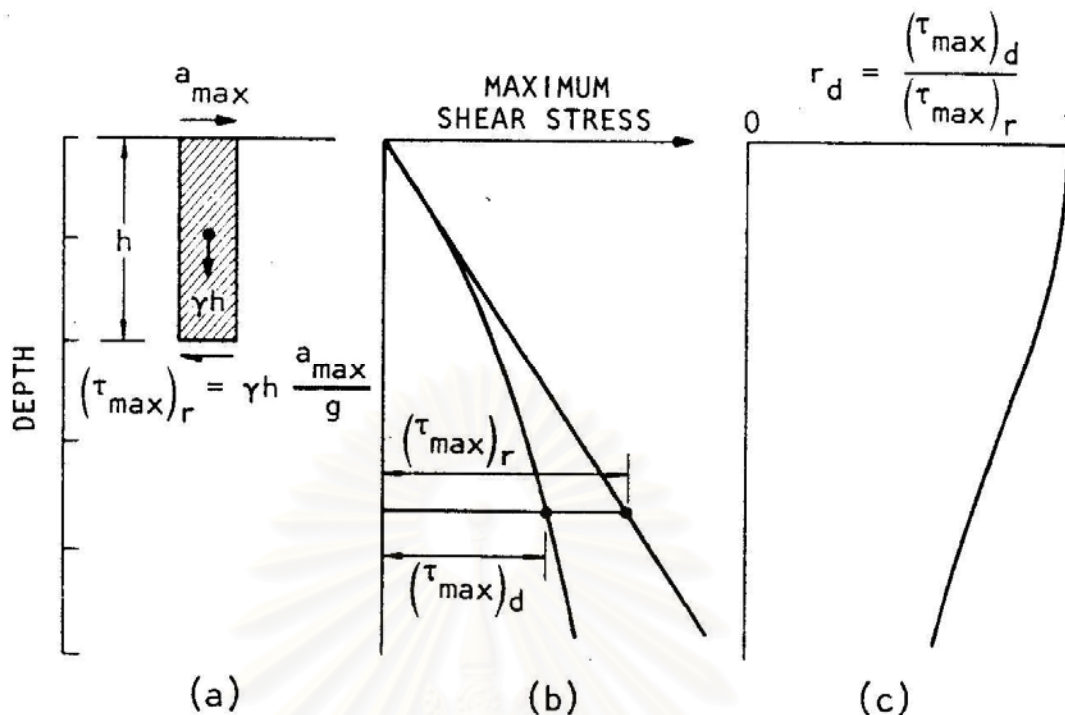


**Fig. 2.27.** Procedure for determining maximum shear stress,  $(\tau_{\max})_r$  (Seed and Idriss, 1982)

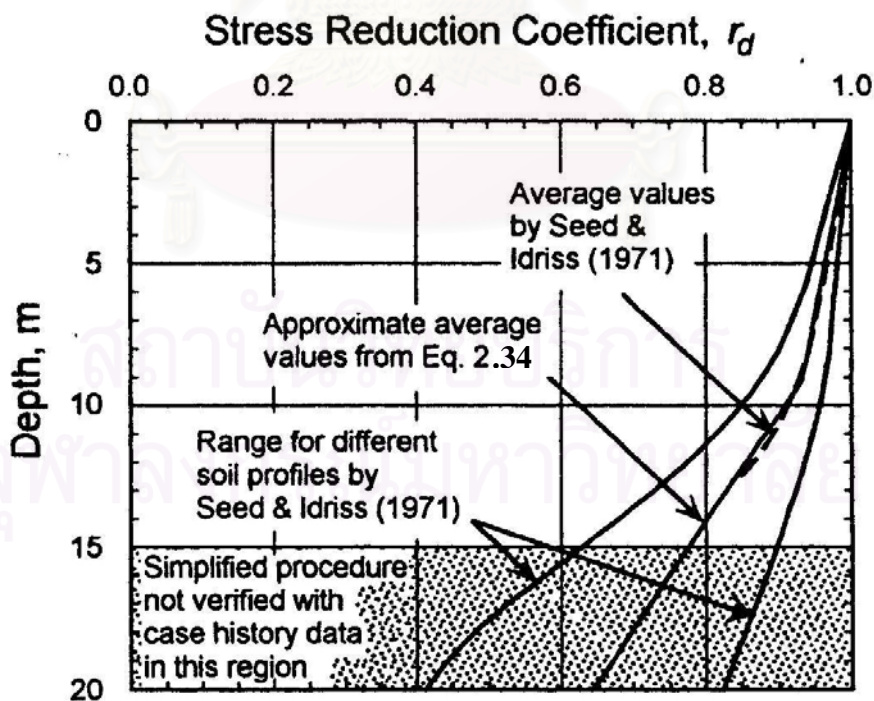


**Fig. 2.28.**  $r_d$  versus depth curves developed by Seed and Idriss (1971) with add mean-value lines plotted from Eq. (2.34) (Youd and Idriss, 2001)

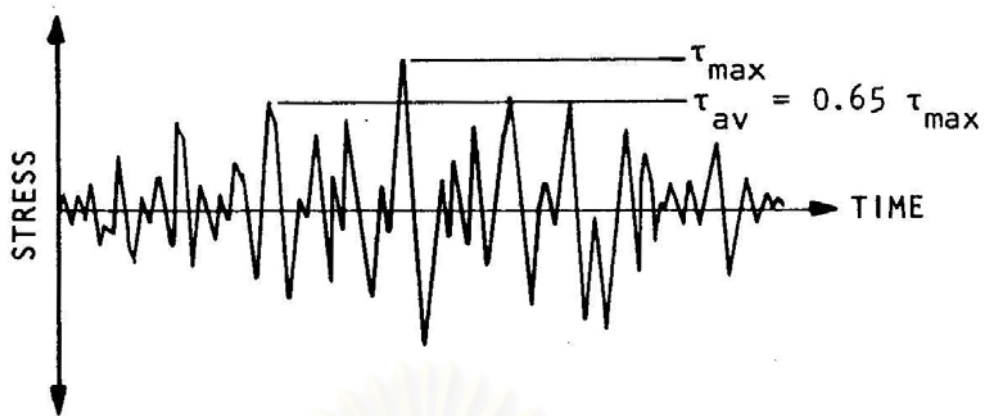


Fig. 2.29. Time history of shear stresses during earthquake (Seed and Idriss, 1982)

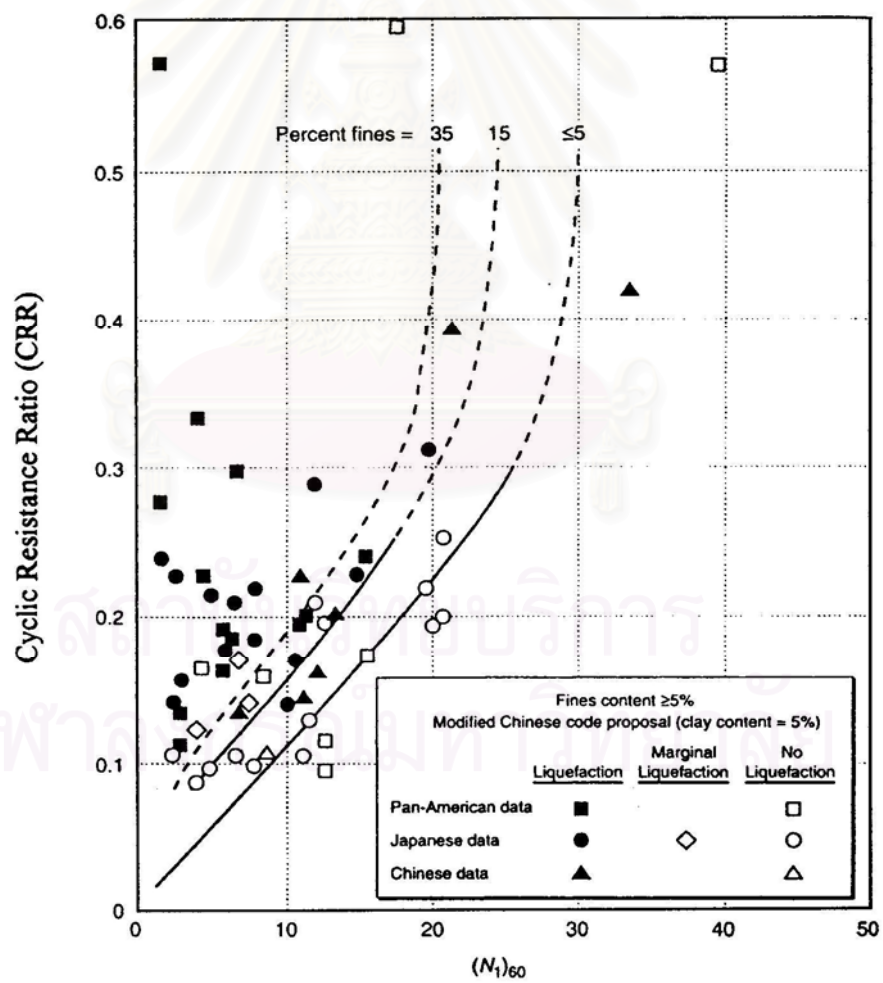
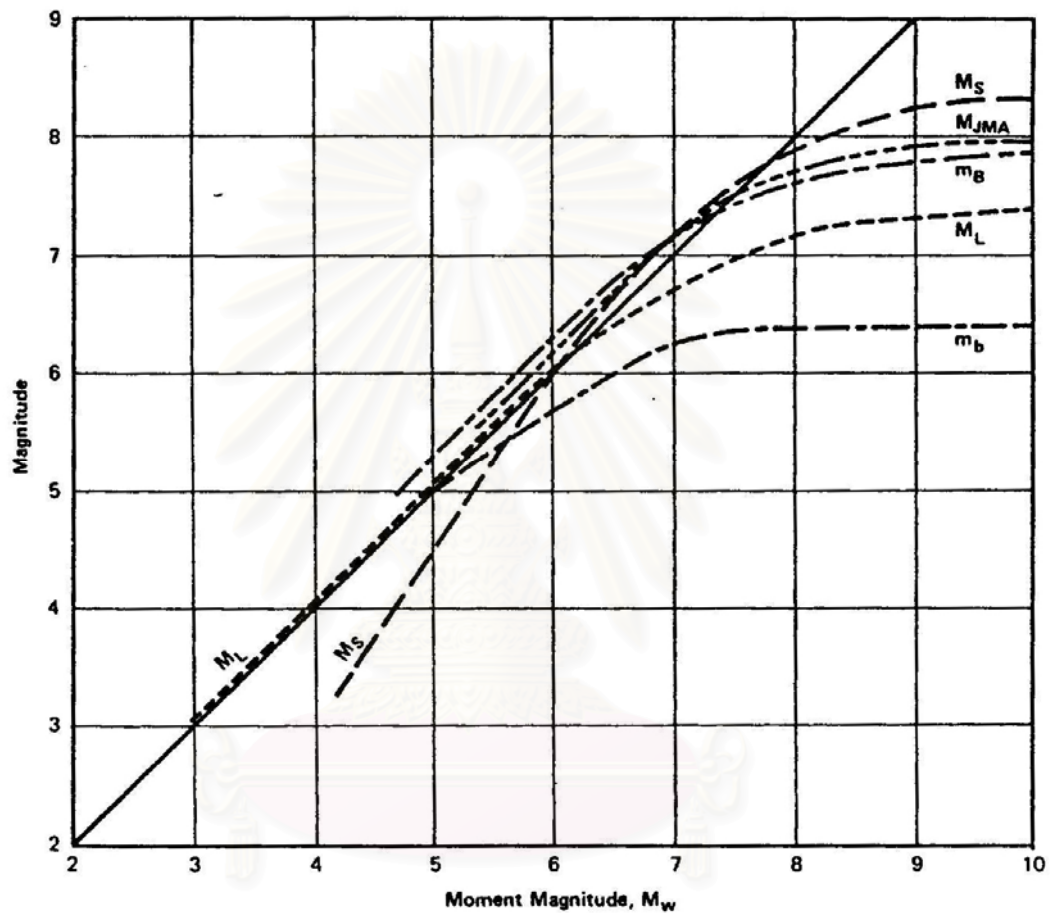
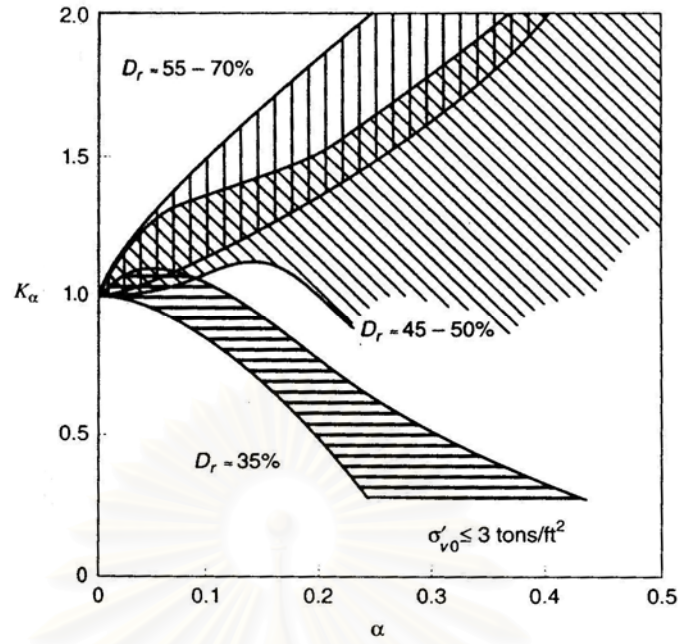


Fig. 2.30. Plot used to determine the cyclic resistance ratio for clean and silty sands for  $M = 7.5$  earthquakes (Seed et al., 1985)



**Fig. 2.31.** Approximate relationships between the moment magnitude scale  $M_w$  and other magnitude scales. Shown are the short-period body wave magnitude scale  $m_b$ , the local magnitude scale  $M_L$ , the long-period body wave magnitude scale  $m_B$ , the Japan Meteorological Agency magnitude scale  $M_{JMA}$ , and the surface-wave magnitude scale  $M_S$  (reproduced from Day, 2002)



**Fig. 2.32.** Variation of correction factor,  $K_\alpha$ , with initial shear/normal stress ratio (Seed and Harder, 1990)

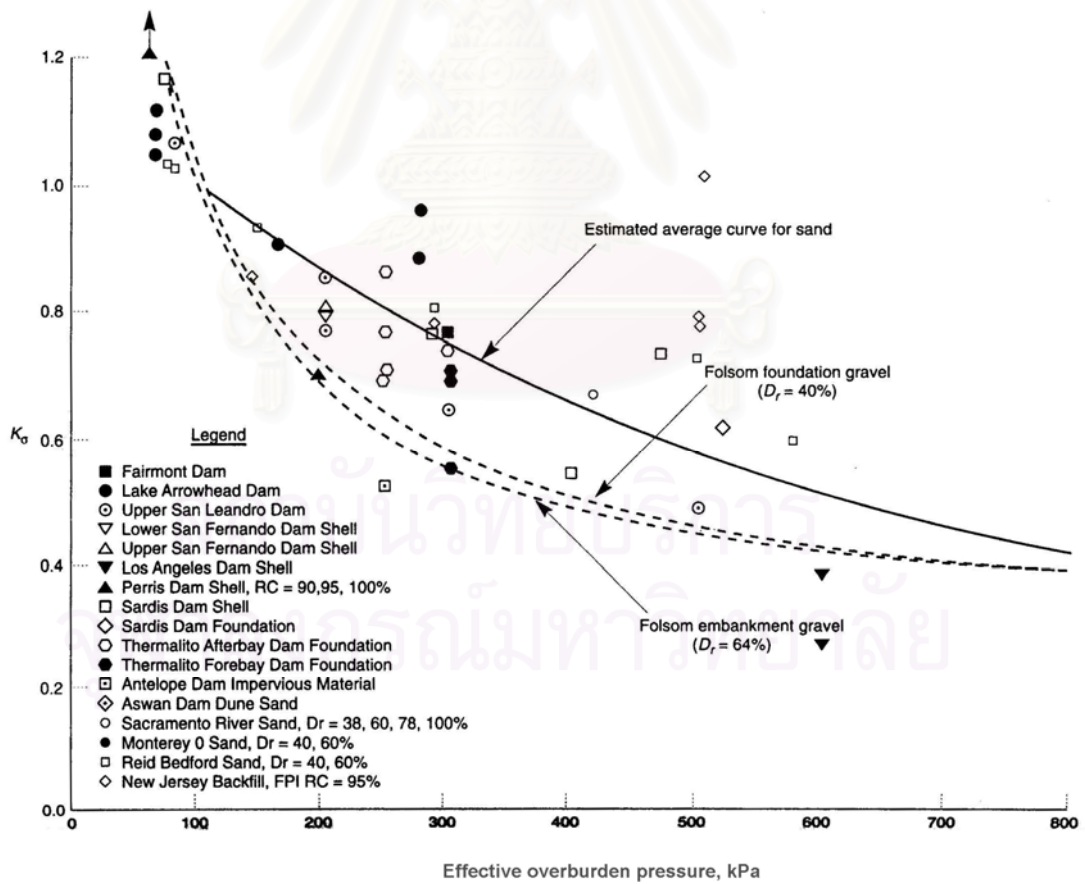


**Fig. 2.33.** Variation of correction factor,  $K_\sigma$ , with effective overburden pressure (Seed and Harder, 1990)

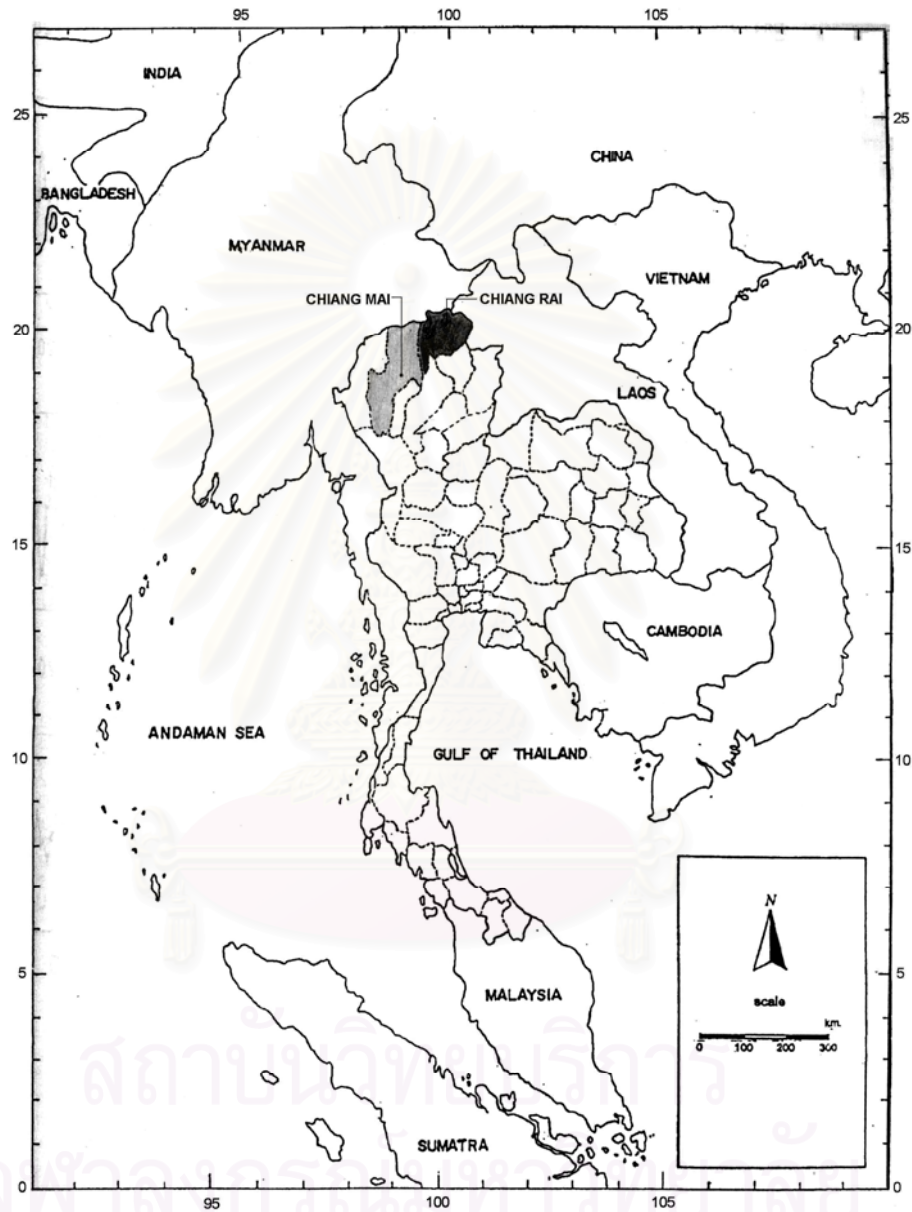


**Fig. 3.1.** Location of the study area



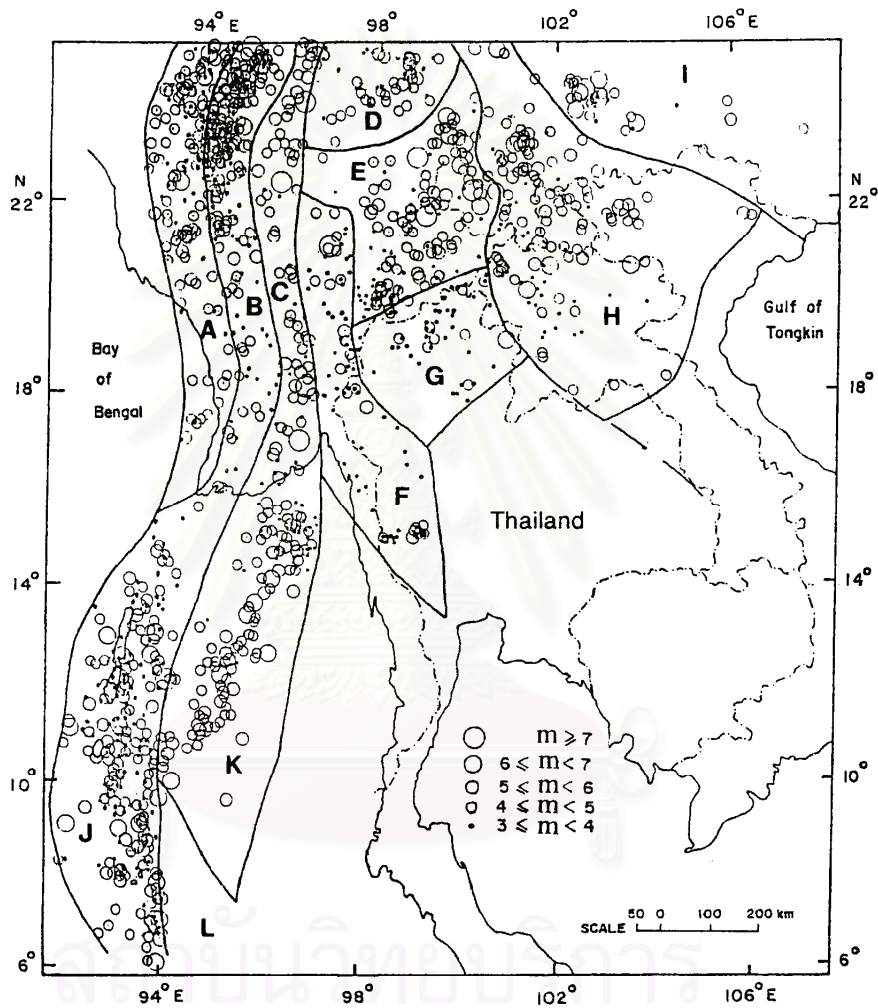
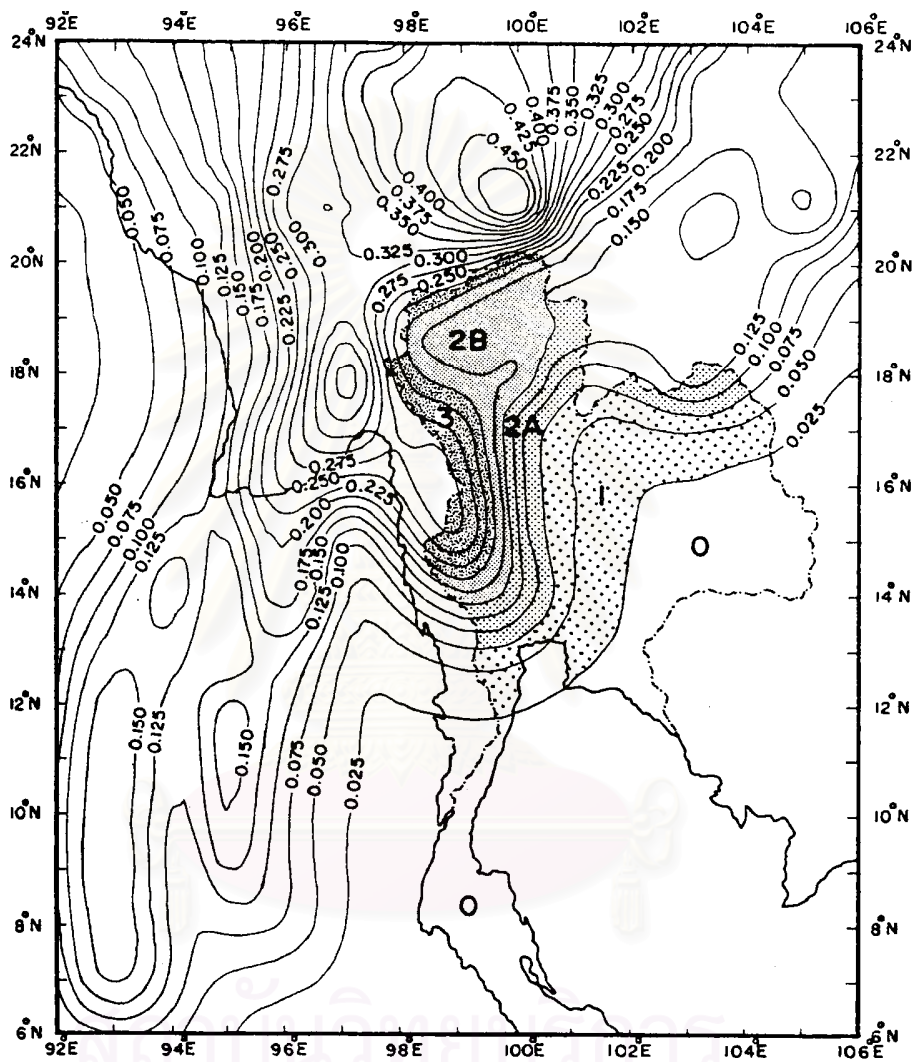
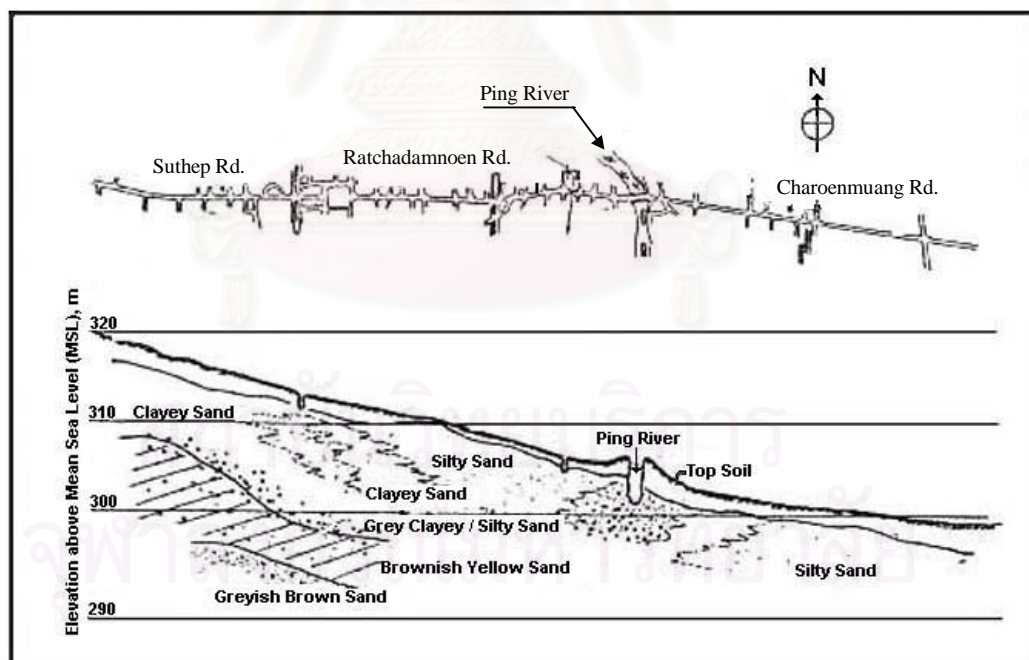
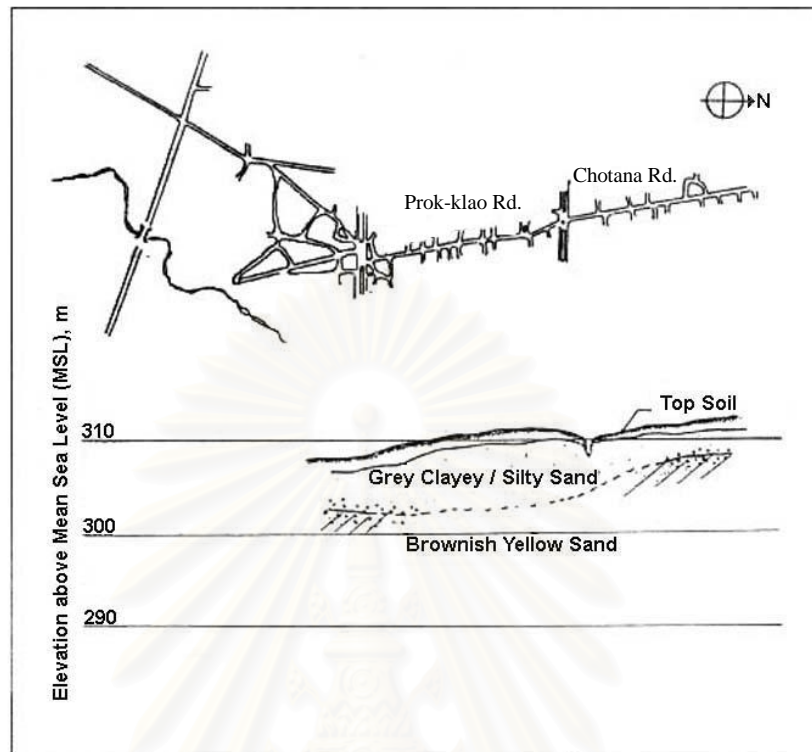


Fig. 3.2. Seismic source zones in Thailand and vicinity (Nutalaya et al., 1985)



**Fig. 3.3.** Map showing contours of peak ground acceleration (in units of acceleration of gravity) with 10% chance of being exceeded in a 50-year exposure time, and seismic zones for earthquake-resistant design (Wanitchai and Lisantono, 1996)



**Fig. 3.4.** Typical subsoil section in Chiang Mai Province (modified from Anantasech and Thanadpipat, 1985)

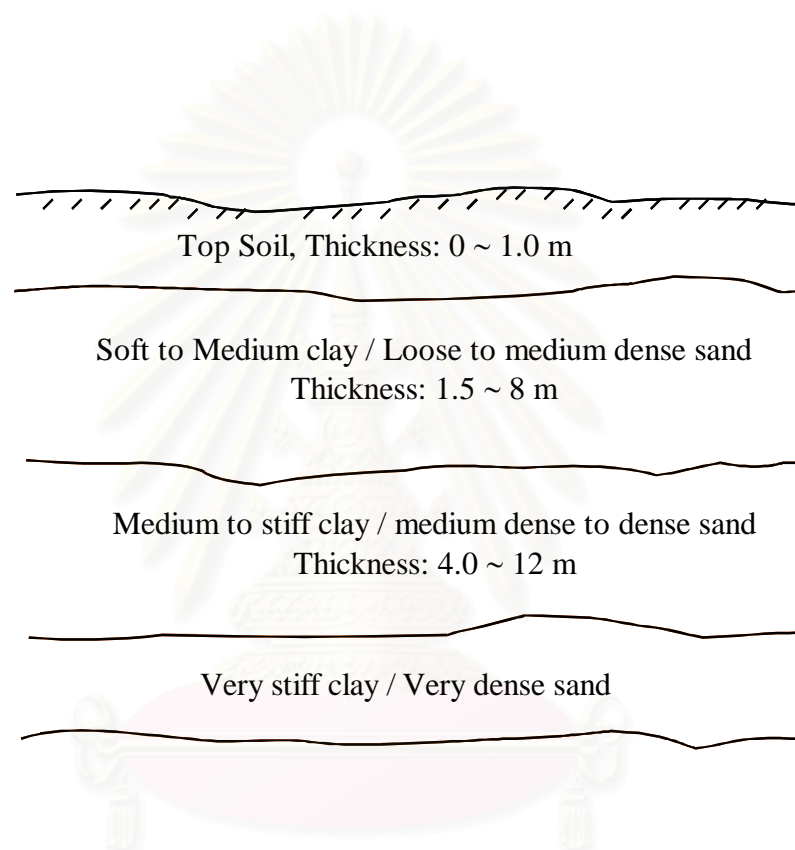


**Fig. 3.5.** Typical subsoil profile in Chiang Rai province

สถาบันวิทยบริการ  
จุฬาลงกรณ์มหาวิทยาลัย

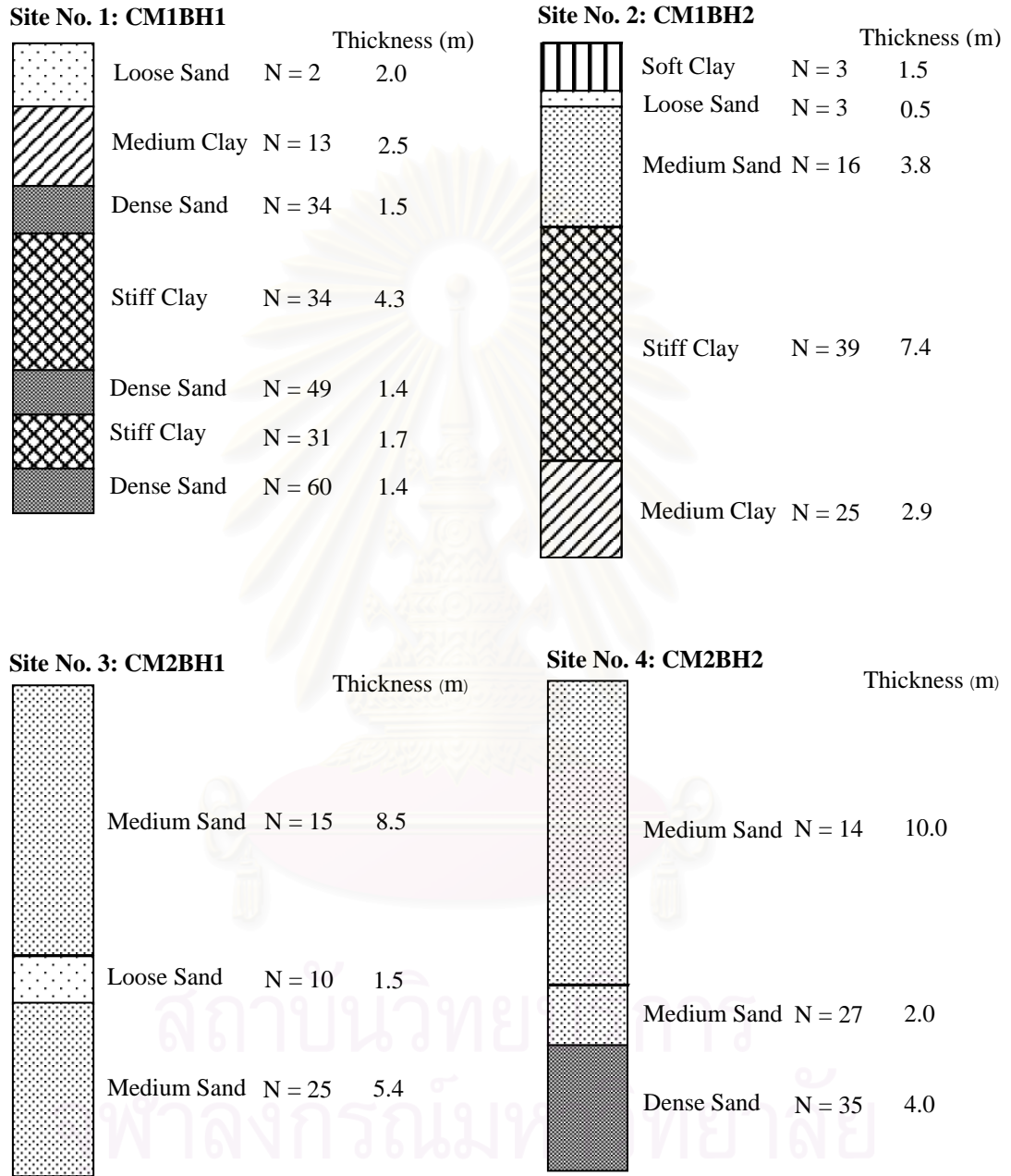


**Fig. 3.6.** Examples of the soil profiles and soil properties collected from Chiang Mai

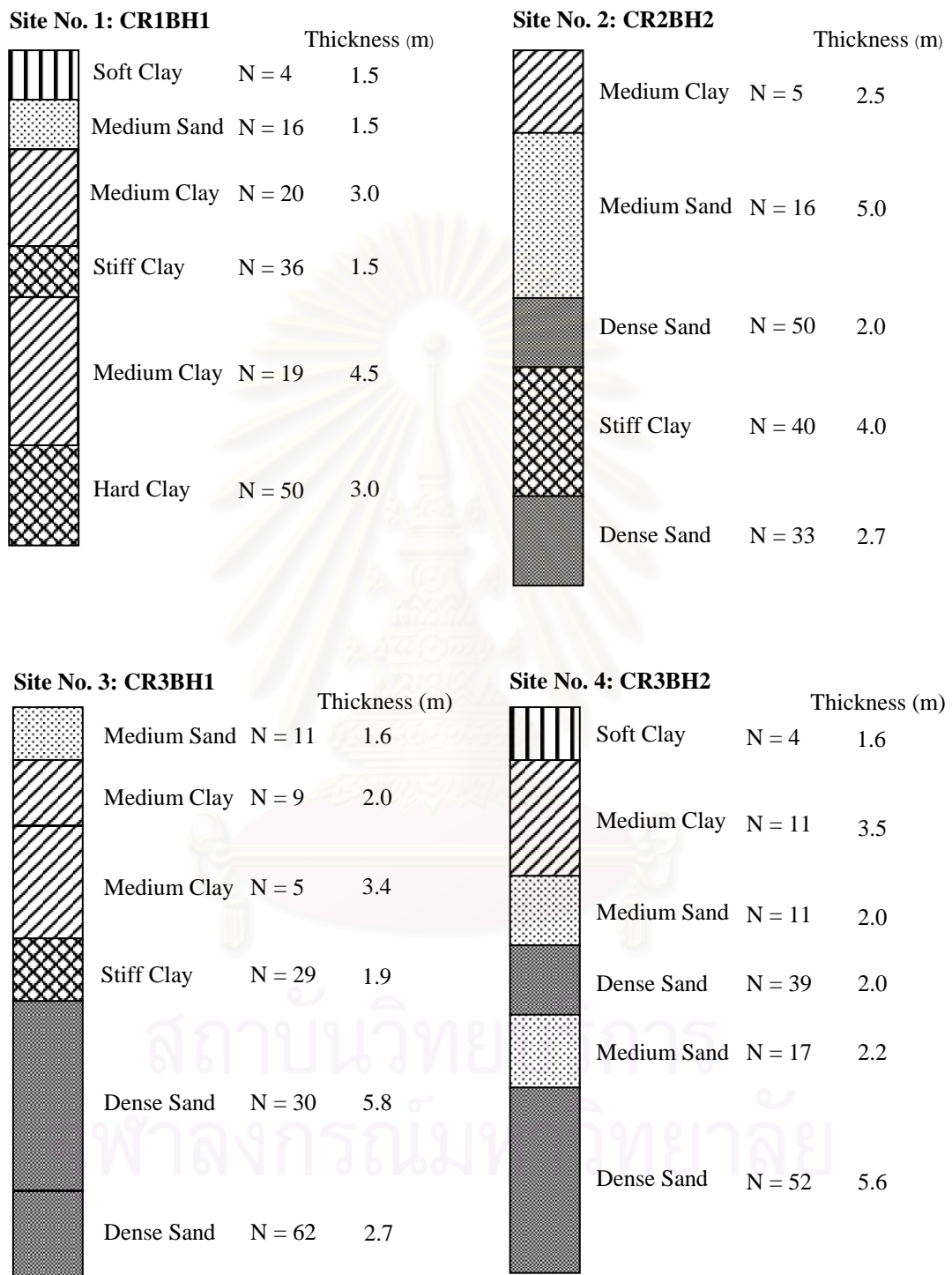


**Fig. 3.7.** Examples of the soil profiles and soil properties collected from Chiang Rai

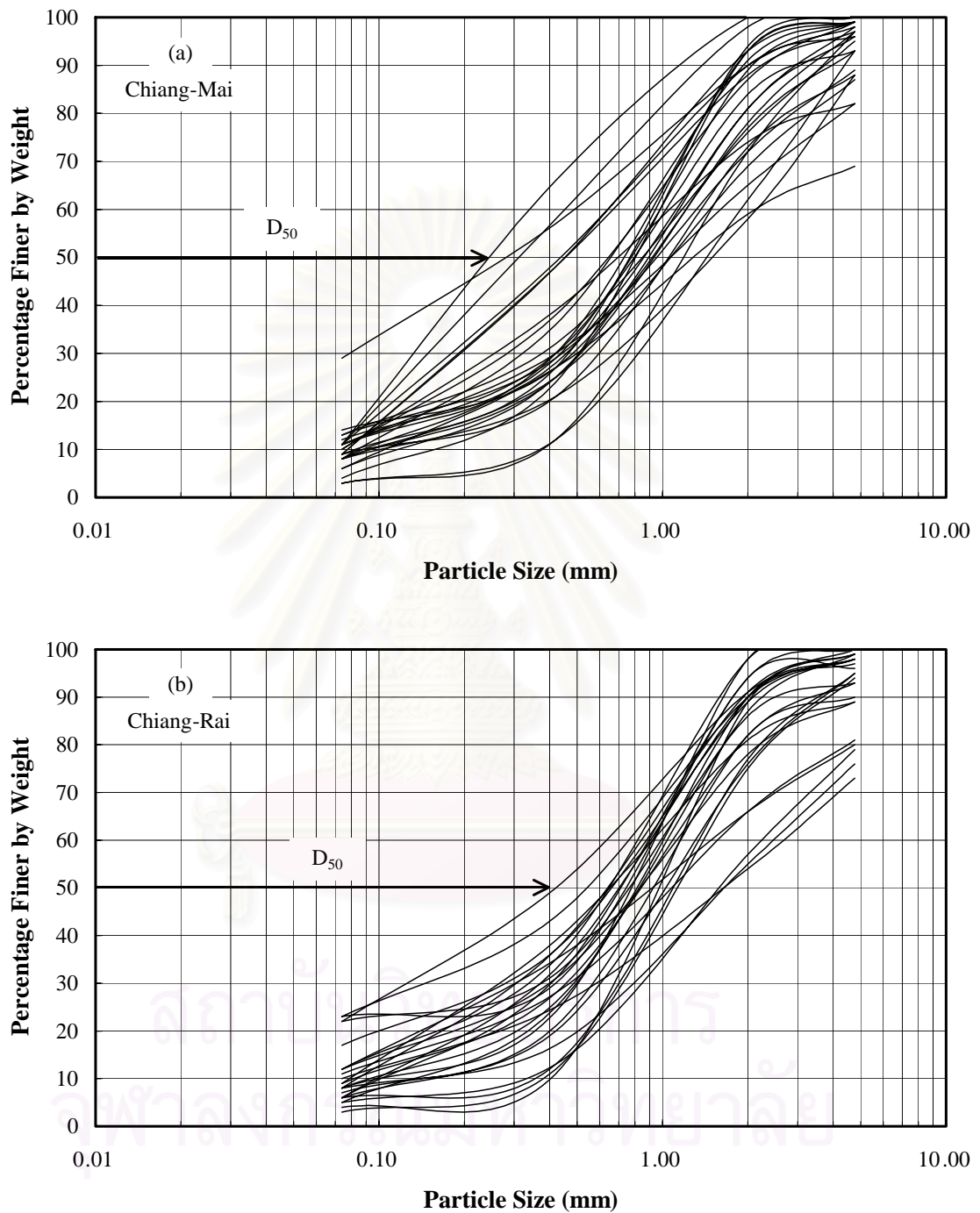


**Fig. 3.8.** Grain size distribution of sands: (a) Chiang Mai; (b) Chiang Rai

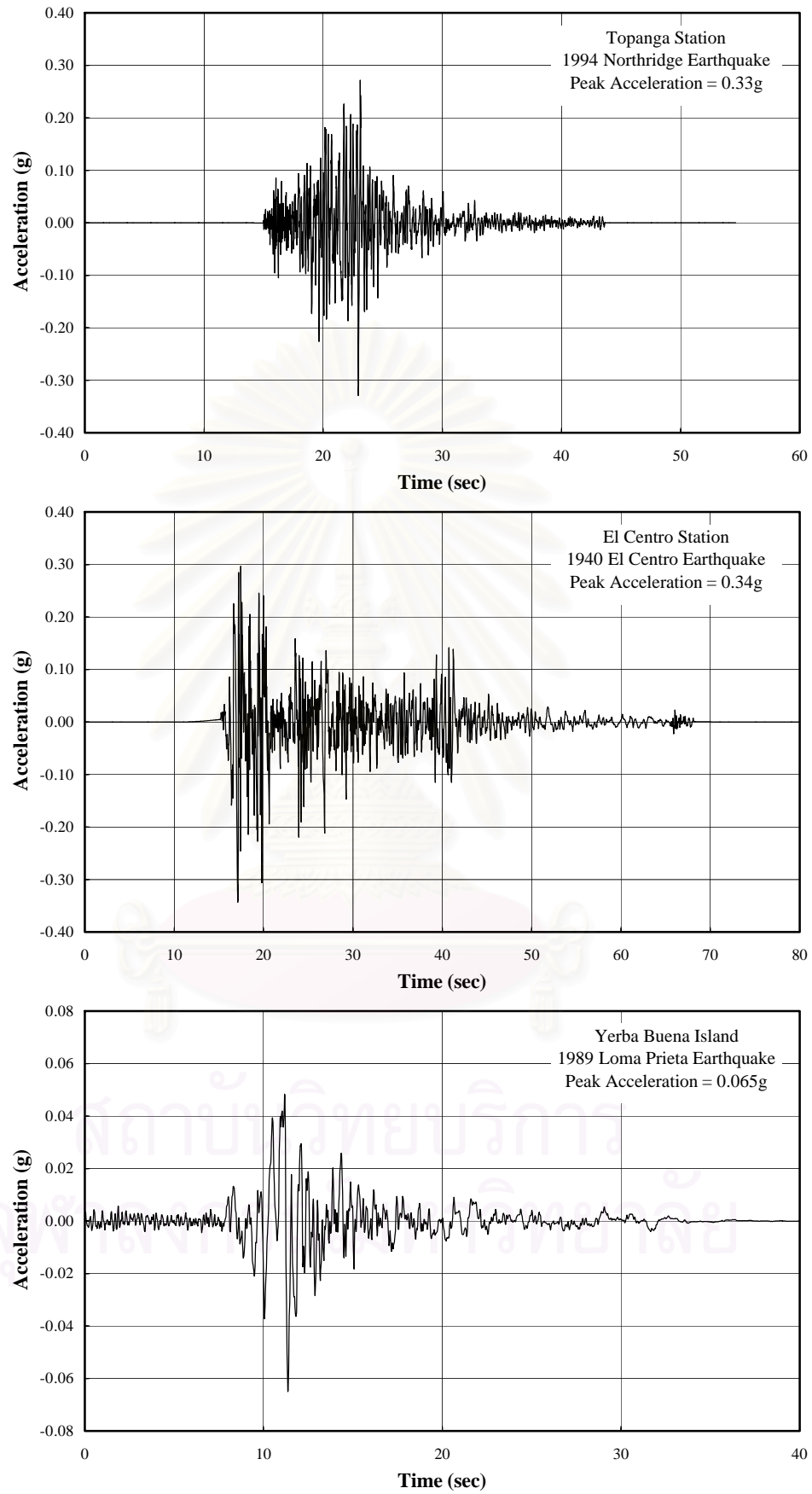


**Fig. 3.9.** Acceleration time history of input motions



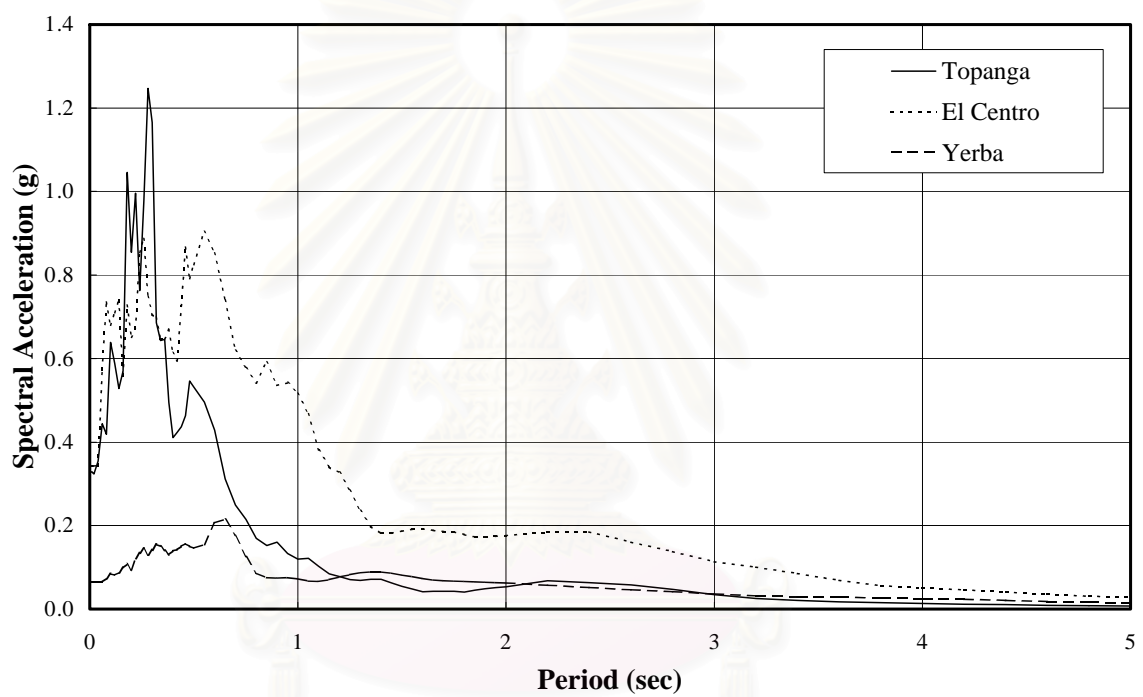


**Fig. 3.10.** Acceleration response spectra of input motions used in this study

สถาบันวิทยบริการ  
จุฬาลงกรณ์มหาวิทยาลัย

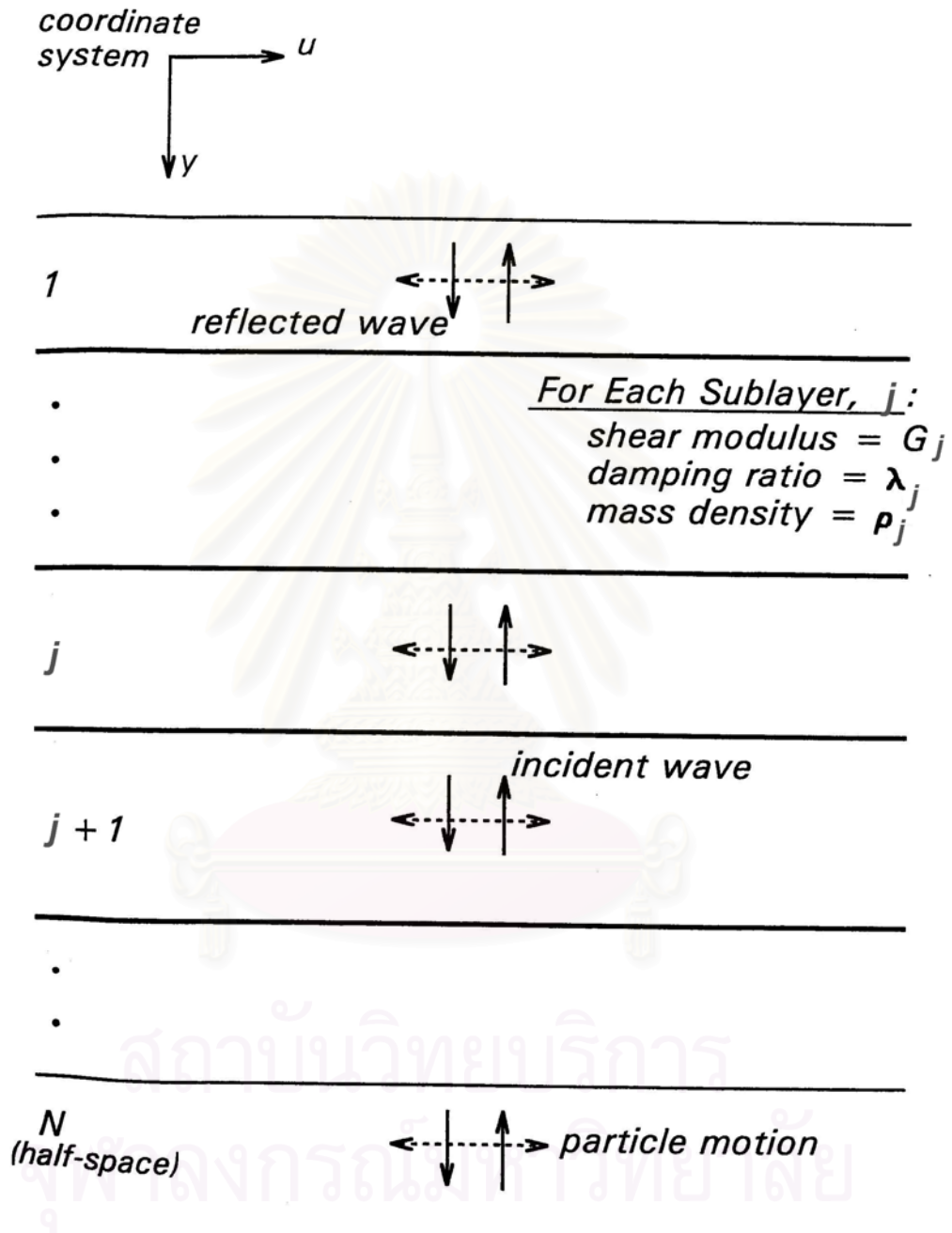


**Fig. 4.1.** One-dimensional idealization of a horizontally layered soil deposit over a uniform half-space (Idriss and Sun, 1992)

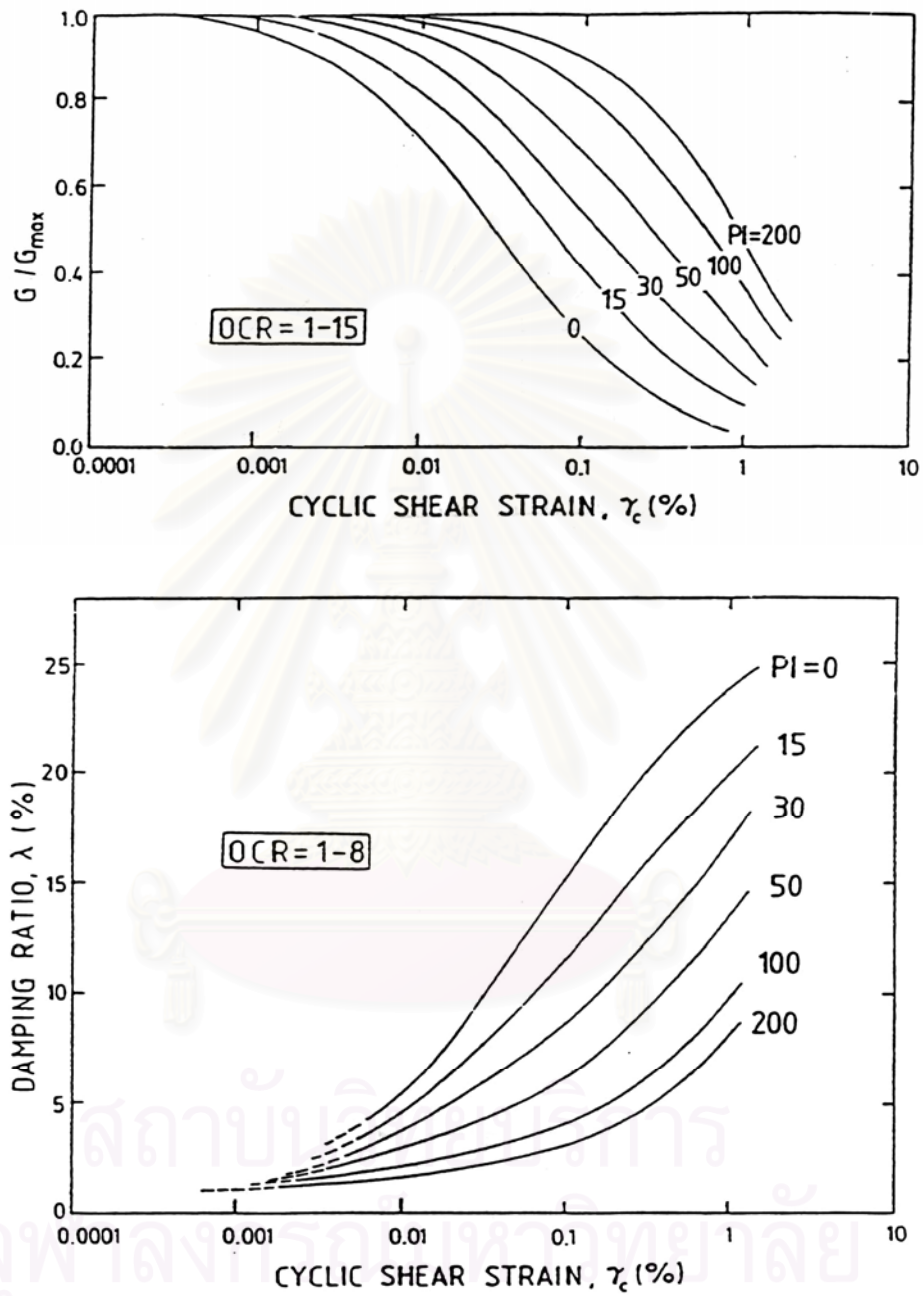


**Fig. 4.2.** Shear modulus and damping variation with shear strain for clays of varying plasticity (Vucetic and Dobry, 1991)

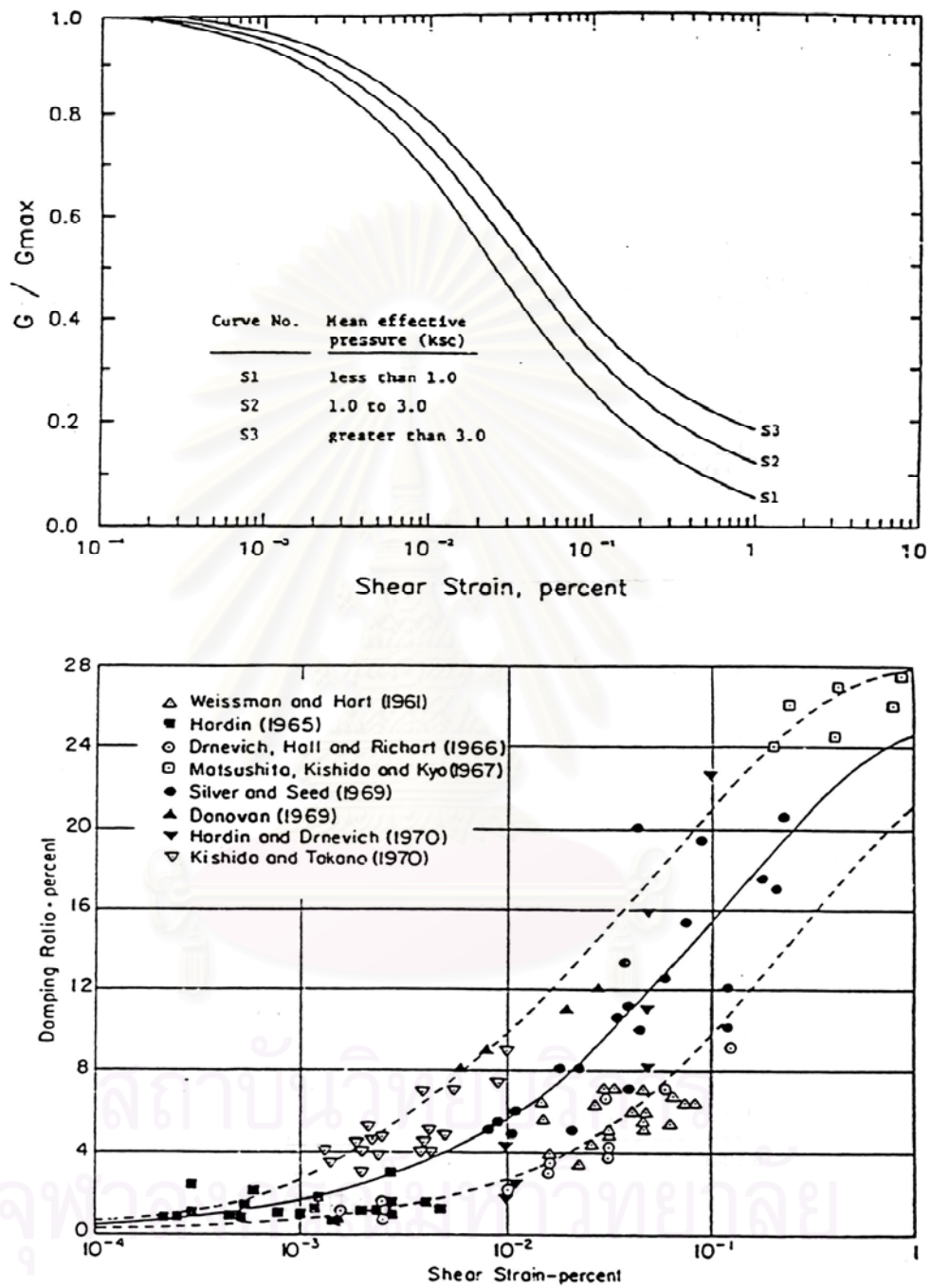


**Fig. 4.3.** Shear modulus and damping variation with shear strain for sands (Seed et al., 1984)

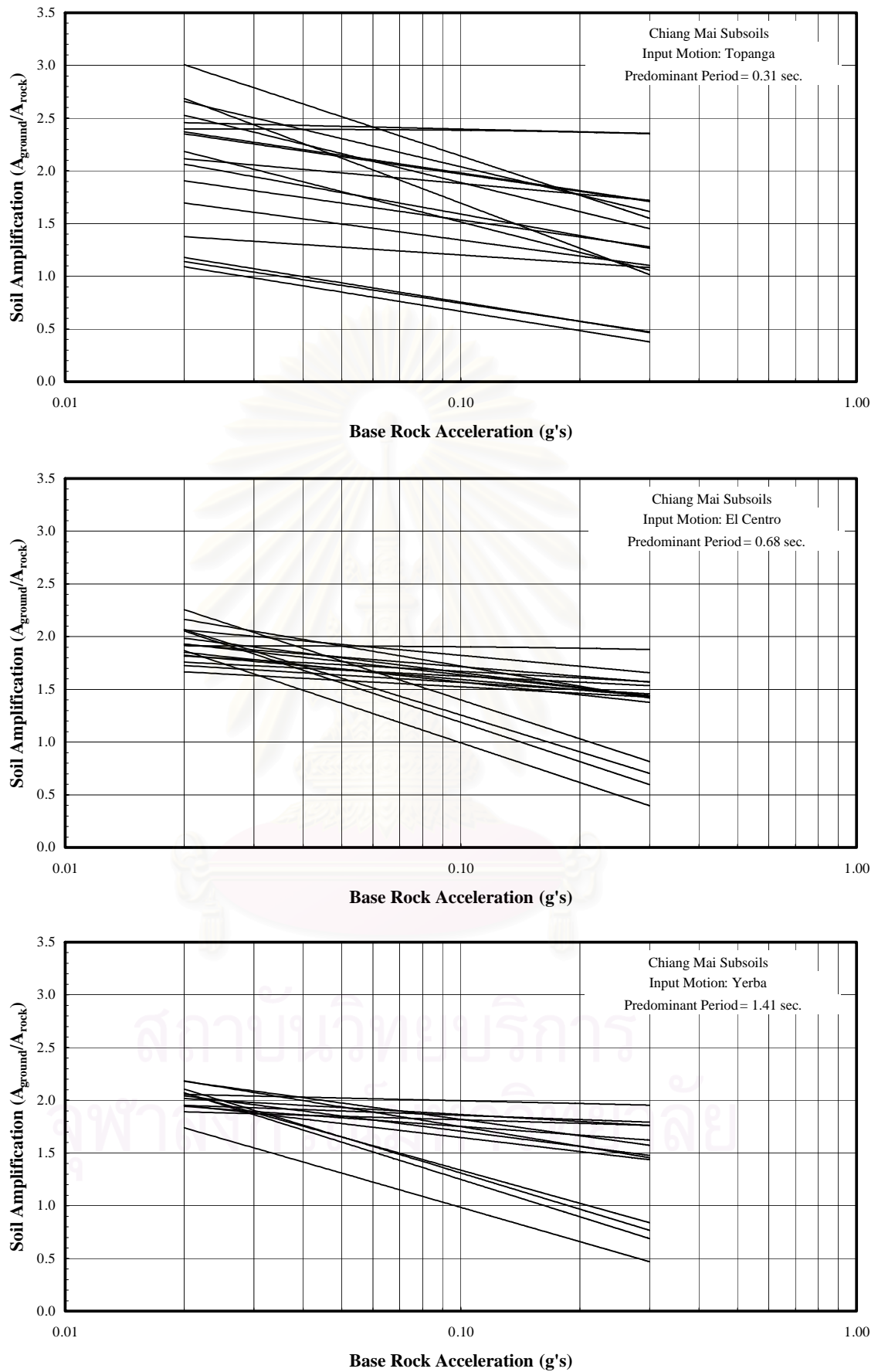


**Fig. 4.4.** Variations of amplification factors with base rock acceleration in Chiang Mai

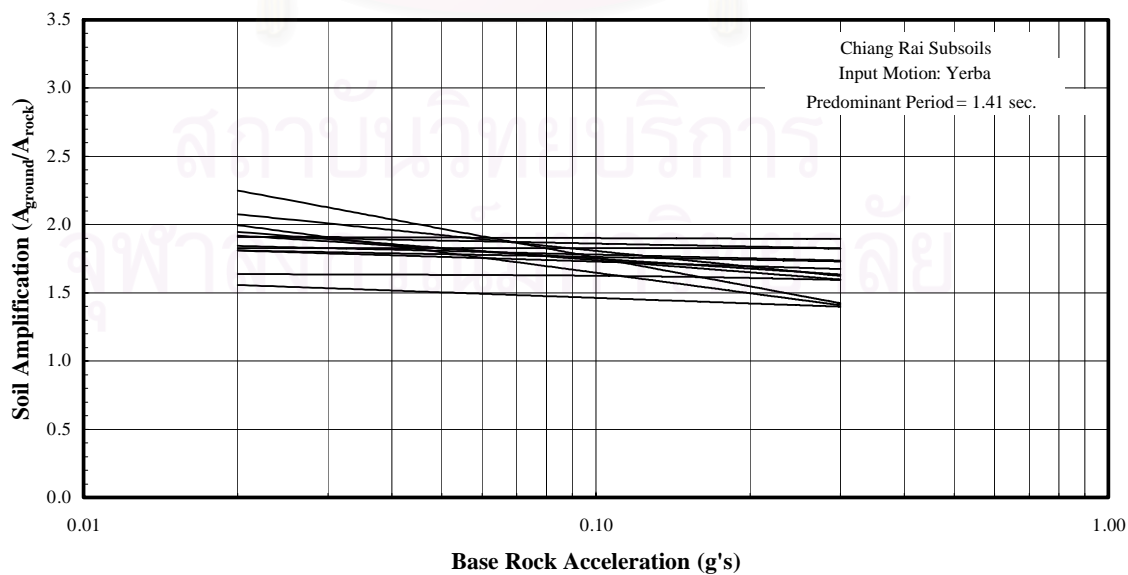
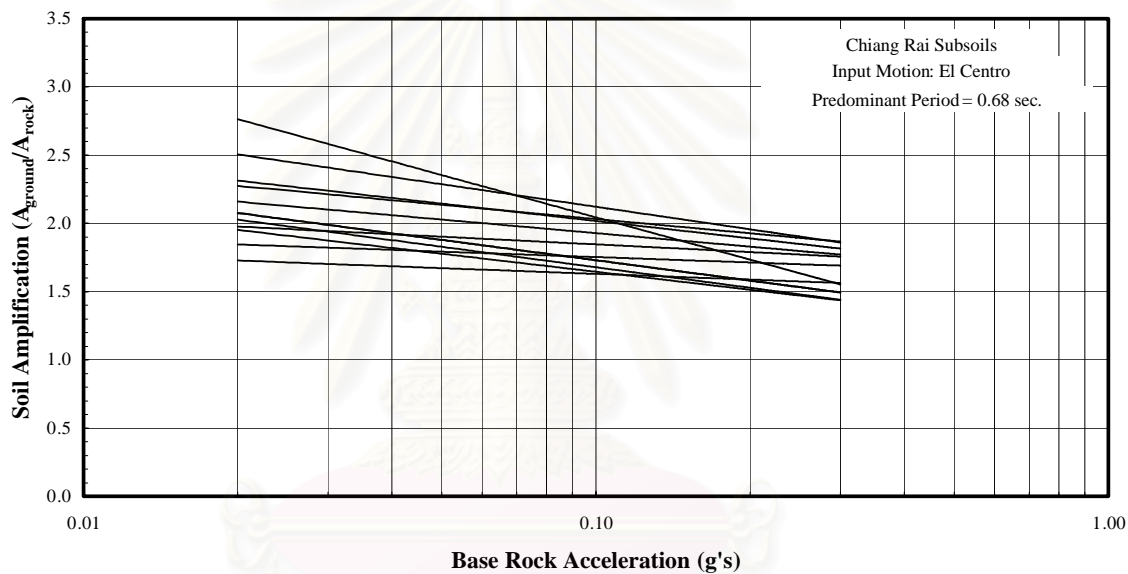
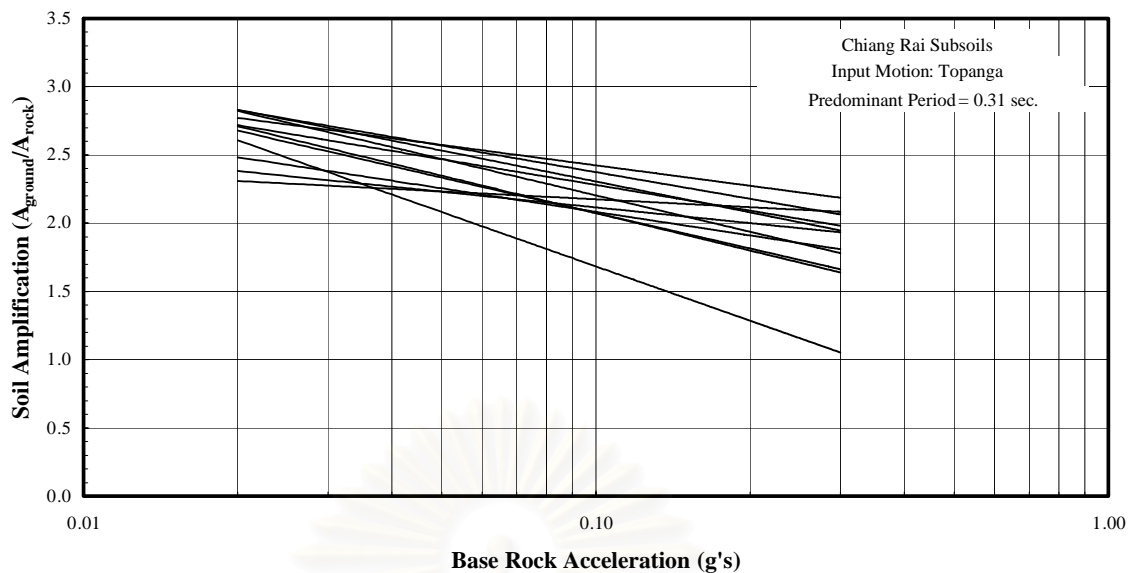


**Fig. 4.5.** Variations of amplification factors with base rock acceleration in Chiang Rai

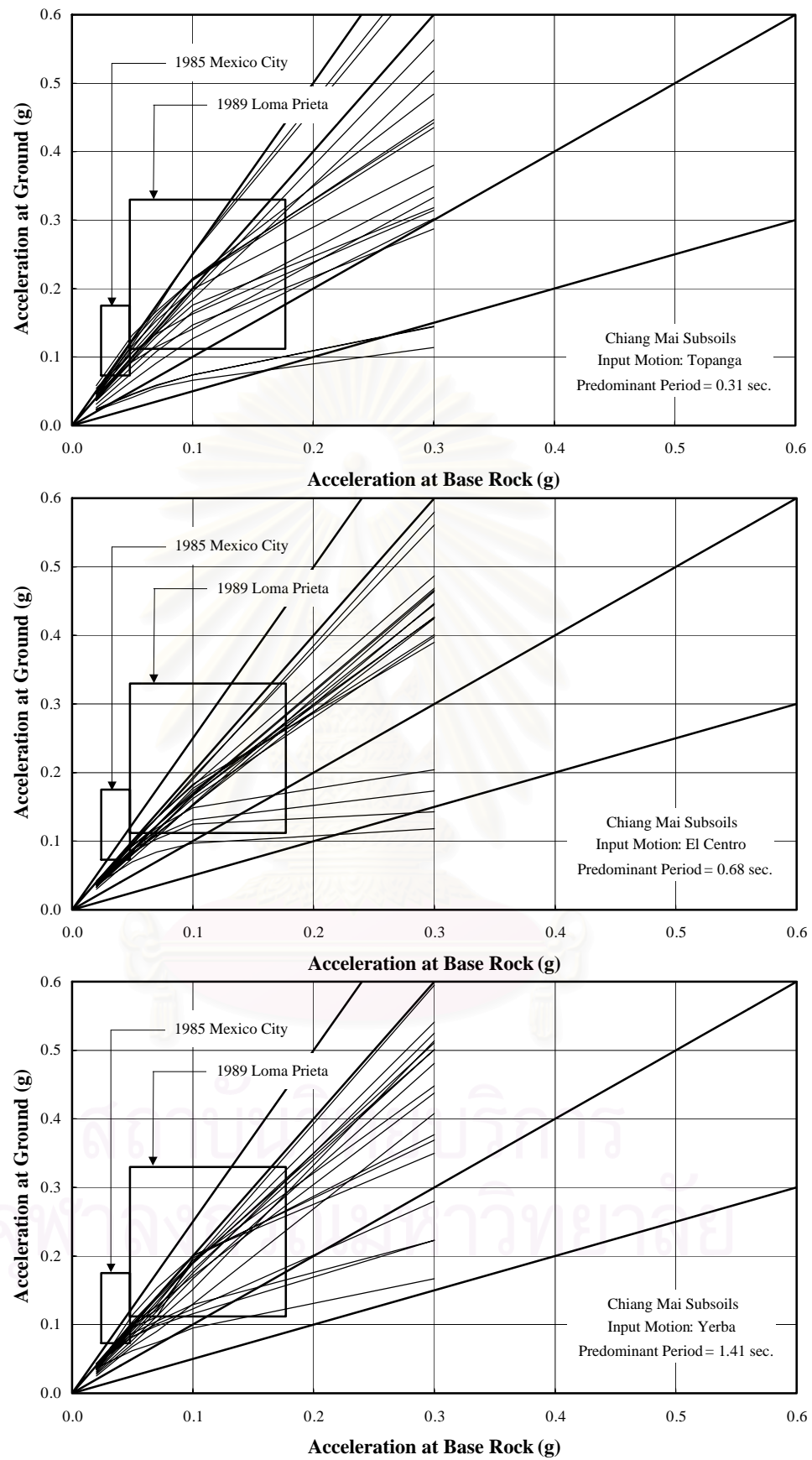


**Fig. 4.6.** Comparison between peak ground accelerations of Chiang Mai and observed results from 1985 Mexico and 1989 Loma Prieta earthquakes (modified from Idriss, 1991)

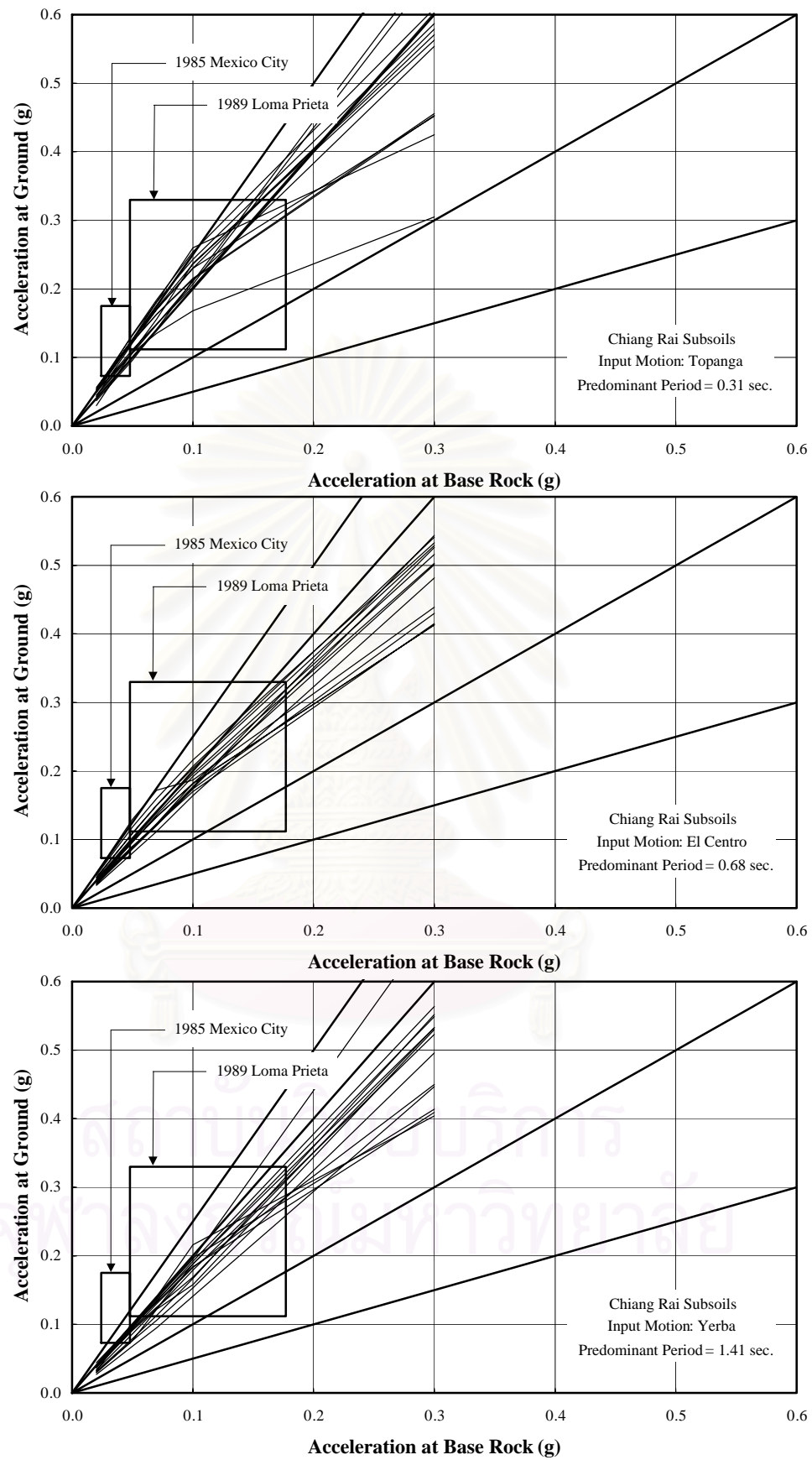


**Fig. 4.7.** Comparison between peak ground accelerations of Chiang Rai and observed results from 1985 Mexico and 1989 Loma Prieta earthquakes (modified from Idriss, 1991)



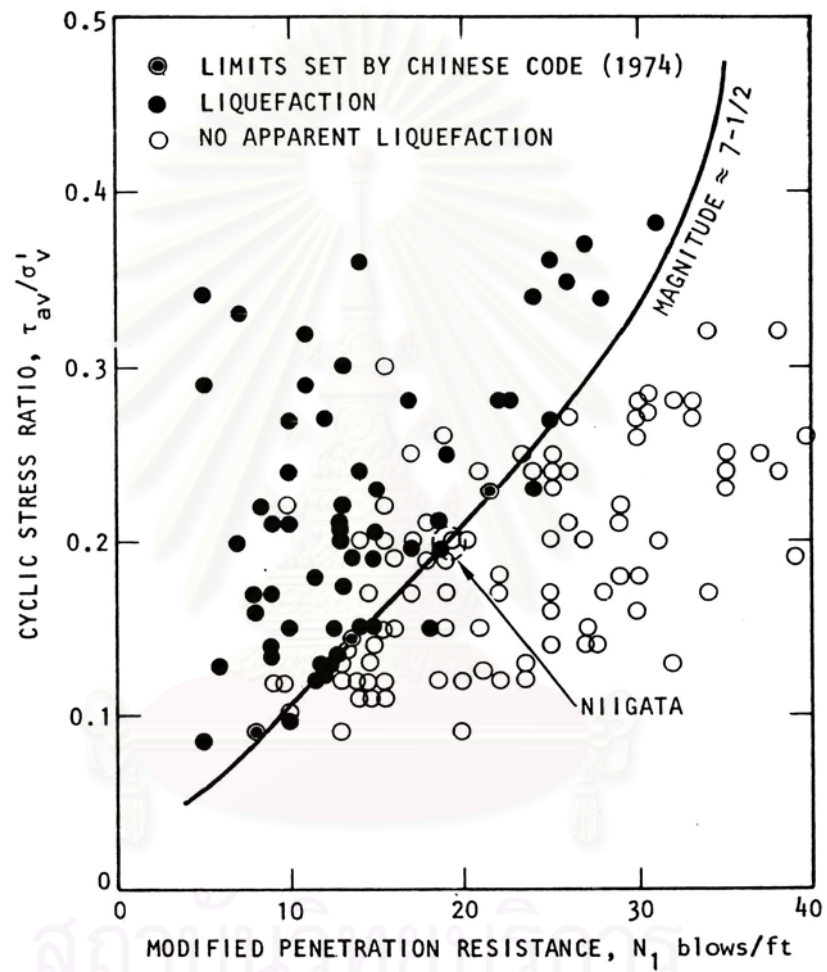


**Fig. 5.1.** Example of deterministic method of liquefaction evaluation derived from empirical data for soils with  $D_{50} > 0.25$  mm (Seed et al., 1983)

CASE	BCAT	LIQ1	LIQ2	M	H	EP	DER	DUR	A	CSR	CSR <sub>N</sub>	ZW	ZL	SIGT	SIGE	N	N1	CE	N160	FC
0101	2	0.	-1.	6.6	-1.	-1.	39.	20.	.12	.14	-1.	.9	6.1	-1.	.55	6.	8.0	-1.	-1.	-1.
0102	2	0.	-1.	6.6	-1.	-1.	39.	20.	.12	.14	-1.	.9	6.1	1.07	.55	12.	16.0	-1.	-1.	-1.
0201	2	0.	-1.	6.1	-1.	-1.	47.	12.	.08	.09	-1.	.9	6.1	-1.	.55	6.	8.0	-1.	-1.	-1.
0202	2	0.	-1.	6.1	-1.	-1.	47.	12.	.08	.09	-1.	.9	6.1	-1.	.55	12.	16.0	-1.	-1.	-1.
0301	2	1.	-1.	8.4	-1.	-1.	32.	75.	.35	.39	-1.	.9	13.7	-1.	1.30	17.	15.0	-1.	-1.	-1.
0301	4	1.	-1.	-2.	-1.	30.	-1.	-1.	-1.	-1.	-1.	.8	-2.	-1.	-1.	-2.	-1.	-1.	-1.	-2.
0301	7	1.	1.0	7.9	-1.	-1.	-1.	-1.	.32	-1.	.364	.8	10.0	1.90	.98	20.	20.2	-1.	-1.	0.
0301	8	1.	-1.	7.9	-1.	-1.	-1.	-1.	.32	.355	.376	.8	10.0	1.93	1.02	20.	19.6	1.30	25.5	0.
0302	2	1.	-1.	8.4	-1.	-1.	32.	75.	.35	.37	-1.	1.8	9.1	-1.	1.00	10.	10.0	-1.	-1.	-1.
0302	4	1.	-1.	-2.	-1.	30.	-1.	-1.	-1.	-1.	-1.	2.0	-2.	-1.	-1.	-2.	-1.	-1.	-1.	-2.
0302	7	1.	1.0	7.9	-1.	-1.	-1.	-1.	.32	-1.	.317	2.0	7.0	1.33	.83	10.	11.1	-1.	-1.	5.
0302	8	1.	-1.	7.9	-1.	-1.	-1.	-1.	.32	.31	.33	2.0	7.0	1.35	.86	10.	10.6	1.17	12.5	6.
0303	2	0.	-1.	8.4	-1.	-1.	32.	75.	.35	.35	-1.	1.8	7.6	-1.	.85	19.	21.0	-1.	-1.	-1.
0303	4	0.	-1.	-2.	-1.	30.	-1.	-1.	-1.	-1.	-1.	1.9	-1.	-1.	-1.	-2.	-1.	-1.	-1.	-2.
0303	7	1.	1.0	7.9	-1.	-1.	-1.	-1.	.28	-1.	.275	1.9	6.0	1.14	.73	17.	20.2	-1.	-1.	3.
0303	8	1.	-1.	7.9	-1.	-1.	-1.	-1.	.32	.316	.33	1.9	6.0	1.17	.75	17.	12.0	1.35	25.0	3.
0304	2	1.	-1.	8.4	-1.	-1.	32.	75.	.35	.35	-1.	2.4	6.1	-1.	.75	16.	19.0	-1.	-1.	-1.
0304	4	1.	-1.	-2.	-1.	30.	-1.	-1.	-1.	-1.	-1.	2.0	-2.	-1.	-1.	-2.	-1.	-1.	-1.	-2.
0304	7	1.	1.0	7.9	-1.	-1.	-1.	-1.	.29	-1.	.245	2.4	6.0	.95	.69	13.	15.9	-1.	-1.	4.
0304	8	1.	-1.	7.9	-1.	-1.	-1.	-1.	.32	.275	.29	2.4	6.0	1.00	.72	13.	15.0	1.17	17.0	4.
0306	3	0.	-1.	8.4	-1.	-1.	-1.	-1.	.35	-1.	-1.	1.8	12.2	-1.	-1.	-1.	48.0	-1.	-1.	-1.
0306	6	1.	-1.	8.4	-1.	55.	-1.	-1.	-1.	-1.	-1.	-1.	-1.	-1.	.74	-1.	15.4	-1.	-1.	-1.
0307	6	1.	-1.	8.4	-1.	51.	-1.	-1.	-1.	-1.	-1.	-1.	-1.	-1.	.45	-1.	20.3	-1.	-1.	-1.
0401	6	1.	-1.	7.5	-1.	79.	-1.	-1.	-1.	-1.	-1.	-1.	-1.	-1.	.62	-1.	10.5	-1.	-1.	-1.
0402	6	1.	-1.	7.5	-1.	65.	-1.	-1.	-1.	-1.	-1.	-1.	-1.	-1.	.37	-1.	10.7	-1.	-1.	-1.
0403	6	0.	-1.	7.5	-1.	68.	-1.	-1.	-1.	-1.	-1.	-1.	-1.	-1.	.54	-1.	12.1	-1.	-1.	-1.
0404	6	1.	-1.	7.5	-1.	37.	-1.	-1.	-1.	-1.	-1.	-1.	-1.	-1.	.39	-1.	4.0	-1.	-1.	-1.
0405	6	1.	-1.	7.5	-1.	13.	-1.	-1.	-1.	-1.	-1.	-1.	-1.	-1.	.47	-1.	7.5	-1.	-1.	-1.
0501	3	1.	-1.	8.3	-1.	-1.	-1.	-1.	-1.	-1.	-1.	2.4	4.6	-1.	.60	16.	20.4	-1.	-1.	-1.
0501	4	1.	-1.	-2.	25.	-1.	-1.	-1.	-1.	-1.	-1.	2.4	4.6	-1.	-1.	16.	-1.	-1.	-1.	-1.
0502	3	1.	-1.	8.3	-1.	-1.	-1.	-1.	-1.	-1.	-1.	2.4	7.6	-1.	.85	16.	17.4	-1.	-1.	-1.
0502	4	1.	-1.	-2.	25.	-1.	-1.	-1.	-1.	-1.	-1.	2.4	7.6	-1.	-1.	16.	-1.	-1.	-1.	-1.
0503	3	1.	-1.	8.3	-1.	-1.	-1.	-1.	-1.	-1.	-1.	2.4	4.9	-1.	.98	52.	52.2	-1.	-1.	-1.
0504	3	1.	-1.	8.3	-1.	-1.	-1.	-1.	-1.	-1.	-1.	1.5	4.6	-1.	.52	24.	33.3	-1.	-1.	-1.
0504	4	1.	-1.	-2.	-1.	-1.	-1.	-1.	-1.	-1.	-1.	1.5	4.6	-1.	-1.	24.	-1.	-1.	-1.	-1.

Fig. 5.2. Example of liquefaction data catalog (Liao and Whitman, 1986a)

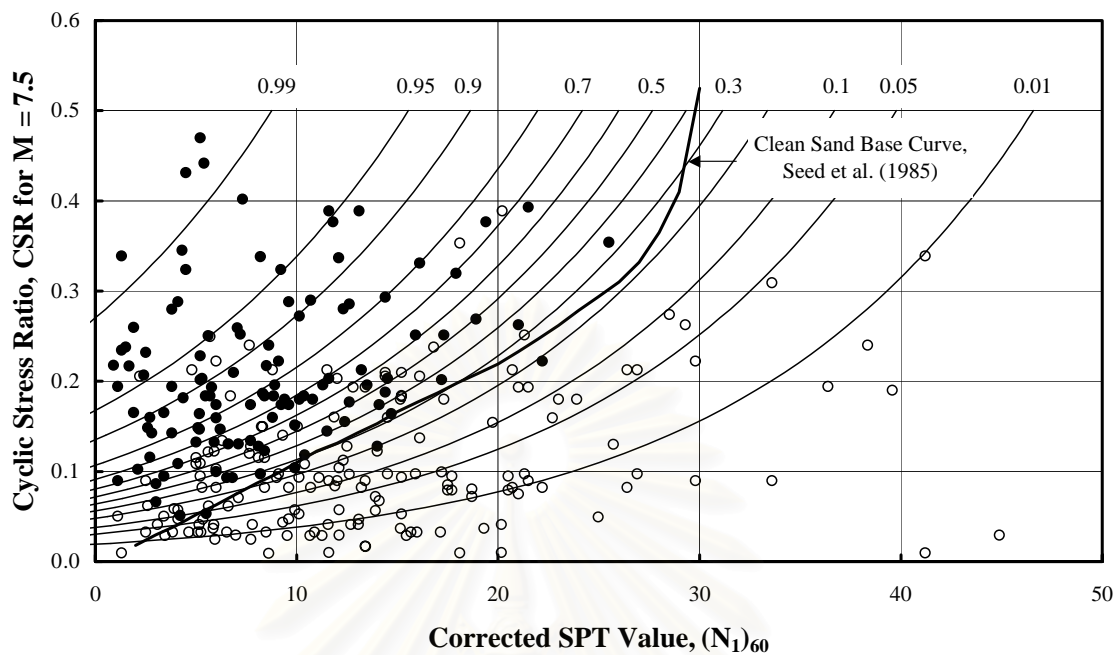


**Fig. 5.3.** Contours of equal probability of liquefaction ( $P_L$ ) for magnitude,  $M = 7.5$  with deterministic line by Seed et al. (1985)

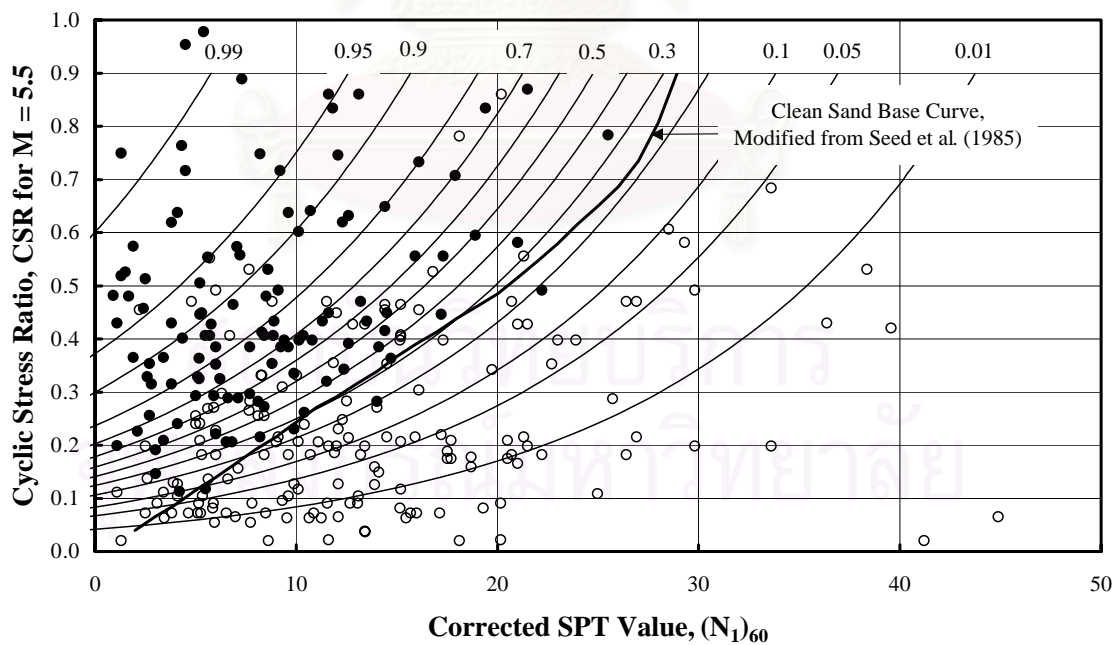


**Fig. 5.4.** Contours of equal probability of liquefaction ( $P_L$ ) for magnitude,  $M = 5.5$  with deterministic line modified from Seed et al. (1985)

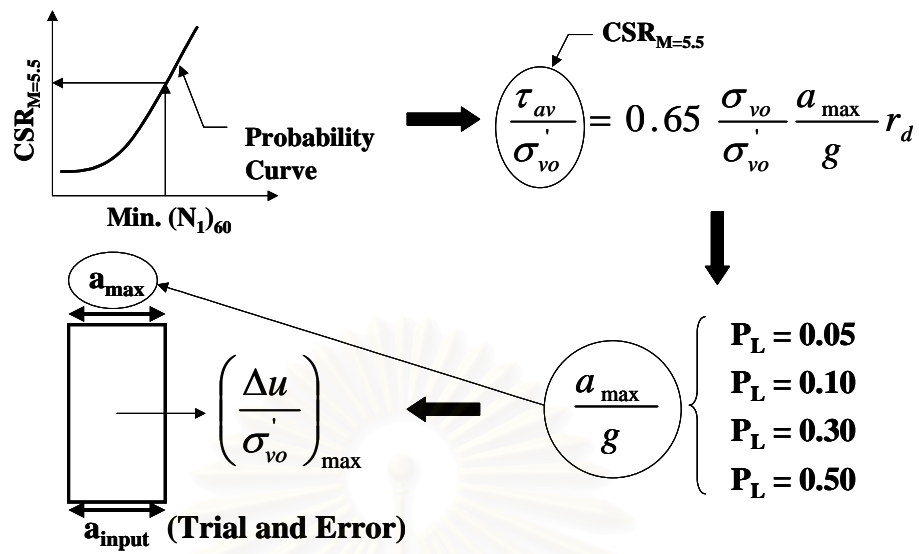


Fig. 6.1. Flow diagram for evaluation of pore water pressure generation

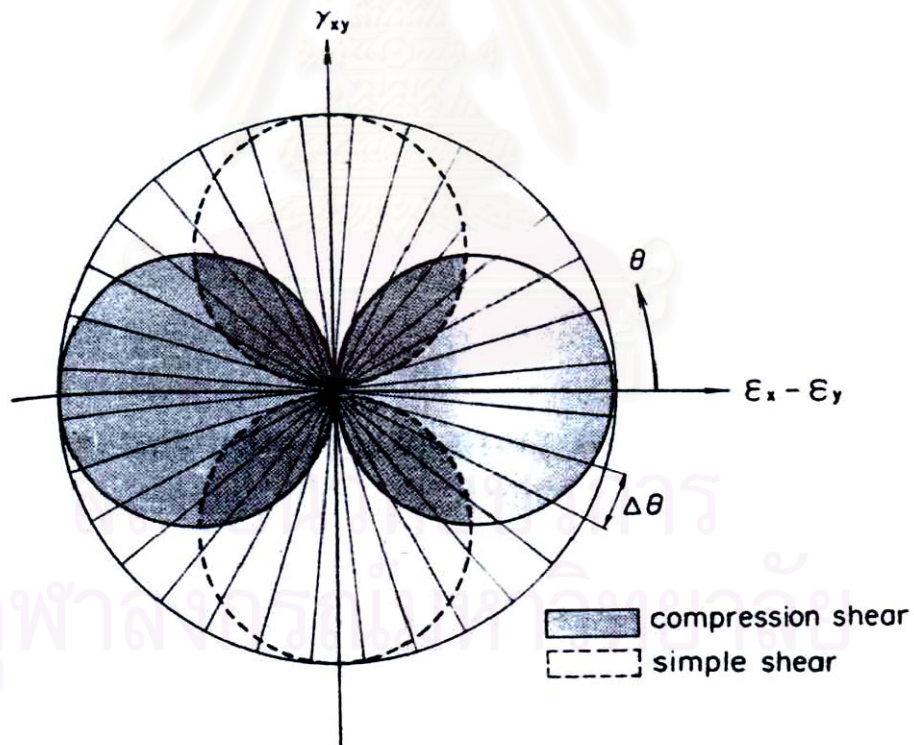
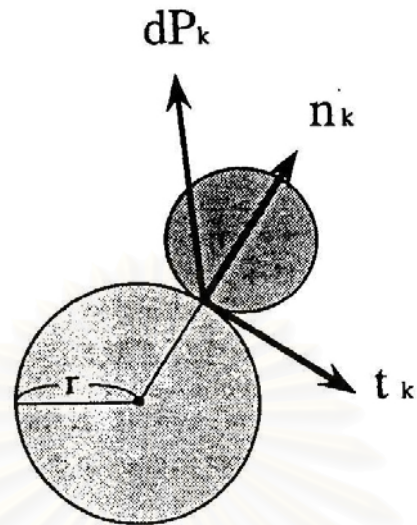
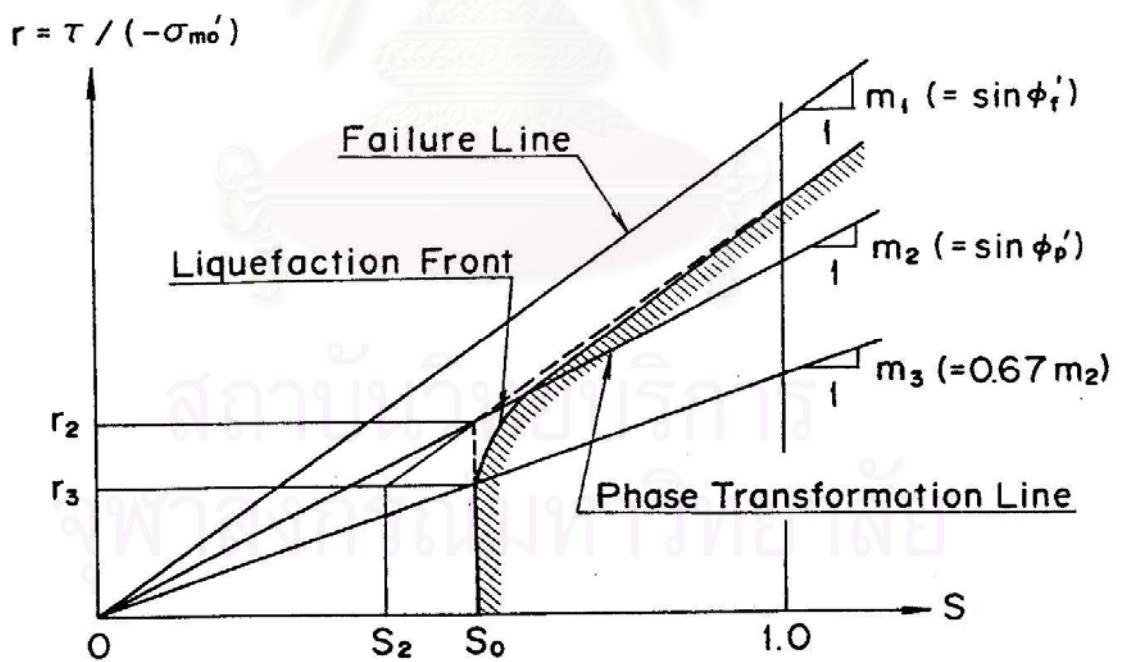


Fig. 6.2. Schematic figure for multiple simple shear mechanisms (pairs of circles indicate mobilized virtual shear strain in positive and negative modes of compression shear and simple shear) (Iai et al., 1992)



**Fig. 6.3.** Schematic figure of contact normal  $n_k$ , tangential direction  $t_k$  and contact force increment  $dP_k$  (Iai et al., 1993)



**Fig. 6.4.** Schematic figure of liquefaction front, state variable  $S$  and shear stress ratio  $r$  (Iai et al., 1992)

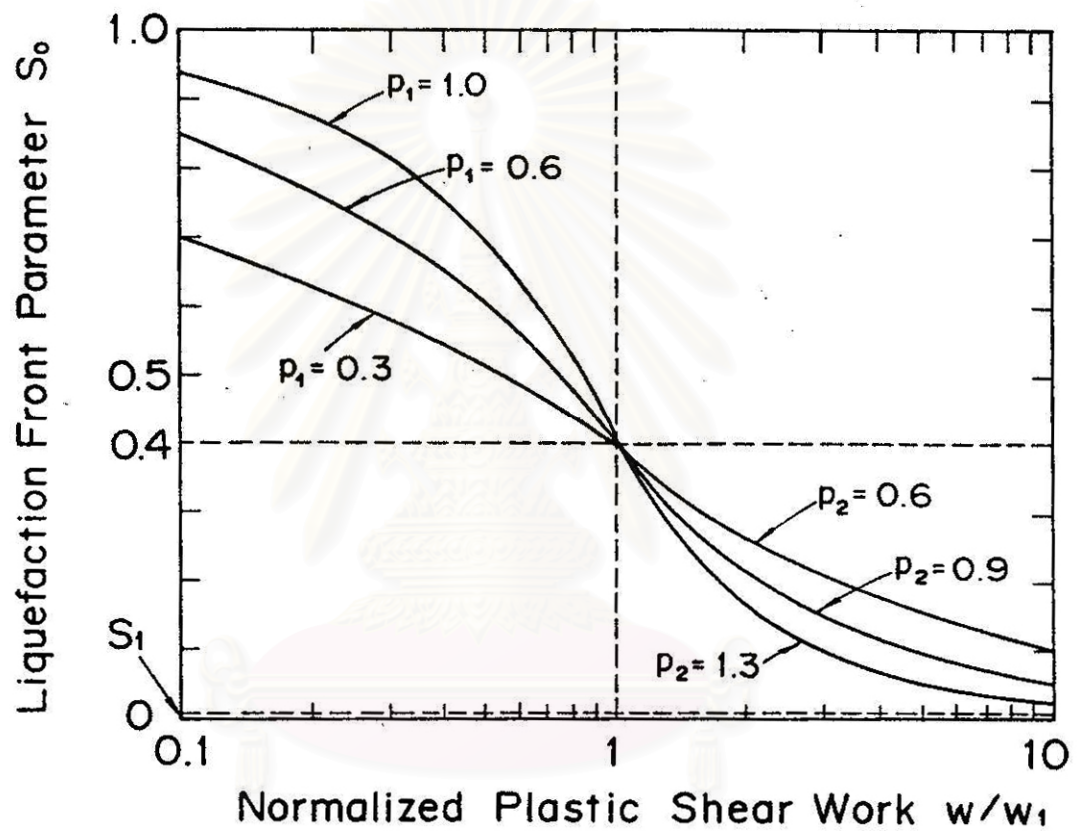


**Fig. 6.5.** Relationship between normalized plastic shear work  $w$  and liquefaction front parameter  $S_0$  (Iai et al., 1992)

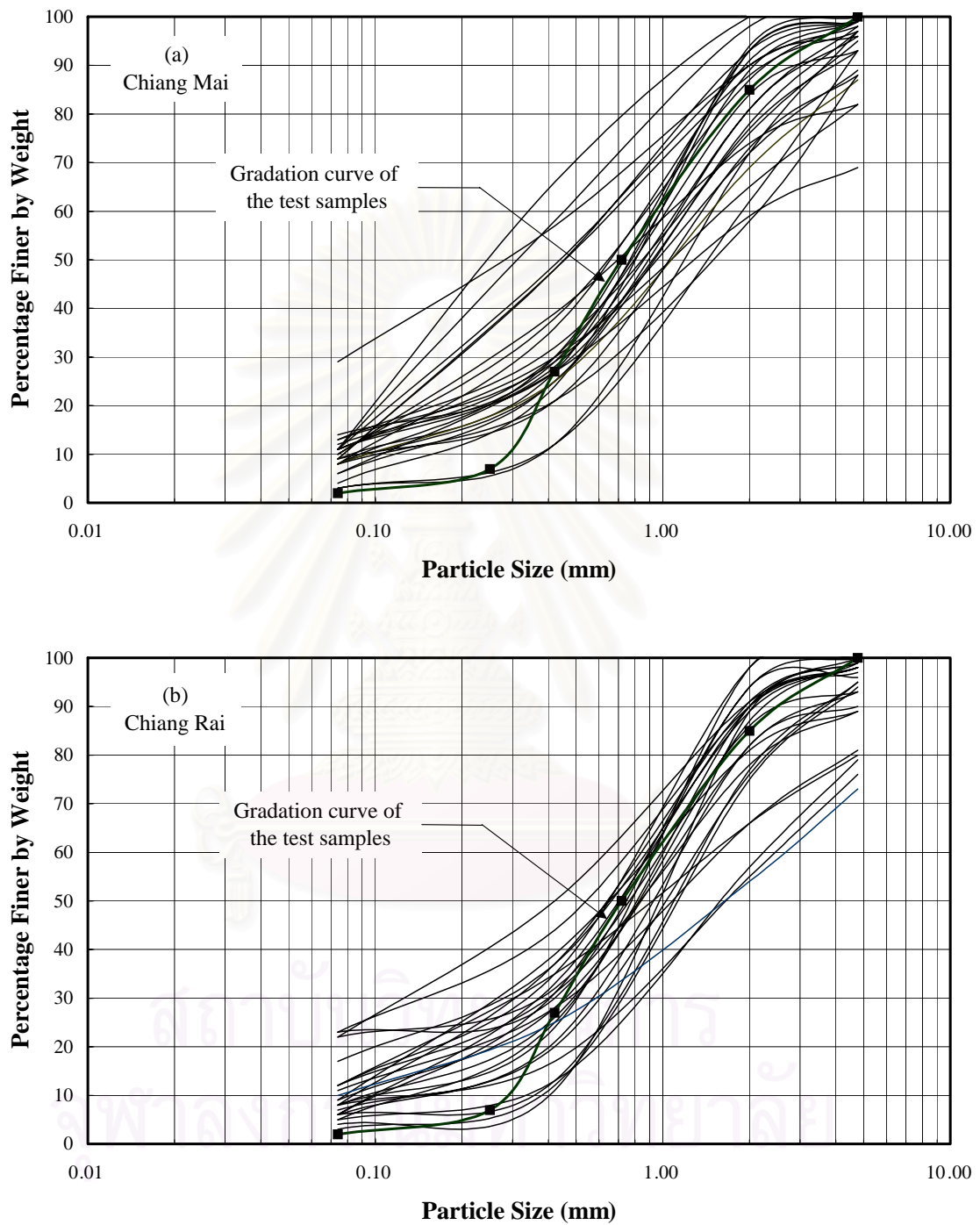


**Fig. 6.6.** Grain size distribution of sands: (a) Chiang Mai; (b) Chiang Rai

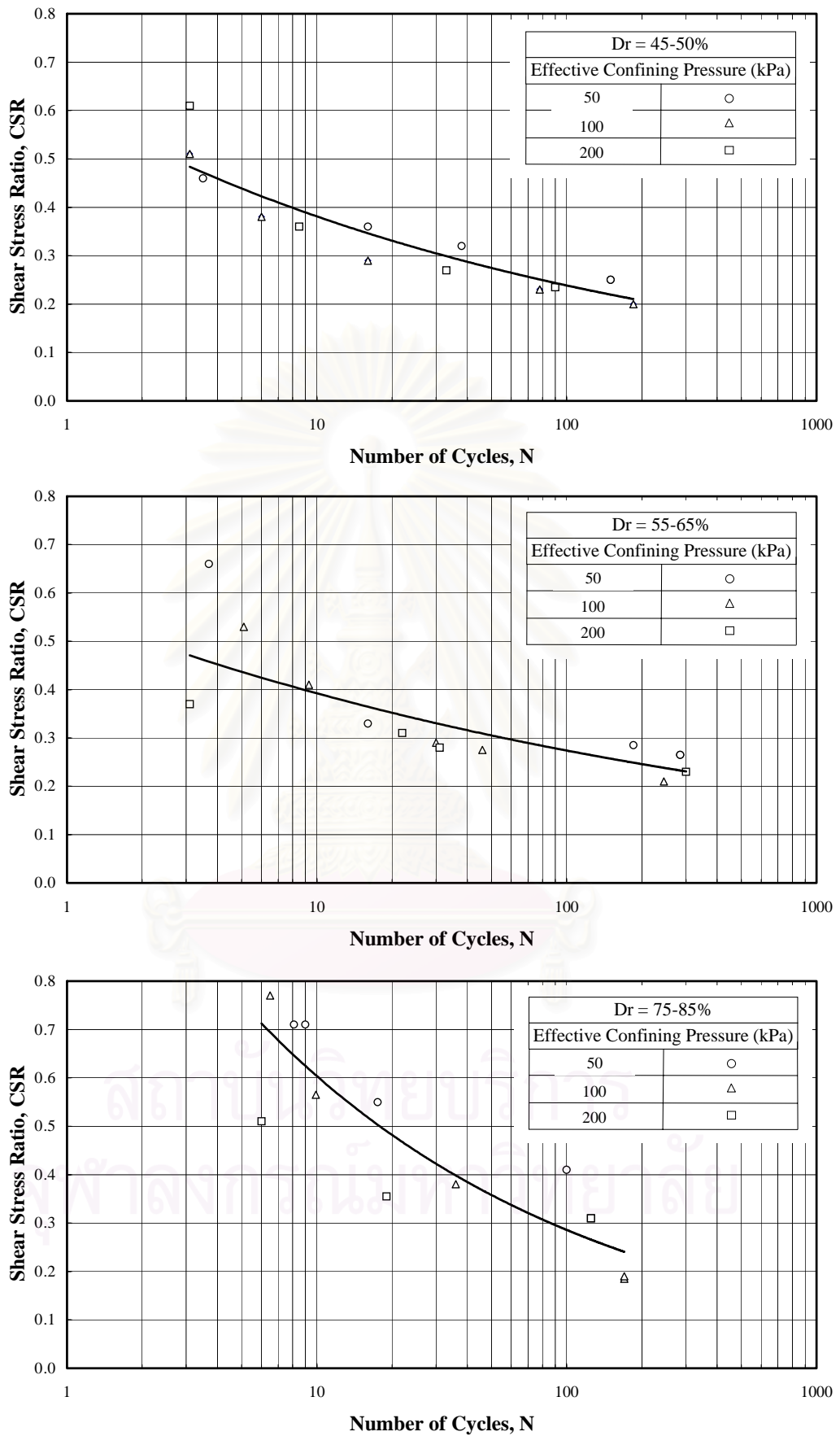


**Fig. 6.7.** Liquefaction resistance curves from undrained cyclic triaxial test (Gauchan, 1984)



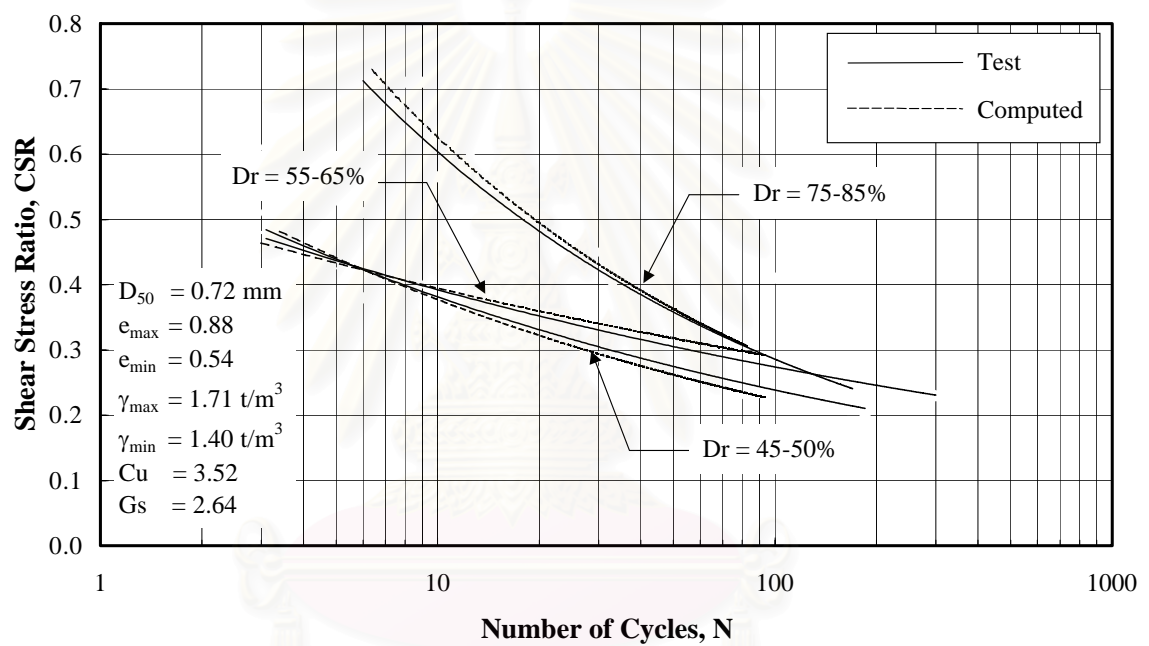


**Fig. 6.8.** Test and computed liquefaction resistance curves

สถาบันวิทยบริการ  
จุฬาลงกรณ์มหาวิทยาลัย

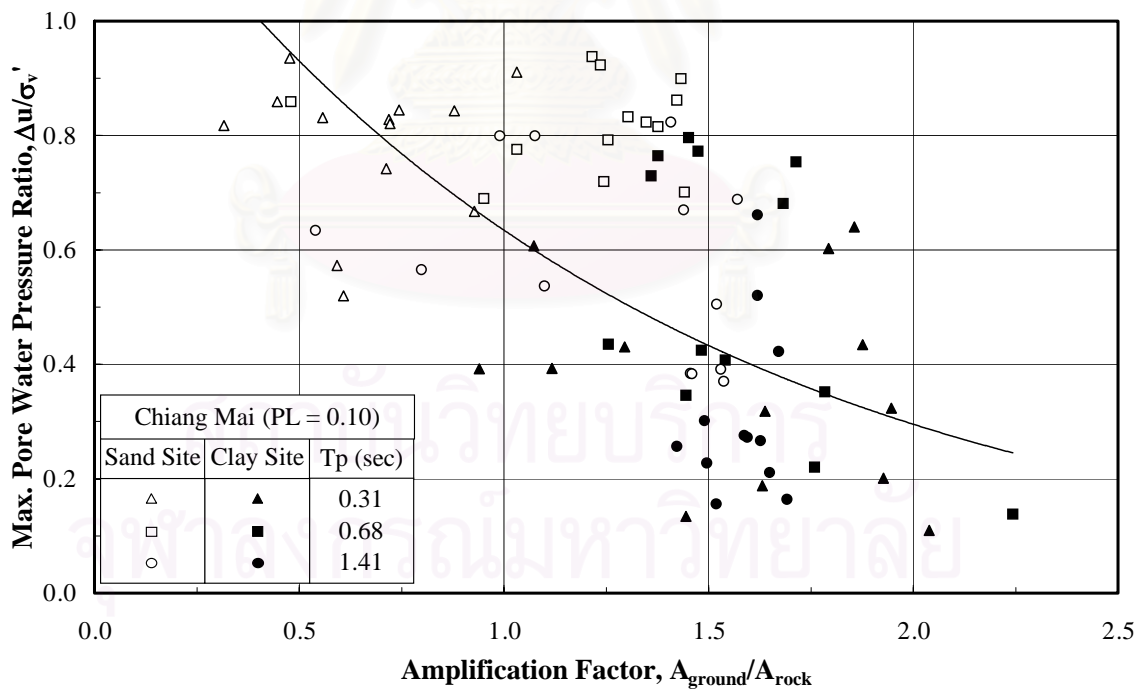
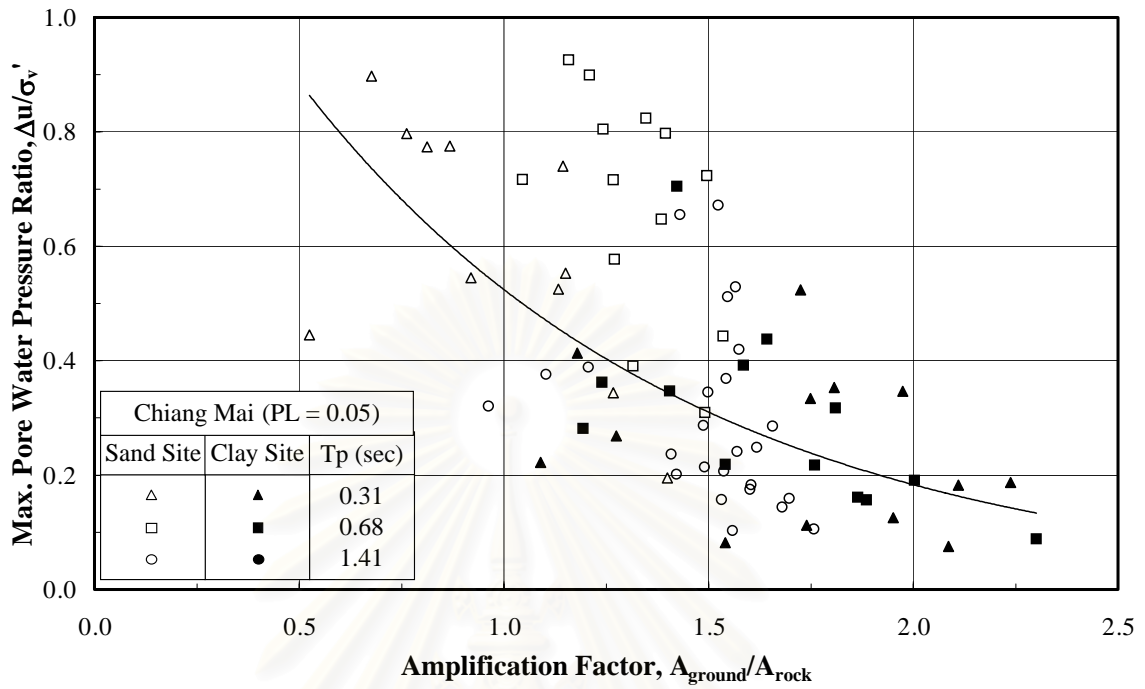


**Fig. 6.9.** Relationship between amplification factor and maximum pore water pressure ratio for Chiang Mai

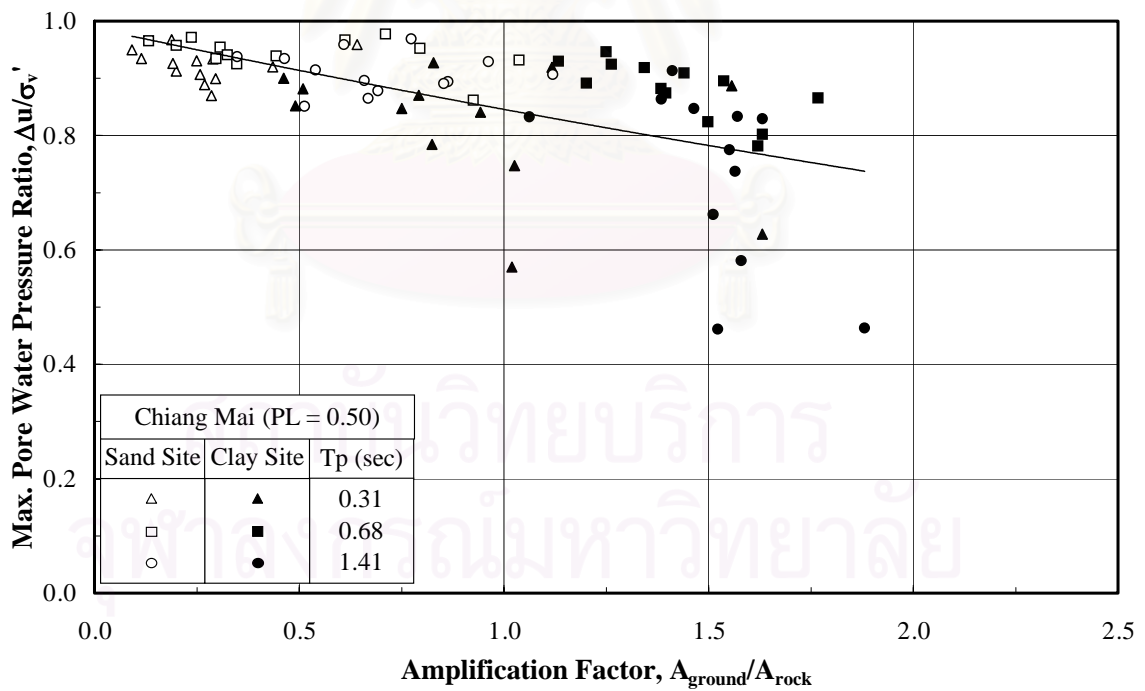
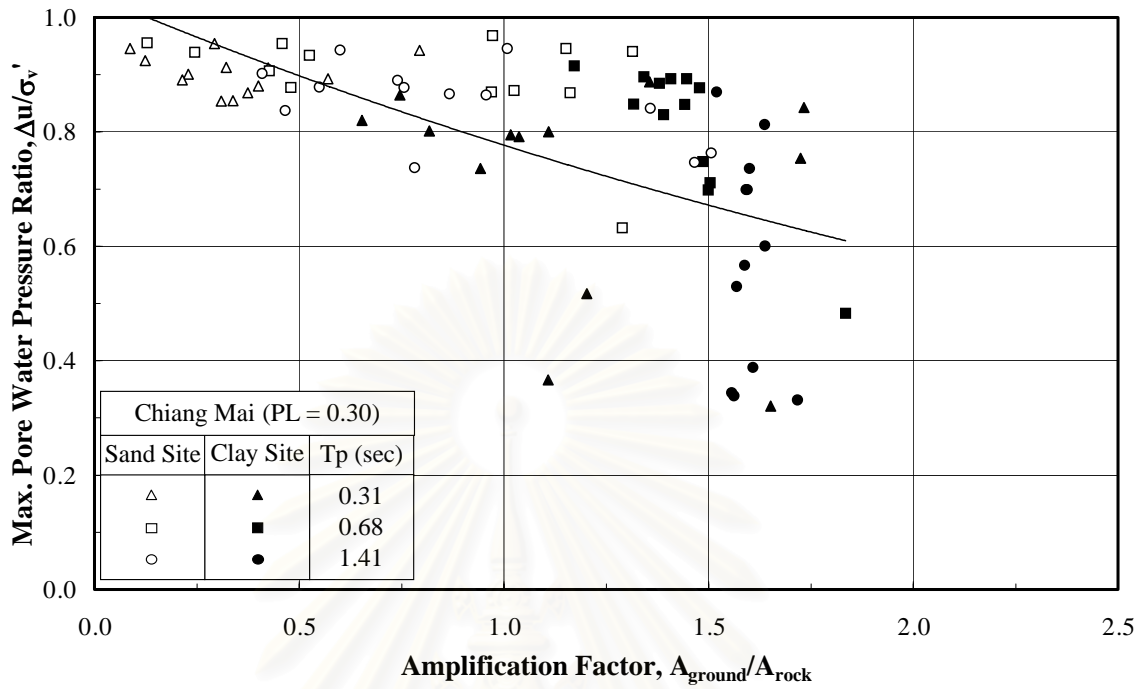


**Fig. 6.9.** Relationship between amplification factor and maximum pore water pressure ratio for Chiang Mai (cont.)

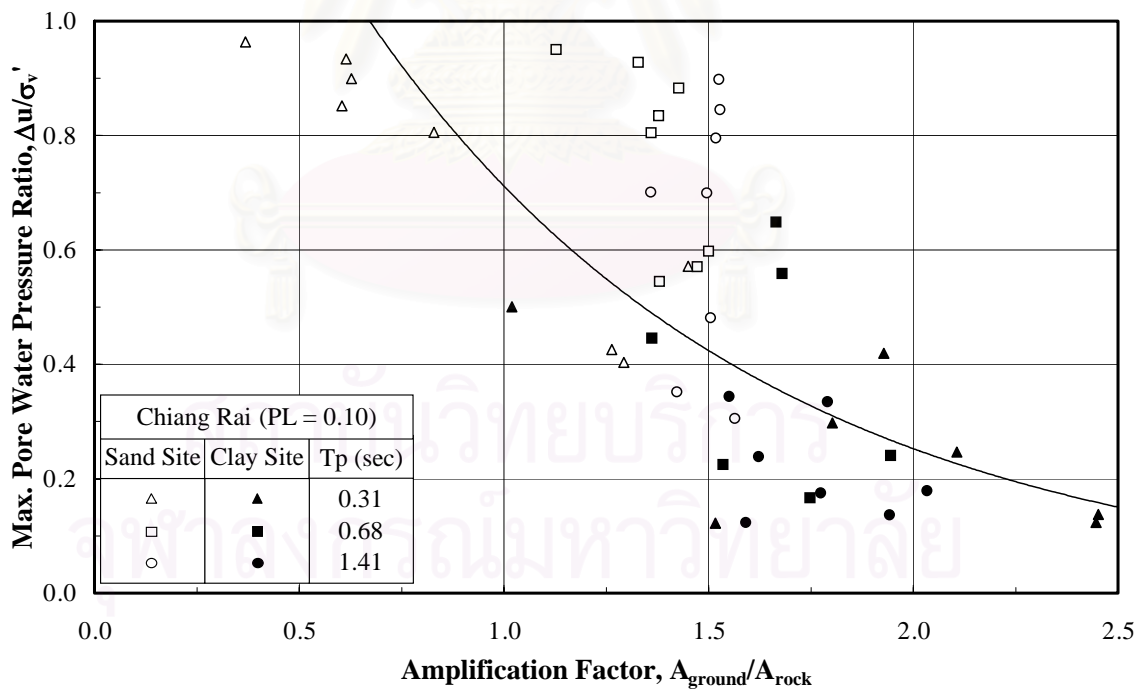
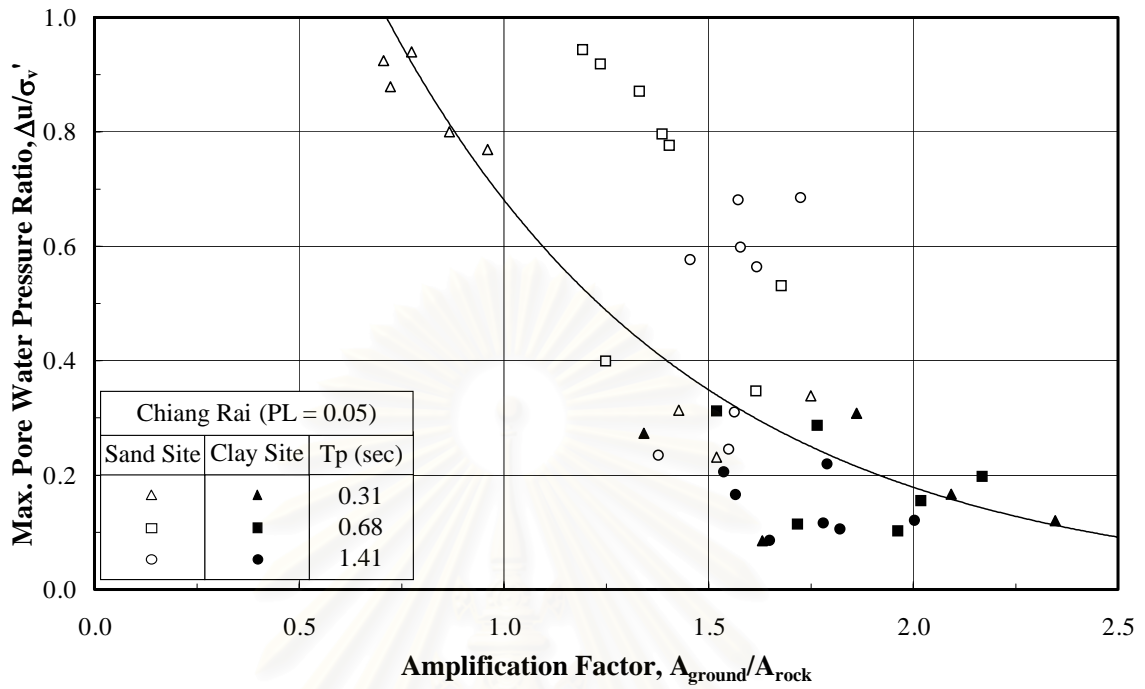


**Fig. 6.10.** Relationship between amplification factor and maximum pore water pressure ratio for Chiang Rai

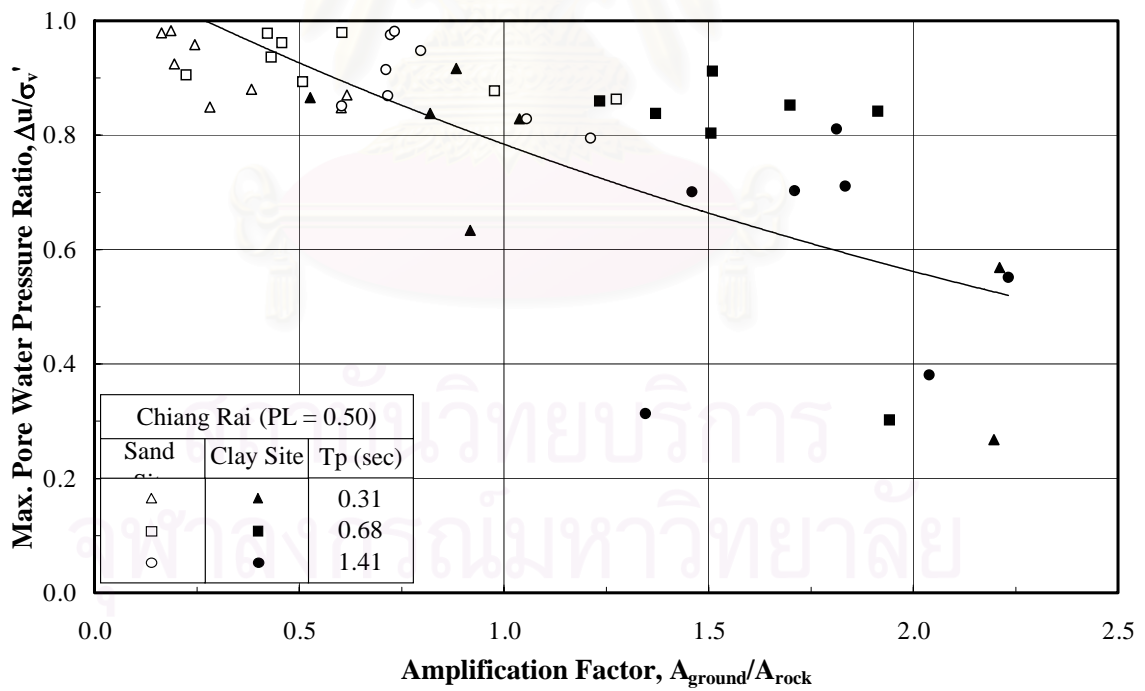
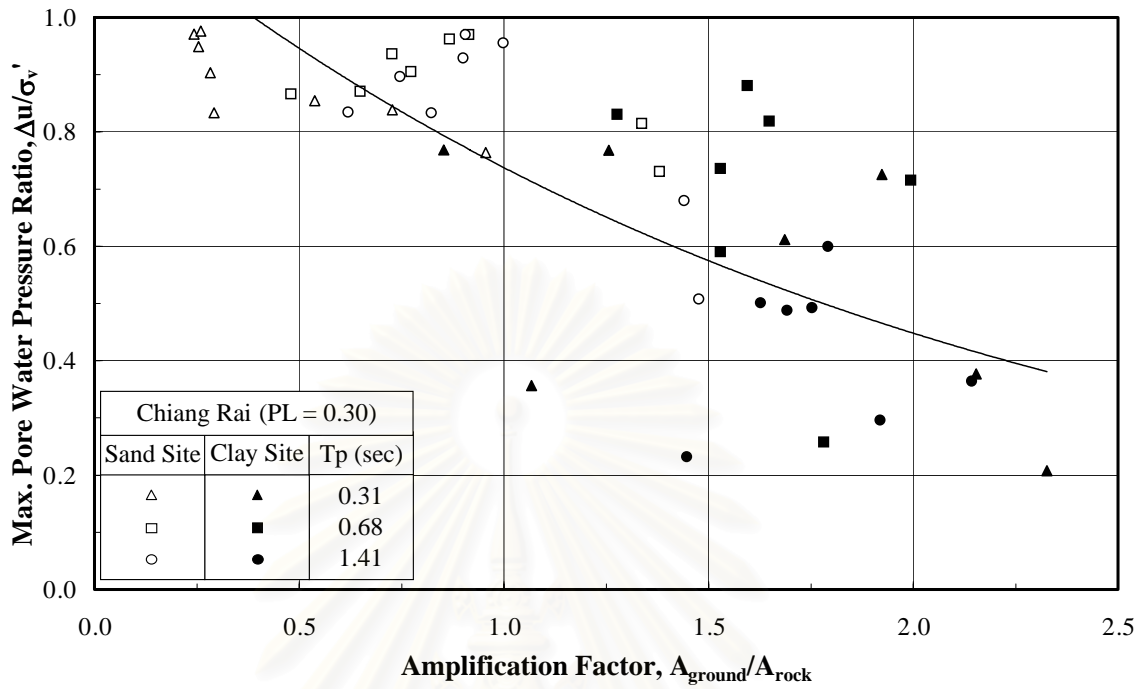


**Fig. 6.10.** Relationship between amplification factor and maximum pore water pressure ratio for Chiang Rai (cont.)

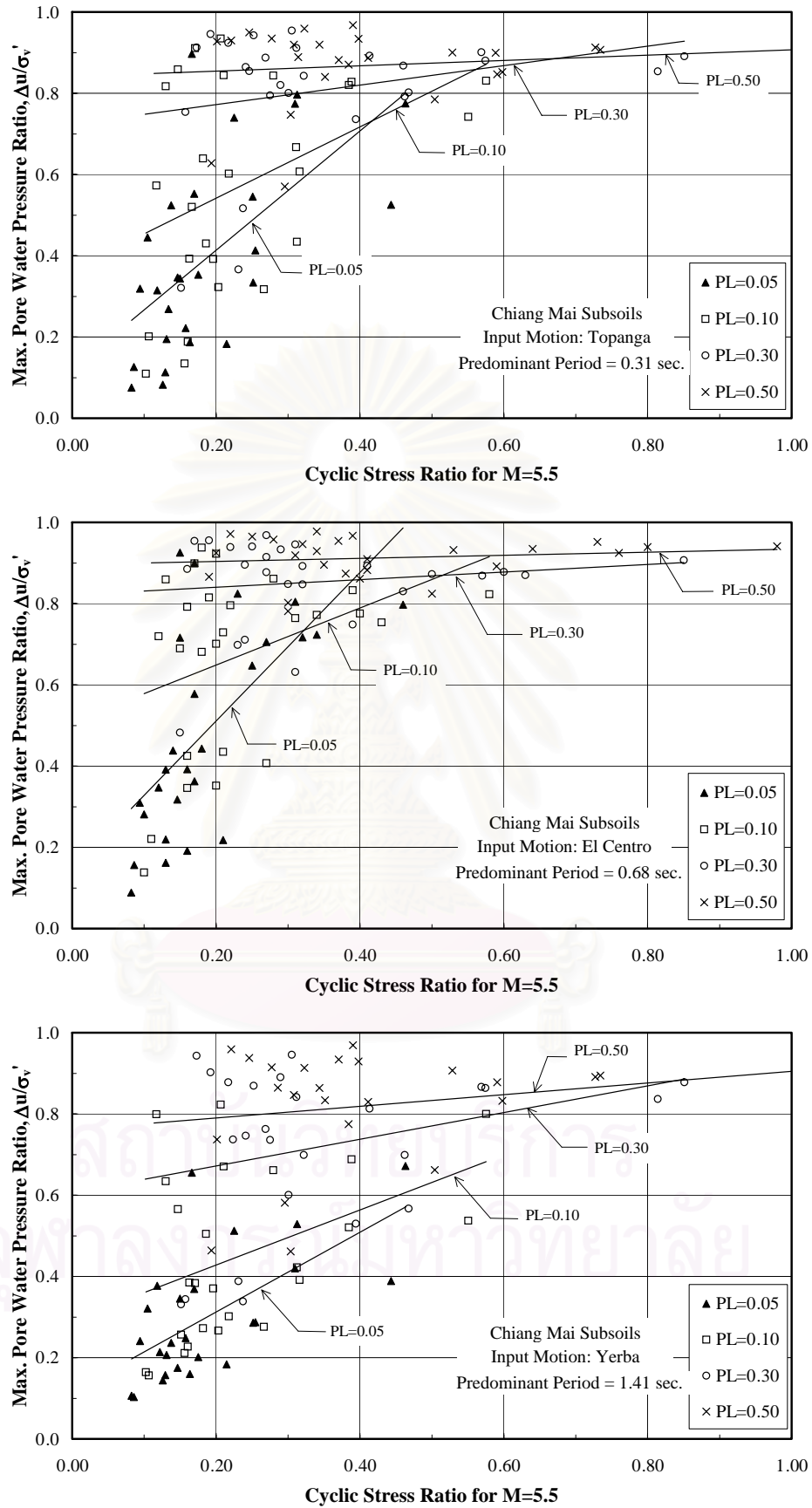


**Fig. 6.11.** Relationship between cyclic stress ratio for earthquake magnitude of 5.5 and maximum pore water pressure ratio for Chiang Mai

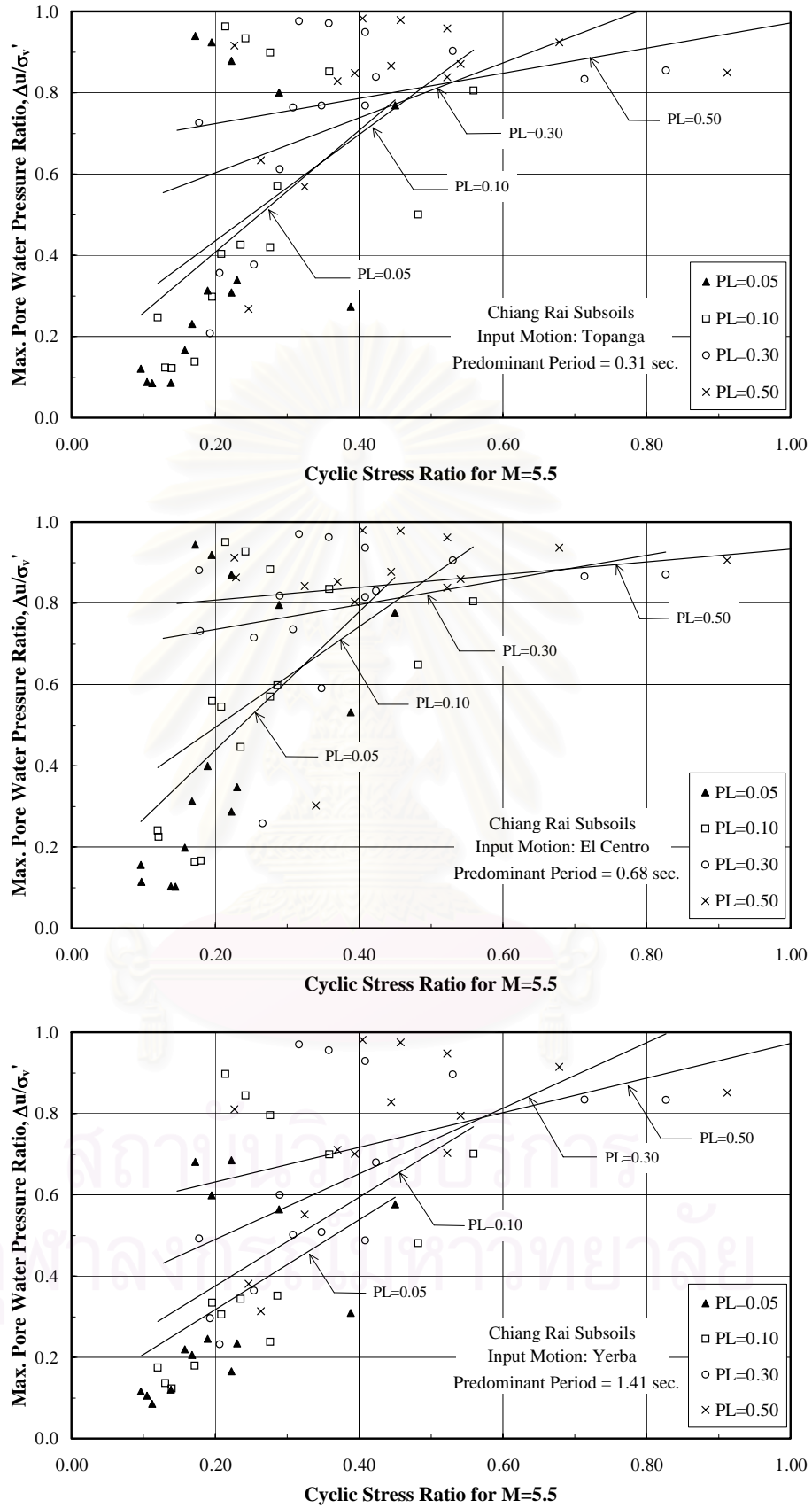


**Fig. 6.12.** Relationship between cyclic stress ratio for earthquake magnitude of 5.5 and maximum pore water pressure ratio for Chiang Rai

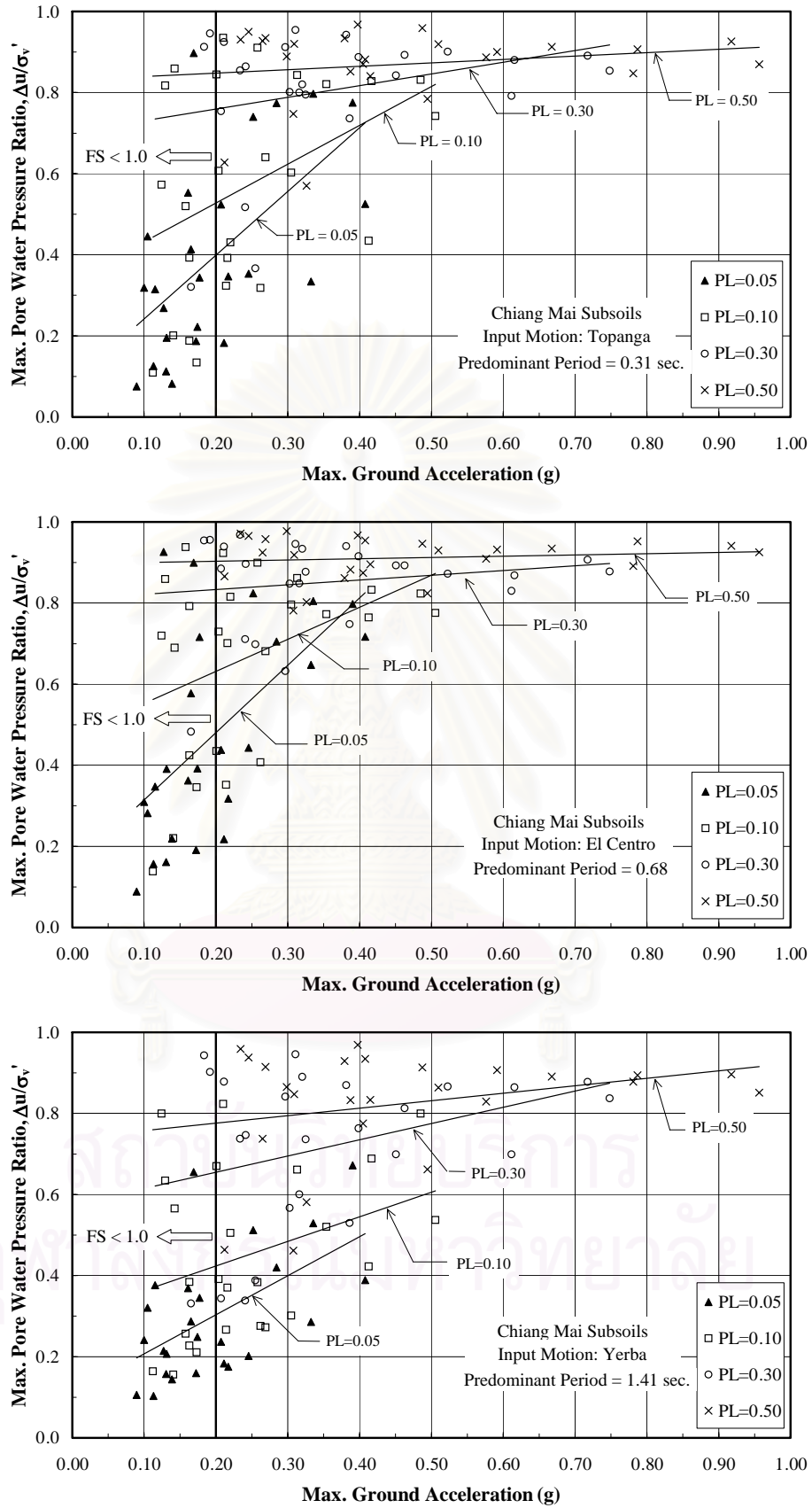


**Fig. 6.13.** Relationship between maximum ground acceleration and maximum pore water pressure ratio for Chiang Mai



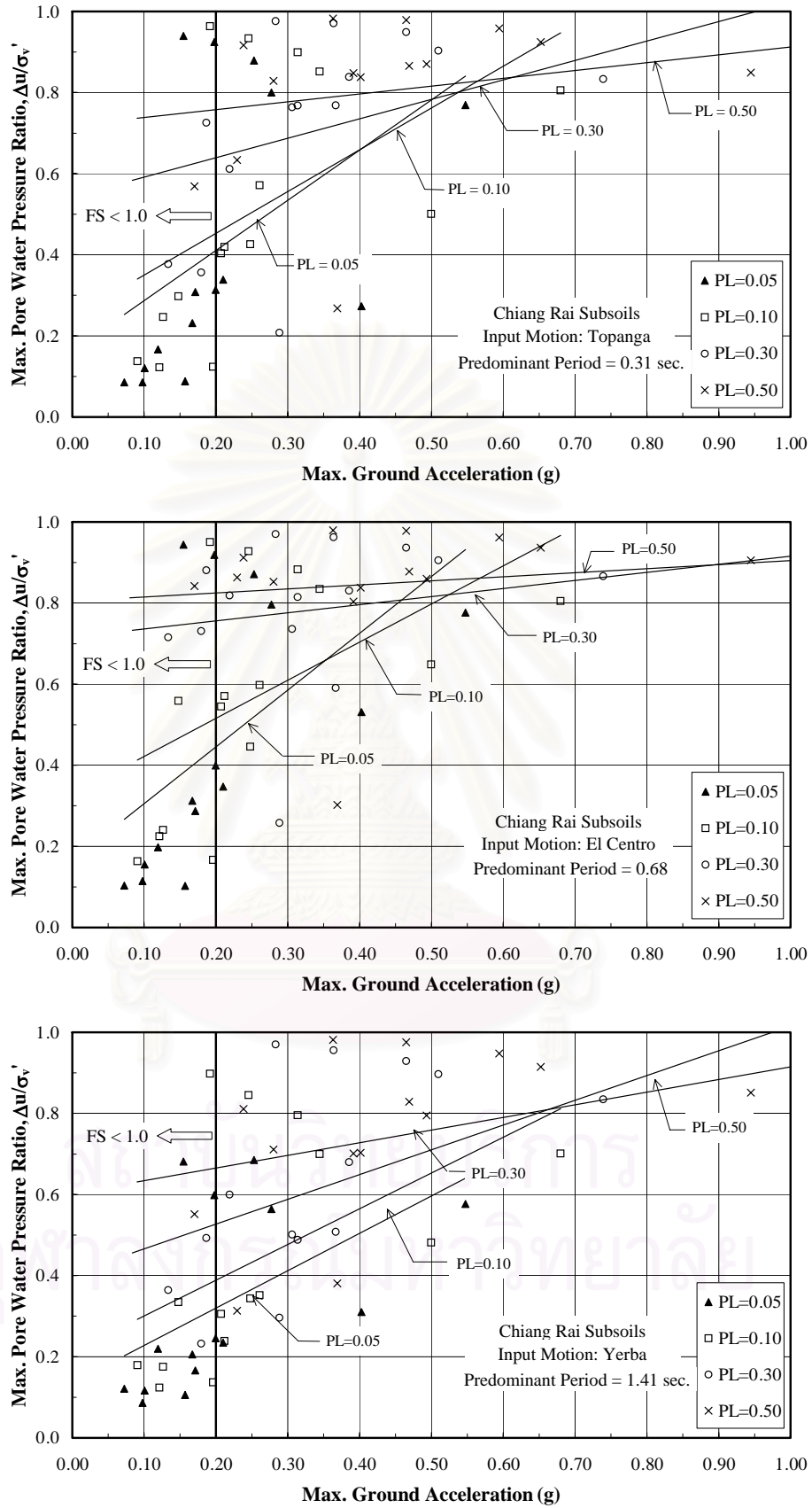


**Fig. 6.14.** Relationship between maximum ground acceleration and maximum pore water pressure ratio for Chiang Rai

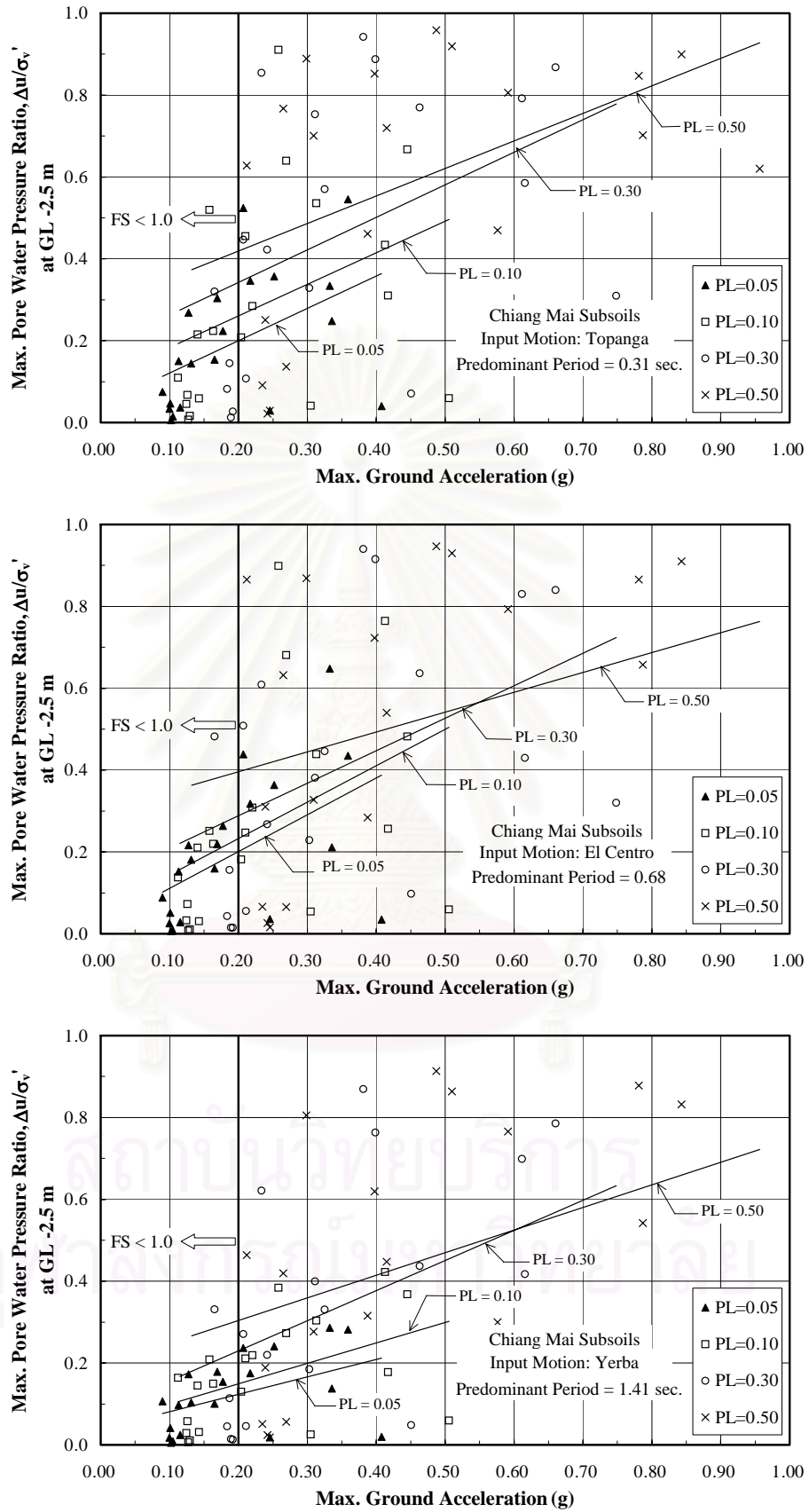


**Fig. 6.15.** Relationship between maximum ground acceleration and maximum pore water pressure ratio at GL -2.5 m for Chiang Mai

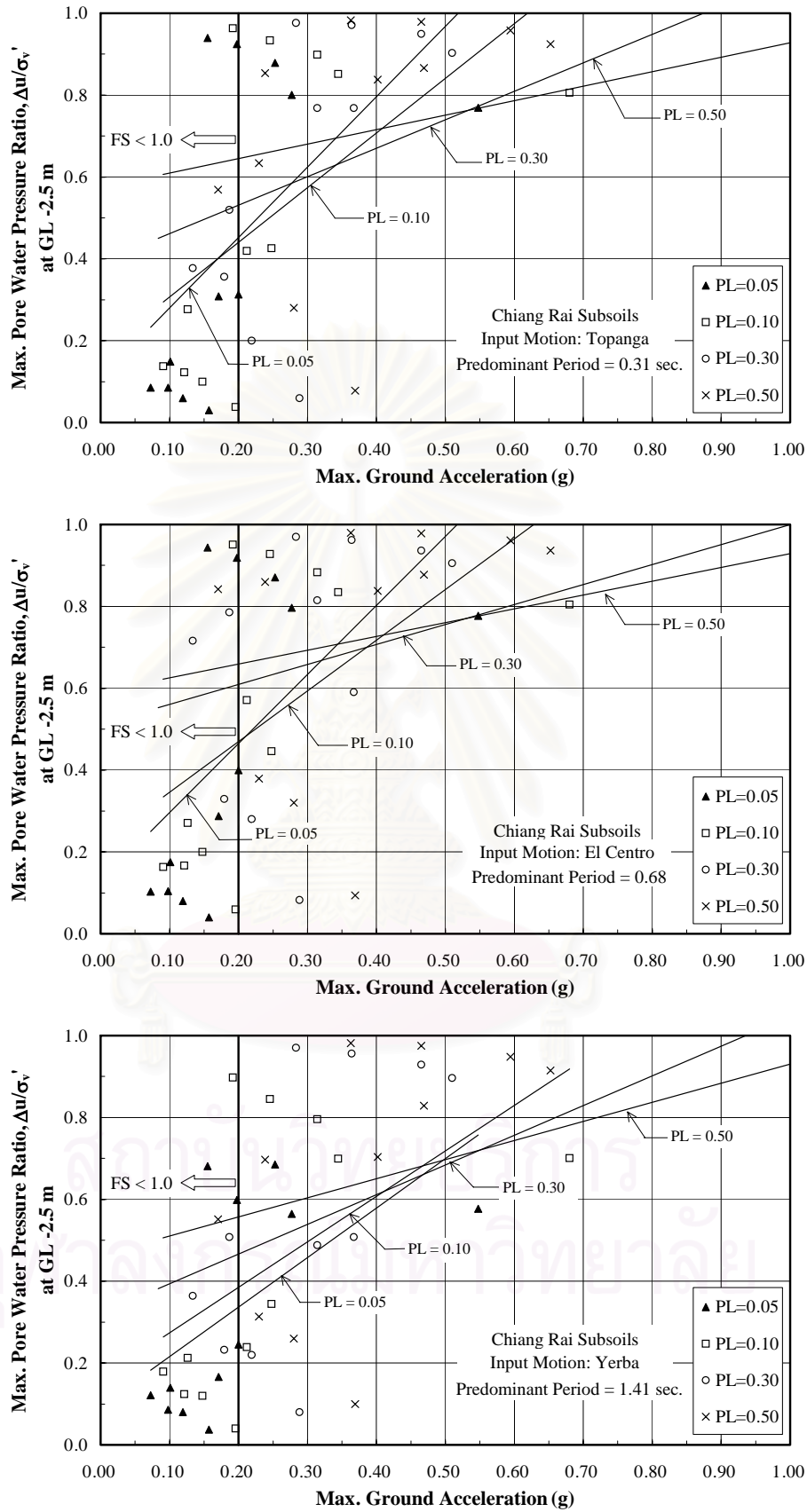
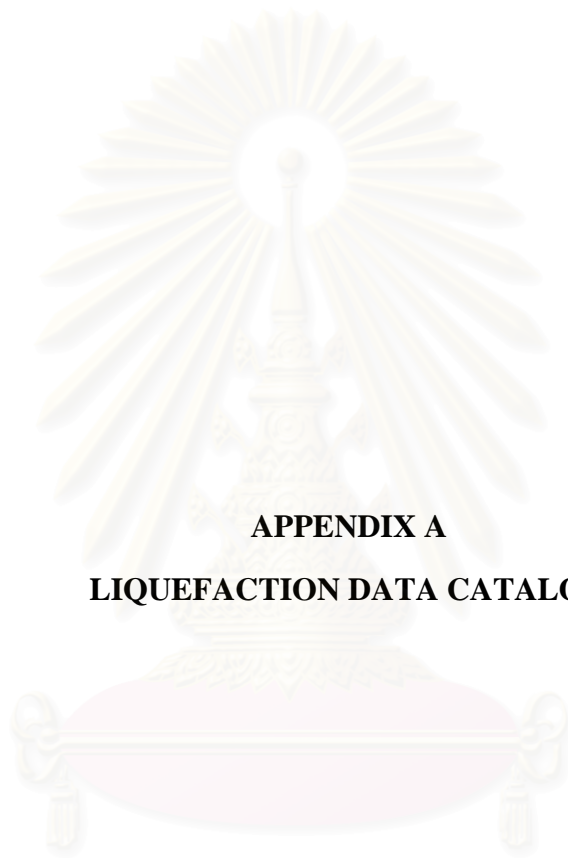


**Fig. 6.16.** Relationship between maximum ground acceleration and maximum pore water pressure ratio at GL -2.5 m for Chiang Rai



**APPENDICES**

สถาบันวิทยบริการ  
จุฬาลงกรณ์มหาวิทยาลัย



**APPENDIX A**  
**LIQUEFACTION DATA CATALOG**

สถาบันวิทยบริการ  
จุฬาลงกรณ์มหาวิทยาลัย

## Liquefaction data catalog compiled by Liao and Whitman (1986a)

Data From Previously Published Catalogs																				
CASE	BCAT	LIQ1	LIQ2	M	H	EP	DER	DUR	A	CSR	CSRN	ZW	ZL	SIGT	SIGE	N	N1	CE	N160	FC
0101	2	0.	-1.	6.6	-1.	-1.	39.	20.	.12	.14	-1.	.9	6.1	-1.	.65	6.	8.0	-1.	-1.	-1.
0102	2	0.	-1.	6.6	-1.	-1.	39.	20.	.12	.14	-1.	.9	6.1	1.07	.65	12.	16.0	-1.	-1.	-1.
0201	2	0.	-1.	6.1	-1.	-1.	47.	12.	.08	.09	-1.	.9	6.1	-1.	.55	6.	8.0	-1.	-1.	-1.
0202	2	0.	-1.	6.1	-1.	-1.	47.	12.	.08	.09	-1.	.9	6.1	-1.	.55	12.	16.0	-1.	-1.	-1.
0301	2	1.	-1.	8.4	-1.	-1.	32.	75.	.35	.39	-1.	.9	13.7	-1.	1.30	17.	15.0	-1.	-1.	-1.
0301	4	1.	-1.	-2.	-1.	30.	-1.	-1.	-1.	-2.	-1.	.8	-2.	-1.	-1.	-2.	-1.	-1.	-1.	-2.
0301	7	1.	1.0	7.9	-1.	-1.	-1.	-1.	.32	-1.	.364	.8	10.0	1.90	.98	20.	20.2	-1.	-1.	0.
0301	8	1.	-1.	7.9	-1.	-1.	-1.	-1.	.32	.356	.376	.8	10.0	1.93	1.02	20.	19.6	1.30	26.6	0.
0302	2	1.	-1.	8.4	-1.	-1.	32.	75.	.35	.37	-1.	1.8	9.1	-1.	1.00	10.	10.0	-1.	-1.	-1.
0302	4	1.	-1.	-2.	-1.	30.	-1.	-1.	-1.	-1.	-1.	2.0	-2.	-1.	-1.	-2.	-1.	-1.	-1.	-2.
0302	7	1.	1.0	7.9	-1.	-1.	-1.	-1.	.32	-1.	.317	2.0	7.0	1.33	.83	10.	11.1	-1.	-1.	6.
0302	8	1.	-1.	7.9	-1.	-1.	-1.	-1.	.32	.31	.33	2.0	7.0	1.35	.86	10.	10.6	1.17	12.6	6.
0303	2	0.	-1.	8.4	-1.	-1.	32.	75.	.35	.35	-1.	1.8	7.6	-1.	.65	19.	21.0	-1.	-1.	-1.
0303	4	0.	-1.	-2.	-1.	30.	-1.	-1.	-1.	-1.	-1.	1.9	-1.	-1.	-1.	-2.	-1.	-1.	-1.	-2.
0303	7	1.	1.0	7.9	-1.	-1.	-1.	-1.	.28	-1.	.276	1.9	6.0	1.14	.73	17.	20.2	-1.	-1.	3.
0303	8	1.	-1.	7.9	-1.	-1.	-1.	-1.	.32	.316	.33	1.9	6.0	1.17	.75	17.	19.0	1.39	26.0	3.
0304	2	1.	-1.	8.4	-1.	-1.	32.	75.	.35	.36	-1.	2.4	6.1	-1.	.75	16.	19.0	-1.	-1.	-1.
0304	4	1.	-1.	-2.	-1.	30.	-1.	-1.	-1.	-1.	-1.	2.0	-2.	-1.	-1.	-2.	-1.	-1.	-1.	-2.
0304	7	1.	1.0	7.9	-1.	-1.	-1.	-1.	.28	-1.	.246	2.4	6.0	.95	.69	13.	15.9	-1.	-1.	4.
0304	8	1.	-1.	7.9	-1.	-1.	-1.	-1.	.32	.276	.29	2.4	6.0	1.00	.72	13.	15.0	1.17	17.0	4.
0306	3	0.	-1.	8.4	-1.	-1.	-1.	-1.	.35	-1.	-1.	1.8	12.2	-1.	-1.	-1.	48.0	-1.	-1.	-1.
0306	6	1.	-1.	8.4	-1.	55.	-1.	-1.	-1.	-1.	-1.	-1.	-1.	-1.	.74	-1.	16.4	-1.	-1.	-1.
0307	6	1.	-1.	8.4	-1.	51.	-1.	-1.	-1.	-1.	-1.	-1.	-1.	-1.	.45	-1.	20.3	-1.	-1.	-1.
0401	6	1.	-1.	7.5	-1.	79.	-1.	-1.	-1.	-1.	-1.	-1.	-1.	-1.	.62	-1.	10.6	-1.	-1.	-1.
0402	6	1.	-1.	7.5	-1.	55.	-1.	-1.	-1.	-1.	-1.	-1.	-1.	-1.	.37	-1.	10.7	-1.	-1.	-1.
0403	6	0.	-1.	7.5	-1.	58.	-1.	-1.	-1.	-1.	-1.	-1.	-1.	-1.	.64	-1.	12.1	-1.	-1.	-1.
0404	6	1.	-1.	7.5	-1.	37.	-1.	-1.	-1.	-1.	-1.	-1.	-1.	-1.	.39	-1.	4.0	-1.	-1.	-1.
0405	6	1.	-1.	7.5	-1.	13.	-1.	-1.	-1.	-1.	-1.	-1.	-1.	-1.	.47	-1.	7.5	-1.	-1.	-1.
0501	3	1.	-1.	8.3	-1.	-1.	-1.	-1.	-1.	-1.	-1.	2.4	4.6	-1.	.60	16.	20.4	-1.	-1.	-1.
0501	4	1.	-1.	-2.	25.	-1.	-1.	-1.	-1.	-1.	-1.	2.4	4.6	-1.	-1.	16.	-1.	-1.	-1.	-1.
0502	3	1.	-1.	8.3	-1.	-1.	-1.	-1.	-1.	-1.	-1.	2.4	7.6	-1.	.85	16.	17.4	-1.	-1.	-1.
0502	4	1.	-1.	-2.	25.	-1.	-1.	-1.	-1.	-1.	-1.	2.4	7.6	-1.	-1.	16.	-1.	-1.	-1.	-1.
0503	3	1.	-1.	8.3	-1.	-1.	-1.	-1.	-1.	-1.	-1.	2.4	4.9	-1.	.98	52.	52.2	-1.	-1.	-1.
0504	3	1.	-1.	8.3	-1.	-1.	-1.	-1.	-1.	-1.	-1.	1.5	4.6	-1.	.62	24.	33.3	-1.	-1.	-1.
0504	4	1.	-1.	-2.	-1.	-1.	-1.	-1.	-1.	-1.	-1.	1.5	4.6	-1.	-1.	24.	-1.	-1.	-1.	-1.

## Liquefaction data catalog compiled by Liao and Whitman (1986a) (cont.)

CASE	BCAT	LIQ1	LIQ2	M	H	EP	DER	DUR	A	CSR	CSR <sub>N</sub>	ZW	ZL	SIGT	SIGE	N	N1	CE	N160	FC
0505	6	1.	-1.	8.3	-1.	48.	-1.	-1.	-1.	-1.	-1.	-1.	-1.	-1.	.48	-1.	8.7	-1.	-1.	-1.
0505	6	1.	-1.	8.3	-1.	48.	-1.	-1.	-1.	-1.	-1.	-1.	-1.	-1.	.69	-1.	5.8	-1.	-1.	-1.
0506	6	1.	-1.	8.3	-1.	184.	-1.	-1.	-1.	-1.	-1.	-1.	-1.	-1.	.43	-1.	10.3	-1.	-1.	-1.
0601	6	0.	-1.	6.9	-1.	51.	-1.	-1.	-1.	-1.	-1.	-1.	-1.	-1.	.74	-1.	15.4	-1.	-1.	-1.
0602	6	0.	-1.	6.9	-1.	57.	-1.	-1.	-1.	-1.	-1.	-1.	-1.	-1.	.46	-1.	20.3	-1.	-1.	-1.
0701	7	1.	0.7	7.9	-1.	-1.	-1.	-1.	.20	.163	-1.	4.0	7.0	1.25	.95	10.	10.3	-1.	-1.	10.
0701	8	1.	-1.	7.9	-1.	-1.	-1.	-1.	.20	.16	.17	4.0	7.0	1.28	.98	10.	10.0	1.09	11.0	10.
0702	7	1.	0.7	7.9	-1.	-1.	-1.	-1.	.20	-1.	.168	4.0	8.0	1.44	1.04	1.	1.0	-1.	-1.	14.
0703	7	1.	0.7	7.9	-1.	-1.	-1.	-1.	.20	-1.	.130	4.0	4.3	.73	.71	2.2	2.7	-1.	-1.	22.
0703	8	1.	-1.	7.9	-1.	-1.	-1.	-1.	.20	.13	.14	4.0	4.3	.75	.73	2.	2.5	1.09	2.5	22.
0704	7	1.	1.0	7.9	-1.	-1.	-1.	-1.	.20	-1.	.225	1.0	8.0	1.52	.82	16.5	18.5	-1.	-1.	1.
0704	8	1.	-1.	7.9	-1.	-1.	-1.	-1.	.20	.225	.24	1.0	8.0	1.58	.85	16.	17.0	1.21	20.5	1.
0705	7	1.	0.7	7.9	-1.	-1.	-1.	-1.	.20	-1.	.167	1.0	5.0	.95	.65	11.9	15.0	-1.	-1.	5.
0705	8	1.	-1.	7.9	-1.	-1.	-1.	-1.	.20	.22	.23	1.0	5.0	1.00	.57	12.	15.5	1.09	16.5	5.
0706	7	0.	0.5	7.9	-1.	-1.	-1.	-1.	.20	-1.	.162	3.0	5.0	.95	.75	5.7	6.7	-1.	-1.	20.
0706	8	0.	.5	7.9	-1.	-1.	-1.	-1.	.20	.16	.17	3.0	5.0	1.00	.78	6.	6.5	1.09	7.0	20.
0707	7	0.	0.5	7.9	-1.	-1.	-1.	-1.	.20	-1.	.18	3.0	8.0	1.52	1.02	2.	2.0	-1.	-1.	33.
0708	8	0.	-1.	7.9	-1.	114.	-1.	-1.	-1.	-1.	-1.	-1.	-1.	-1.	.62	-1.	10.5	-1.	-1.	-1.
0709	8	0.	-1.	7.9	-1.	102.	-1.	-1.	-1.	-1.	-1.	-1.	-1.	-1.	.37	-1.	10.7	-1.	-1.	-1.
0710	8	0.	-1.	7.9	-1.	105.	-1.	-1.	-1.	-1.	-1.	-1.	-1.	-1.	.54	-1.	12.1	-1.	-1.	-1.
0711	8	1.	-1.	7.9	-1.	95.	-1.	-1.	-1.	-1.	-1.	-1.	-1.	-1.	.39	-1.	4.0	-1.	-1.	-1.
0712	8	1.	-1.	7.9	-1.	77.	-1.	-1.	-1.	-1.	-1.	-1.	-1.	-1.	.47	-1.	7.5	-1.	-1.	-1.
0713	8	1.	-1.	7.9	-1.	72.	-1.	-1.	-1.	-1.	-1.	-1.	-1.	-1.	.42	-1.	6.5	-1.	-1.	-1.
0714	8	1.	-1.	7.9	-1.	75.	-1.	-1.	-1.	-1.	-1.	-1.	-1.	-1.	.47	-1.	15.1	-1.	-1.	-1.
0801	2	1.	-1.	6.3	-1.	-1.	11.	15.	.20	.18	-1.	4.6	7.5	-1.	-1.	-1.	-1.	-1.	-1.	-1.
0801	5	1.	-1.	6.3	-1.	11.	-1.	15.	.20	-1.	-1.	4.5	7.5	-1.	-1.	3.	-1.	-1.	-1.	-1.
0801	6	1.	1.0	6.3	-1.	11.	-1.	-1.	-1.	-1.	-1.	-1.	-1.	-1.	1.06	-1.	2.9	-1.	-1.	-1.
0901	6	1.	-1.	7.0	-1.	20.	-1.	-1.	-1.	-1.	-1.	-1.	-1.	-1.	.62	-1.	10.5	-1.	-1.	-1.
0902	6	1.	-1.	7.0	-1.	19.	-1.	-1.	-1.	-1.	-1.	-1.	-1.	-1.	.37	-1.	10.7	-1.	-1.	-1.
0903	6	0.	-1.	7.0	-1.	34.	-1.	-1.	-1.	-1.	-1.	-1.	-1.	-1.	.54	-1.	12.1	-1.	-1.	-1.
0904	6	1.	-1.	7.0	-1.	51.	-1.	-1.	-1.	-1.	-1.	-1.	-1.	-1.	.39	-1.	4.0	-1.	-1.	-1.
0905	6	0.	-1.	7.0	-1.	55.	-1.	-1.	-1.	-1.	-1.	-1.	-1.	-1.	.47	-1.	7.5	-1.	-1.	-1.

## Liquefaction data catalog compiled by Liao and Whitman (1986a) (cont.)

CASE	BCAT	LIQ1	LIQ2	M	R	EP	DER	DUR	A	CSR	CSRW	ZV	ZL	SIGT	SIGE	N	N1	CE	N160	FC
1001	3	0.	-1.	6.3	-1.	-1.	-1.	-1.	-1.	-1.	-1.	3.0	-2.	-1.	-2.	-2.	-2.	-1.	-1.	-1.
1002	3	0.	-1.	6.3	-1.	-1.	-1.	-1.	-1.	-1.	-1.	5.5	-2.	-1.	-2.	-2.	-2.	-1.	-1.	-1.
1003	3	0.	-1.	6.3	-1.	-1.	-1.	-1.	-1.	-1.	-1.	3.0	-2.	-1.	-2.	-2.	-2.	-1.	-1.	-1.
1004	3	0.	-1.	6.3	-1.	-1.	-1.	-1.	-1.	-1.	-1.	3.0	-2.	-1.	-2.	-2.	-2.	-1.	-1.	-1.
1005	7	0.	-1.	6.3	-1.	-1.	-1.	-1.	.20	-1.	.163	-1.	-1.	-1.	-1.	-1.	7.0	-1.	-1.	-1.
1005	8	0.	-1.	6.3	-1.	-1.	-1.	-1.	.20	.205	.165	1.8	8.2	1.51	.90	8.	8.0	1.00	8.0	25.
1006	8	0.	-1.	6.3	-1.	-1.	-1.	-1.	.18	.155	.125	1.8	8.1	1.11	.71	7.	8.5	1.00	8.5	2.
1101	2	1.	-1.	7.0	-1.	-1.	8.	30.	.25	.155	-1.	4.5	4.5	-1.	-1.	-1.	-1.	-1.	-1.	-1.
1101	5	1.	-1.	-2.	-1.	-1.	-1.	-1.	.25	-1.	-1.	4.5	4.5	-1.	-1.	9.	-1.	-1.	-1.	-1.
1101	6	1.	-1.	7.0	-1.	8.	-1.	-1.	-1.	-1.	-1.	-1.	-1.	-1.	.77	-1.	9.8	-1.	-1.	-1.
1102	2	1.	-1.	7.0	-1.	-1.	8.	30.	.25	.155	-1.	6.1	7.6	-1.	-1.	-1.	-1.	-1.	-1.	-1.
1102	5	1.	-1.	7.0	-1.	-1.	-1.	-1.	.25	-1.	-1.	6.0	7.5	-1.	-1.	4.	-1.	-1.	-1.	-1.
1102	6	1.	-1.	7.0	-1.	8.	-1.	-1.	.25	-1.	-1.	-1.	-1.	-1.	1.17	-1.	3.8	-1.	-1.	-1.
1103	2	1.	-1.	7.0	-1.	-1.	8.	30.	.25	.28	-1.	1.5	6.1	-1.	-1.	-1.	-1.	-1.	-1.	-1.
1103	5	1.	-1.	7.0	-1.	-1.	-1.	-1.	.25	-1.	-1.	1.5	6.0	-1.	-1.	1.	-1.	-1.	-1.	-1.
1103	6	1.	-1.	7.0	-1.	8.	-1.	-1.	-1.	-1.	-1.	-1.	-1.	-1.	.69	-1.	1.1	-1.	-1.	-1.
1201	2	1.	-1.	8.0	-1.	-1.	.161	70.	.03	.08	-1.	1.5	4.0	-1.	.50	4.	5.0	-1.	-1.	-1.
1201	4	1.	-1.	-2.	-1.	.165	-1.	-1.	-1.	-1.	-1.	2.0	-2.	-1.	-1.	-2.	-1.	-1.	-1.	-2.
1201	7	1.	1.0	8.0	-1.	-1.	-1.	-1.	.20	-1.	.193	2.0	5.0	.91	.51	8.	10.4	-1.	-1.	10.
1201	8	1.	-1.	8.0	-1.	-1.	-1.	-1.	.20	.18	.195	2.1	5.2	1.00	.59	8.	9.5	1.17	11.0	10.
1202	2	1.	-1.	8.0	-1.	-1.	.161	70.	.08	.09	-1.	.5	2.4	-1.	.25	1.	2.0	-1.	-1.	-1.
1202	4	1.	-1.	-2.	-1.	.165	-1.	-1.	-1.	-1.	-1.	.5	-2.	-1.	-1.	-2.	-1.	-1.	-1.	-2.
1202	7	1.	1.0	8.0	-1.	-1.	-1.	-1.	.20	-1.	.243	.5	3.5	.68	.36	1.	1.6	-1.	-1.	-1.
1202	8	1.	-1.	8.0	-1.	-1.	-1.	-1.	.20	.225	.24	.5	3.7	.70	.40	1.	1.5	1.17	1.5	27.
1203	4	3.	-1.	-2.	-1.	.165	-1.	-1.	-1.	-1.	-1.	2.5	-2.	-1.	-1.	-2.	-1.	-1.	-1.	-2.
1203	7	1.	1.0	8.0	-1.	-1.	-1.	-1.	.20	-1.	.148	2.5	3.0	.51	.46	2.	2.9	-1.	-1.	30.
1203	8	1.	-1.	8.0	-1.	-1.	-1.	-1.	.20	.145	.155	2.4	3.0	.55	.49	2.	2.5	1.17	3.0	30.
1204	7	1.	1.0	8.0	-1.	-1.	-1.	-1.	.15	-1.	.181	2.0	7.0	1.33	.83	10.	11.1	-1.	-1.	5.
1204	8	1.	-1.	8.0	-1.	-1.	-1.	-1.	.15	.155	.165	2.1	7.0	1.35	.85	10.	10.5	1.17	12.5	5.
1301	7	0.	1.0	7.3	-1.	-1.	-1.	-1.	.35	-1.	.392	.8	4.0	.69	.35	7.	11.2	-1.	-1.	35.
1302	2	0.	-1.	7.2	-1.	-1.	6.	30.	.30	.32	-1.	.9	7.0	-1.	.70	28.	34.0	-1.	-1.	-1.
1302	4	0.	-1.	-2.	-1.	5.	-1.	-1.	-1.	-1.	-1.	.8	-2.	-1.	-1.	-2.	-1.	-1.	-1.	-2.
1302	7	0.	0.0	7.3	-1.	-1.	-1.	-1.	.35	-1.	.388	.8	8.0	1.44	.72	29.	34.7	-1.	-1.	2.
1302	8	0.	-1.	7.3	-1.	-1.	-1.	-1.	.35	.395	.385	.9	8.2	1.57	.83	29.	31.5	1.30	40.5	2.
1303	2	1.	-1.	7.2	-1.	-1.	6.	30.	.30	.30	-1.	3.4	7.0	-1.	.95	18.	18.0	-1.	-1.	-1.
1303	4	1.	-1.	-2.	-1.	5.	-1.	-1.	-1.	-1.	-1.	3.7	-2.	-1.	-1.	-2.	-1.	-1.	-1.	-2.
1303	7	1.	1.0	7.3	-1.	-1.	-1.	-1.	.35	-1.	.287	3.7	7.0	1.25	.93	19.	19.8	-1.	-1.	4.
1303	8	1.	-1.	7.3	-1.	-1.	-1.	-1.	.35	.29	.28	3.7	7.0	1.35	1.01	19.	18.5	1.30	24.0	4.
1304	2	1.	-1.	7.3	-1.	-1.	6.	30.	.30	.29	-1.	1.2	3.0	-1.	.38	3.	5.0	-1.	-1.	-1.
1304	4	1.	-1.	-2.	-1.	5.	-1.	-1.	-1.	-1.	-1.	1.2	-2.	-1.	-1.	-2.	-1.	-1.	-1.	-2.
1304	7	1.	1.	7.3	-1.	-1.	-1.	-1.	.40	-1.	.375	1.2	4.0	.75	.48	8.	11.5	-1.	-1.	0.
1304	8	1.	-1.	7.3	-1.	-1.	-1.	-1.	.40	.395	.38	1.2	4.0	.75	.49	8.	11.0	1.17	13.0	0.



## Liquefaction data catalog compiled by Liao and Whitman (1986a) (cont.)

CASE	BCAT	LIQ1	LIQ2	M	H	EP	DER	DUR	A	CSR	CSR <sub>N</sub>	ZW	ZL	SIGT	SIGE	N	N1	CE	N100	FC
1305	2	1.	-1.	7.2	-1.	-1.	6.	30.	.30	.33	-1.	.9	8.1	-1.	.60	5.	7.0	-1.	-1.	-1.
1305	4	1.	-1.	-2.	-1.	5.	-1.	-1.	-1.	-1.	-1.	.9	-2.	-1.	-1.	-2.	-1.	-1.	-1.	-2.
1305	7	0.	0.5	7.3	-1.	-1.	-1.	-1.	.40	-1.	.450	.9	6.0	1.02	.52	8.	11.1	-1.	-1.	21.
1306	7	0.	0.5	7.3	-1.	-1.	-1.	-1.	.40	-1.	.451	.9	7.5	1.31	.65	20.	25.2	-1.	-1.	0.
1306	6	0.	-1.	7.3	-1.	-1.	-1.	-1.	.40	.48	.45	.9	7.8	1.42	.75	20.	22.5	1.30	29.0	0.
1401	3	0.	-1.	5.4	-1.	-1.	-1.	-1.	-1.	-1.	-1.	2.4	17.1	-1.	1.50	22.	17.9	-1.	-1.	-1.
1501	3	0.	-1.	5.5	-1.	-1.	-1.	-1.	-1.	-1.	-1.	4.6	6.1	-1.	.94	4.	4.1	-1.	-1.	-1.
1502	2	1.	-1.	5.5	-1.	-1.	6.	18.	.18	.13	-1.	2.4	3.0	-1.	.60	7.	10.0	-1.	-1.	-1.
1502	7	1.	1.0	5.5	-1.	-1.	-1.	-1.	.19	.10	-1.	-1.	-1.	.60	.49	8.	6.1	-1.	-1.	3.
1502	8	1.	-1.	5.3	-1.	-1.	-1.	-1.	.19	.13	.085	2.4	3.0	.62	.46	6.	7.0	.76	5.5	3.
1503	3	0.	-1.	5.5	-1.	-1.	-1.	-1.	-1.	-1.	-1.	3.7	4.0	-1.	.68	14.	16.9	-1.	-1.	-1.
1504	3	0.	-1.	5.5	-1.	-1.	-1.	-1.	-1.	-1.	-1.	2.4	4.6	-1.	.60	16.	20.6	-1.	-1.	-1.
1505	3	0.	-1.	5.5	-1.	-1.	-1.	-1.	-1.	-1.	-1.	2.4	7.6	-1.	.85	16.	17.4	-1.	-1.	-1.
1506	3	0.	-1.	5.5	-1.	-1.	-1.	-1.	-1.	-1.	-1.	1.5	6.1	-1.	.96	52.	52.5	-1.	-1.	-1.
1507	3	0.	-1.	5.5	-1.	-1.	-1.	-1.	-1.	-1.	-1.	1.5	4.6	-1.	.52	24.	33.3	-1.	-1.	-1.
1508	3	0.	-1.	5.5	-1.	-1.	-1.	-1.	-1.	-1.	-1.	1.5	6.1	-1.	.63	6.	7.5	-1.	-1.	-1.
1509	3	0.	-1.	5.5	-1.	-1.	-1.	-1.	-1.	-1.	-1.	4.6	6.1	-1.	.94	20.	20.6	-1.	-1.	-1.
1510	3	0.	-1.	5.5	-1.	-1.	-1.	-1.	-1.	-1.	-1.	2.4	4.6	-1.	.60	20.	25.7	-1.	-1.	-1.
1511	3	0.	-1.	5.5	-1.	-1.	-1.	-1.	-1.	-1.	-1.	.9	1.2	-1.	.19	4.	9.2	-1.	-1.	-1.
1512	3	0.	-1.	5.5	-1.	-1.	-1.	-1.	-1.	-1.	-1.	.9	1.2	-1.	.19	6.	13.9	-1.	-1.	-1.
1513	3	0.	-1.	5.5	-1.	-1.	-1.	-1.	-1.	-1.	-1.	1.2	3.7	-1.	.41	6.	9.4	-1.	-1.	-1.
1514	3	0.	-1.	5.5	-1.	-1.	-1.	-1.	-1.	-1.	-1.	1.2	4.3	-1.	.46	6.	8.8	-1.	-1.	-1.
1515	3	0.	-1.	5.5	-1.	-1.	-1.	-1.	-1.	-1.	-1.	3.0	3.7	-1.	.60	11.	14.2	-1.	-1.	-1.
1516	3	0.	-1.	5.5	-1.	-1.	-1.	-1.	-1.	-1.	-1.	3.0	4.0	-1.	.02	10.	12.7	-1.	-1.	-1.
1517	3	0.	-1.	5.5	-1.	-1.	-1.	-1.	-1.	-1.	-1.	1.8	5.8	-1.	.64	12.	15.0	-1.	-1.	-1.
1518	3	0.	-1.	5.5	-1.	-1.	-1.	-1.	-1.	-1.	-1.	1.2	5.8	-1.	.58	15.	20.9	-1.	-1.	-1.
1519	3	0.	-1.	5.5	-1.	-1.	-1.	-1.	-1.	-1.	-1.	1.6	3.7	-1.	.48	10.	14.5	-1.	-1.	-1.
1520	3	0.	-1.	5.5	-1.	-1.	-1.	-1.	-1.	-1.	-1.	2.4	7.6	-1.	.85	3.	3.3	-1.	-1.	-1.
1521	3	0.	-1.	5.5	-1.	-1.	-1.	-1.	-1.	-1.	-1.	2.4	9.1	-1.	.97	5.	5.1	-1.	-1.	-1.
1522	3	0.	-1.	5.5	-1.	-1.	-1.	-1.	-1.	-1.	-1.	1.8	5.8	-1.	.64	7.	8.7	-1.	-1.	-1.
1523	3	0.	-1.	5.5	-1.	-1.	-1.	-1.	-1.	-1.	-1.	1.8	5.8	-1.	.64	5.	6.2	-1.	-1.	-1.
1524	3	0.	-1.	5.5	-1.	-1.	-1.	-1.	-1.	-1.	-1.	1.8	3.0	-1.	.43	9.	13.8	-1.	-1.	-1.
1525	3	0.	-1.	5.5	-1.	-1.	-1.	-1.	-1.	-1.	-1.	1.8	4.6	-1.	.55	5.	6.8	-1.	-1.	-1.
1526	3	0.	-1.	5.5	-1.	-1.	-1.	-1.	-1.	-1.	-1.	1.8	4.6	-1.	.60	8.	11.3	-1.	-1.	-1.

## Liquefaction data catalog compiled by Liao and Whitman (1986a) (cont.)

CASE	BCAT	LIQ1	LIQ2	M	H	EP	DER	DUR	A	CSR	CSRN	ZW	ZL	SIGT	SIGE	N	N1	CE	N160	FC
1527	3	0.	-1.	5.5	-1.	-1.	-1.	-1.	-1.	-1.	-1.	1.8	4.6	-1.	.50	5.	7.1	-1.	-1.	-1.
1528	3	0.	-1.	5.5	-1.	-1.	-1.	-1.	-1.	-1.	-1.	1.8	4.6	-1.	.50	15.	21.3	-1.	-1.	-1.
1529	3	0.	-1.	5.5	-1.	-1.	-1.	-1.	-1.	-1.	-1.	1.8	3.0	-1.	.43	3.	4.6	-1.	-1.	-1.
1530	3	0.	-1.	5.5	-1.	-1.	-1.	-1.	-1.	-1.	-1.	2.1	2.7	-1.	.43	7.	10.6	-1.	-1.	-1.
1531	3	0.	-1.	5.5	-1.	-1.	-1.	-1.	-1.	-1.	-1.	.8	1.5	-1.	.18	13.	30.6	-1.	-1.	-1.
1532	3	0.	-1.	5.5	-1.	-1.	-1.	-1.	-1.	-1.	-1.	1.2	4.3	-1.	.46	7.	10.3	-1.	-1.	-1.
1533	3	0.	-1.	5.5	-1.	-1.	-1.	-1.	-1.	-1.	-1.	1.2	4.6	-1.	.41	5.	7.8	-1.	-1.	-1.
1534	3	0.	-1.	5.5	-1.	-1.	-1.	-1.	-1.	-1.	-1.	1.2	3.7	-1.	.35	12.	20.2	-1.	-1.	-1.
1601	2	1.	-1.	8.4	-1.	-1.	113.	75.	.15	.15	-1.	3.7	4.6	-1.	.75	6.	7.0	-1.	-1.	-1.
1602	2	1.	-1.	8.4	-1.	-1.	113.	75.	.15	.15	-1.	3.7	4.6	-1.	.75	8.	10.0	-1.	-1.	-1.
1603	2	0.	-1.	8.4	-1.	-1.	113.	75.	.15	.15	-1.	3.7	6.1	-1.	.90	15.	19.0	-1.	-1.	-1.
1604	1	0.	-1.	-1.	-1.	-1.	-1.	-1.	.15	.135	-1.	3.7	7.0	-1.	-1.	10.	-1.	-1.	-1.	-1.
1604	5	0.	-1.	8.4	-1.	-1.	113.	-1.	.15	-1.	-1.	3.5	7.0	-1.	-1.	10.	-1.	-1.	-1.	-1.
1605	1	0.	-1.	-1.	-1.	-1.	-1.	-1.	.15	.140	-1.	3.7	7.9	-1.	-1.	35.	-1.	-1.	-1.	-1.
1605	5	0.	-1.	8.4	-1.	-1.	113.	-1.	.15	-1.	-1.	3.5	8.0	-1.	-1.	35.	-1.	-1.	-1.	-1.
1701	2	1.	-1.	8.3	-1.	-1.	97.	180.	.15	.18	-1.	.0	6.1	-1.	.55	5.	7.0	-1.	-1.	-1.
1701	4	1.	-1.	-2.	-2.	142.	-1.	-1.	-1.	-1.	-1.	.0	-2.	-1.	-1.	-2.	-1.	-1.	-1.	10.
1701	7	1.	1.0	8.3	-1.	-1.	-1.	-1.	.15	-1.	.210	.0	6.0	1.14	.54	5.	4.9	-1.	-1.	40.
1702	2	1.	-1.	8.3	-1.	-1.	97.	180.	.15	.15	-1.	2.4	6.1	-1.	.75	5.	6.0	-1.	-1.	-1.
1702	4	1.	-1.	-2.	-2.	142.	-1.	-1.	-1.	-1.	-1.	-2.	-2.	-1.	-1.	-2.	-1.	-1.	-1.	10.
1702	7	1.	1.0	8.3	-1.	-1.	-1.	-1.	.15	-1.	.165	2.4	5.0	1.14	.73	5.	4.2	-1.	-1.	40.
1703	2	0.	-1.	8.3	-1.	-1.	113.	180.	.12	.146	-1.	.0	7.6	-1.	.75	-2.	-2.	-1.	-1.	-1.
1703	4	0.	-1.	-2.	-2.	145.	-1.	-1.	-1.	-1.	-1.	3.1	-2.	-1.	-1.	-2.	-1.	-1.	-1.	-1.
1704	2	1.	-1.	8.3	-1.	-1.	89.	180.	.16	.185	-1.	.0	6.1	-1.	.55	10.	14.0	-1.	-1.	-1.
1704	4	1.	-2.	-2.	-2.	126.	-1.	-1.	-1.	-1.	-1.	.0	-2.	-1.	-1.	-2.	-1.	-1.	-1.	10.
1704	7	1.	1.0	8.3	-1.	-1.	-1.	-1.	.16	-1.	.224	.0	6.0	1.14	.54	10.	9.8	-1.	-1.	10.
1705	2	1.	-1.	8.3	-1.	-1.	58.	180.	.25	.25	-1.	1.5	6.1	-1.	.65	13.	16.0	-1.	-1.	-1.
1705	4	1.	-1.	-2.	-1.	-1.	1.	-1.	-1.	-1.	-1.	-2.	-2.	-1.	-1.	-2.	-1.	-1.	-1.	-1.
1705	7	1.	1.0	8.3	-1.	-1.	-1.	-1.	.25	-1.	.25	1.5	6.0	1.10	.63	13.	11.9	-1.	-1.	0.
1706	1	1.	-1.	-1.	-1.	-1.	-1.	120.	.15	.192	-1.	.0	4.6	-1.	-1.	16.	-1.	-1.	-1.	-1.
1801	2	1.	-1.	7.5	-1.	-1.	52.	40.	.18	.195	-1.	.9	6.1	-1.	.60	8.	8.0	-1.	-1.	-1.
1801	5	1.	-1.	7.5	-1.	-1.	52.	40.	.18	-1.	-1.	1.0	6.0	-1.	-1.	8.	-1.	-1.	-1.	-1.
1802	2	1.	-1.	7.5	-1.	-1.	52.	40.	.18	.195	-1.	.9	7.6	-1.	.75	15.	18.0	-1.	-1.	-1.
1802	5	1.	-1.	7.5	-1.	-1.	52.	40.	.18	-1.	-1.	1.0	7.5	-1.	-1.	8.	-1.	-1.	-1.	-1.
1803	2	0.	-1.	7.5	-1.	-1.	52.	40.	.18	.195	-1.	.9	6.1	-1.	.60	12.	16.0	-1.	-1.	-1.
1803	5	0.	-1.	7.5	-1.	-1.	52.	40.	.18	-1.	-1.	1.0	6.0	-1.	-1.	12.	-1.	-1.	-1.	-1.
1804	2	0.	-1.	7.5	-1.	-1.	52.	40.	.18	.12	-1.	3.7	7.6	-1.	1.00	6.	6.0	-1.	-1.	-1.

## Liquefaction data catalog compiled by Liao and Whitman (1986a) (cont.)

CASE	BCAT	LIQ1	LIQ2	M	H	EP	DER	DUR	A	CER	CSRH	ZW	ZL	SIGT	SIGE	N	N1	CE	N100	FC
1904	5	0.	-1.	7.5	-1.	-1.	82.	40.	.16	-1.	-1.	3.5	7.5	-1.	-1.	6.	-1.	-1.	-1.	-1.
1905	1	1.	-1.	-1.	-1.	-1.	-1.	20.	.16	.194	-1.	.9	6.1	-1.	-1.	7.	-1.	-1.	-1.	-1.
1905	5	1.	-1.	7.5	-1.	-1.	82.	20.	.16	-1.	-1.	1.0	6.0	-1.	-1.	7.	-1.	-1.	-1.	-1.
1906	1	0.	-1.	-1.	-1.	-1.	-1.	20.	.16	.158	-1.	3.7	8.8	-1.	-1.	7.	-1.	-1.	-1.	-1.
1906	5	0.	-1.	7.5	-1.	-1.	-1.	20.	.16	-1.	-1.	3.5	8.5	-1.	-1.	7.	-1.	-1.	-1.	-1.
1907	1	0.	-1.	-1.	-1.	-1.	-1.	20.	.16	.194	-1.	.9	6.1	-1.	-1.	12.	-1.	-1.	-1.	-1.
1907	5	0.	-1.	7.5	-1.	-1.	-1.	20.	.16	-1.	-1.	1.0	6.0	-1.	-1.	12.	-1.	-1.	-1.	-1.
1908	3	0.	-1.	7.5	-1.	-1.	-1.	-1.	-1.	-1.	-1.	3.0	12.2	-1.	-1.	-1.	55.0	-1.	-1.	-1.
1909	4	0.	-1.	7.5	-2.	51.	-1.	-1.	-1.	-1.	-1.	.9	-2.	-1.	-1.	-2.	-1.	-1.	-1.	-1.
1910	4	1.	-1.	7.5	-2.	51.	-1.	-1.	-1.	-1.	-1.	.9	-2.	-1.	-1.	-2.	-1.	-1.	-1.	-1.
1911	4	1.	-1.	7.5	-2.	51.	-1.	-1.	-1.	-1.	-1.	.9	-2.	-1.	-1.	-2.	-1.	-1.	-1.	-1.
1912	4	1.	-1.	7.5	-2.	51.	-1.	-1.	-1.	-1.	-1.	.9	-2.	-1.	-1.	-2.	-1.	-1.	-1.	-1.
1913	4	1.	-1.	7.5	-2.	51.	-1.	-1.	-1.	-1.	-1.	.9	-2.	-1.	-1.	-2.	-1.	-1.	-1.	-1.
1914	7	1.	1.0	7.5	-1.	-1.	-1.	-1.	.16	-1.	.170	1.0	7.0	1.33	.73	8.	9.5	-1.	-1.	2.
1914	8	1.	-1.	7.5	-1.	-1.	-1.	-1.	.16	.18	.18	.9	7.0	1.35	.74	8.	9.0	1.09	10.0	2.
1916	7	0.	0.5	7.5	-1.	-1.	-1.	-1.	.16	-1.	.170	1.0	7.0	1.33	.73	12.	14.2	-1.	-1.	2.
1916	8	0.	0.5	7.5	-1.	-1.	-1.	-1.	.16	.18	.18	.9	7.0	1.35	.74	12.	13.5	1.09	15.0	2.
1916	7	0.	0.0	7.5	-1.	-1.	-1.	-1.	.16	-1.	.151	2.0	7.0	1.31	.81	18.	20.3	-1.	-1.	2.
1916	8	0.	-1.	7.5	-1.	-1.	-1.	-1.	.16	.18	.18	1.8	7.0	1.35	.83	18.	19.5	1.21	23.5	2.
1917	7	1.	1.0	7.5	-1.	-1.	-1.	-1.	.16	-1.	.168	1.0	10.0	1.90	1.00	10.	10.0	-1.	-1.	2.
1917	8	1.	-1.	7.5	-1.	-1.	-1.	-1.	.16	.18	.18	.9	10.1	1.93	1.02	10.	10.0	1.09	10.5	2.
1918	7	0.	0.5	7.5	-1.	-1.	-1.	-1.	.16	-1.	.168	1.0	10.0	1.90	1.00	16.	18.0	-1.	-1.	2.
1918	8	0.	0.5	7.5	-1.	-1.	-1.	-1.	.16	.18	.18	.9	10.1	1.93	1.02	16.	15.5	1.09	17.0	2.
1919	7	0.	0.0	7.5	-1.	-1.	-1.	-1.	.16	-1.	.134	2.0	10.0	1.68	1.08	20.	19.1	-1.	-1.	2.
1919	8	0.	-1.	7.5	-1.	-1.	-1.	-1.	.16	.185	.185	1.8	10.1	1.93	1.11	20.	19.0	1.21	22.5	2.
1920	7	1.	1.0	7.5	-1.	-1.	-1.	-1.	.16	-1.	.205	.0	4.3	.82	.39	4.	6.2	-1.	-1.	10.
1920	8	1.	-1.	7.5	-1.	-1.	-1.	-1.	.16	.21	.21	.0	4.3	.82	.40	4.	6.0	1.09	6.5	10.
1921	7	0.	0.0	7.5	-1.	-1.	-1.	-1.	.16	-1.	.161	1.3	6.0	1.14	.67	27.	33.5	-1.	-1.	0.
1921	8	0.	-1.	7.5	-1.	-1.	-1.	-1.	.16	.195	.195	1.2	6.1	1.17	.68	27.	32.0	1.21	38.5	0.
1922	7	0.	0.0	7.5	-1.	-1.	-1.	-1.	.16	-1.	.128	2.5	6.0	.95	.70	12.	14.6	-1.	-1.	0.
1922	8	0.	-1.	7.5	-1.	-1.	-1.	-1.	.16	.165	.165	2.4	6.1	1.17	.81	12.	13.0	1.09	14.5	0.
1923	7	1.	1.0	7.5	-1.	-1.	-1.	-1.	.16	-1.	.177	.6	4.5	.88	.47	6.	8.7	-1.	-1.	0.
1923	8	1.	-1.	7.5	-1.	-1.	-1.	-1.	.16	.185	.185	.6	4.5	.88	.48	6.	8.5	1.09	9.0	0.
1901	3	0.	0.0	4.9	-1.	-1.	-1.	-1.	-1.	-1.	-1.	2.4	17.1	-1.	1.50	22.	17.9	-1.	-1.	-1.
2001	2	1.	-1.	6.3	-1.	-1.	55.	15.	.13	.085	-1.	.9	.9	-1.	.165	3.	5.0	-1.	-1.	-1.
2001	8	1.	-1.	6.3	-1.	-1.	-1.	-1.	.13	.085	.07	.9	.9	.16	.16	3.	5.0	.50	3.5	-1.
2101	1.	-1.	6.3	-2.	8.	-1.	-1.	-1.	-1.	-1.	-1.	1.8	-2.	-1.	-1.	7.	-1.	-1.	-1.	-2.
2102	4	1.	-1.	6.3	-2.	8.	-1.	-1.	-1.	-1.	-1.	1.4	-2.	-1.	-1.	7.	-1.	-1.	-1.	20.

## Liquefaction data catalog compiled by Liao and Whitman (1986a) (cont.)

CASE	BCAT	LIQ1	LIQ2	M	H	EP	DER	DUR	A	CSR	CSRN	ZW	ZL	SIGT	SIGE	N	N1	CE	N:60	FC
2201	1	1.	-1.	-1.	-1.	-1.	-1.	20.	.19	.237	-1.	.9	5.8	-1.	-1.	13.	-1.	-1.	-1.	-1.
2201	2	1.	-1.	7.8	-1.	-1.	161.	45.	.18	.205	-1.	.9	4.8	-1.	.60	6.	9.0	-1.	-1.	-1.
2201	4	1.	-1.	-2.	20.	-1.	160.	-1.	-1.	-1.	-1.	1.0	-2.	-1.	-1.	-2.	-1.	-1.	-1.	-2.
2201	5	1.	1.0	7.8	-1.	283.	-1.	45.	.18	-1.	-1.	1.0	4.5	-1.	-1.	6.	-1.	-1.	-1.	-1.
2201	6	1.	-1.	7.8	-1.	160.	-1.	-1.	-1.	-1.	-1.	-1.	-1.	-1.	.28	-1.	5.8	-1.	-1.	-1.
2201	7	1.	-1.	7.9	-1.	-1.	-1.	-1.	.20	-1.	.214	1.0	4.0	.76	.48	5.	7.3	-1.	-1.	20.
2201	8	1.	-1.	7.9	-1.	-1.	-1.	-1.	.20	.21	.22	.9	4.0	.76	.48	5.	7.0	1.17	8.0	20.
2202	1	0.	-1.	-1.	-1.	-1.	-1.	20.	.21	.205	-1.	1.5	3.7	-1.	-1.	18.	-1.	-1.	-1.	-1.
2202	2	0.	-1.	7.8	-1.	-1.	-2.	45.	.21	.185	-1.	1.5	3.0	-1.	-1.	15.	23.0	-1.	-1.	-1.
2202	5	0.	0.0	7.8	-1.	172.	-1.	45.	.21	-1.	-1.	1.5	3.0	-1.	-1.	15.	-1.	-1.	-1.	-1.
2203	1	1.	-1.	-1.	-1.	-1.	-1.	20.	.21	.210	-1.	1.5	3.7	-1.	-1.	6.	-1.	-1.	-1.	-1.
2203	5	1.	-1.	7.8	-1.	172.	-1.	20.	.21	-1.	-1.	1.5	3.5	-1.	-1.	6.	-1.	-1.	-1.	-1.
2204	2	0.	-1.	7.8	-1.	-1.	-2.	45.	.21	.23	-1.	.9	3.7	-1.	.40	14.	21.	-1.	-1.	-1.
2204	5	0.	-1.	7.8	-1.	172.	-1.	45.	.21	-1.	-1.	1.0	3.5	-1.	-1.	14.	-1.	-1.	-1.	-1.
2205	2	1.	-1.	7.8	-1.	-1.	-2.	45.	.21	.185	-1.	1.5	2.1	-1.	.40	6.	9.	-1.	-1.	-1.
2205	5	1.	-1.	7.8	-1.	172.	-1.	45.	.21	-1.	-1.	2.0	3.5	-1.	-1.	6.	-1.	-1.	-1.	-1.
2208	4	0.	-1.	7.8	-2.	160.	-1.	-1.	-1.	-1.	-1.	1.0	-2.	-1.	-1.	-2.	-1.	-1.	-1.	-2.
2207	4	0.	-1.	7.8	-2.	160.	-1.	-1.	-1.	-1.	-1.	1.5	-2.	-1.	-1.	-2.	-1.	-1.	-1.	-2.
2207	7	0.	0.0	7.9	-1.	-1.	-1.	-1.	.23	-1.	.222	2.0	6.0	1.14	.74	28.	33.1	-1.	-1.	5.
2207	8	0.	-1.	7.9	-1.	-1.	-1.	-1.	.23	.215	.23	2.1	6.1	1.17	.78	28.	31.0	1.21	37.5	5.
2208	4	0.	-1.	7.8	-2.	160.	-1.	-1.	-1.	-1.	-1.	1.3	-2.	-1.	-1.	-2.	-1.	-1.	-1.	-2.
2208	7	0.	0.0	7.9	-1.	-1.	-1.	-1.	.23	-1.	.248	1.0	4.0	.76	.48	15.	23.4	-1.	-1.	5.
2208	8	0.	-1.	7.9	-1.	-1.	-1.	-1.	.23	.24	.255	.9	4.0	.76	.48	15.	22.5	1.21	27.5	5.
2209	4	0.	-1.	7.8	-2.	160.	-1.	-1.	-1.	-1.	-1.	1.5	-2.	-1.	-1.	-2.	-1.	-1.	-1.	-2.
2210	4	0.	-1.	7.8	-2.	160.	-1.	-1.	-1.	-1.	-1.	1.5	-2.	-1.	-1.	-2.	-1.	-1.	-1.	-2.
2211	4	0.	-1.	7.8	-2.	160.	-1.	-1.	-1.	-1.	-1.	1.0	-2.	-1.	-1.	-2.	-1.	-1.	-1.	-2.
2212	4	0.	-1.	7.8	-2.	160.	-1.	-1.	-1.	-1.	-1.	1.3	-2.	-1.	-1.	-2.	-1.	-1.	-1.	-2.
2213	7	1.	1.0	7.9	-1.	-1.	-1.	-1.	.23	-1.	.270	.5	4.0	.76	.42	6.	9.1	-1.	-1.	5.
2213	8	1.	-1.	7.9	-1.	-1.	-1.	-1.	.23	.26	.275	.5	4.0	.76	.42	6.	9.0	1.09	9.5	5.
2301	4	0.	-2.	6.1	50.	-1.	-1.	-1.	-1.	-1.	-1.	8.0	-2.	-1.	-1.	-2.	-1.	-1.	-1.	-1.
2302	4	0.	-2.	6.1	50.	-1.	-1.	-1.	-1.	-1.	-1.	8.0	10.0	-1.	-1.	47.	-1.	-1.	-1.	-1.
2303	4	0.	-2.	6.1	50.	-1.	-1.	-1.	-1.	-1.	-1.	2.0	8.3	-1.	-1.	10.	-1.	-1.	-1.	-1.
2304	4	0.	-2.	6.1	50.	-1.	-1.	-1.	-1.	-1.	-1.	2.0	-2.	-1.	-1.	-2.	-1.	-1.	-1.	-1.
2305	4	0.	-2.	6.1	50.	-1.	-1.	-1.	-1.	-1.	-1.	3.5	-2.	-1.	-1.	-2.	-1.	-1.	-1.	-1.
2306	4	0.	-2.	6.1	50.	-1.	-1.	-1.	-1.	-1.	-1.	3.0	-2.	-1.	-1.	-2.	-1.	-1.	-1.	-1.
2501	4	0.	-1.	7.1	-1.	-1.	-1.	-1.	-1.	-1.	-1.	3.7	7.	-1.	-1.	12.	-1.	-1.	-1.	-1.
2601	2	1.	-1.	6.8	-1.	-1.	8.	16.	.40	.28	-1.	4.5	6.1	-1.	1.00	2.	2.0	-1.	-1.	-1.
2601	7	1.	1.0	6.8	-1.	-1.	-1.	-1.	.40	-1.	.237	4.5	6.0	1.14	.98	2.	1.4	-1.	-1.	10.

## Liquefaction data catalog compiled by Liao and Whitman (1986a) (cont.)

CASE	BCAT	LIQ1	LIQ2	M	H	EP	DER	DUR	A	CSR	CSRN	ZW	ZL	SIGT	SIGE	N	N1	CE	N100	FC
2601	8	1.	-1.	6.6	-1.	-1.	-1.	-1.	.45	.325	.28	4.6	6.1	1.14	.98	2.	2.0	.75	1.6	50.
2602	2	1.	-1.	6.6	-1.	-1.	8.	15.	.45	.16	-1.	16.8	16.8	-1.	3.30	24.	11.0	-1.	-1.	-1.
2602	4	1.	-1.	6.6	-2.	-1.	-1.	-1.	-1.	-1.	-1.	-2.	-2.	-1.	-1.	-2.	-1.	-1.	-1.	-1.
2602	7	1.	1.0	6.6	-1.	-1.	-1.	-1.	.45	-1.	.190	16.6	16.6	3.22	3.22	24.	7.4	-1.	-1.	50.
2603	7	1.	1.0	6.6	-1.	-1.	-1.	-1.	.45	-1.	.287	3.0	6.0	1.10	.68	9.	6.9	-1.	-1.	20.
2603	8	1.	-1.	6.6	-1.	-1.	-1.	-1.	.45	.345	.30	3.0	6.1	1.10	.68	9.	9.5	.75	7.0	20.
2604	3	0.	-1.	6.6	-1.	-1.	-1.	-1.	-1.	-1.	-1.	8.3	19.8	-1.	3.42	15.	8.1	-1.	-1.	-1.
2605	3	0.	-1.	6.6	-1.	-1.	-1.	-1.	-1.	-1.	-1.	18.3	25.9	-1.	3.68	32.	16.2	-1.	-1.	-1.
2606	3	0.	-1.	6.6	-1.	-1.	-1.	-1.	-1.	-1.	-1.	14.3	25.9	-1.	2.89	42.	24.7	-1.	-1.	-1.
2607	3	0.	-1.	6.6	-1.	-1.	-1.	-1.	-1.	-1.	-1.	1.5	4.6	-1.	.48	8.	11.6	-1.	-1.	-1.
2608	3	0.	-1.	6.6	-1.	-1.	-1.	-1.	-1.	-1.	-1.	16.8	19.8	-1.	3.43	21.	11.3	-1.	-1.	-1.
2609	3	0.	-1.	6.6	-1.	-1.	-1.	-1.	-1.	-1.	-1.	10.7	15.2	-1.	2.28	30.	19.9	-1.	-1.	-1.
2610	3	0.	-1.	6.6	-1.	-1.	-1.	-1.	-1.	-1.	-1.	10.7	16.8	-1.	2.61	26.	16.0	-1.	-1.	-1.
2611	3	0.	-1.	6.6	-1.	-1.	-1.	-1.	-1.	-1.	-1.	13.7	21.3	-1.	3.26	39.	21.6	-1.	-1.	-1.
2701	4	0.	-1.	7.3	-1.	-1.	-1.	-1.	-1.	-1.	-1.	3.1	-2.	-1.	-1.	-2.	-1.	-1.	-1.	-1.
2801	5	0.	-1.	7.3	-1.	90.	-1.	-1.	.075	-1.	-1.	1.0	8.0	-1.	-1.	15.	-1.	-1.	-1.	-1.
2802	5	0.	-1.	7.3	-1.	90.	-1.	-1.	.075	-1.	-1.	1.0	12.0	-1.	-1.	20.	-1.	-1.	-1.	-1.
2803	5	0.	-1.	7.3	-1.	90.	-1.	-1.	.075	-1.	-1.	2.0	8.0	-1.	-1.	8.5	-1.	-1.	-1.	-1.
2803	8	0.	-1.	7.3	-1.	-1.	-1.	-1.	.10	.095	.095	2.0	8.0	1.14	.73	9.5	11.	1.00	11.0	-1.
2804	5	0.	-1.	7.3	-1.	90.	-1.	-1.	.075	-1.	-1.	2.0	12.0	-1.	-1.	15.5	-1.	-1.	-1.	-1.
2805	5	0.	-1.	7.3	-1.	104.	-1.	-1.	.075	-1.	-1.	2.0	13.0	-1.	-1.	14.5	-1.	-1.	-1.	-1.
2805	8	0.	-1.	7.3	-1.	-1.	-1.	-1.	.10	.095	.09	2.0	13.0	2.58	1.48	14.5	11.6	1.00	11.6	-1.
2806	5	1.	-1.	7.3	-1.	95.	-1.	-1.	.075	-1.	-1.	1.5	6.2	-1.	-1.	6.5	-1.	-1.	-1.	-1.
2807	5	0.	-1.	7.3	-1.	95.	-1.	-1.	.075	-1.	-1.	1.5	6.2	-1.	-1.	6.	-1.	-1.	-1.	-1.
2807	8	1.	-1.	7.3	-1.	-1.	-1.	-1.	.10	.10	.10	1.5	6.2	1.22	.76	6.	6.5	1.00	6.5	-1.
2808	5	0.	-1.	7.3	-1.	67.	-1.	-1.	.075	-1.	-1.	1.5	7.0	-1.	-1.	6.	-1.	-1.	-1.	-1.
2809	5	0.	-1.	7.3	-1.	63.	-1.	-1.	.15	-1.	-1.	1.0	10.5	-1.	-1.	11.	-1.	-1.	-1.	-1.
2809	8	1.	-1.	7.3	-1.	-1.	-1.	-1.	.20	.21	.20	1.5	8.2	1.61	.94	11.	11.0	1.00	13.5	-1.
2810	5	1.	-1.	7.3	-1.	60.	-1.	-1.	.075	-1.	-1.	2.0	3.0	-1.	-1.	6.	-1.	-1.	-1.	-1.
2810	8	1.	-1.	7.3	-1.	-1.	-1.	-1.	.13	.10	.095	2.0	3.0	.58	.48	6.	8.5	.75	6.5	-1.
2811	5	1.	-1.	7.3	-1.	-1.	-1.	-1.	.15	-1.	-1.	2.0	10.0	-1.	-1.	9.	-1.	-1.	-1.	-1.
2811	8	1.	-1.	7.3	-1.	-1.	-1.	-1.	.20	.20	.195	2.0	10.0	1.98	1.18	9.	8.0	1.00	8.0	-1.
2812	6	1.	-1.	7.3	-1.	55.	-1.	-1.	.15	-1.	.51	2.0	10.3	-1.	-1.	9.	-1.	-1.	-1.	-1.
2812	8	1.	-1.	7.3	-1.	-1.	-1.	-1.	.20	.195	.18	2.0	10.3	2.04	1.21	9.	8.0	1.00	8.0	-1.
2813	8	1.	-1.	7.3	-1.	-1.	-1.	-1.	.13	.135	.13	1.5	9.1	1.79	1.03	8.	8.0	1.00	6.5	67.
2814	8	1.	-1.	7.3	-1.	-1.	-1.	-1.	.20	.21	.20	1.5	8.2	1.61	.94	13.	13.5	1.00	13.5	48.

## Liquefaction data catalog compiled by Liao and Whitman (1986a) (cont.)

CASE	BCAT	LIQ1	LIQ2	M	R	EP	DER	DUR	A	CSR	CSR <sub>N</sub>	Z <sub>w</sub>	Z <sub>L</sub>	SIGT	SIGE	N	N <sub>1</sub>	CE	N <sub>100</sub>	FC
2815	8	0.	-1.	7.3	-1.	-1.	-1.	-1.	.10	.105	.10	1.5	8.2	1.61	.94	9.	9.0	1.00	9.0	-1.
2901	7	1.	1.0	7.5	-1.	-1.	-1.	-1.	.135	-1.	.159	1.5	4.6	.60	.29	8.	9.3	-1.	-1.	3.
2901	8	1.	-1.	7.5	-1.	-1.	-1.	-1.	.135	.19	.19	1.5	10.4	1.42	.88	8.	8.0	.75	5.0	3.
2902	7	0.	0.5	7.5	-1.	-1.	-1.	-1.	.135	-1.	.135	2.0	4.6	.58	.35	8.	9.3	-1.	-1.	3.
2902	8	0.	0.5	7.5	-1.	-1.	-1.	-1.	.135	.135	.135	2.4	4.3	.56	.34	8.	12.0	.75	9.0	3.
2904	7	1.	1.0	7.5	-1.	-1.	-1.	-1.	.135	-1.	.126	3.3	7.0	1.03	.64	14.	12.7	-1.	-1.	3.
2905	8	1.	0.5	7.5	-1.	-1.	-1.	-1.	.135	.18	.18	2.4	11.5	1.57	.91	15.	15.5	.75	11.5	3.
2906	8	0.	-1.	7.5	-1.	-1.	-1.	-1.	.135	.15	.15	-2.	10.7	1.40	.73	16.	18.5	.75	14.0	3.
3001	5	1.	-1.	7.8	-1.	43.	-1.	-1.	.15	-1.	-1.	1.4	2.3	-1.	-1.	11.	-1.	-1.	-1.	-1.
3001	8	1.	-1.	7.6	-1.	-1.	-1.	-1.	.20	.18	.17	1.4	2.3	.43	.33	11.	18.0	.75	13.5	-1.
3002	5	1.	-1.	7.8	-1.	25.	-1.	-1.	.30	-1.	-1.	1.0	7.0	-1.	-1.	4.	-1.	-1.	-1.	-1.
3002	8	1.	-1.	7.6	-1.	-1.	-1.	-1.	.35	.39	.405	1.0	7.0	1.34	.74	4.	4.5	1.00	4.5	-1.
3003	7	1.	-1.	7.8	-1.	-1.	-1.	-1.	-1.	-1.	-1.	-1.	-1.	-1.	-1.	-1.	-1.	-1.	-1.	-1.
3004	7	1.	0.7	7.8	-1.	-1.	-1.	-1.	.20	-1.	.192	.5	11.0	2.20	1.30	-1.	7.0	-1.	-1.	50.
3005	7	0.	0.5	7.8	-1.	-1.	-1.	-1.	.20	-1.	.192	.5	11.0	2.20	1.30	-1.	8.0	-1.	-1.	50.
3006	8	0.	-1.	7.6	-1.	-1.	-1.	-1.	.50	.405	.42	3.0	5.3	1.00	.77	30.	33.5	1.00	33.5	10.
3007	8	1.	-1.	7.8	-1.	-1.	-1.	-1.	.35	.38	.395	.9	5.3	1.04	.60	17.	21.5	1.00	21.5	20.
3008	8	1.	-1.	7.8	-1.	-1.	-1.	-1.	.22	.155	.175	3.7	5.4	.99	.82	20.	22.0	1.00	22.0	3.
3009	8	1.	-1.	7.8	-1.	-1.	-1.	-1.	.20	.155	.16	1.5	2.0	.37	.32	10.	16.5	.75	12.5	12.
3010	8	1.	-1.	7.6	-1.	-1.	-1.	-1.	.13	.14	.145	1.2	6.1	1.19	.70	10.	11.5	1.00	11.5	12.
3011	8	1.	-1.	7.8	-1.	-1.	-1.	-1.	.20	.22	.23	.9	6.1	1.20	.68	9.	11.0	1.00	11.0	-1.
3012	8	0.	-1.	7.8	-1.	-1.	-1.	-1.	.07	.06	.05	4.0	9.1	1.74	1.22	13.	11.5	1.00	11.5	1.
3013	8	1.	-1.	7.8	-1.	-1.	-1.	-1.	.20	.205	.21	1.5	7.0	1.37	.82	11.	12.5	1.00	12.5	2.
3201	8	1.	-1.	7.4	-1.	-1.	-1.	-1.	.20	.155	.16	4.6	8.2	1.45	1.08	9.	8.5	.75	6.0	20.
3203	8	1.	-1.	7.4	-1.	-1.	-1.	-1.	.20	.155	.16	6.7	11.9	1.55	1.04	12.	11.5	.75	8.5	-1.
3204	8	0.	-1.	7.4	-1.	-1.	-1.	-1.	.20	.20	.195	1.2	3.7	.64	.40	14.	21.5	.75	16.0	4.
3205	8	0.	-1.	7.4	-1.	-1.	-1.	-1.	.20	.155	.15	2.1	3.0	.54	.44	14.	19.5	.75	14.5	3.
3206	8	1.	-1.	7.4	-1.	-1.	-1.	-1.	.20	.195	.19	1.8	5.2	.91	.58	8.	8.0	.75	6.0	51.
3301	7	1.	1.0	7.0	-1.	-1.	-1.	-1.	.25	-1.	.244	1.0	7.0	1.33	.73	-1.	1.2	-1.	-1.	90.
3401	7	0.	0.0	6.7	-1.	-1.	-1.	-1.	.10	-1.	.092	1.0	6.3	1.21	.58	10.	12.3	-1.	-1.	0.
3401	8	0.	-1.	6.7	-1.	-1.	-1.	-1.	.10	.11	.095	.9	6.4	1.23	.58	10.	12.0	1.09	13.0	0.

## Liquefaction data catalog compiled by Liao and Whitman (1986a) (cont.)

CASE	BCAT	LIQ1	LIQ2	M	H	EP	DER	DUR	A	CSR	CSR <sub>N</sub>	ZW	ZL	SIGT	SIGE	M	N1	CE	M180	FC
3403	7	0.	0.7	8.7	-1.	-1.	-1.	-1.	.12	-1.	.117	.5	3.3	.63	.42	5.	8.1	-1.	-1.	5.
3403	8	1.	-1.	8.7	-1.	-1.	-1.	-1.	.12	.135	.115	.5	3.4	.64	.37	5.	8.0	1.00	8.0	5.
3404	7	0.	0.0	8.7	-1.	-1.	-1.	-1.	.12	-1.	.098	1.3	3.3	.63	.42	7.	10.6	-1.	-1.	4.
3404	8	0.	-1.	8.7	-1.	-1.	-1.	-1.	.12	.115	.10	1.2	3.4	.64	.43	7.	10.0	1.00	10.0	4.
3405	7	0.	0.0	8.7	-1.	-1.	-1.	-1.	.12	-1.	.100	1.8	5.3	.95	.60	2.	2.5	-1.	-1.	60.
3405	8	0.	-1.	8.7	-1.	-1.	-1.	-1.	.12	.12	.105	1.8	5.5	1.01	.64	2.	2.5	1.00	2.5	60.
3405	7	0.	0.0	8.7	-1.	-1.	-1.	-1.	.12	-1.	.109	.9	4.3	.82	.48	11.	15.0	-1.	-1.	0.
3405	8	0.	-1.	8.7	-1.	-1.	-1.	-1.	.12	-1.	.115	.9	4.3	.82	.48	11.	15.0	1.00	15.0	0.
3408	7	0.	0.0	8.7	-1.	-1.	-1.	-1.	.12	-1.	.094	1.7	4.3	.82	.55	4.	5.4	-1.	-1.	10.
3408	8	0.	-1.	8.7	-1.	-1.	-1.	-1.	.12	.11	.095	1.8	4.3	.82	.58	4.	5.0	1.00	5.0	10.
3409	7	0.	0.0	8.7	-1.	-1.	-1.	-1.	.12	-1.	.098	1.3	3.3	.63	.42	13.	19.7	-1.	-1.	7.
3409	8	0.	-1.	8.7	-1.	-1.	-1.	-1.	.12	.115	.10	1.2	3.4	.64	.43	13.	19.0	1.12	21.5	7.
3410	7	0.	0.0	8.7	-1.	-1.	-1.	-1.	.12	-1.	.125	.3	4.3	.82	.42	8.	13.7	-1.	-1.	12.
3410	8	0.	-1.	8.7	-1.	-1.	-1.	-1.	.12	.145	.13	.3	4.3	.82	.42	8.	12.0	1.00	12.0	12.
3412	7	0.	0.0	8.7	-1.	-1.	-1.	-1.	.14	-1.	.089	4.3	6.3	1.05	.85	9.	9.9	-1.	-1.	5.
3412	8	0.	-1.	8.7	-1.	-1.	-1.	-1.	.14	.11	.095	4.3	6.4	1.08	.87	9.	9.5	1.00	9.5	5.
3413	7	0.	0.0	8.7	-1.	-1.	-1.	-1.	.14	-1.	.111	2.4	6.3	1.11	.72	8.	9.8	-1.	-1.	4.
3413	8	0.	-1.	8.7	-1.	-1.	-1.	-1.	.14	.13	.115	2.4	6.4	1.17	.77	8.	9.0	1.00	9.0	4.
3414	7	0.	0.0	8.7	-1.	-1.	-1.	-1.	.14	-1.	.080	3.0	3.3	.61	.59	11.	14.8	-1.	-1.	5.
3414	8	0.	-1.	8.7	-1.	-1.	-1.	-1.	.14	.095	.08	3.0	3.4	.63	.61	11.	13.5	1.00	13.5	5.
3417	7	0.	0.0	8.7	-1.	-1.	-1.	-1.	.14	-1.	.093	2.5	4.0	.76	.61	6.	7.8	-1.	-1.	10.
3417	8	0.	-1.	8.7	-1.	-1.	-1.	-1.	.14	.11	.095	2.4	4.0	.76	.61	6.	7.5	1.09	8.0	10.
3419	7	0.	0.0	8.7	-1.	-1.	-1.	-1.	.14	-1.	.100	2.5	5.0	.95	.70	9.	10.9	-1.	-1.	20.
3419	8	0.	-1.	8.7	-1.	-1.	-1.	-1.	.14	.12	.105	2.4	5.2	1.00	.72	9.	10.5	1.09	11.5	20.
3421	7	0.	0.0	8.7	-1.	-1.	-1.	-1.	.14	-1.	.105	2.5	6.0	1.14	.79	12.	13.7	-1.	-1.	3.
3421	8	0.	-1.	8.7	-1.	-1.	-1.	-1.	.14	.125	.11	2.4	6.1	1.17	.81	12.	13.0	1.09	14.5	3.
3424	7	0.	0.0	8.7	-1.	-1.	-1.	-1.	.12	-1.	.098	1.4	4.0	.76	.60	4.	5.7	-1.	-1.	10.
3424	8	0.	-1.	8.7	-1.	-1.	-1.	-1.	.12	.11	.10	1.5	4.0	.76	.62	4.	5.5	1.09	6.0	10.
3501	7	0.	0.0	7.4	-1.	-1.	-1.	-1.	.20	-1.	.205	1.0	6.3	1.21	.68	10.	12.3	-1.	-1.	0.
3501	8	1.	-1.	7.4	-1.	-1.	-1.	-1.	.20	.22	.22	.9	6.4	1.23	.68	10.	12.0	1.09	13.0	0.
3502	7	0.	0.0	7.4	-1.	-1.	-1.	-1.	.32	-1.	.314	.9	3.3	.63	.39	19.	29.6	-1.	-1.	4.
3502	8	0.	-1.	7.4	-1.	-1.	-1.	-1.	.32	.33	.325	.9	3.4	.64	.40	19.	28.5	1.12	31.5	4.
3503	7	0.	0.7	7.4	-1.	-1.	-1.	-1.	.32	-1.	.350	.5	3.3	.63	.42	5.	8.1	-1.	-1.	3.
3503	8	1.	-1.	7.4	-1.	-1.	-1.	-1.	.32	.355	.35	.5	3.4	.64	.37	5.	8.0	1.00	8.0	5.
3504	7	0.	0.0	7.4	-1.	-1.	-1.	-1.	.32	-1.	.292	1.3	3.3	.63	.42	7.	10.6	-1.	-1.	4.
3504	8	1.	-1.	7.4	-1.	-1.	-1.	-1.	.32	.305	.30	1.2	3.4	.64	.43	7.	10.0	1.00	10.0	4.
3505	7	0.	0.0	7.4	-1.	-1.	-1.	-1.	.24	-1.	.224	1.8	5.3	.95	.60	2.	2.5	-1.	-1.	60.
3505	8	1.	-1.	7.4	-1.	-1.	-1.	-1.	.24	.235	.23	1.8	5.5	1.01	.64	2.	2.5	1.00	2.5	60.
3505	7	0.	0.0	7.4	-1.	-1.	-1.	-1.	.24	-1.	.245	.9	4.3	.82	.48	11.	15.0	-1.	-1.	0.
3505	8	1.	-1.	7.4	-1.	-1.	-1.	-1.	.24	.255	.25	.9	4.3	.82	.48	11.	15.0	1.00	15.0	0.
3507	7	0.	0.0	7.4	-1.	-1.	-1.	-1.	.24	-1.	.205	2.2	5.3	.99	.68	20.	24.6	-1.	-1.	0.
3507	8	0.	-1.	7.4	-1.	-1.	-1.	-1.	.24	.22	.215	2.1	5.5	1.05	.72	20.	23.0	1.12	25.0	0.
3508	7	0.	0.0	7.4	-1.	-1.	-1.	-1.	.24	-1.	.210	1.7	4.3	.82	.56	4.	5.4	-1.	-1.	10.

## Liquefaction data catalog compiled by Liao and Whitman (1986a) (cont.)

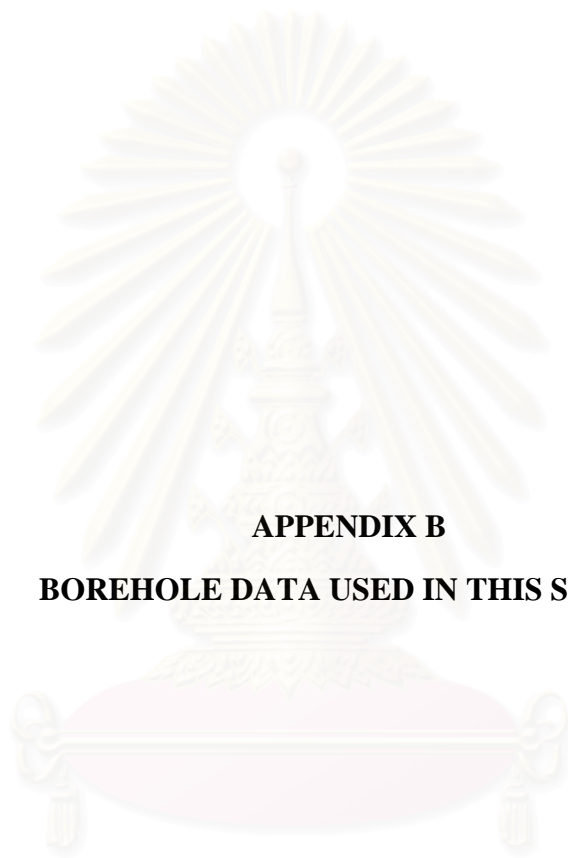
CASE	BCAT	LIQ1	LIQ2	M	R	EP	DER	DUR	A	CSR	CSR <sub>N</sub>	ZW	ZL	SIGT	SIGE	N	M1	CE	N160	FC
3508	8	1.	-1.	7.4	-1.	-1.	-1.	-1.	.24	.216	.216	1.8	4.3	.82	.68	4.	5.0	1.00	5.0	10.
3509	7	0.	0.0	7.4	-1.	-1.	-1.	-1.	.24	-1.	.219	1.3	3.3	.63	.42	13.	19.7	-1.	-1.	7.
3509	8	1.	-1.	7.4	-1.	-1.	-1.	-1.	.24	.23	.225	1.2	3.4	.64	.43	13.	19.0	1.12	21.6	7.
3510	7	0.	0.0	7.4	-1.	-1.	-1.	-1.	.24	-1.	.281	.3	4.3	.82	.42	8.	12.1	-1.	-1.	12.
3510	8	1.	-1.	7.4	-1.	-1.	-1.	-1.	.24	.29	.29	.3	4.3	.82	.42	8.	12.0	1.00	12.0	12.
3511	7	0.	0.0	7.4	-1.	-1.	-1.	-1.	.24	-1.	.241	1.3	7.3	1.39	.79	17.	19.4	-1.	-1.	17.
3511	8	0.	-1.	7.4	-1.	-1.	-1.	-1.	.24	.26	.255	1.2	7.3	1.41	.80	17.	18.5	1.12	21.0	17.
3512	7	0.	0.0	7.4	-1.	-1.	-1.	-1.	.24	-1.	.172	4.3	6.3	1.05	.85	9.	9.9	-1.	-1.	5.
3512	8	1.	-1.	7.4	-1.	-1.	-1.	-1.	.24	.186	.18	4.3	6.4	1.08	.87	9.	9.5	1.00	9.5	5.
3513	7	0.	0.0	7.4	-1.	-1.	-1.	-1.	.24	-1.	.214	2.4	6.3	1.11	.72	8.	9.5	-1.	-1.	4.
3513	8	1.	-1.	7.4	-1.	-1.	-1.	-1.	.24	.225	.22	2.4	6.4	1.17	.77	8.	9.0	1.00	9.0	4.
3514	7	0.	0.0	7.4	-1.	-1.	-1.	-1.	.28	-1.	.179	3.0	3.3	.61	.68	11.	14.6	-1.	-1.	5.
3514	8	1.	-1.	7.4	-1.	-1.	-1.	-1.	.28	.186	.185	3.0	3.4	.63	.61	11.	13.5	1.00	13.5	5.
3515	7	0.	0.0	7.4	-1.	-1.	-1.	-1.	.28	-1.	.223	3.0	6.0	1.12	.82	23.	25.7	-1.	-1.	0.
3515	8	0.	-1.	7.4	-1.	-1.	-1.	-1.	.28	.235	.23	3.0	6.1	1.17	.67	23.	24.0	1.21	29.0	0.
3516	7	0.	0.0	7.4	-1.	-1.	-1.	-1.	.24	-1.	.202	2.5	6.0	1.14	.79	10.	11.4	-1.	-1.	10.
3516	8	0.	-1.	7.4	-1.	-1.	-1.	-1.	.24	.215	.21	2.4	6.1	1.17	.82	10.	11.0	1.09	12.	10.
3517	7	0.	0.0	7.4	-1.	-1.	-1.	-1.	.24	-1.	.180	2.5	4.3	.78	.61	6.	7.6	-1.	-1.	10.
3517	8	1.	-1.	7.4	-1.	-1.	-1.	-1.	.24	.19	.185	2.4	4.0	.76	.81	6.	7.5	1.09	8.0	10.
3518	7	0.	0.0	7.4	-1.	-1.	-1.	-1.	.24	-1.	.208	2.5	7.0	1.33	.88	21.	22.6	-1.	-1.	5.
3518	8	0.	-1.	7.4	-1.	-1.	-1.	-1.	.24	.225	.22	2.4	7.0	1.36	.89	21.	22.0	1.21	26.5	5.
3519	7	0.	0.0	7.4	-1.	-1.	-1.	-1.	.24	-1.	.193	2.5	5.0	.95	.70	9.	10.9	-1.	-1.	20.
3519	8	1.	-1.	7.4	-1.	-1.	-1.	-1.	.24	.205	.206	2.4	5.2	1.00	.72	9.	10.5	1.09	11.5	20.
3520	7	0.	0.0	7.4	-1.	-1.	-1.	-1.	.24	-1.	.187	2.5	4.5	.85	.65	10.	12.5	-1.	-1.	25.
3520	8	0.	-1.	7.4	-1.	-1.	-1.	-1.	.24	.20	.195	2.4	4.6	.88	.65	10.	12.0	1.09	13.0	25.
3521	7	0.	0.0	7.4	-1.	-1.	-1.	-1.	.24	-1.	.202	2.5	6.0	1.14	.79	12.	13.7	-1.	-1.	3.
3521	8	1.	-1.	7.4	-1.	-1.	-1.	-1.	.24	.22	.215	2.4	6.1	1.17	.81	12.	13.0	1.09	14.5	3.
3522	7	0.	0.0	7.4	-1.	-1.	-1.	-1.	.24	-1.	.209	2.4	6.0	1.09	.73	15.	17.8	-1.	-1.	11.
3522	8	0.	-1.	7.4	-1.	-1.	-1.	-1.	.24	.22	.22	2.4	6.1	1.13	.77	15.	16.5	1.21	20.0	11.
3523	7	0.	0.0	7.4	-1.	-1.	-1.	-1.	.24	-1.	.188	3.6	7.0	1.27	.93	17.	17.7	-1.	-1.	12.
3523	8	0.	-1.	7.4	-1.	-1.	-1.	-1.	.24	.20	.195	3.7	7.0	1.30	.98	17.	17.0	1.21	20.5	12.
3524	7	0.	0.0	7.4	-1.	-1.	-1.	-1.	.20	-1.	.183	1.4	4.0	.76	.50	4.	5.7	-1.	-1.	10.
3524	8	1.	-1.	7.4	-1.	-1.	-1.	-1.	.20	.185	.18	1.5	4.0	.76	.52	4.	5.5	1.09	6.0	10.
3525	7	0.	0.0	7.4	-1.	-1.	-1.	-1.	.20	-1.	.195	1.4	5.0	1.14	.68	15.	18.5	-1.	-1.	10.
3525	8	0.	-1.	7.4	-1.	-1.	-1.	-1.	.20	.205	.20	1.5	5.1	1.17	.71	15.	17.5	1.21	21.0	10.
3901	7	0.	0.0	6.6	-1.	-1.	-1.	-1.	.60	-1.	.449	1.8	4.0	.74	.52	31.	43.2	-1.	-1.	11.
3901	8	0.	-1.	6.6	-1.	-1.	-1.	-1.	.78	.67	.575	1.8	3.7	.69	.51	28.	38.0	1.05	39.5	25.
3902	7	0.	0.0	6.6	-1.	-1.	-1.	-1.	.60	-1.	.449	1.8	4.0	.74	.52	4.	5.5	-1.	-1.	25.
3902	8	0.	-1.	6.6	-1.	-1.	-1.	-1.	.78	.67	.575	1.8	3.7	.69	.51	1.	1.5	1.05	1.5	29.
3903	7	0.	0.0	6.6	-1.	-1.	-1.	-1.	.60	-1.	.449	1.8	4.0	.74	.52	11.	15.3	-1.	-1.	19.
3903	8	0.	-1.	6.6	-1.	-1.	-1.	-1.	.78	.695	.595	1.8	4.3	.81	.57	13.	16.5	1.05	17.5	37.



## Liquefaction data catalog compiled by Liao and Whitman (1986a) (cont.)

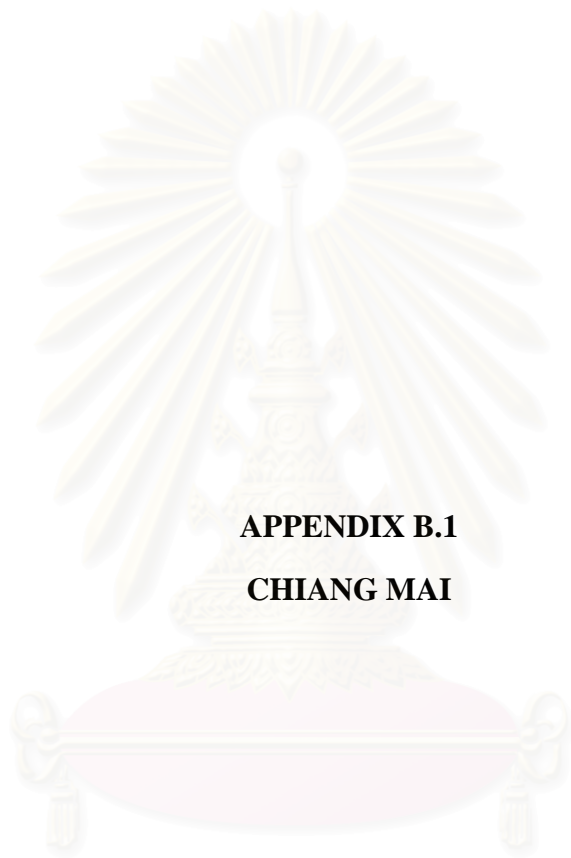
CASE	BCAT	LIQ1	LIQ2	M	H	EP	DER	DUR	A	CSR	CSRN	ZW	ZL	SIGT	SIGE	N	N1	CE	N160	FC
3904	7	1.	0.7	6.6	-1.	-1.	-1.	-1.	.20	-1.	.206	.2	2.0	.38	.20	3.	5.7	-1.	-1.	66.
3904	8	1.	-1.	6.6	-1.	-1.	-1.	-1.	.24	.265	.23	.3	1.8	.36	.21	3.	5.5	.79	4.6	80.
3905	7	1.	0.7	6.6	-1.	-1.	-1.	-1.	.20	-1.	.209	.2	5.0	.95	.47	7.	10.1	-1.	-1.	34.
3905	8	1.	-1.	6.6	-1.	-1.	-1.	-1.	.24	.28	.24	.3	4.3	.85	.45	11.	15.0	1.05	16.0	18.
3918	8	1.	-1.	6.6	-1.	-1.	-1.	-1.	.20	.16	.135	2.1	3.4	.62	.60	2.	2.5	1.05	3.0	75.
3919	8	0.	-1.	6.6	-1.	-1.	-1.	-1.	.20	.13	.115	2.1	2.3	.41	.39	11.	16.5	.79	13.0	30.
3925	8	1.	-1.	6.6	-1.	-1.	-1.	-1.	.51	.39	.335	1.5	2.1	.39	.33	3.	5.0	.79	4.0	31.
4101	7	0.	0.0	6.1	-1.	-1.	-1.	-1.	.10	-1.	.086	1.0	6.0	1.08	.58	5.	6.6	-1.	-1.	13.
4101	8	0.	-1.	6.1	-1.	-1.	-1.	-1.	.10	.12	.095	.9	6.1	1.10	.59	5.	6.5	1.09	7.0	13.
4102	7	1.	0.7	6.1	-1.	-1.	-1.	-1.	-1.	-1.	.143	-1.	-1.	-1.	-1.	-1.	6.6	-1.	-1.	13.
4102	8	0.	0.6	6.1	-1.	-1.	-1.	-1.	.145	.17	.135	.9	6.1	1.10	.59	5.	6.5	1.09	7.0	13.
4103	7	0.	0.0	6.1	-1.	-1.	-1.	-1.	.10	-1.	.094	1.0	14.0	2.52	1.08	4.	3.8	-1.	-1.	27.
4103	8	0.	-1.	6.1	-1.	-1.	-1.	-1.	.10	.105	.085	.9	14.3	2.59	1.25	4.	3.5	1.09	4.0	27.
4104	7	1.	0.7	6.1	-1.	-1.	-1.	-1.	-1.	-1.	.165	-1.	-1.	-1.	1.08	4.	3.8	-1.	-1.	27.
4104	8	1.	0.5	6.1	-1.	-1.	-1.	-1.	.145	.155	.12	.9	14.3	2.59	1.25	4.	3.5	1.09	4.0	27.
4204	8	0.	-1.	5.6	-1.	-1.	-1.	-1.	.21	.235	.165	.3	1.8	.36	.21	3.	5.5	.79	4.5	80.
4205	8	0.	-1.	5.6	-1.	-1.	-1.	-1.	.21	.245	.175	.3	4.3	.85	.45	11.	15.0	1.05	16.0	18.
4218	8	1.	-1.	5.6	-1.	-1.	-1.	-1.	.20	.16	.11	2.1	3.4	.62	.60	2.	2.5	1.05	3.0	75.
4219	8	0.	-1.	5.6	-1.	-1.	-1.	-1.	.20	.13	.095	2.1	2.3	.41	.39	11.	16.5	.79	13.0	30.
4225	8	1.	-1.	5.6	-1.	-1.	-1.	-1.	.26	.28	.20	.9	4.9	.98	.55	9.	11.0	1.05	11.5	40.
4226	8	1.	-1.	5.6	-1.	-1.	-1.	-1.	.32	.28	.185	2.7	4.3	.79	.64	5.	6.5	1.05	6.5	92.
4227	8	0.	-1.	5.6	-1.	-1.	-1.	-1.	.09	.07	.05	1.5	2.1	.39	.33	3.	5.0	.79	4.0	31.

สถาบันวิทยบริการ  
จุฬาลงกรณ์มหาวิทยาลัย



**APPENDIX B**  
**BOREHOLE DATA USED IN THIS STUDY**

สถาบันวิทยบริการ  
จุฬาลงกรณ์มหาวิทยาลัย

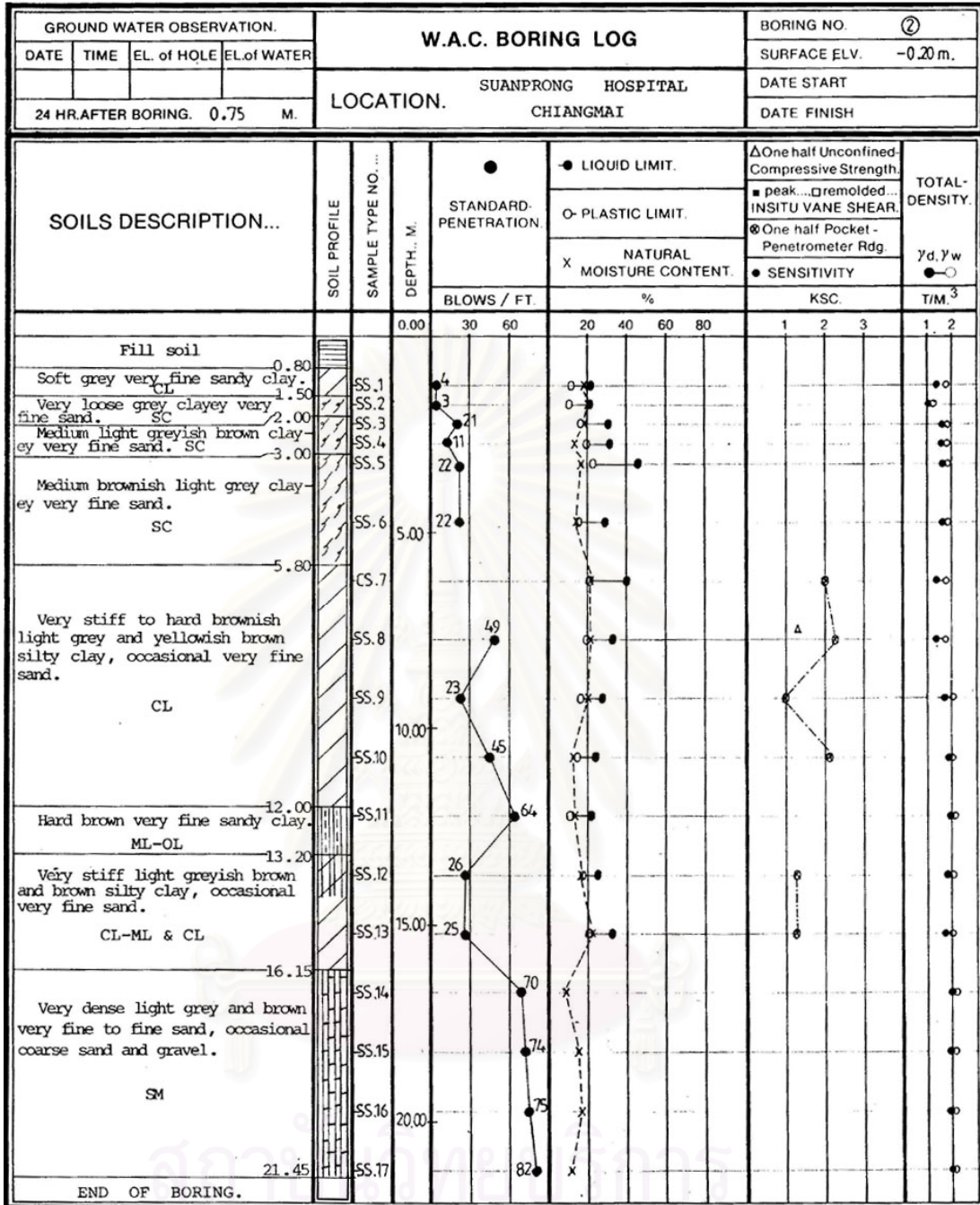


**APPENDIX B.1**  
**CHIANG MAI**

สถาบันวิทยบริการ  
จุฬาลงกรณ์มหาวิทยาลัย

GROUND WATER OBSERVATION.				W.A.C. BORING LOG				BORING NO. ①				
DATE	TIME	EL. of HOLE	EL. of WATER	LOCATION. SUANPRONG HOSPITAL CHIANGMAI				SURFACE ELV. -0.20m.				
24 HR. AFTER BORING.		0.78 M.						DATE START				
								DATE FINISH				
SOILS DESCRIPTION...	SOIL PROFILE	SAMPLE TYPE NO. ...	DEPTH. M.	STANDARD-PENETRATION BLOWS / FT.	● LIQUID LIMIT.				△ One half Unconfined-Compressive Strength.			TOTAL-DENSITY. γ <sub>d</sub> , γ <sub>w</sub> T/M. <sup>3</sup>
					○ PLASTIC LIMIT.				■ peak... □ remolded... INSITU VANE SHEAR.			
					X NATURAL MOISTURE CONTENT.				⊗ One half Pocket - Penetrometer Rdg.			
					%				KSC.			
Fill soil			0.00	30 60	20 40 60 80	1 2 3	1 2					
Very loose grey and brown clayey very fine sand. SC		SS.1	0.80	3	0							
		SS.2		2	0							
		SS.3	2.00	5	0							
Medium to very stiff light grey and brown silty clay, occasional very fine sand. CL		SS.4		13	0							
		SS.5		19	0							
Dense light grey and brown clayey very fine sand. SC		SS.6	4.50	34	0							
		SS.7	6.00	41	0							
Hard to very stiff light grey, yellowish brown and brown silty clay, trace of very fine sand. CL		SS.8		36	0							
		SS.9		25	0							
Dense light grey very fine sand. SM		SS.10	10.00	49	0							
Very stiff light grey and yellowish brown silty clay, trace of very fine sand. CL		SS.11	11.70	31	0							
Very dense grey very fine sand. SM		SS.12	13.40	60	0							
Very stiff light grey and brown silty clay. CL		SS.13	14.80	21	0							
		SS.14	16.00	140	0							
Very dense brownish grey and brown very fine to fine sand. SM		SS.15		98	0							
		SS.16	20.00	102	0							
END OF BORING.		SS.17	21.45	132	0							

จุฬาลงกรณ์มหาวิทยาลัย



จุฬาลงกรณ์มหาวิทยาลัย

BORING LOG					BORING NO. : BH-1		ELEVATION (m) : -														
PROJECT : BCP "เจริญเมือง 2 เชียงใหม่"					DEPTH (m) : 15.45		GWL (m) : -3.15														
LOCATION : อ.เมือง จ.เชียงใหม่					COORD. N : _____		DATE STARTED : 02/04/97														
					E : _____		DATE FINISHED : 02/04/97														
SOIL DESCRIPTION	DEPTH (m.)	GRAPHIC LOG	METHOD	SAMPLE NO	RECOVERY (cm)	SPT-N VALUE (blows/ft)				NATURAL MOISTURE CONTENT (%)				Su (t/sq.m)				TOTAL UNIT WEIGHT (t/cu.m)			
						10	20	30	40	20	40	60	80	1	2	3	4	16	18	20	
MEDIUM DENSE CLAYEY FINE TO MEDIUM SAND, BROWN (SC)	1.0		PA																		
			SS	1	25	11															
			SS	2	30	16															
	2.00	2.0	SS	3	25	19															
MEDIUM DENSE FINE TO MEDIUM SAND, BROWN (SM, SP-SM)			SS	4	30	14															
		3.0	PA																		
			SS	5	35	12															
		4.0	PA																		
			SS	6	30	18															
		5.0	PA																		
			SS	7	40	17															
		6.0	PA																		
		7.0	PA																		
			SS	8	30	13															
		8.50	PA																		
	LOOSE FINE TO COARSE SAND, BROWN (SP-SM)			SS	9	35	9														
		10.00	10.0	PA																	
MEDIUM DENSE TO DENSE FINE TO COARSE SAND WITH GRAVEL, GREY (SP-SM)			SS	10	32	24															
		11.0	PA																		
			SS	11	30	27															
		12.0	PA																		
			SS	12	30	18															
		14.0	PA																		
END OF BORING REFUSAL			SS	13	15	36															
	15.45	15.0	PA																		

PA = POWER AUGERING	HA = HAND AUGERING	WO = WASH OUT	ST = SHELBY TUBE	SS = SPLIT SPOON
PARTY CHIEF: SARADECH CH	MADE BY: VIPAWEE G	GEOLOGIST: UDOMPORN CH	FILE: BCP-CH1	DISK: 9/1 CHIANG MAI



K. ENGINEERING CONSULTANTS CO., LTD.																			
BORING LOG					BORING NO. BH-1		GROUND ELEV.(m.)												
PROJECT อาคาร 7 ชั้น หลังโรงแรมเชียงใหม่ภูคำ					DEPTH (m.) 12.45		OBSERVED WL (m.) - 2.00												
LOCATION ค่าเทอเมือง จังหวัดเชียงใหม่					COORD. _____		DATE STARTED 27/8/94												
							DATE FINISHED 27/8/94												
SOIL DESCRIPTION	DEPTH (m.)	GRAPHIC LOG	METHOD	SAMPLING RECOVERY	SPT - N (blows / ft)				PL W <sub>n</sub> LL (%)			S <sub>u</sub> (t/m <sup>2</sup> )				γ <sub>s</sub> (t/m <sup>3</sup> )			
					10	20	30	40	20	40	60	80	1	2	3	4	1.6	1.8	2.0
VERY STIFF CLAY, BROWNISH GREY (CL)	1		PA																
	2		SS 1	1	15														
	3		SS 2	2	24														
	3.40		SS 3	3	32														
LOOSE CLAYEY FINE TO MEDIUM SAND, GREY (SC)	4		PA																
	5.50		SS 4	4	30														
MEDIUM DENSE SILTY MEDIUM SAND, GREY (SM)	6		WO																
	7.00		SS 5	5	10														
MEDIUM DENSE CLAYEY SAND, BROWN (SC)	8		WO																
	9		SS 6	6	20														
	10		WO																
	11		SS 7	7	20														
	12		WO																
	12.45		SS 8	8	31														
END OF BORING			WO																
			SS 9	9	50														221
			WO																
			SS 10	10	47														

สถาบันวิศวกรรม  
จุฬาลงกรณ์มหาวิทยาลัย



SOIL DESCRIPTION		DEPTH (m.)	GRAPHIC LOG	METHOD	SAMPLING RECOVERY	SPT-N (blows/ft)	PL (%)	w	LL	Su (t/sq.m)				TOTAL UNIT WEIGHT γ <sub>t</sub> (t/cu.m.)					
										○ UCT	△ PP	X FVT	□ TV	1	2	3	4	1.6	1.8
LOOSE CLAYEY SAND WITH GRAVEL, BROWN (SC)		1.00		PA	1	7	0												
VERY LOOSE SILTY FINE SAND, GREY (SM)		2.00		SS 2	2	2	0												
LOOSE TO MEDIUM DENSE CLAYEY SAND, TRACE OF GRAVEL, BROWN AND GREY (SC)		4.00		SS 4	4	8	0												
HARD FINE SANDY CLAY, GREY AND BROWN (CL)		5.50		WO	5	27	0												
DENSE CLAYEY SAND, GREY AND BROWN (SC)		8.70		SS 7	7	41	0												
VERY STIFF FINE SANDY CLAY, GREY (CL)		10.00		WO	8	400	0												
MEDIUM DENSE TO DENSE CLAYEY SAND TRACE OF GRAVEL, GREY AND BROWN (SC)		12.45		SS 10	10	38	0												
END OF BORING				WO	11	15	0												
				SS 11	12	12	0												
				WO	12	33	0												

PA = POWER AUGERING    HA = HAND AUGERING    WO = WASH OUT    ST = SHELBY TUBE    SS = SPLIT SPOON  
 PARTY CHIEF : SAYAN K.    DRILLER : SARAWUT Y.    GEOLOGIST : NATTAPOL K.    DRAFTMAN : SS    TYPIST : VS

BORING LOG				BORING NO : BH- 2	GROUND ELEV (m) :		
PROJECT : <u>ธนาคารกรุงศรีอยุธยา สาขาเขตนา</u>				DEPTH (m) : 12.45	WATER LEVEL (m) : -1.50		
LOCATION : <u>อ.เมือง จ.เชียงใหม่</u>				COORD :	DATE STARTED : 1/6/95		
					DATE FINISHED : 1/6/95		
SOIL DESCRIPTION	DEPTH (m.)	GRAPHIC LOG	METHOD SAMPLING RECOVERY	SPT-N (blows/ft)	PL wn LL (%)	Su (t/sq.m)	TOTAL UNIT WEIGHT (t/cu.m.)
				10 20 30 40	20 40 60 80	1 2 3 4	1.6 1.8 2.0
MEDIUM CLAYEY SAND WITH GRAVEL, BROWN (SC) 1.00	1	PA	SS 1	8	11		
LOOSE SILTY FINE TO MEDIUM SAND, BROWN (SM) 1.50	2	SS 2	SS 3	8	11		
LOOSE CLAYEY FINE TO MEDIUM SAND BROWN (SC) 2.00	3	SS 4	SS 5	29	11		
MEDIUM DENSE TO DENSE CLAYEY SAND, LI-GREY, BROWN (SC) 4.00	4	PA	SS 6	33	11		
HARD CLAY TRACE OF SAND, BROWN (CL) 5.50	5	WO	SS 7	45	11		
VERY STIFF TO HARD FINE TO MEDIUM SANDY CLAY, GREY AND BROWN (CL) 10.00	6	WO	SS 8	30	11		
	7	WO	SS 9	33	11		
	8	WO	SS 10	16	11		
	9	WO	SS 11	50/8	11		
VERY DENSE CLAYEY SAND, GREY AND BROWN (SC) 11.50	11	WO	SS 12	42	11		
DENSE SILTY CLAYEY FINE TO MEDIUM SAND, GREY (SM-SC) 12.45	12	WO					
END OF BORING							

PA = POWER AUGERING    HA = HAND AUGERING    WO = WASH OUT    ST = SHELBY TUBE    SS = SPLIT SPOON  
 PARTY CHIEF : SAYAN K.    DRILLER : SARAWUT Y.    GEOLOGIST : NATTAJDLK    DRAFTMAN : SS    TYPIST : VS

<b>BORING LOG</b>		BORING NO. : <b>BH - 1</b>		GROUND ELEV. (m) : _____												
PROJECT : <b>สถาบันบริการน้ำดื่มจาก ทก.เชียงใหม่ ทวีศ</b>		DEPTH (m) : <b>15.45</b>		WATER LEVEL (m) : <b>-0.90</b>												
LOCATION : <b>อ.เมือง จ.เชียงใหม่</b>		DATE STARTED : <b>22/3/96</b>		DATE FINISHED : <b>22/3/96</b>												
SOIL DESCRIPTION	DEPTH (m)	GRAPHIC LOG	METHOD	SAMPLING	RECOVERY	SPT-N (blows/ft)	PL wn LL (%)			Su (t/sq.m)				TOTAL UNIT WEIGHT γ <sub>t</sub> (t/cu.m.)		
							10	20	30	40	20	40	60		80	1
SOFT FINE TO MEDIUM SANDY CLAY, GREY (CH/SC)	1.00		PA	SS 1		3										
MEDIUM DENSE CLAYEY - SILTY FINE TO MEDIUM SAND, GREY (SC,SM)	2.70		SS 2	SS 3		13										
			SS 4			11										
STIFF FINE SANDY CLAY, GREY (CL)	4.00		PA	SS 5		14										
			WO													
			SS 6			18										
			WO													
MEDIUM DENSE FINE TO COARSE SAND WITH CLAY, GREY (SC)	11.50		SS 7			15										
			WO													
			SS 8			19										
			WO													
			SS 9			19										
			WO													
			SS 10			21										
			WO													
MEDIUM DENSE TO DENSE CLAYEY-SILTY FINE TO COARSE SAND WITH CLAY, GREY (SC,SM)	15.45		SS 11			15										
			WO													
			SS 12			25										
			WO													
END OF BORING			SS 13			40										

PA = POWER AUGERING      HA = HAND AUGERING      WO = WASH OUT      ST = SHELBY TUBE      SS = SPLIT SPOON  
 PARTY CHIEF : SAYAN K.      DRILLER : LERTCHAI S.      GEOLOGIST : UC.      DRAFTSMAN : PN      TYPIST : WS

<b>BORING LOG</b>		BORING NO. : <u>BH-1</u>		GROUND ELEV (m) : _____												
PROJECT : <u>อาคารที่พักคนไข้ 30 เตียง</u>		DEPTH (m) : <u>13.95</u>		WATER LEVEL (m) : <u>-1.50</u>												
LOCATION : <u>ค่ายกาวิละ อ.เมือง จ.เชียงใหม่</u>		COORD. : _____		DATE STARTED : <u>14/05/91</u>												
				DATE FINISHED : <u>15/05/91</u>												
SOIL DESCRIPTION	DEPTH (m)	GRAPHIC LOG	METHOD	SAMPLING	RECOVERY	SPT-N (blows/ft)	PL $\frac{w}{m}$ LL (%)			Su (t/sq.m)				TOTAL UNIT WEIGHT $\gamma_t$ (t/cu.m.)		
							10	20	30	40	20	40	60		80	1
STIFF FINE SANDY CLAY, BROWN (CL-ML)	1.00	[PA]	PA	SS 1	8	8										
		[PA]	PA	SS 2	9	9										
LOOSE SILTY-CLAYEY FINE TO MEDIUM SAND, BROWN (SM-SC, SP-SM)	2.50	[PA]	PA	SS 3	6	6										
		[PA]	PA	SS 4	8	8										
MEDIUM FINE SANDY CLAY, BROWN (CL/SC)	4.00	[PA]	PA	SS 5	4	4										
		[WO]	WO	SS 6	6	6										
		[WO]	WO	SS 7	18	18										
LOOSE TO MEDIUM DENSE SILTY SAND, GREY (SM, SP, SP-SM)		[WO]	WO	SS 8	13	13										
		[WO]	WO	SS 9	7	7										
		[WO]	WO	SS 10	27	27										
	13.00	[WO]	WO	SS 11	24	24										
VERY DENSE SILTY SAND/GRAVEL, GREY (SP-SM)	13.95	[WO]	WO	SS 12	55	55										
END OF BORING																

PA = POWER AUGERING	HA = HAND AUGERING	WO = WASH OUT	ST = SHELBY TUBE	SS = SPLIT SPOON
PARTY CHIEF : SAYAN K.	DRILLER : SANIT S.	GEOLOGIST : P I .	DRAFTMAN : WK.	TYPIST : tp

SOIL DESCRIPTION		DEPTH (m.)	GRAPHIC LOG	METHOD	SAMPLING RECOVERY	SPT-N (blows/ft)	PL wn LL (%)		Su (Usq.m)				TOTAL UNIT WEIGHT (T <sub>1</sub> ) (Ucu.m.)		
							20	40	1	2	3	4	16	18	20
CONCRETE SLAB		0.07		PA	1	11									
MEDIUM DENSE CLAYEY FINE TO MEDIUM SAND, LI-BROWN (SC/CL)		1.00		SS	2	9									
				SS	3	8									
				SS	4	6									
LOOSE SILTY FINE TO MEDIUM SAND, LI-BROWN (SM, SP-SM)		4.00		PA	5	4									
				WO	6	16									
VERY STIFF CLAY, DARK GREY (CL)		8.50		WO	7	17									
				SS	8	17									
				WO	9	13									
MEDIUM DENSE TO DENSE SILTY FINE TO COARSE SAND, YELLOWISH BROWN (SM, SP-SM)		13.00		WO	10	23									
				SS	11	32									
				WO	12										
DENSE SANDY GRAVEL, GREY, BROWN (GP-GM)		15.45		SS	12	42									
				WO	13	42									
END OF BORING															

PA = POWER AUGERING	HA = HAND AUGERING	WO = WASH OUT	ST = SHELBY TUBE	SS = SPLIT SPOON
PARTY CHIEF : KOBKIT T.	DRILLER : SERM J.	GEOLOGIST : PI	DRAFTMAN : WK	TYPIST : WS

<b>BORING LOG</b>				BORING NO : ABH-1		GROUND ELEV (m) : _____						
PROJECT : <u>ก่อสร้างทางแยกต่างระดับกลุ่มที่ 37-1</u>				DEPTH (m) : <u>49.65</u>		WATER LEVEL (m) : <u>-0.70</u>						
LOCATION : <u>อ.เมือง จ.เชียงใหม่</u>				COORD. : _____		DATE STARTED : <u>14/7/95</u>						
						DATE FINISHED : <u>17/7/95</u>						
SOIL DESCRIPTION	DEPTH (m)	GRAPHIC LOG	METHOD SAMPLING RECOVERY	SPT-N (blows/ft)	PL wn LL (%)		Su (t/sq.m)				TOTAL UNIT WEIGHT (t/cu.m)	
					20	40	60	80	1	2		3
				10 20 30 40								16 1.8 20
MEDIUM DENSE SILTY FINE TO COARSE SAND, BROWN (SM) 1.50	1	PA SS 1	SS 2	24								
LOOSE TO MEDIUM DENSE FINE TO COARSE SAND, BROWN (SP,SM) 3.50	2	PA SS 3	SS 4	4								
MEDIUM TO VERY STIFF CLAY TRACE FINE TO MEDIUM SAND, GREY AND BROWN (CL,CH) 10.50	3	PA SS 4	SS 5	18								
	4	WO SS 5	SS 6	11								
	5	WO SS 6	SS 7	18								
	6	ST 1	ST 1						17.06			
	7	WO ST 2	ST 2									
	8	WO ST 2	ST 2						15.43			
MEDIUM DENSE TO DENSE CLAYEY/SILTY FINE SAND, GREY AND BROWN (SM,SC/CL) 14.00	9	WO SS 7	SS 8	7								
	10	WO SS 7	SS 8	43								
	11	WO SS 8	SS 9									
MEDIUM DENSE SILTY GRAVELLY SAND LIGHT GREN (GP-GM) 16.00	12	WO SS 9	SS 10	30								
	13	WO SS 10	SS 11	28								
	14	WO SS 11	SS 12	52								
VERY DENSE SILTY SANDY GRAVEL, LIGHT GREN (GP-GM) 18.50	15	WO SS 12	SS 13	50								
	16	WO SS 13	SS 14	4								
	17	WO SS 14	SS 15									
SOFT CLAY, DARK GREY (CL) 20.50	18	WO SS 15	SS 16									
	19	WO ST 4	ST 4									
	20	WO ST 4	ST 4									

PA = POWER AUGERING      HA = HAND AUGERING      WO = WASH OUT      ST = SHELBY TUBE      SS = SPLIT SPOON  
 PARTY CHIEF : KERKSIN I.      DRILLER : SANEH K.      GEOLOGIST :      DRAFTMAN : WK      TYPIST : WS

<b>BORING LOG</b>				BORING NO. : <u>ABH-1</u>		GROUND ELEV (m) : _____			
PROJECT : <u>ก่อสร้างทางแยกต่างระดับกลุ่มที่ 37-1</u>				DEPTH (m) : <u>49.65</u>		WATER LEVEL (m) : <u>-0.70</u>			
LOCATION : <u>อ.เมือง จ.เชียงใหม่</u>				COORD. : _____		DATE STARTED : <u>14/7/95</u>			
						DATE FINISHED : <u>17/7/95</u>			
SOIL DESCRIPTION	DEPTH (m)	GRAPHIC LOG	METHOD SAMPLING	RECOVERY	SPT-N (blows/ft)	PL wn LL (%)		Su (t/sq.m)	TOTAL UNIT WEIGHT $\gamma_t$ (t/cu.m.)
						10	20 30 40		
VERY LOOSE TO LOOSE SILTY SAND, DARK GREY  (SM) 22.00	21		WO						
	22		SS 14		12				
DENSE TO VERY DENSE SILTY SANDY GRAVEL, LIGHT GREY  (GP-GM) 24.00	23		WO						
	24		SS 15		50/7				
	25		WO						
	26		SS 16		34				
VERY STIFF TO HARD CLAY, GREY  (CH) 28.00	27		WO						
	28		SS 17		18				
	29		WO						
	30		SS 18		50/10				
VERY DENSE SILTY GRAVEL, SILTY SAND, LIGHT-GREY  (SP-SM,GP-SM) 37.00	31		WO						
	32		SS 19		60/5				
	33		WO						
	34		SS 20		50/8				
	35		WO						
	36		SS 21		50/4				
	37		WO						
	38		SS 22		52/5				
	39		WO						
	40		SS 23		50/5				
VERY DENSE SILTY SAND/GRAVEL, LIGHT BROWN  (SM/GM)	41		WO						
	42		SS 24		63/5				
	43		WO						
	44		SS 25		50/6				
	45		WO						
	46		SS 26		63/5				
	47		TC						

PA = POWER AUGERING	HA = HAND AUGERING	WO = WASH OUT	ST = SHELBY TUBE	SS = SPLIT SPOON
PARTY CHIEF : KERKSIN I.	DRILLER : SANEH K.	GEOLOGIST :	DRAFTMAN : WK	TYPIST : ws

<b>BORING LOG</b>				BORING NO. : <u>ABH-1</u>		GROUND ELEV (m) : _____															
PROJECT : <u>ก่อสร้างทางแยกต่างระดับกลุ่มที่ 37-1</u>				DEPTH (m) : <u>49.65</u>		WATER LEVEL (m) : <u>-0.70</u>															
LOCATION : <u>อ.เมือง จ.เชียงใหม่</u>				COORD : _____		DATE STARTED : <u>14/7/95</u>															
						DATE FINISHED : <u>17/7/95</u>															
SOIL DESCRIPTION	DEPTH (m)	GRAPHIC LOG	METHOD	SAMPLING	RECOVERY	SPT-N (blows/ft)				PL wn LL (%)				Su (t/sq.m)				TOTAL UNIT WEIGHT (t/cu.m.)			
						10	20	30	40	20	40	60	80	1	2	3	4	1.6	1.8	2.0	
VERY DENSE SILTY SAND/GRAVEL, LIGHT BROWN  (SM/GM)	41	TC	SS 27			50/4'															
	42	TC	SS 28			50/4'															
	43	TC	SS 29			50/1.20															
	44																				
	45																				
	46																				
	47																				
48																					
49																					
49.65																					
END OF BORING																					

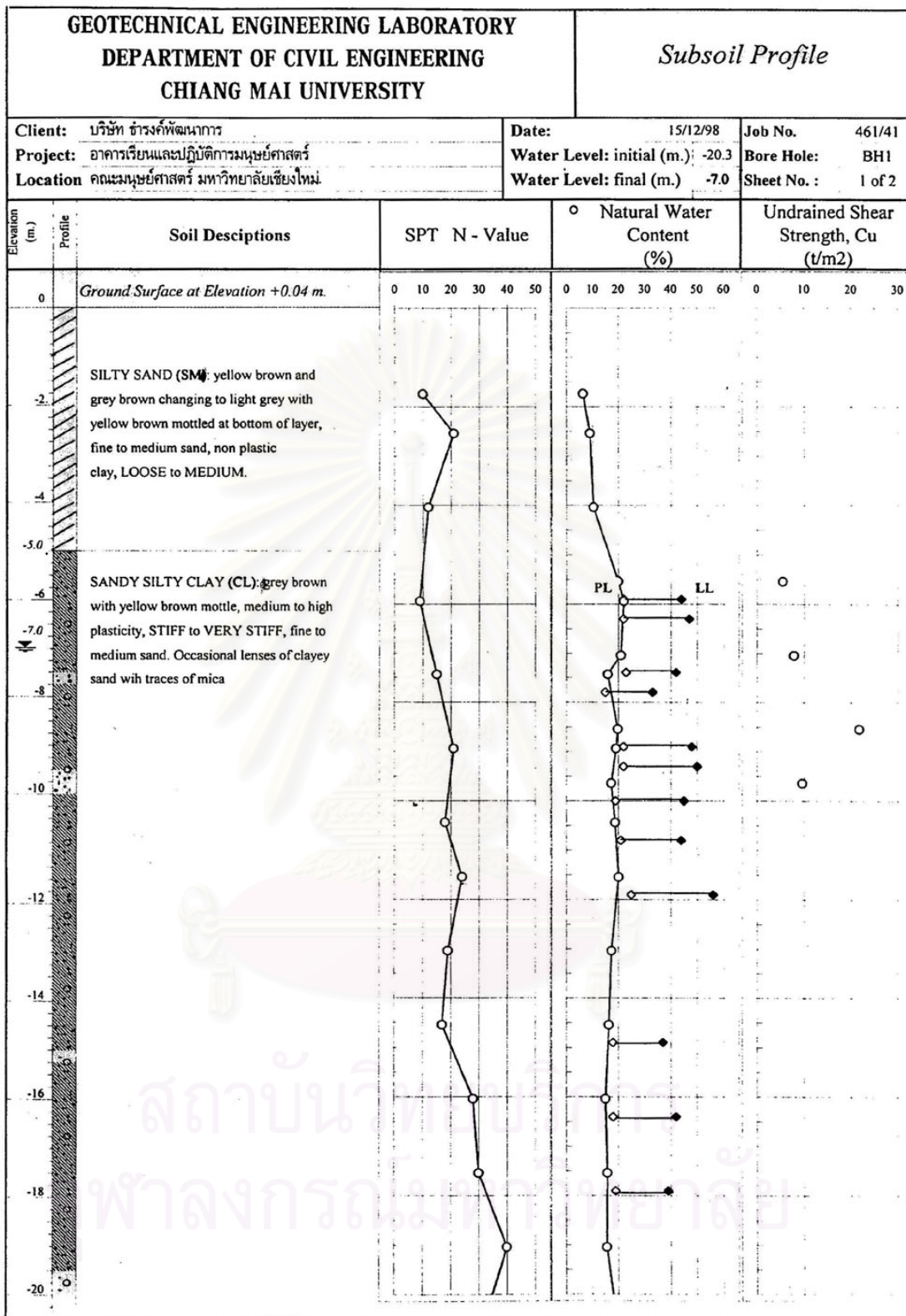
PA = POWER AUGERING    HA = HAND AUGERING    WO = WASH OUT    ST = SHELBY TUBE    SS = SPLIT SPOON  
 PARTY CHIEF : KERKSIN I.    DRILLER : SANEH K.    GEOLOGIST : \_\_\_\_\_    DRAFTMAN : WK    TYPIST : WS

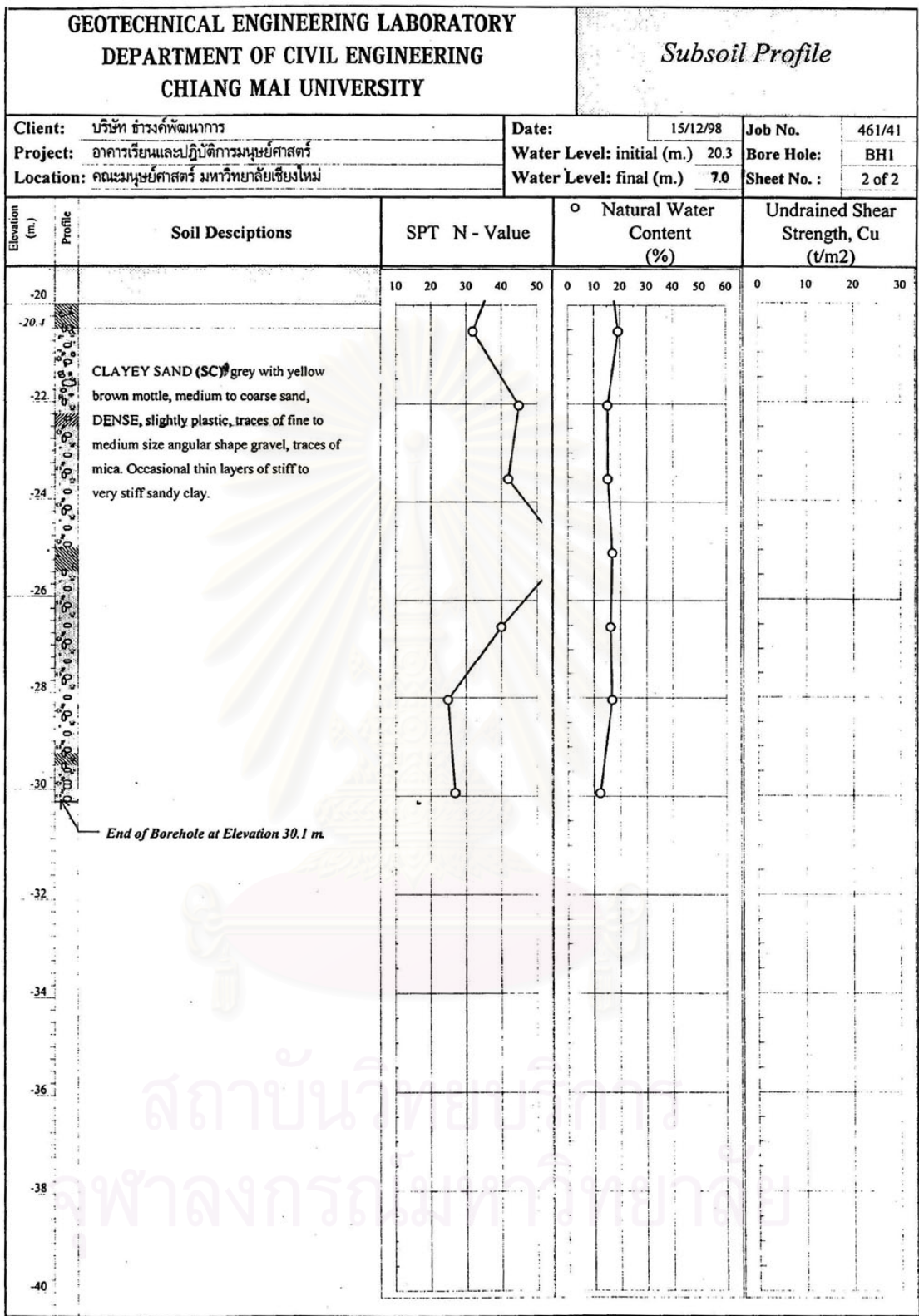


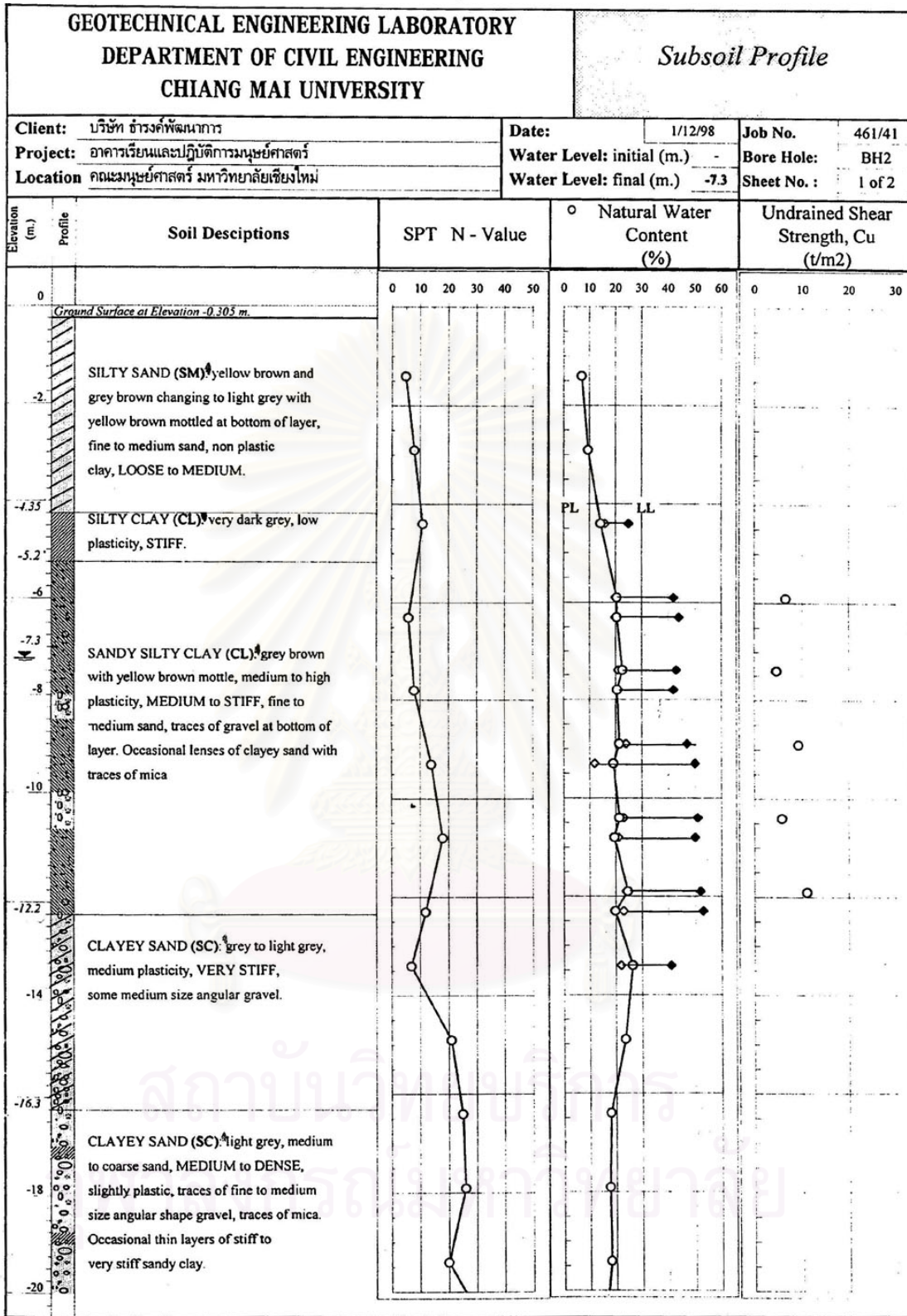
<b>BORING LOG</b>		BORING NO. : ABH-2		GROUND ELEV. (m) : _____										
PROJECT : <u>ก่อสร้างทางแยกต่างระดับกลุ่มที่ 37-1</u>		DEPTH (m) : <u>31.95</u>		WATER LEVEL (m) : <u>-2.40</u>										
LOCATION : <u>อ.เมือง จ.เชียงใหม่</u>		COORD. : _____		DATE STARTED : <u>12/7/95</u>										
				DATE FINISHED : <u>2/7/95</u>										
SOIL DESCRIPTION	DEPTH (m)	GRAPHIC LOG	METHOD	SAMPLING	RECOVERY	SPT-N (blows/ft)	PL (%)	wm	LL	Su (t/sq.m)	TOTAL UNIT WEIGHT γ <sub>t</sub> (t/cu.m.)			
												10	20	30
MEDIUM DENSE CLAYEY FINE TO COARSE SAND WITH GRAVEL, YELLOWISH BROWN (SC)	3.00	PA SS 1 SS 2 PA SS 3 SS 4 SS 5	PA SS SS SS SS	1 2 3 4 5	100% 100% 100% 100% 100%	15 10 17 11 19	10	1	1					
VERY STIFF CLAY, GREY AND BROWN (CL)	8.30	WO SS 6 WO SS 7 WO ST 1 WO ST 2	WO SS WO SS WO ST WO ST	6 7 8 9 10 11 12	100% 100% 100% 100% 100% 100% 100% 100%	24 29 19 19 19 19 19	10	1	1	13.69				
DENSE SILTY FINE TO MEDIUM SAND, DARK GREY (SP-SM)	12.45	WO SS 8 WO SS 9	WO SS WO SS	13 14 15	100% 100% 100% 100%	26 27	10	1	1					
DENSE SILTY SAND GRAVEL, LIGHT GREY (GP-GM)	15.45	WO SS 10 WO SS 11	WO SS WO SS	16 17 18	100% 100% 100% 100%	31 44	10	1	1					
HARD CLAY, YELLOWISH BROWN (CL)	17.00	WO SS 12	WO SS	19 20	100% 100%	30	10	1	1					
CLAYEY GRAVEL (GC)	18.00	WO ST 3	WO ST	21 22	100% 100%	30	10	1	1					
HARD CLAY TRACE FINE SAND, BROWN AND GREY (CH)	20.00	WO SS 13 WO SS 14	WO SS WO SS	23 24 25 26	100% 100% 100% 100%	50 50	10	1	1					
PA = POWER AUGERING		HA = HAND AUGERING		WO = WASH OUT		ST = SHELBY TUBE		SS = SPLIT SPOON						
PARTY CHIEF : KERK SIN I.		DRILLER : SANEH K.		GEOLOGIST :		DRAFTMAN : WK		TYPIST : WS						

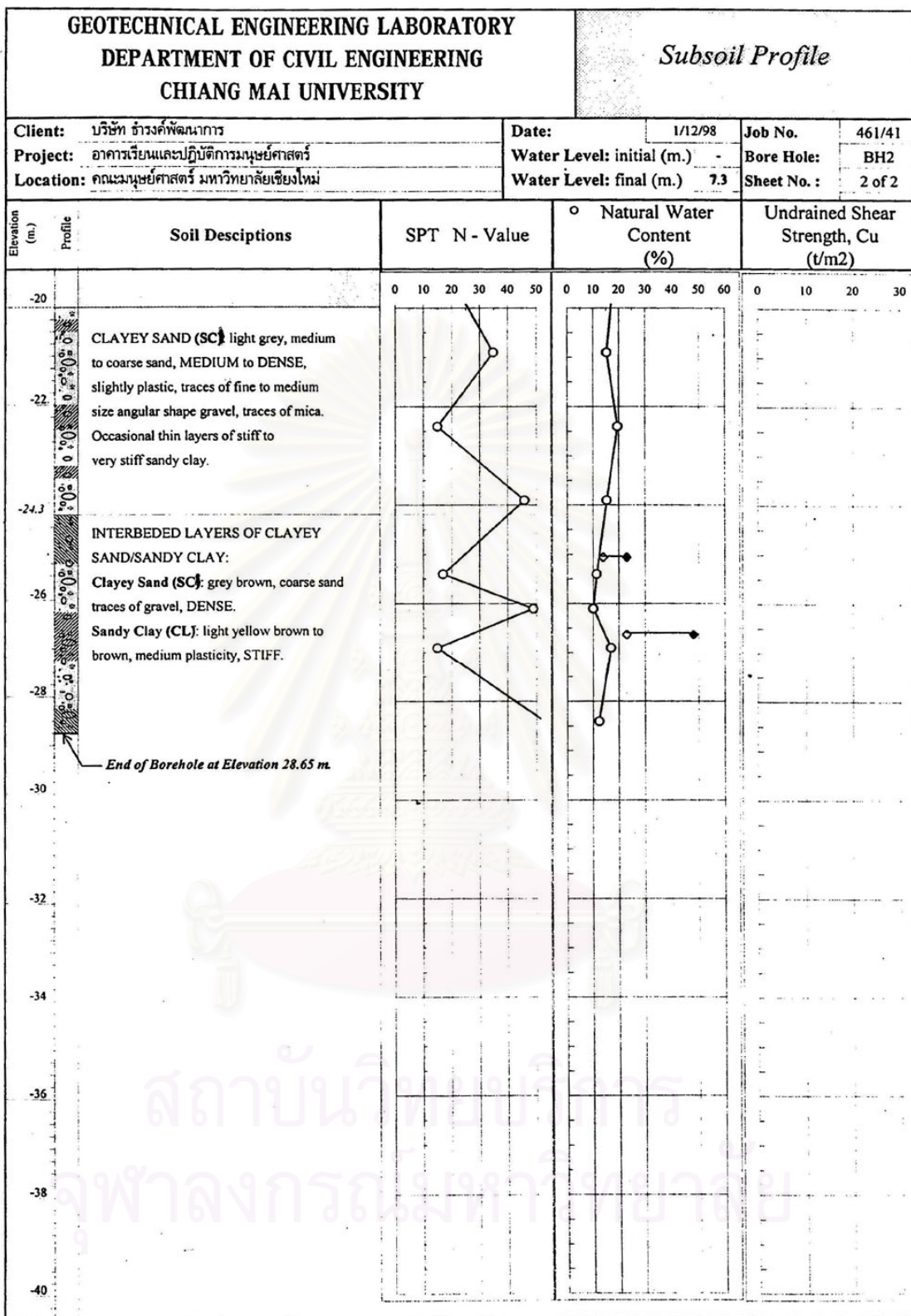
<b>BORING LOG</b>				BORING NO : <u>ABH-2</u>		GROUNDELEV (m) : _____								
PROJECT : <u>ก่อสร้างทางแยกต่างระดับกลุ่มที่ 37-1</u>				DEPTH (m) : <u>31.95</u>		WATER LEVEL (m) : <u>- 2.40</u>								
LOCATION : <u>อ.เมือง จ.เชียงใหม่</u>				COORD : _____		DATE STARTED : <u>12/7/95</u>								
						DATE FINISHED : <u>21/7/95</u>								
SOIL DESCRIPTION	DEPTH (m.)	GRAPHIC LOG	METHOD	SAMPLING	RECOVERY	SPT-N (blows/ft)	PL (%)	wn	LL	Su (t/sq.m)				TOTAL UNIT WEIGHT γ <sub>t</sub> (t/cu.m.)
										1	2	3	4	
						10 20 30 40	20 40 60 80							1.6 1.8 2.0
DENSE SILTY FINE TO MEDIUM SAND AND CLAYEY FINE SAND, LIGHT GREY  (SM, SC)	21		WO	SS 15		33								
	22		WO											
24.10	23		WO	SS 16		25								
	24		WO	SS 17		44								
HARD CLAY, DARK GREY  (CL) 26.00	25		WO	SS 18		34								
VERY DENSE SILTY FINE TO COARSE SAND, LIGHT GREY  (SM)	26		WO											
	27		WO	SS 19		31								
28	28		WO											
	29		WO	SS 20		50/10								
VENG DENSE SILTY SAND/GRAVEL, LIGHT GREY  (SM/GM) 31.95	30		WO	SS 21		50/4								
	31		WO											
END OF BORING				SS 22		50/4								

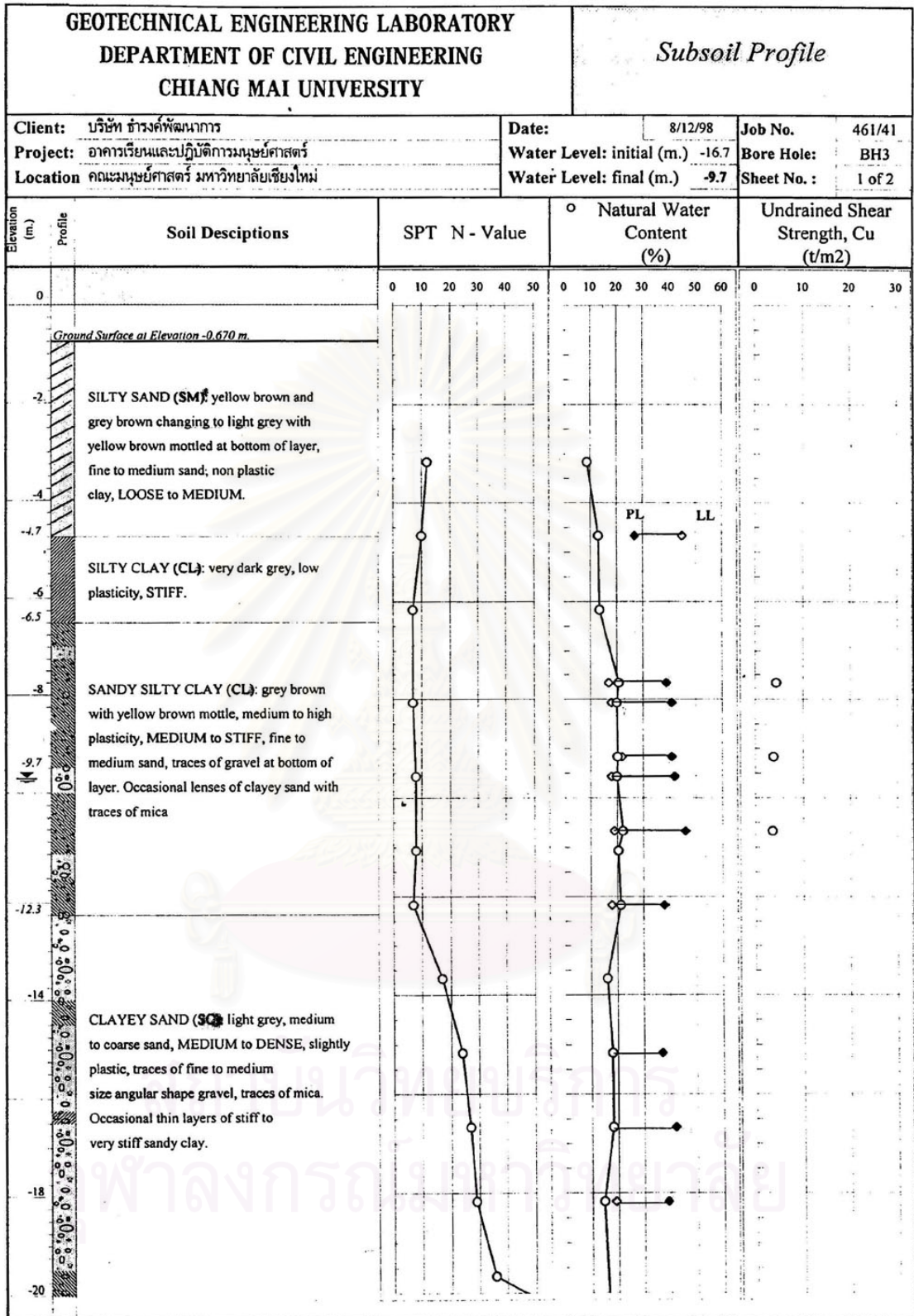
PA = POWER AUGERING	HA = HAND AUGERING	WO = WASH OUT	ST = SHELBY TUBE	SS = SPLIT SPOON
PARTY CHIEF : KERKSIN I.	DRILLER : SANEH K.	GEOLOGIST :	DRAFTMAN W/K	TYPIST : WS

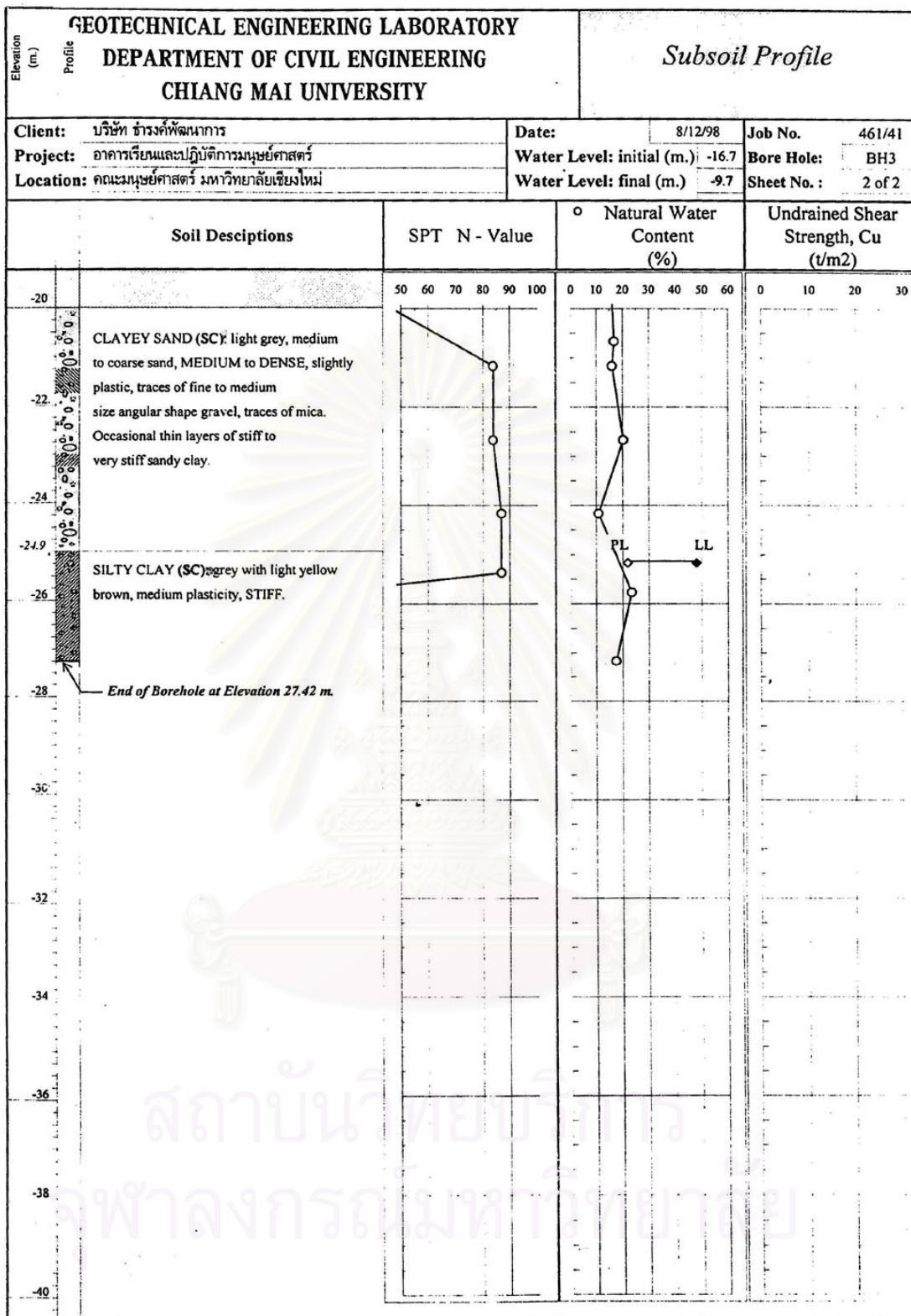




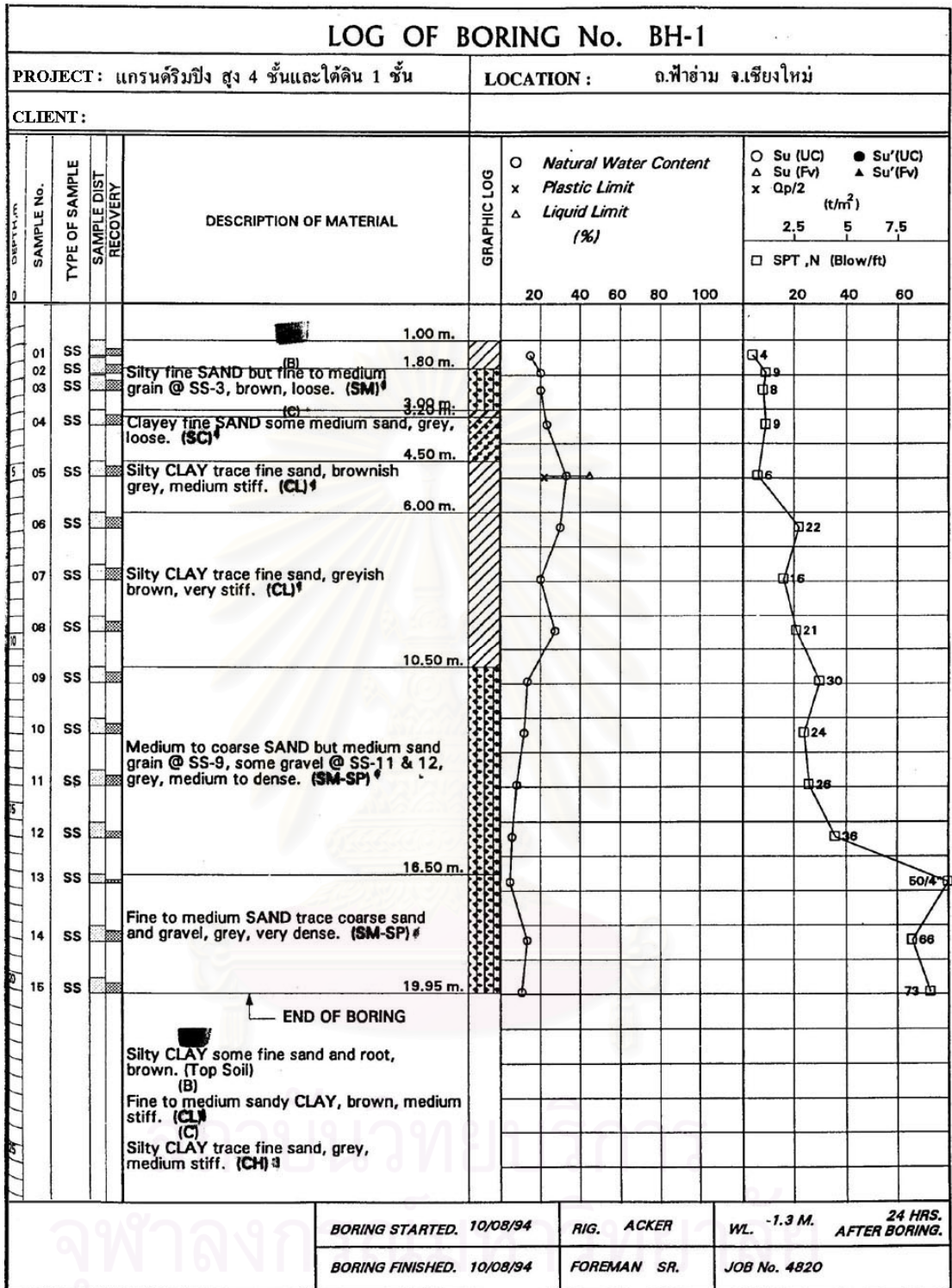


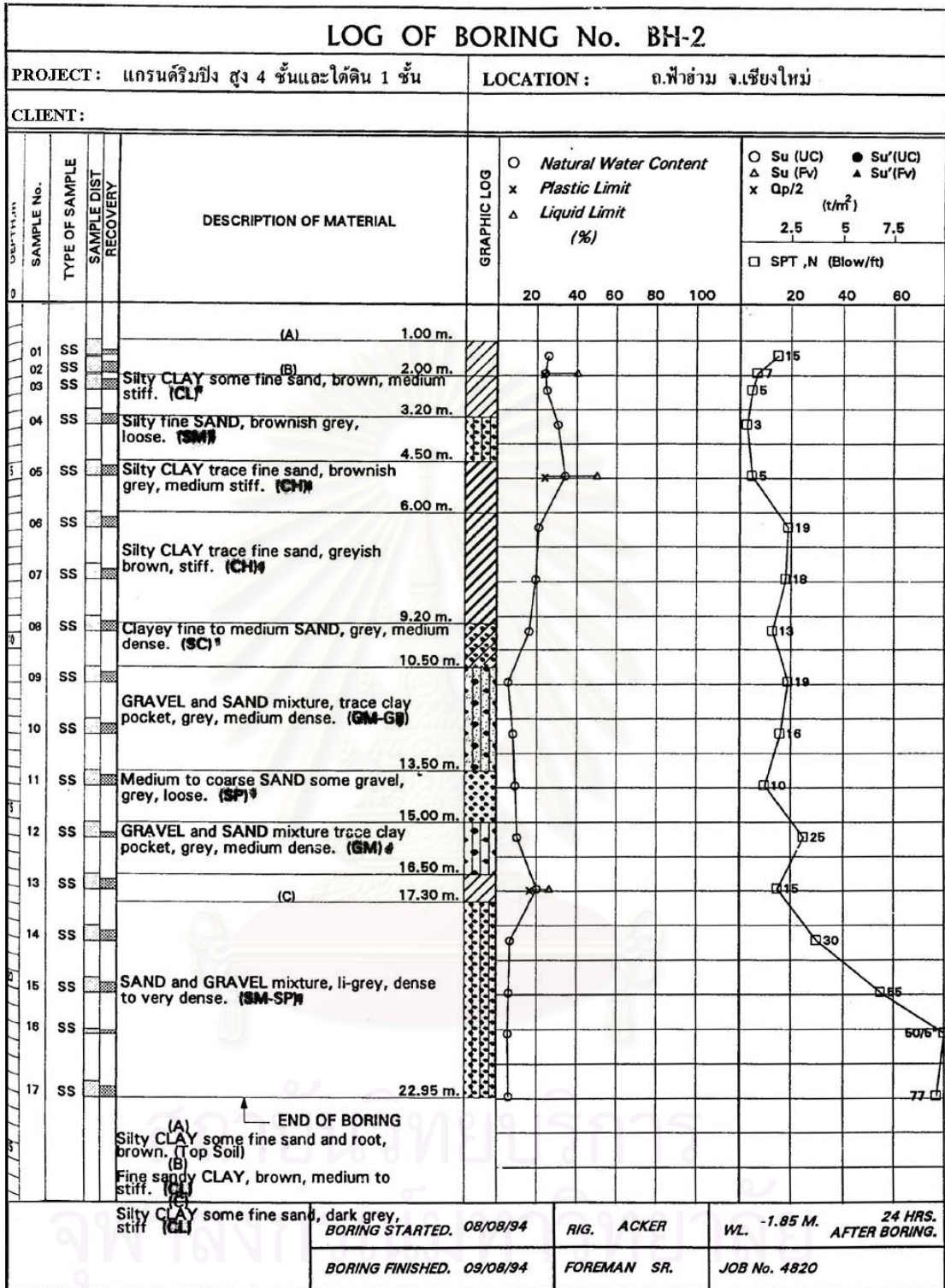






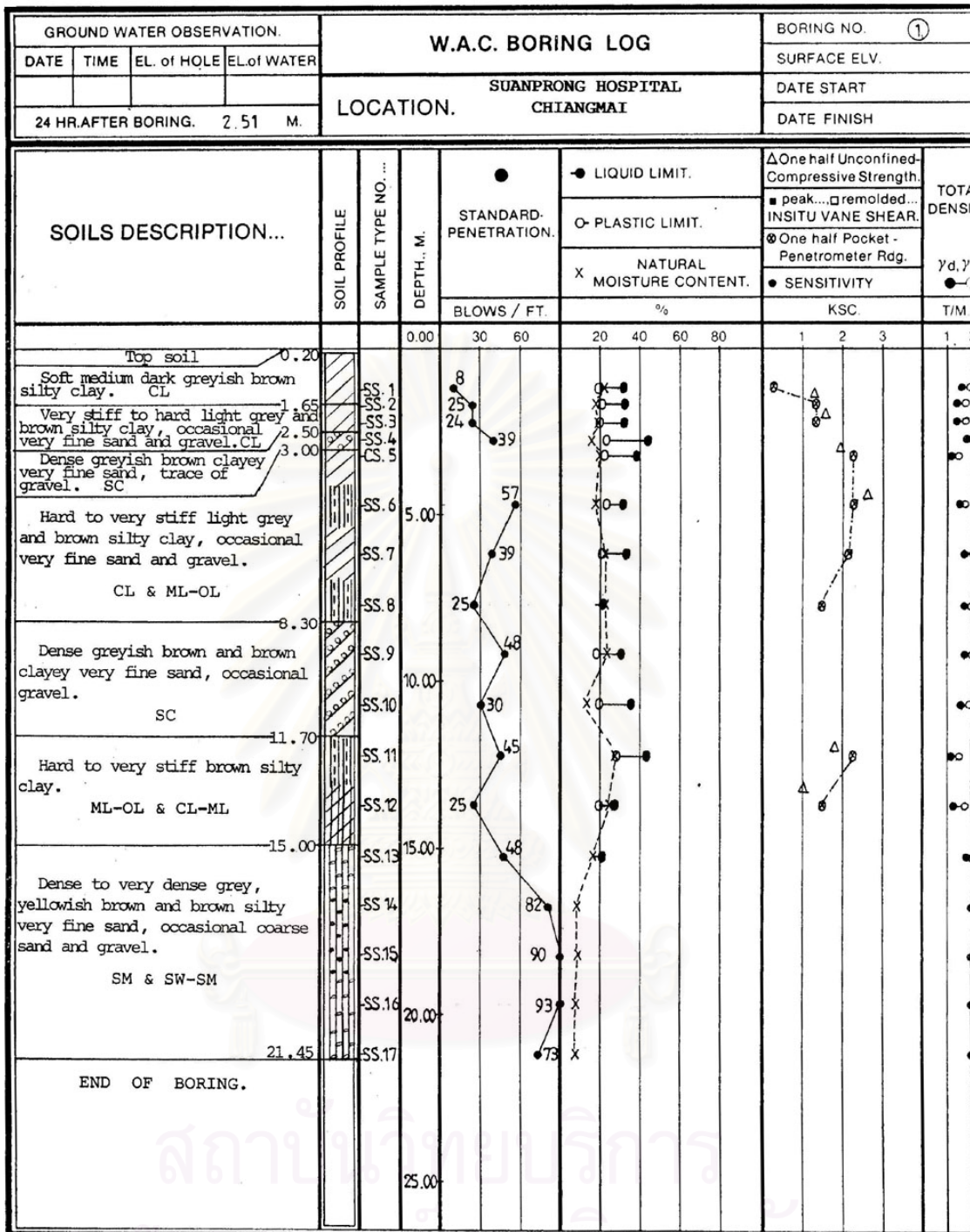




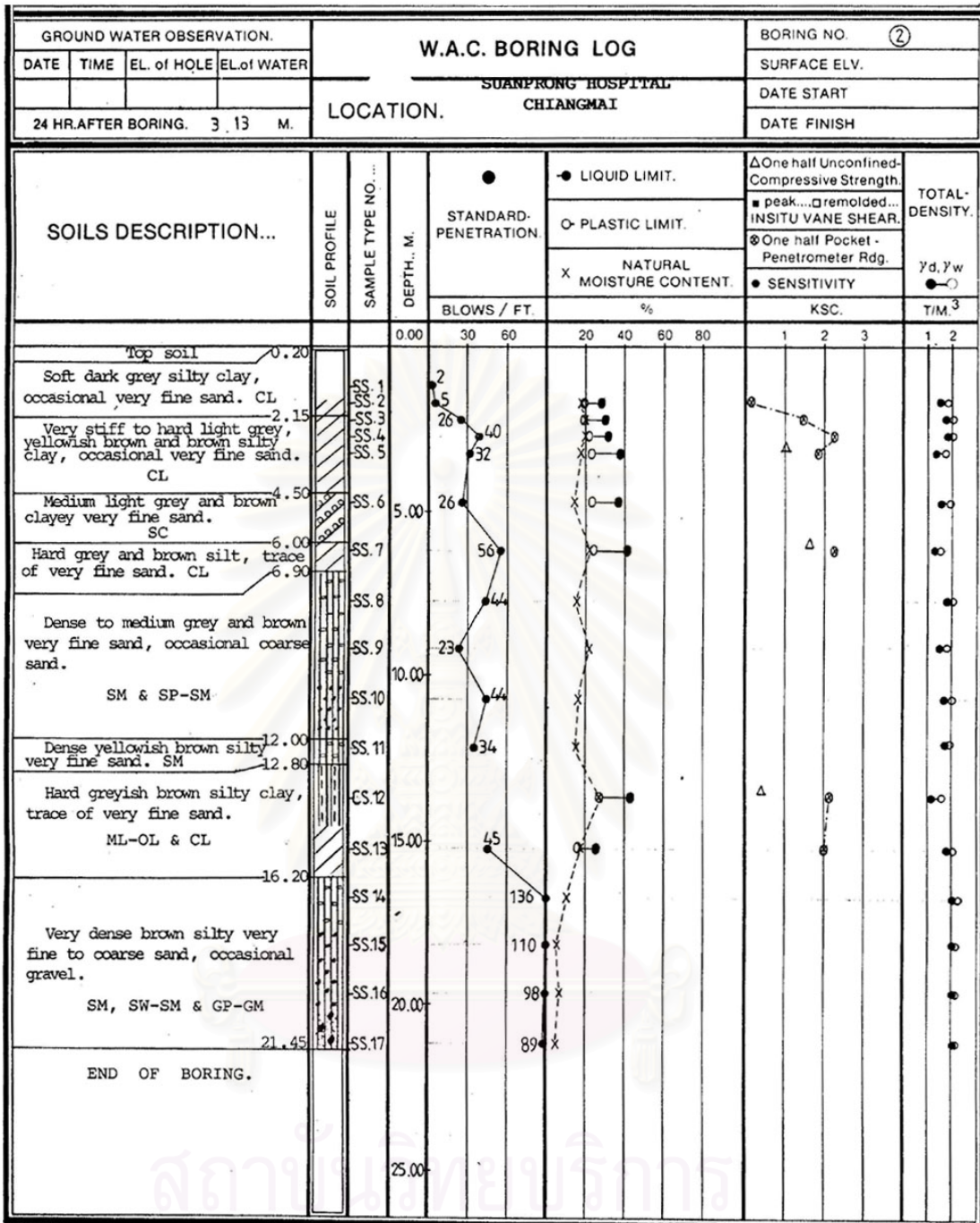


LOG OF BORING No. BH-3													
PROJECT: แกรนด์ริมปีง สูง 4 ชั้นและใต้ดิน 1 ชั้น				LOCATION: อ.ฟ้าฮ่าม จ.เชียงใหม่									
CLIENT:													
DEPTH, m	SAMPLE NO.	TYPE OF SAMPLE	SAMPLE DIST RECOVERY	DESCRIPTION OF MATERIAL	GRAPHIC LOG	Natural Water Content			Su (UC) ● Su'(UC)				
						Plastic Limit			Su (Fv) ▲ Su'(Fv)				
						Liquid Limit (%)			(t/m <sup>2</sup> )				
									2.5	5	7.5		
									□ SPT ,N (Blow/ft)				
						20	40	60	80	100	20	40	60
0													
01	SS			(A) 1.00 m.									
02	SS			(B) 1.50 m.									
03	SS			(C) 2.20 m.									
04	SS			Clayey fine SAND, brown, loose. (SC)									
05	SS			(D) 3.00 m.									
06	SS			Silty fine SAND trace to some medium sand, brown, loose. (SM)									
07	SS			4.50 m.									
08	SS			Silty CLAY trace fine sand, grey, medium stiff. (CL)									
09	SS			6.00 m.									
10	SS			Silty CLAY trace fine sand, brownish grey, stiff to very stiff. (CL)									
11	SS			9.20 m.									
12	SS			Clayey fine SAND trace to some medium sand, grey, medium dense. (SC)									
13	SS			10.50 m.									
14	SS			Medium to coarse SAND some gravel, trace to some fine sand, grey, medium to very dense. (SM-SP)									
15	SS			19.58 m.									
16	SS			END OF BORING									
17				(A) Silty CLAY some fine sand with root, brown. (Top Soil)									
18				(B) Clayey fine to coarse SAND and gravel, brown, loose. (SC)									
19				(C) Silty CLAY trace fine sand, greyish brown, medium stiff. (CL)									
20				(D) Silty CLAY trace fine sand, brown, stiff (CL)									

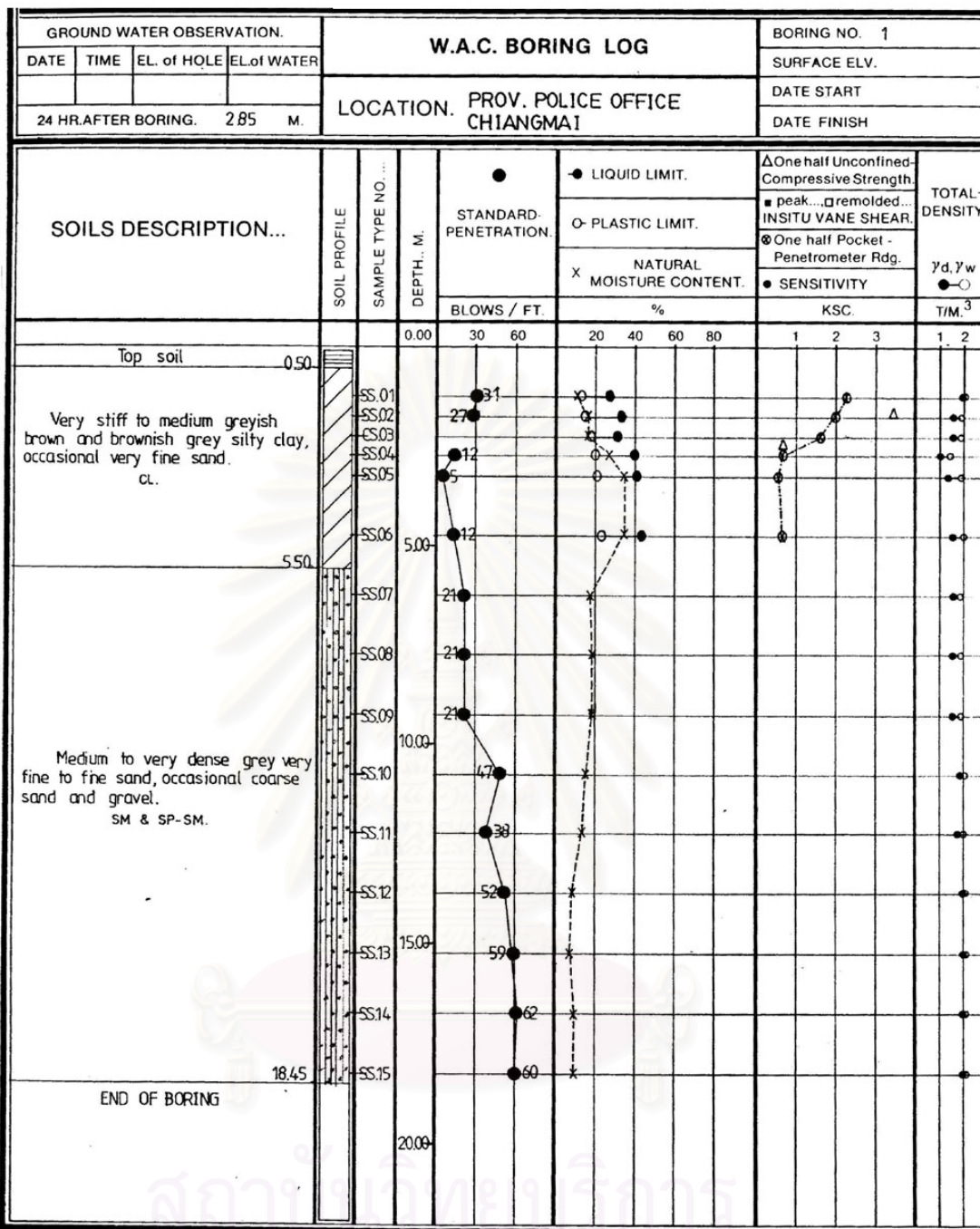
BORING STARTED. 10/08/94	RIG. ACKER	WL. -2.35 M. 24 HRS. AFTER BORING.
BORING FINISHED. 10/08/94	FOREMAN SR.	JOB No. 4820



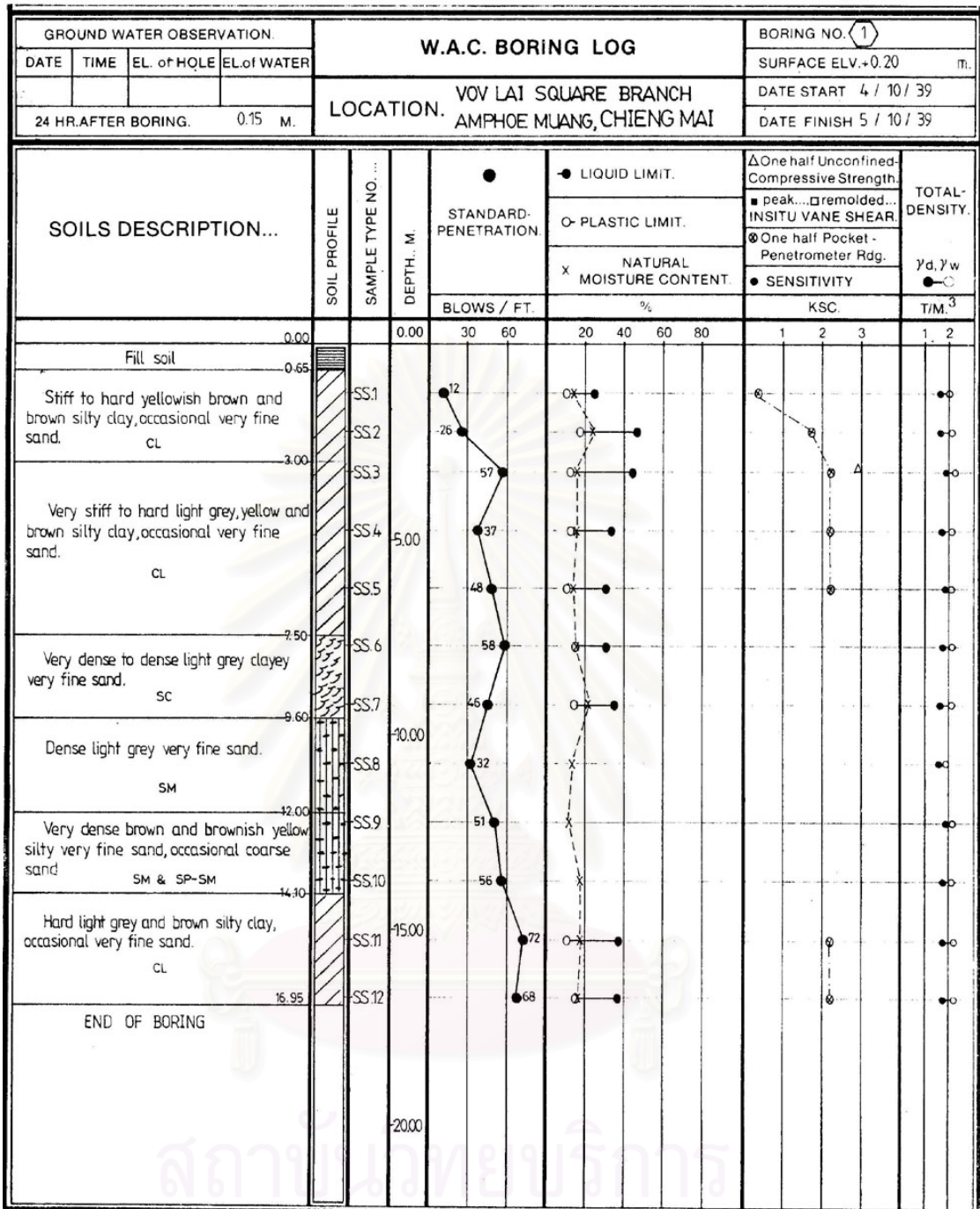
สถาบันวิศวกรรมบริการ  
 ๑๖๖ ถนนวิภาวดีรังสิต กรุงเทพฯ ๑๐๑๖๐



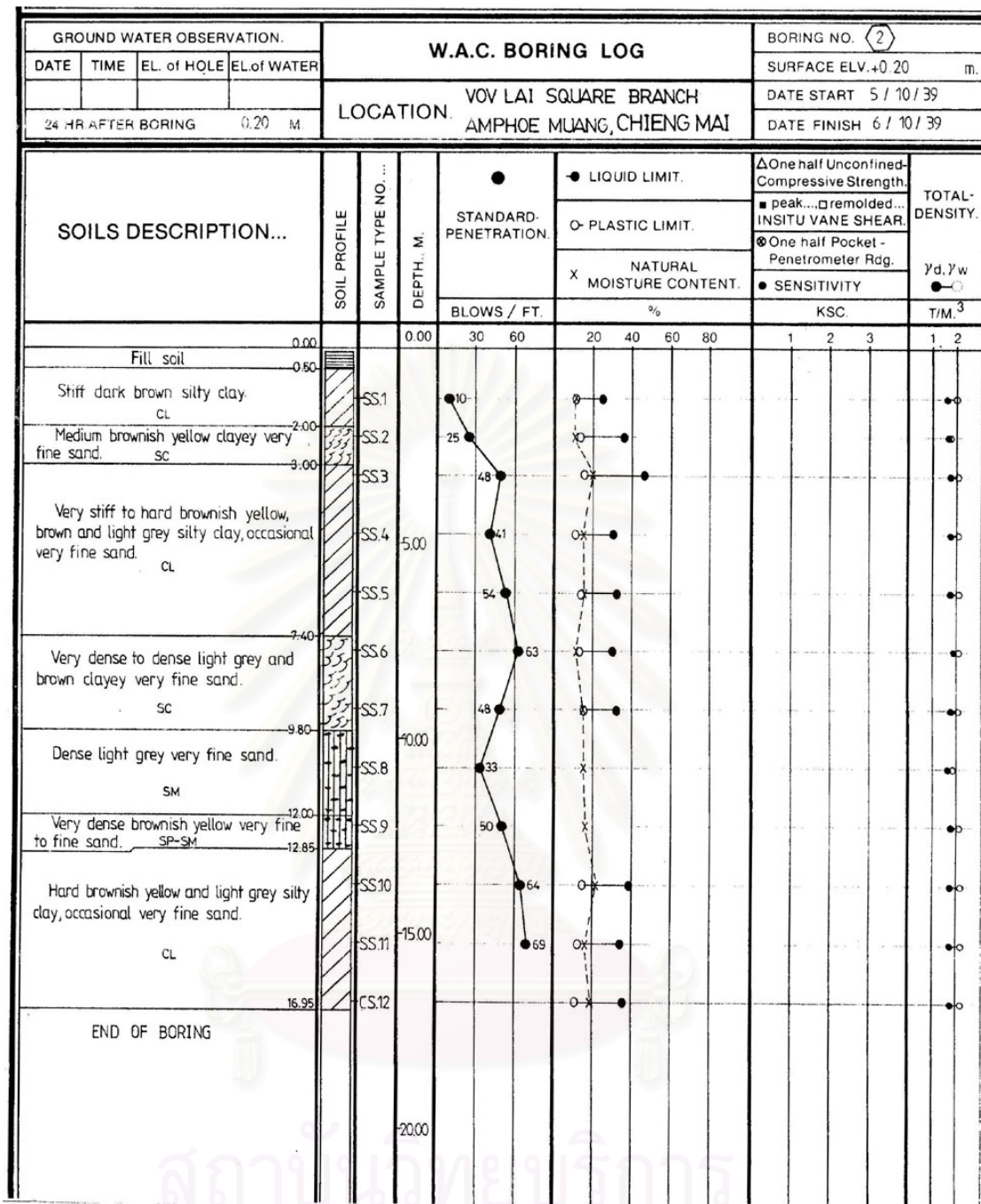
สถาบันวิจัยบริการ  
จุฬาลงกรณ์มหาวิทยาลัย



จุฬาลงกรณ์มหาวิทยาลัย



สถาบันมหาวิทยาลัย  
จุฬาลงกรณ์มหาวิทยาลัย



สถาบันมหาวิทยาลัย  
จุฬาลงกรณ์มหาวิทยาลัย

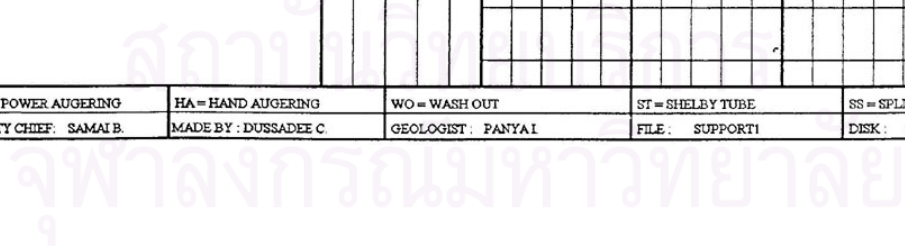


BORING LOG				BORING NO. :	BH-1	ELEVATION (m.) :	-													
PROJECT : SELF SUPPORT TOWER				DEPTH (m) :	25.45	GWL (m) :	-3.20													
LOCATION : A MUANG, CHIANGMAI				COORD. N :	-	DATE STARTED :														
				E :	-	DATE FINISHED :														
SOIL DESCRIPTION	DEPTH (m.)	GRAPHIC LOG	METHOD	SAMPLE NO.	RECOVERY (cm)	SPT-N VALUE (blows/ft.)				NATURAL MOISTURE CONTENT (%)				Su (t/sq.m)				TOTAL UNIT WEIGHT (t/cu.m.)		
						10	20	30	40	20	40	60	80	1	2	3	4	1.6	1.8	2.0
HARD FINE TO MEDIUM SANDY CLAY, GREY (CL)	1.0	[Symbol]	PA																	
			SS	1	10															
	1.50		SS	2	20															
STIFF CLAY, GREY (CL)	2.0		SS	3	10															
			SS	4	15															
	3.0		PA																	
			SS	5	25															
4.0			WO																	
4.50			WO																	
LOOSE CLAYEY FINE SAND, GREY (SC)	5.0		SS	6	20															
	6.0		WO																	
	6.70		SS	7	25															
	7.0		WO																	
MEDIUM DENSE FINE TO MEDIUM SAND, GREY (SP-SM)	8.0		SS	8	10															
	8.40		WO																	
STIFF FINE SANDY CLAY, GREY (CL/SC)	9.0		WO																	
	9.60		SS	9	30															
	10.0		WO																	
MEDIUM DENSE TO DENSE SAND WITH GRAVEL, GREY (SP-SM)	11.0		SS	10	10															
			WO																	
	12.0		SS	11	10															
			WO																	
	13.0		SS	12	10															
			WO																	
	14.0		SS	13	10															
			WO																	
	15.0		SS	14	15															
			WO																	
	16.0		SS	15	30															
17.0		SS	16	30																
17.70		WO																		
VERY STIFF CLAY, GREY (CL)	18.0		SS	15	30															
	19.0		WO																	
	20.0		SS	16	30															
			WO																	

PA = POWER AUGERING      HA = HAND AUGERING      WO = WASH OUT      ST = SHELBY TUBE      SS = SPLIT SPOON  
 PARTY CHIEF: SAMAI B      MADE BY: DUSSADEE C.      GEOLOGIST: PANYAL      FILE: SUPPORT1      DISK: 9/1 CHIANG MAI

BORING LOG					BORING NO. : BH-1		ELEVATION (m) : -														
PROJECT : SELF SUPPORT TOWER					DEPTH (m) : 25.45		GWL (m) : -3.20														
LOCATION : A. MUANG, CHIANGMAI					COORD. N : -		DATE STARTED : -														
					E : -		DATE FINISHED : -														
SOIL DESCRIPTION	DEPTH (m)	GRAPHIC LOG	METHOD	SAMPLE NO.	RECOVERY (cm)	SPT-N VALUE (blows/ft)				NATURAL MOISTURE CONTENT (%)				Su (t/sq.m)				TOTAL UNIT WEIGHT (t/cu.m)			
						10	20	30	40	20	40	60	80	1	2	3	4	1.6	1.8	2.0	
VERY STIFF CLAY, GREY (CL)	20.40		WO																		
MEDIUM DENSE CLAYEY FINE TO MEDIUM SAND, GREY (SC)	22.50		SS	17	30					22											
			WO																		
	23.0		SS	18	30					53											
			WO																		
VERY DENSE SILT SAND, GREY (SM)	25.45		SS	19	30					52											
			WO																		
			SS	20	30					56											
END OF BORING																					

PA = POWER AUGERING	HA = HAND AUGERING	WO = WASH OUT	ST = SHELBY TUBE	SS = SPLIT SPOON
PARTY CHIEF: SAMAI B.	MADE BY: DUSSADEE C.	GEOLOGIST: PANYAI	FILE: SUPPORT1	DISK: 9/1 CHIANG MAI



SOIL DESCRIPTION		DEPTH (m)	GRAPHIC LOG	METHOD	SAMPLING	RECOVERY	SPT-N (blows/ft)				PL wn LL (%)		Su (t/sq.m)				TOTAL UNIT WEIGHT $\gamma_t$ (t/cu.m.)		
							10	20	30	40	20	40	60	80	1	2	3	4	1.8
MEDIUM SANDY CLAY, BROWN (CL)	2.00			PA	SS I		4												
					SS 2		8												
LOOSE SILTY FINE SAND, GREY (SM)	2.50				SS 3		6												
					SS 4		7												
MEDIUM FINE SANDY CLAY, GREY (CL)	4.00			PA	ST I														
					SS 5		5												
STIFF CLAY WITH FINE SAND, GREY (CL)	5.00				WO														
					SS 6		13												
MEDIUM DENSE CLAYEY FINE TO MEDIUM SAND, BROWN (SC/CL)	6.00				ST 2														
					SS 7		38												
VERY STIFF TO HARD FINE TO MEDIUM SANDY CLAY, BROWN (CL/SC)	8.50				WO														
					SS 8		20												
VERY STIFF CLAY WITH FINE SAND, GREY (CL)	12.00				WO														
					SS 9		17												
					WO														
					SS 10		26												
VERY STIFF TO HARD FINE SANDY CLAY, BROWN (CL)	14.00				WO														
					SS 11		38												
					WO														
					SS 12		29												
HARD CLAY, BROWN (CL)	16.00				WO														
					ST 3														
					SS 13		39												
					WO														
DENSE CLAYEY FINE TO MEDIUM SAND, BROWN (SC/CL)	18.00				SS 14		41												
					WO														
VERY STIFF CLAY, GREY (CL)	19.30				SS 15		26												
					WO														
VERY DENSE SILTY FINE SAND, GREY (SM)	20.00				SS 16		50												
					WO		9												

PA = POWER AUGERING    HA = HAND AUGERING    WO = WASH OUT    ST = SHELBY TUBE    SS = SPLIT SPOON  
 PARTY CHIEF : SONGSAK S    DRILLER : BOONSONG C    GEOLOGIST : PANYA . I    DRAFTMAN : SS    TYPIST : WS

BORING LOG				BORING NO. : BH-1	GROUND ELEV (m) : _____														
PROJECT : โรงเรียนทิวเขาเพชร 2				DEPTH (m.) : 27.05	WATER LEVEL (m) : -0.40														
LOCATION : อ.เมือง จ.เชียงใหม่				COORD. : _____	DATE STARTED : 28/6/95														
					DATE FINISHED : 30/6/95														
SOIL DESCRIPTION	DEPTH (m.)	GRAPHIC LOG	METHOD	SAMPLING	RECOVERY	SPT-N (blows/ft)		PL wn LL (%)		Su (t/sq.m)				TOTAL UNIT WEIGHT γ <sub>t</sub> (t/cu.m.)					
						10	20	30	40	20	40	60	80		1	2	3	4	1.6
VERY DENSE SILTY FINE SAND, BROWN (SM) 22.50	21		WO																
	22		SS 17																
VERY DENSE SILTY FINE TO MEDIUM SAND, GREY 25.00	23		WO																
	24		SS 18																
VERY DENSE GRAVELLY SAND, GREY, BROWN 27.05	25		WO																
	26		SS 19																
END OF BORING	27		WO																
			SS 20																
			SS 21																
PA = POWER AUGERING	HA = HAND AUGERING		WO = WASH OUT	ST = SHELBY TUBE	SS = SPLIT SPOON														
PARTY CHIEF :	DRILLER :		GEOLOGIST :	DRAFTMAN :	TYPIST : WS														

SOIL DESCRIPTION		DEPTH (m)	GRAPHIC LOG	METHOD	SAMPLING	RECOVERY	SPT-N (blows/ft)				PL wn LL (%)		Su (t/sq.m)				TOTAL UNIT WEIGHT $\gamma_1$ (t/cu.m.)		
							10	20	30	40	20	40	60	80	1	2	3	4	1.6
SOFT FINE TO MEDIUM SANDY CLAY, GREY (CL/SC) 1.00		1	PA	SS 1			4												
MEDIUM CLAY WITH FINE TO MEDIUM SAND, GREY (CL) 1.80		1.80		SS 2			5												
MEDIUM DENSE SILTY FINE TO MEDIUM SAND, GREY (SM) 2.00		2.00		SS 3			II												
MEDIUM DENSE SILTY FINE TO MEDIUM SAND, GREY (SM) 2.00		2.00		SS 4			3												
SOFT FINE TO MEDIUM SANDY CLAY, GREY (CL/SC) 3.40		3.40		PA			II												
MEDIUM DENSE SILTY FINE TO MEDIUM SAND, GREY (SM) 4.50		4.50		SS 5			II												
WO				WO															
VERY STIFF CLAY, BROWN (CH) 7.50		7.50		SS 6			19												
WO				WO															
ST 1				ST 1															
SS 7				SS 7			28												
DENSE CLAYEY SAND TRACE GRAVEL, BROWN (SC) 8.50		8.50		SS 8			36												
WO				WO															
MEDIUM DENSE CLAYEY SAND, BROWN (SC) 10.00		10.00		SS 9			25												
WO				WO															
HARD CLAY, BROWN (CL) 12.00		12.00		SS 10			39												
WO				WO															
VERY STIFF FINE TO MEDIUM SANDY CLAY, BROWN (CL) 13.50		13.50		SS 11			25												
WO				WO															
VERY STIFF TO HARD CLAY, BROWN (CH) 17.80		17.80		SS 12			29												
WO				WO															
ST 2				ST 2															
SS 13				SS 13			47												
WO				WO															
SS 14				SS 14			40												
WO				WO															
DENSE FINE SANDY SILT, GREY (ML/SM) 19.50		19.50		SS 15			46												
WO				WO															
VERY DENSE SILTY SAND, GREY (SM) 20.00		20.00		SS 16			50												
WO				WO															

PA = POWER AUGERING    HA = HAND AUGERING    WO = WASH OUT    ST = SHELBY TUBE    SS = SPLIT SPOON  
 PARTY CHIEF : SONGSAK S    DRILLER : BOONSONG C    GEOLOGIST :    DRAFTMAN : SS    TYPIST : WS

<b>BORING LOG</b>					BORING NO. : <b>BH-2</b>		GROUND ELEV (m) : _____												
PROJECT : <u>โครงการเคอเมทรี 2</u> LOCATION : <u>อ.เมือง จ.เชียงใหม่</u>					DEPTH (m.) : <b>28.70</b>		WATER LEVEL (m) : _____												
					COORD. : _____		DATE STARTED : <b>25/6/95</b>												
						DATE FINISHED : <b>26/6/95</b>													
SOIL DESCRIPTION	DEPTH (m.)	GRAPHIC LOG	METHOD	SAMPLING RECOVERY	SPT-N (blows/ft)				PL wn LL (%)			Su (t/sq.m)				TOTAL UNIT WEIGHT $\gamma_t$ (t/cu.m.)			
					10	20	30	40	20	40	60	80	1	2	3	4	1.6	1.8	2.0
VERY DENSE SILTY SAND, GREY (SM)	21	[Pattern]	WO																
			SS 17																
	22		WO																
			SS 18																
	23	WO																	
	24	WO																	
	25	WO																	
	25.50																		
VERY DENSE GRAVELLY MEDIUM TO COARSE SAND TRACE SILT, GREY (SP-SM)	26	[Pattern]	WO																
			SS 20																
VERY DENSE SANDY GRAVEL TRACE SILT GREY (GP-GM)	27	[Pattern]	WO																
			SS 21																
	28	[Pattern]	WO																
	28.70		SS 22																
END OF BORING																			

PA = POWER AUGERING	HA = HAND AUGERING	WO = WASH OUT	ST = SHELBY TUBE	SS = SPLIT SPOON
PARTY CHIEF : _____	DRILLER : _____	GEOLOGIST : _____	DRAFTSMAN : _____	TYPIST : WS

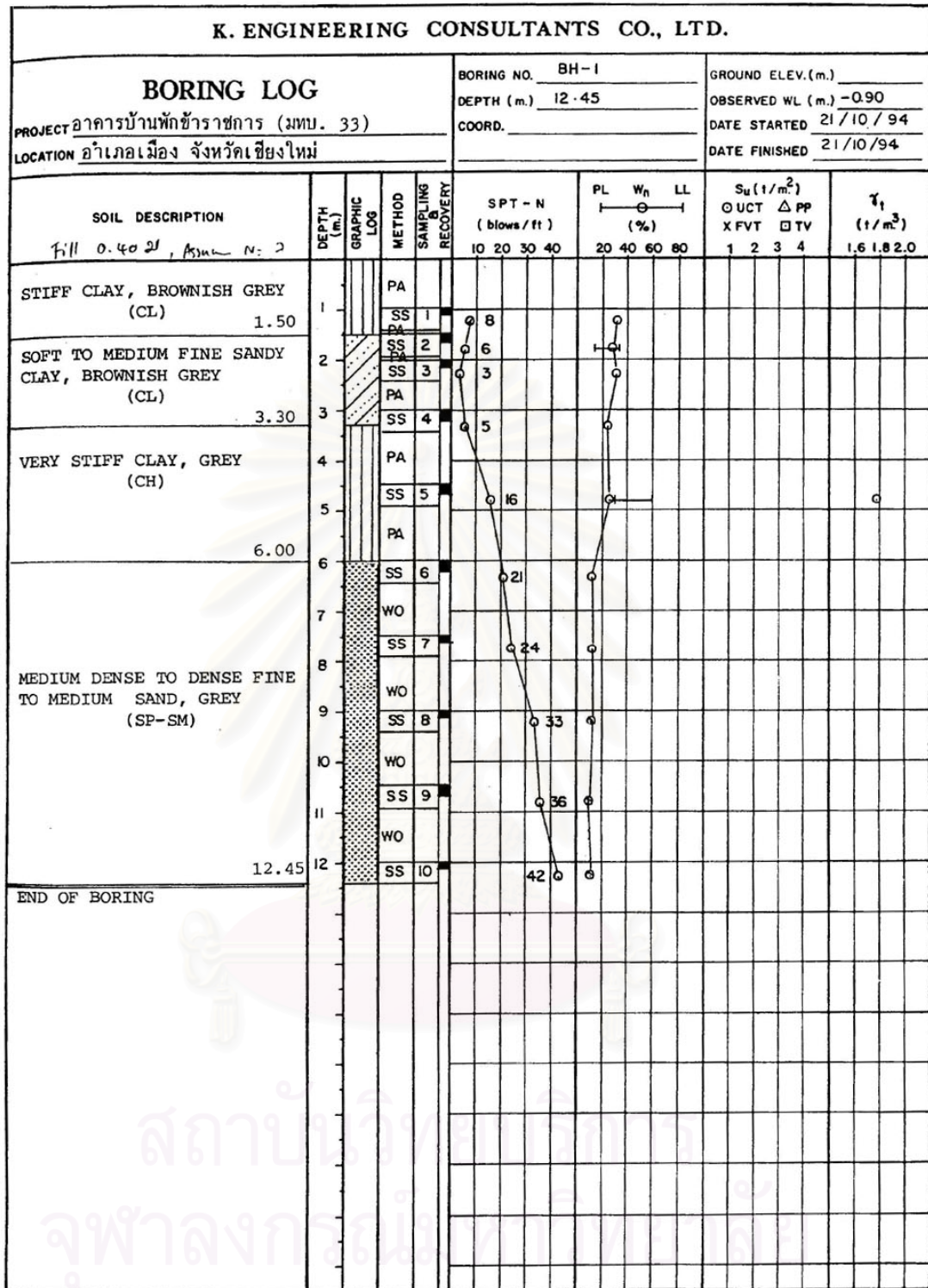
SOIL DESCRIPTION		DEPTH (m.)	GRAPHIC LOG	METHOD	SAMPLING RECOVERY	SPT-N (blows/ft)	PL wn LL (%)	Su (t/sq.m)				TOTAL UNIT WEIGHT $\gamma_t$ (t/cu.m.)
								○ UCT	△ PP	X FVT	□ TV	
						10 20 30 40	20 40 60 80	1	2	3	4	1.6 1.8 2.0
VERY SOFT TO SOFT CLAY, WITH FINE SAND, BROWN, DARK BROWN (CL)		1 - 3.00	PA	SS	1	2	1-1					
			PA	SS	2	2	1-1					
			PA	SS	3	3	1-1					
MEDIUM CLAY, DARK BROWN (CH)		3.00 - 4.50	PA	SS	4	5						
			WO									
VERY STIFF CLAY, DARK BROWN (CH)		4.50 - 5.90	SS	SS	5	26	1-1					
			WO									
DENSE CLAYEY FINE TO MEDIUM SAND, DARK BROWN (SC)		5.90 - 7.30	SS	SS	6	44	1-1					
			WO									
STIFF TO VERY STIFF CLAY, DARK BROWN (CL)		7.30 - 10.00	SS	SS	7	25						
			WO									
			SS	SS	8	9	1-1					
			WO									
MEDIUM DENSE SILTY SAND, GREY, BROWN (SP-SM)		10.00 - 13.50	SS	SS	9	25						
			WO									
			SS	SS	10	25						
			WO									
VERY DENSE SANDY GRAVEL, BROWN (GP-GM)		13.50 - 15.16	SS	SS	11	55						
			WO									
END OF BORING		15.16	SS	SS	12	50/7						

PA = POWER AUGERING	HA = HAND AUGERING	WO = WASH OUT	ST = SHELBY TUBE	SS = SPLIT SPOON
PARTY CHIEF: PK	DRILLER: SARAWUT Y	GEOLOGIST: PANYA I.	DRAFTMAN: SS	TYPIST: WS

<b>BORING LOG</b>				BORING NO. : <u>BH- 2</u>		GROUND ELEV (m) : _____													
PROJECT : <u>ธนาคารไทยพาณิชย์ สาขาอยุธยา</u>				DEPTH (m) : <u>15.00</u>		WATER LEVEL (m) : <u>-0.50</u>													
LOCATION : <u>อำเภอเมือง จังหวัดเชียงใหม่</u>				COORD. : _____		DATE STARTED : <u>3/12/94</u>													
						DATE FINISHED : <u>3/12/94</u>													
SOIL DESCRIPTION	DEPTH (m.)	GRAPHIC LOG	METHOD	SAMPLING	RECOVERY	SPT-N (blows/ft)	PL wn LL (%)		Su (t/sq.m)	TOTAL UNIT WEIGHT γ <sub>t</sub> (t/cu.m.)									
							10	20			30	40	20	40	60	80	1	2	3
VERY SOFT CLAY, DARK GREY (CL)	1.50	[Hatched]	PA	SS 1	1	2													
MEDIUM CLAY WITH FINE SAND, DARK BROWN (CL)	4.50	[Hatched]	WO	SS 2	2	4													
VERY STIFF CLAY, DARK BROWN (CL)	5.90	[Hatched]	WO	SS 3	3	23													
DENSE CLAYEY FINE TO MEDIUM SAND, DARK BROWN (SC)	7.30	[Dotted]	WO	SS 4	4	42													
VERY STIFF CLAY, DARK BROWN (CH)	9.00	[Hatched]	WO	SS 5	5	25													
MEDIUM CLAY, DARK BROWN (CH)	10.00	[Hatched]	WO	SS 6	6	7													
MEDIUM DENSE TO DENSE FINE TO MEDIUM SAND, DARK BROWN (SP-SM)	13.50	[Dotted]	WO	SS 7	7	27													
VERY DENSE SANDY GRAVEL, BROWN (GP-GM)	15.00	[Cross-hatched]	WO	SS 8	8	31													
END OF BORING				SS 9	9	55													
				SS 10	10	50													

PA = POWER AUGERING      HA = HAND AUGERING      WO = WASH OUT      ST = SHELBY TUBE      SS = SPLIT SPOON  
 PARTY CHIEF : PK      DRILLER : SARAWUT Y.      GEOLOGIST : PANYA I.      DRAFTMAN : SS      TYPIST : WS





สถาบันวิจัยและพัฒนา  
 จุฬาลงกรณ์มหาวิทยาลัย





BORING LOG				BORING NO :	BH-1	ELEVATION (m)	-														
PROJECT : UNDERPASS ตอนชั้นเทรคเซ็นเตอร์				DEPTH (m) :	18.45	GWL (m)	-1.50														
LOCATION : อ.เมือง จ.เชียงใหม่				COORD N :	-	DATE STARTED	27/10/96														
				E :	-	DATE FINISHED	27/10/96														
SOIL DESCRIPTION	DEPTH (m)	GRAPHIC LOG	METHOD	SAMPLE NO	RECOVERY (cm.)	SPT-N VALUE (blows/ft.)				NATURAL MOISTURE CONTENT (%)				Su (t/sq.m.)				TOTAL UNIT WEIGHT (t/cu.m.)			
						10	20	30	40	20	40	60	80	1	2	3	4	1.6	1.8	2.0	
VERY SOFT FINE TO MEDIUM SANDY CLAY, BROWN (CL/SC)	1.0	[Hatched]	PA																		
	1.50		SS 1	25	2																
VERY STIFF CLAY WITH FINE SAND, BROWN (CL)	2.0	[Vertical Lines]	SS 2	25	7																
	3.0		ST 1	25																	
	3.5		PA																		
	4.0		ST 2	25																	
	4.5		PA																		
	5.0		ST 3	25																	
LOOSE CLAYEY-SILTY FINE SAND, BROWN (SC-SM)	5.5	[Dotted]	PA																		
	6.0		SS 3	-	6																
VERY STIFF FINE SANDY CLAY, BROWN (CL)	6.5	[Vertical Lines]	WO																		
	7.0		SS 4	25	8																
MEDIUM DENSE TO DENSE FINE TO MEDIUM SAND, GREY (SP)	7.5	[Dotted]	WO																		
	8.0		SS 5	40	18																
MEDIUM DENSE SAND WITH GRAVEL, BROWN (SP-SM)	8.5	[Vertical Lines]	WO																		
	9.0		SS 6	40	14																
	10.0		WO																		
	11.0		SS 7	30	36																
DENSE SILTY/GRAVELLY SAND, BROWN (SM/GM)	11.5	[Dotted]	WO																		
	12.0		SS 8	25	19																
	13.0		WO																		
END OF BORING	13.50	[Vertical Lines]	SS 9	25	17																
	14.0		WO																		
END OF BORING	15.0	[Vertical Lines]	SS 10	25	22																
	16.0		WO																		
END OF BORING	17.0	[Vertical Lines]	SS 11	25	15																
	18.0		WO																		
END OF BORING	18.45	[Vertical Lines]	SS 12	25	35																
			WO																		

PA = POWER AUGERING      HA = HAND AUGERING      WO = WASH OUT      ST = SHELBY TUBE      SS = SPLIT SPOON  
 PARTY CHIEF : SAYANK.      MADE BY : PACHAREE C.      GEOLOGIST : PANYA I.      FILE : UNDER-1      DISK : 9 CHIANG MAI

จุฬาลงกรณ์มหาวิทยาลัย



<b>BORING LOG</b>		BORING NO : <u>BH - 1</u>		GROUND ELEV (m) : _____			
PROJECT : <u>สถานีบริการน้ำมันบางจาก BCP - ราชเชียงใหม่</u> LOCATION : <u>อ.เมือง จ.เชียงใหม่</u>		DEPTH (m) : <u>15.45</u>		WATER LEVEL (m) : <u>-1.80</u>			
		COORD : _____		DATE STARTED : <u>21/3/96</u>			
				DATE FINISHED : <u>21/3/96</u>			
SOIL DESCRIPTION	DEPTH (m)	GRAPHIC LOG	METHOD SAMPLING RECOVERY	SPT-N (blows/ft)	PL wn LL (%)	Su (t/sq.m)	TOTAL UNIT WEIGHT $\gamma_t$ (t/cu.m.)
MEDIUM FINE TO MEDIUM SANDY CLAY, GREY (CL)	1.00	PA	SS 1	6	1		
SOFT FINE TO MEDIUM SANDY CLAY, GREY (CL)	2.80	PA	SS 2	2	1		
			SS 3	4	1		
			SS 4	4			
STIFF TO VERY STIFF FINE TO MEDIUM SANDY CLAY, GREY (CL)	5.80	PA	SS 5	11	1		22.1
			WO				
			SS 6	18			
MEDIUM DENSE CLAYEY FINE TO MEDIUM SAND, GREY (SC)	7.00	PA	SS 7	15	1		
			WO				
STIFF TO VERY STIFF FINE TO MEDIUM SANDY CLAY, GREY (CL)	13.50	PA	SS 8	26			
			WO				
			SS 9	28			
			WO				
			SS 10	18	1		
			WO				
MEDIUM DENSE SILTY FINE TO MEDIUM SAND, GREY (SM)	14.50	PA	SS 11	14	1		
			WO				
VERY DENSE SILTY FINE TO MEDIUM SAND, GREY (SM)	15.45	PA	SS 12	29			
			WO				
END OF BORING							
SS 13				52			

PA = POWER AUGERING	HA = HAND AUGERING	WO = WASH OUT	ST = SHELBY TUBE	SS = SPLIT SPOON
PARTY CHIEF : SAYAN K.	DRILLER : LERTCHAI S.	GEOLOGIST : UC.	DRAFTSMAN : PN.	TYPIST : WS

BORING LOG					BORING NO. : BH-1		ELEVATION (m) : -														
PROJECT : เรือนำจังหวัดเชียงใหม่ (แห่งใหม่)					DEPTH (m) : 16.00		GWL (m) : -0.10														
LOCATION : อ.ช้างเผือก อ.เมือง จ.เชียงใหม่					COORD. N : -		DATE STARTED : 31/10/96														
					E : -		DATE FINISHED : 01/11/96														
SOIL DESCRIPTION	DEPTH (m)	GRAPHIC LOG	METHOD	SAMPLE NO.	RECOVERY (cm)	SPT-N VALUE (blows/ft.)				NATURAL MOISTURE CONTENT (%)				Su (t/sq.m)				TOTAL UNIT WEIGHT (t/cu.m)			
						10	20	30	40	20	40	60	80	1	2	3	4	1.6	1.8	2.0	
GARBAGE	1.0	[Redacted]	PA																		
	2.0																				
	3.0																				
	4.0																				
	5.0																				
	6.00																				
VERY STIFF FINE SANDY CLAY, GREY (CL/SC)	7.0		SS	1	40																
	7.50		WO																		
MEDIUM DENSE TO DENSE CLAYEY FINE SAND, BROWN (SC,SC/CL)	8.0		SS	2	40																
			WO																		
	9.0		SS	3	30																
			WO																		
	10.0		SS	4	35																
			WO																		
VERY DENSE SILTY FINE TO MEDIUM SAND, BROWN (SM)	11.0		SS	5	40																
			WO																		
	12.0		SS	6	25																
			WO																		
13.50		SS	7	20																	
		WO																			
14.0		SS	8	-																	
		WO																			
15.0		SS	7	20																	
		WO																			
16.00		SS	8	-																	
END OF BORING	ROCK		SS	8	-																
			WO																		
			SS	8	-																
			WO																		

PA = POWER AUGERING    HA = HAND AUGERING    WO = WASH OUT    ST = SHELBY TUBE    SS = SPLIT SPOON  
 PARTY CHIEF: SAYAN K.    MADE BY: DUSSADEE C.    GEOLOGIST: PANYAI    FILE: CHANG-1    DISK: 9 CHIANG MAI

ศูนย์บริการโลหิตแห่งชาติ สภากาชาดไทย

BORING LOG				BORING NO. : BH-2		ELEVATION (m) : -														
PROJECT : เรือนจำจังหวัดเชียงใหม่ (แห่งใหม่)				DEPTH (m) : 19.50		GWL (m) : -1.30														
LOCATION : ต.ช้างศึก อ.เมือง จ.เชียงใหม่				COORD. N : -		DATE STARTED : 01/11/96														
				E : -		DATE FINISHED : 02/11/96														
SOIL DESCRIPTION	DEPTH (m.)	GRAPHIC LOG	METHOD	SAMPLE NO.	RECOVERY (cm)	SPT-N VALUE (blows/ft)				NATURAL MOISTURE CONTENT (%)				Su (t/sqm)				TOTAL UNIT WEIGHT (t/cu.m)		
						10	20	30	40	20	40	60	80	1	2	3	4	1.6	1.8	2.0
VERY STIFF TO HARD CLAY WITH FINE SAND, BROWN, REDDISH BROWN (CH)	1.0	[Graphic Log]	PA																	
	2.00		SS 1	40	22															
DENSE CLAYEY FINE TO MEDIUM SAND, BROWN (SC)	2.0	[Graphic Log]	SS 2	30																
	3.0		SS 3	40	30															
	4.00		PA																	
	4.0		SS 4	40	38															
VERY STIFF FINE TO MEDIUM SANDY CLAY, BROWN (CL/SC)	5.00	[Graphic Log]	PA																	
	5.0		SS 5	40	25															
	6.0		PA																	
MEDIUM DENSE TO DENSE CLAYEY FINE TO MEDIUM SAND, BROWN (SC)	6.0	[Graphic Log]	SS 6	40																
	7.0		PA																	
	8.0		SS 7	35	24															
	9.0		WO																	
	10.0		SS 8	40	30															
VERY STIFF FINE SANDY CLAY, GREY (SC/SC)	10.50	[Graphic Log]	WO																	
	11.0		SS 9	40	49															
DENSE CLAYEY FINE TO MEDIUM SAND, BROWN (SC)	11.80	[Graphic Log]	WO																	
	12.0		SS 10	40	27															
DENSE CLAYEY FINE TO MEDIUM SAND, BROWN (SC)	13.0	[Graphic Log]	SS 11	40	42															
	13.50		WO																	
DENSE SILTY FINE TO MEDIUM SAND, GREY, BROWN (SM)	14.0	[Graphic Log]	SS 12	35	33															
	14.50		WO																	
VERY STIFF SANDY CLAY, GREY, BROWN (CL)	15.0	[Graphic Log]	SS 13	35	27															
	16.0		WO																	
DENSE TO VERY DENSE CLAYEY FINE SAND, YELLOWISH BROWN (SC)	16.50	[Graphic Log]	SS 14	40	30															
	17.0		WO																	
	18.0		SS 15	40	53															
END OF BORING	19.0	[Graphic Log]	WO																	
	19.50		SS 16	-	50/0*															

PA = POWER AUGERING    HA = HAND AUGERING    WO = WASH OUT    ST = SHELBY TUBE    SS = SPLIT SPOON  
 PARTY CHIEF : EAYANK    MADE BY : DUSSADEE C.    GEOLOGIST : PANYAI    FILE : CHANG-2    DISK : 9 CHIANG MAI



BORING LOG					BORING NO. : BH-3		ELEVATION (m) : -													
PROJECT : เรือนจำจังหวัดเชียงใหม่ (แห่งใหม่)					DEPTH (m) : 18.50		GWL (m) : -2.45													
LOCATION : ต.ช้างเผือก อ.เมือง จ.เชียงใหม่					COORD. N : -		DATE STARTED : 03/11/96													
					E : -		DATE FINISHED : 03/11/96													
SOIL DESCRIPTION	DEPTH (m)	GRAPHIC LOG	METHOD	SAMPLE NO	RECOVERY (cm)	SPT-N VALUE (blows/ft)				NATURAL MOISTURE CONTENT (%)				Su (t/sq.m)				TOTAL UNIT WEIGHT (t/cu.m)		
						10	20	30	40	20	40	60	80	1	2	3	4	1.6	1.8	2.0
DENSE CLAYEY SAND, BROWN (SC)	1.0		PA																	
	1.50		SS	1	40															
VERY STIFF FINE TO MEDIUM SANDY CLAY, BROWN (CH)	2.00		SS	2	40															
	2.00		SS	3	40															
DENSE CLAYEY FINE TO MEDIUM SAND, BROWN (SC)	3.00		PA																	
	4.00		SS	4	40															
	4.00		WO																	
VERY STIFF FINE SANDY CLAY, BROWN (CL/SC)	5.00		SS	5	40															
	5.00		WO																	
MEDIUM DENSE CLAYEY SAND, BROWN (SC)	5.80		SS	6	35															
	6.00		WO																	
HARD FINE TO MEDIUM SANDY CLAY, BROWN (CH)	7.00		SS	7	35															
	7.00		WO																	
MEDIUM DENSE CLAYEY FINE TO MEDIUM SAND, GREY (SC/CL)	8.80		SS	8	45															
	8.80		WO																	
VERY DENSE SILTY FINE TO MEDIUM SAND, GREY (SM)	10.00		SS	9	45															
	10.00		WO																	
	11.00		SS	10	40															
	12.00		WO																	
MEDIUM DENSE TO DENSE CLAYEY FINE SAND, GREY, BROWN (SC,SC/CL)	14.80		SS	11	40															
	13.00		WO																	
	14.00		SS	12	35															
	14.80		WO																	
STIFF CLAY WITH SAND, GREY (CH)	16.50		SS	13	40															
	16.00		WO																	
	17.00		SS	14	15															
	17.00		WO																	
VERY DENSE SILTY SAND WITH GRAVEL, BROWN, GREY (SM)	18.50		SS	15	-															
	18.00		WO																	
END OF BORING	ROCK		SS	16	-															
			WO																	

PA = POWER AUGERING    HA = HAND AUGERING    WO = WASH OUT    ST = SHELBY TUBE    SS = SPLIT SPOON  
 PARTY CHIEF: SAYAN K.    MADE BY: DUSSADEE C.    GEOLOGIST: PANYAI    FILE: CHANG-3    DISK: 9 CHIANG MAI

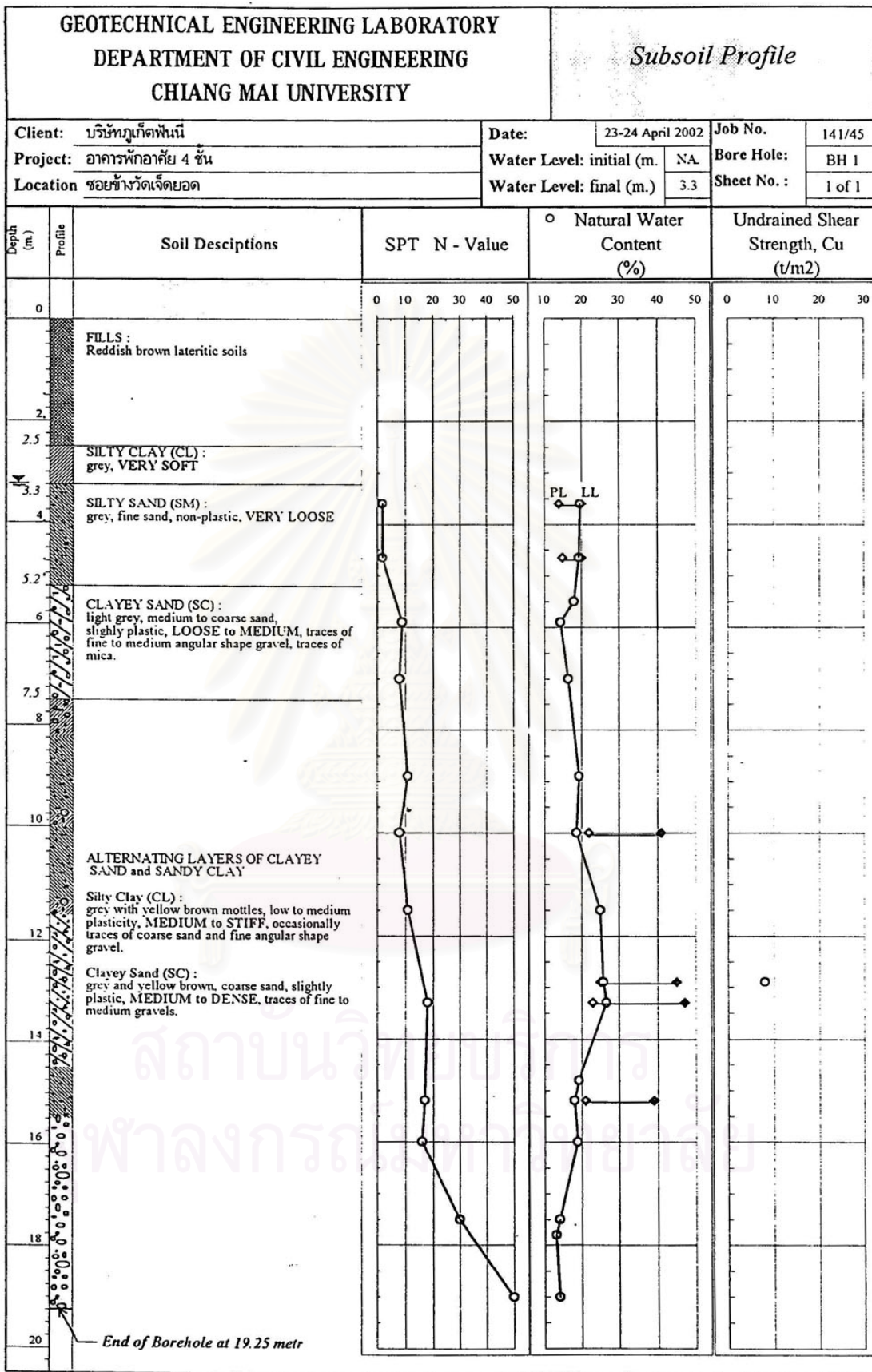


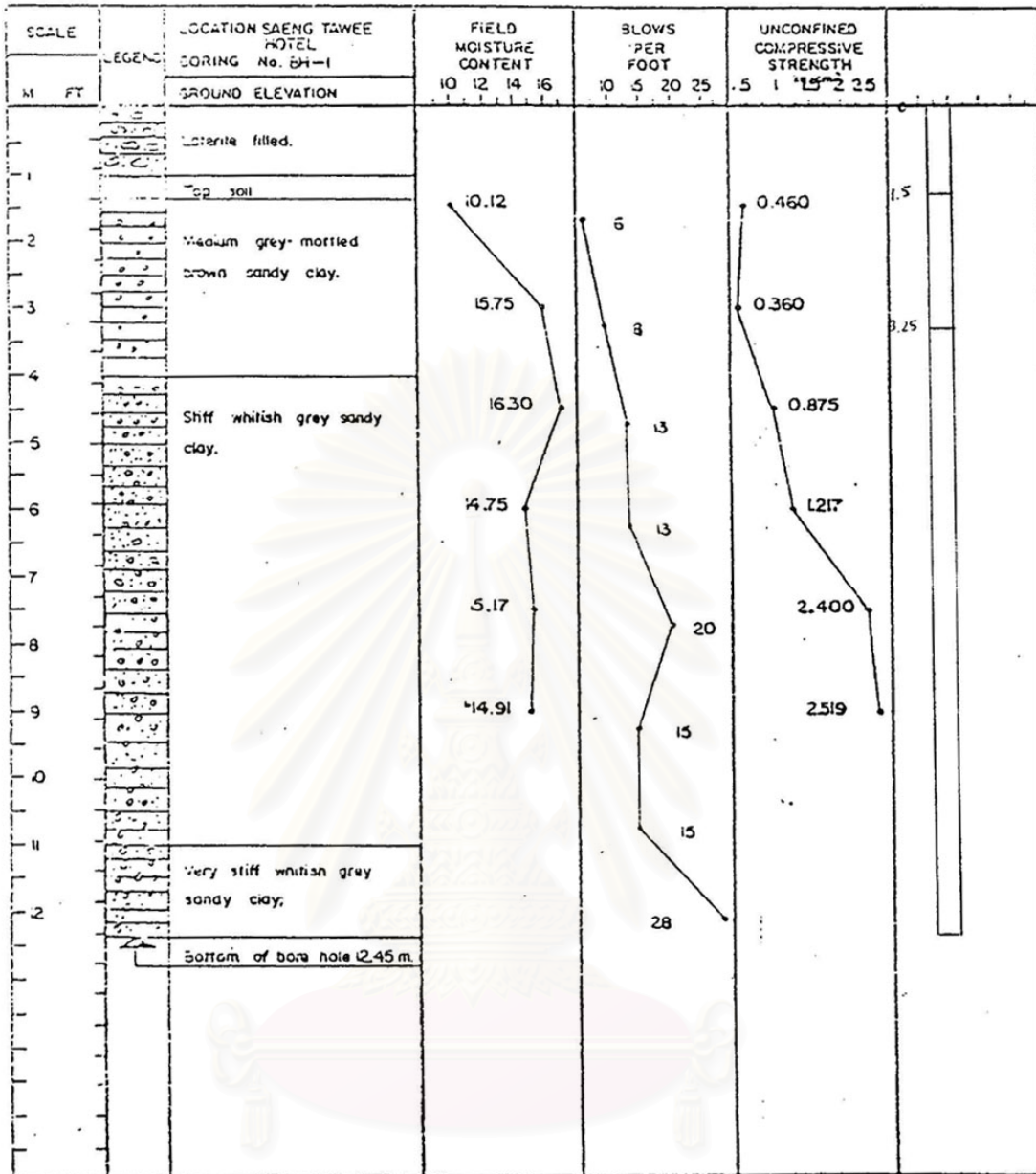
BORING LOG					BORING NO. : BH-5		ELEVATION (m) : -														
PROJECT : เรือนำจังหวัดเชียงใหม่ (แห่งใหม่)					DEPTH (m) : 16.23		GWL (m) : -														
LOCATION : ต.ช้างเผือก อ.เมือง จ.เชียงใหม่					COORD. N : -		DATE STARTED : 04/11/96														
					E : -		DATE FINISHED : 05/11/96														
SOIL DESCRIPTION	DEPTH (m)	GRAPHIC LOG	METHOD	SAMPLE NO	RECOVERY (cm)	SPT-N VALUE (blows/ft.)				NATURAL MOISTURE CONTENT (%)				Su (t/sq.m)				TOTAL UNIT WEIGHT (t/cu.m)			
						10	20	30	40	20	40	60	80	1	2	3	4	1.6	1.8	2.0	
GARBAGE	1.0	[Redacted]	PA																		
	2.0																				
	3.0																				
	4.0																				
	5.0																				
	6.00																				
MEDIUM DENSE CLAYEY FINE TO MEDIUM SAND, GREY (SC)	7.00		SS	1	40				28												
VERY STIFF CLAY, BROWN (CH)	8.00		WO																		
	8.80		SS	2	40				28												
DENSE CLAYEY FINE TO MEDIUM SAND, GREY (SC)	9.00		WO																		
	10.00		SS	3	40				30												
DENSE TO VERY DENSE SILTY SAND WITH GRAVEL, GREY (SM,SP-SM)	11.00		WO																		
			SS	4	35				45												
	12.00		WO																		
			SS	5	35				31												
	13.00		WO																		
			SS	6	40				48												
	14.00		WO																		
			SS	7	30				50/8*												
15.00		WO																			
		SS	8	-				50/1*													
16.00		WO																			
16.23		SS																			
END OF BORING																					

PA = POWER AUGERING      HA = HAND AUGERING      WO = WASH OUT      ST = SHELBY TUBE      SS = SPLIT SPOON  
 PARTY CHIEF : SAYAN K      MADE BY : DUSSADEE C      GEOLOGIST : PANYA I      FILE : CHANG-5      DISK : 9/1 CHIANG MAI

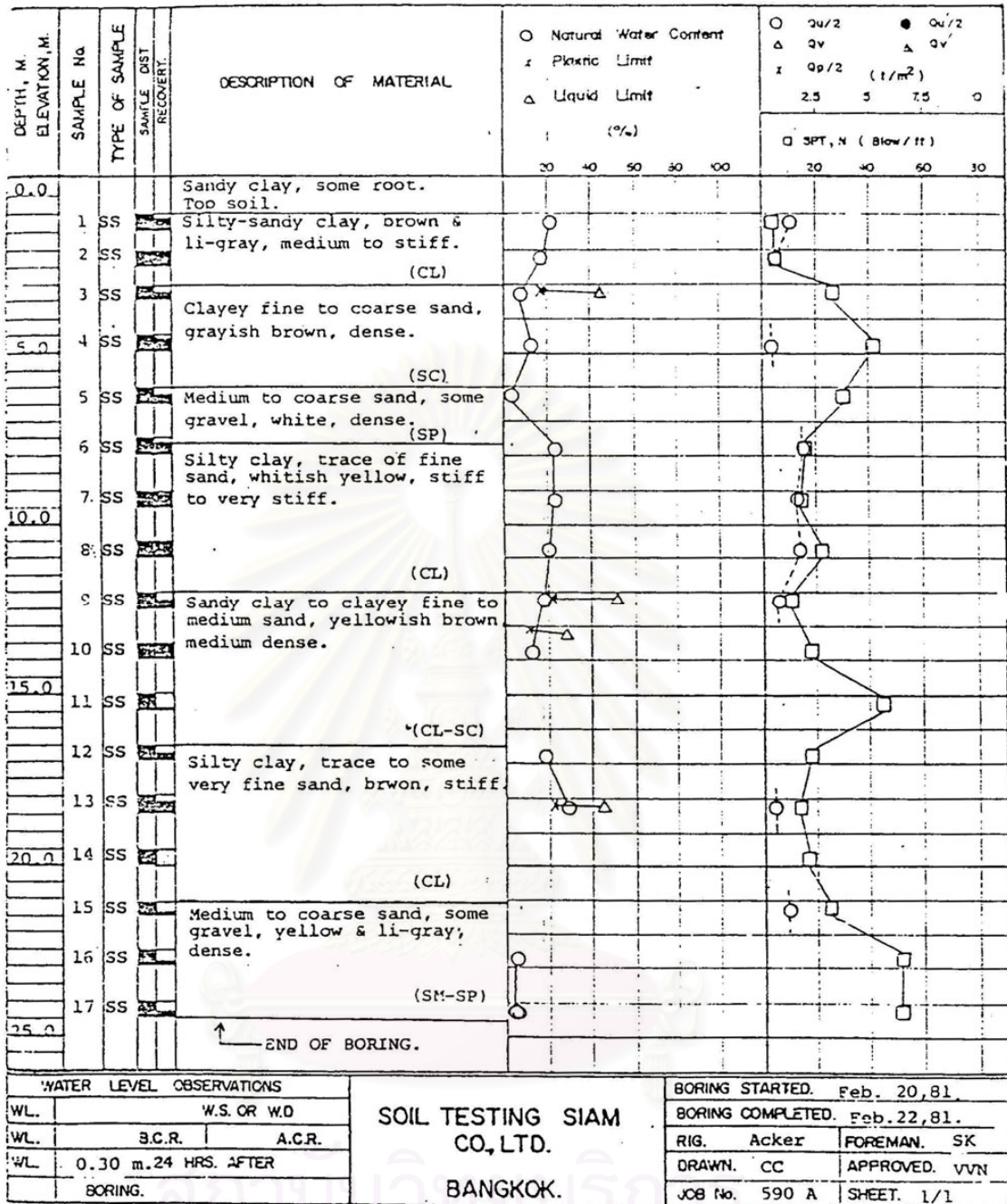
BORING LOG				BORING NO. :	BH-7	ELEVATION (m) :	-											
PROJECT : เรือนำจังหวัดเชียงใหม่ (แห่งใหม่)				DEPTH (m) :	16.50	GWL (m) :	-1.10											
LOCATION : ค.ช้างศึก อ.เมือง จ.เชียงใหม่				COORD N :	-	DATE STARTED :	05/11/96											
				E :	-	DATE FINISHED :	05/11/96											
SOIL DESCRIPTION	DEPTH (m)	GRAPHIC LOG	METHOD	SAMPLE NO	RECOVERY (cm)	SPT-N VALUE		NATURAL MOISTURE CONTENT (%)				Su (t/sqm)				TOTAL UNIT WEIGHT (t/cum)		
						10	20	30	40	20	40	60	80	1	2	3	4	1.6
MEDIUM FINE TO MEDIUM SANDY CLAY, GREY, BROWN (CL/SC)	1.0		PA															
	1.50		SS	1	40	5												
	2.0		SS	2	30	15												
			SS	3	35													
	3.0		PA															
			SS	4	40													
	4.0		PA															
			SS	5	40	33												
	5.0		PA															
			SS	6	35													
MEDIUM DENSE TO VERY DENSE CLAYEY FINE TO MEDIUM SAND, GREY (SC,SC/CL)	6.0		PA															
			SS	7	40	17												
	7.0		WO															
	8.0		SS	8	40	17												
			WO															
	9.0		SS	9	40													
	10.0		WO															
	10.50		SS	10	40	11												
			WO															
STIFF TO VERY STIFF CLAY, GREY, BROWN (CH)	12.0		SS	11	45	18												
	13.0		WO															
	13.50		SS	12	35	45												
	14.0		WO															
DENSE TO VERY DENSE SILTY FINE TO MEDIUM SAND, GREY, BROWN (SM)	15.0		SS	13	25	45												
	16.0		WO															
END OF BORING	16.50		SS	14	-	50/0*												

PA = POWER AUGERING    HA = HAND AUGERING    WO = WASH OUT    ST = SHELBY TUBE    SS = SPLIT SPOON  
 PARTY CHIEF: SAYAN K    MADE BY: DUSSADEE C    GEOLOGIST: PANYAI    FILE: CHANG-7    DISK: 9/1 CHIANG MAI

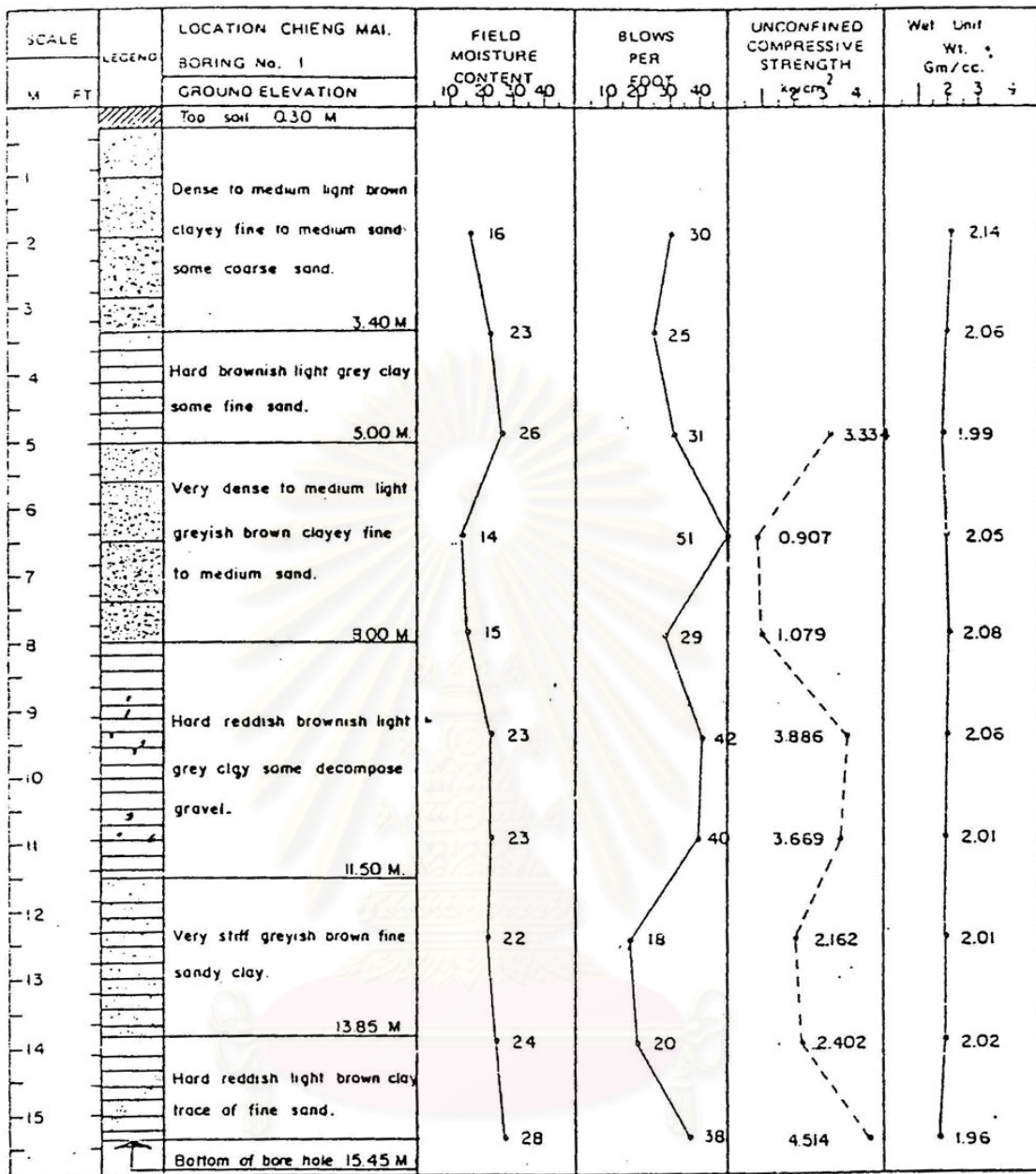




สถาบันวิทยบริการ  
จุฬาลงกรณ์มหาวิทยาลัย

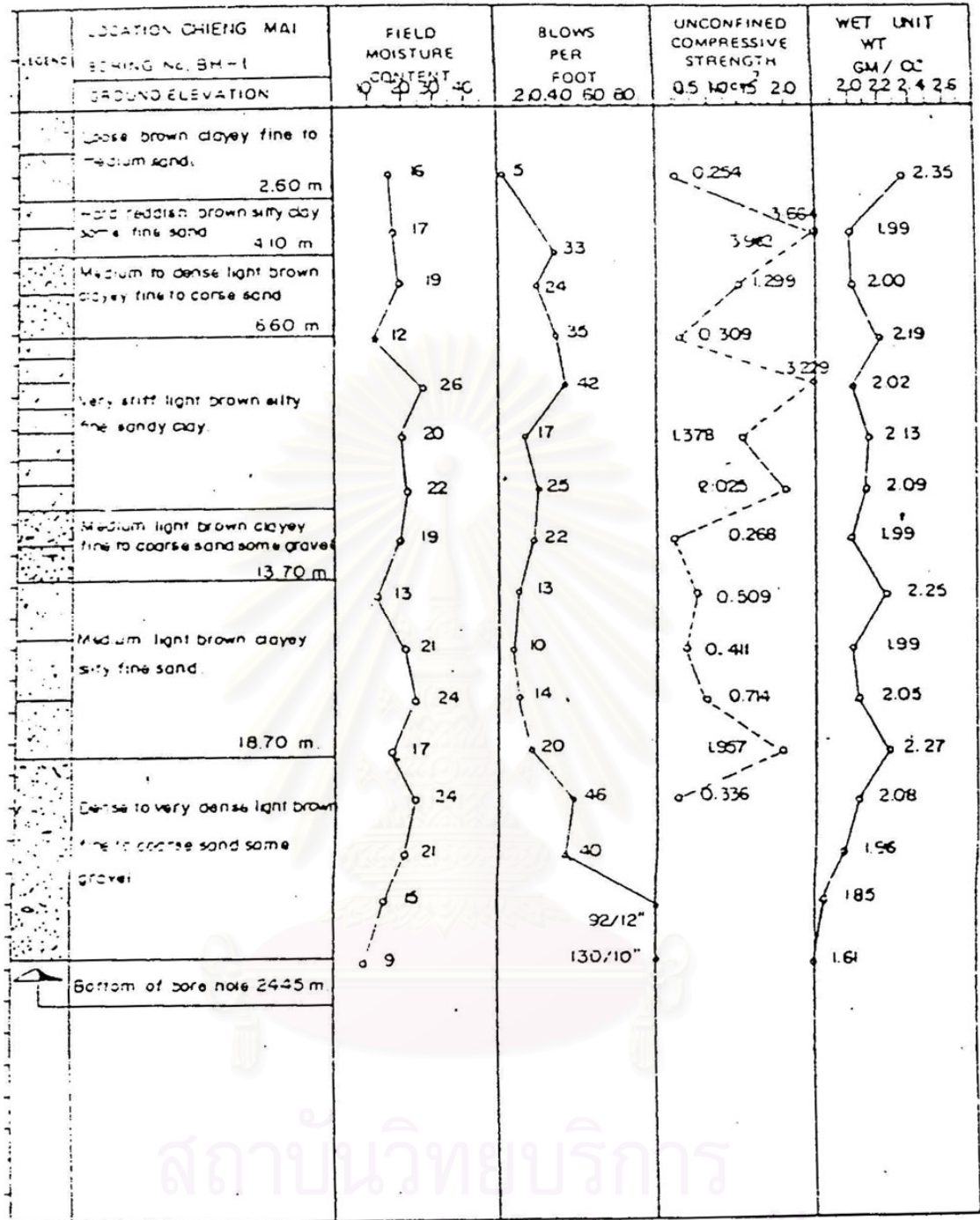


จุฬาลงกรณ์มหาวิทยาลัย

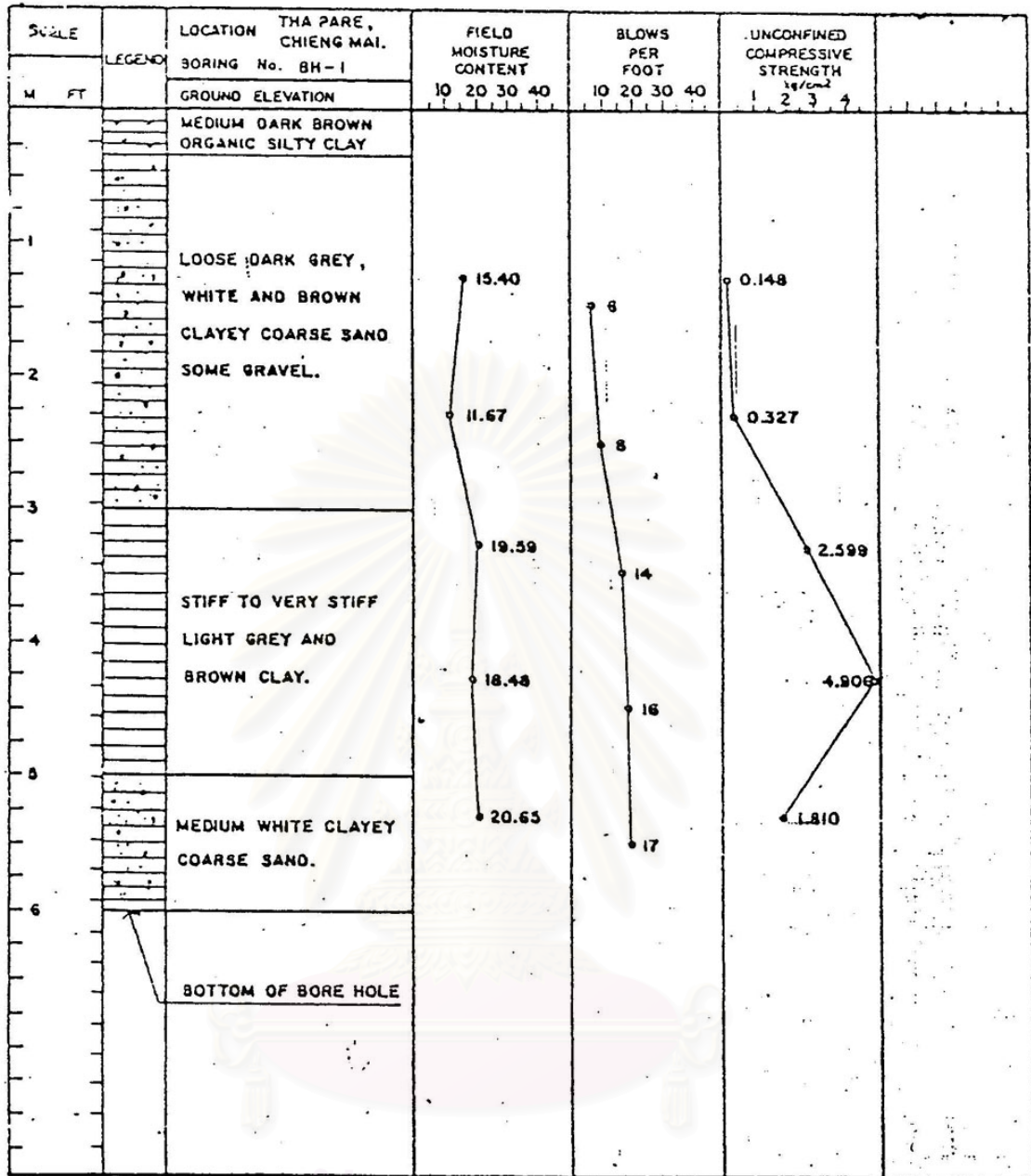


สถาบันวิทยบริการ  
จุฬาลงกรณ์มหาวิทยาลัย

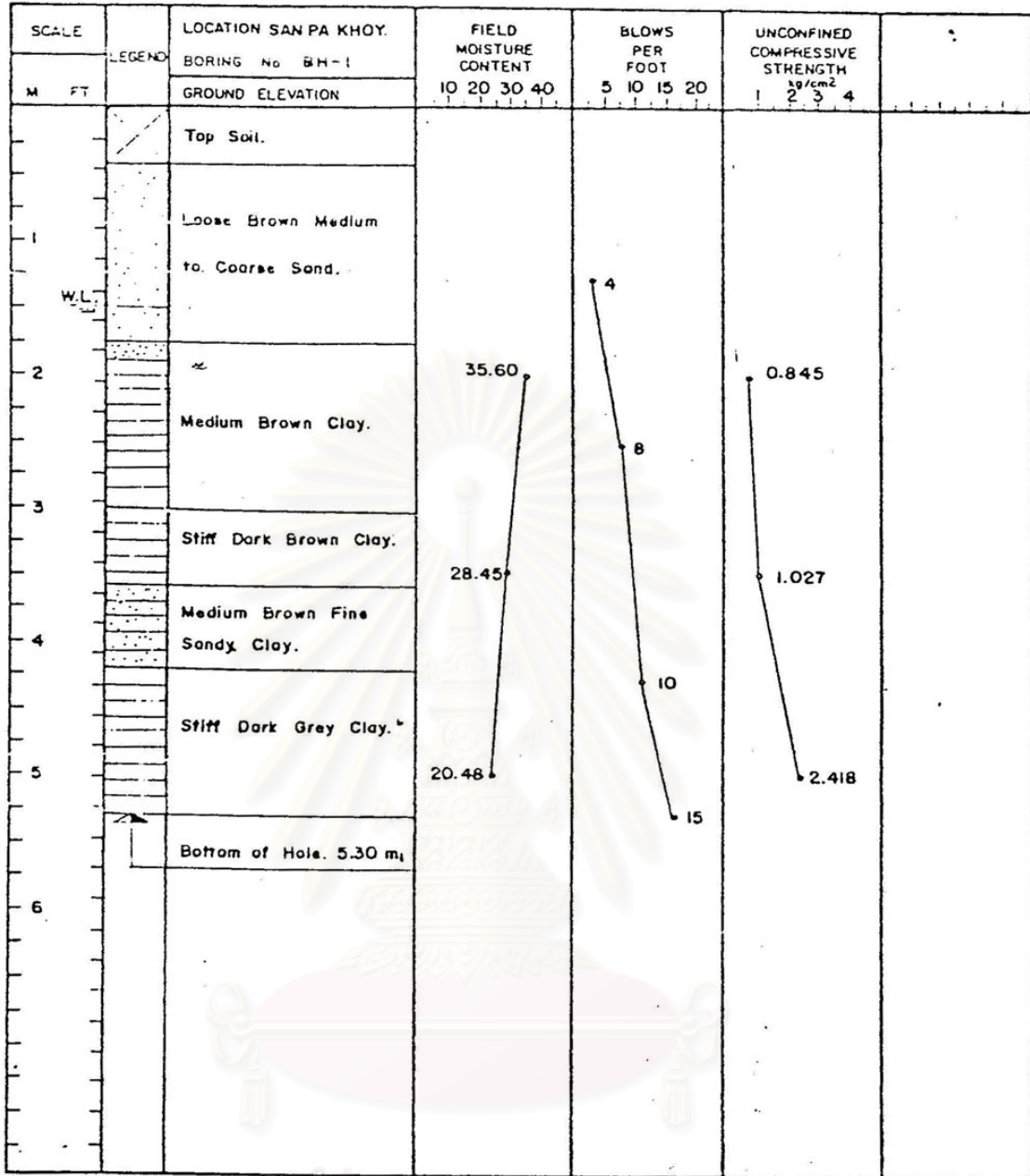




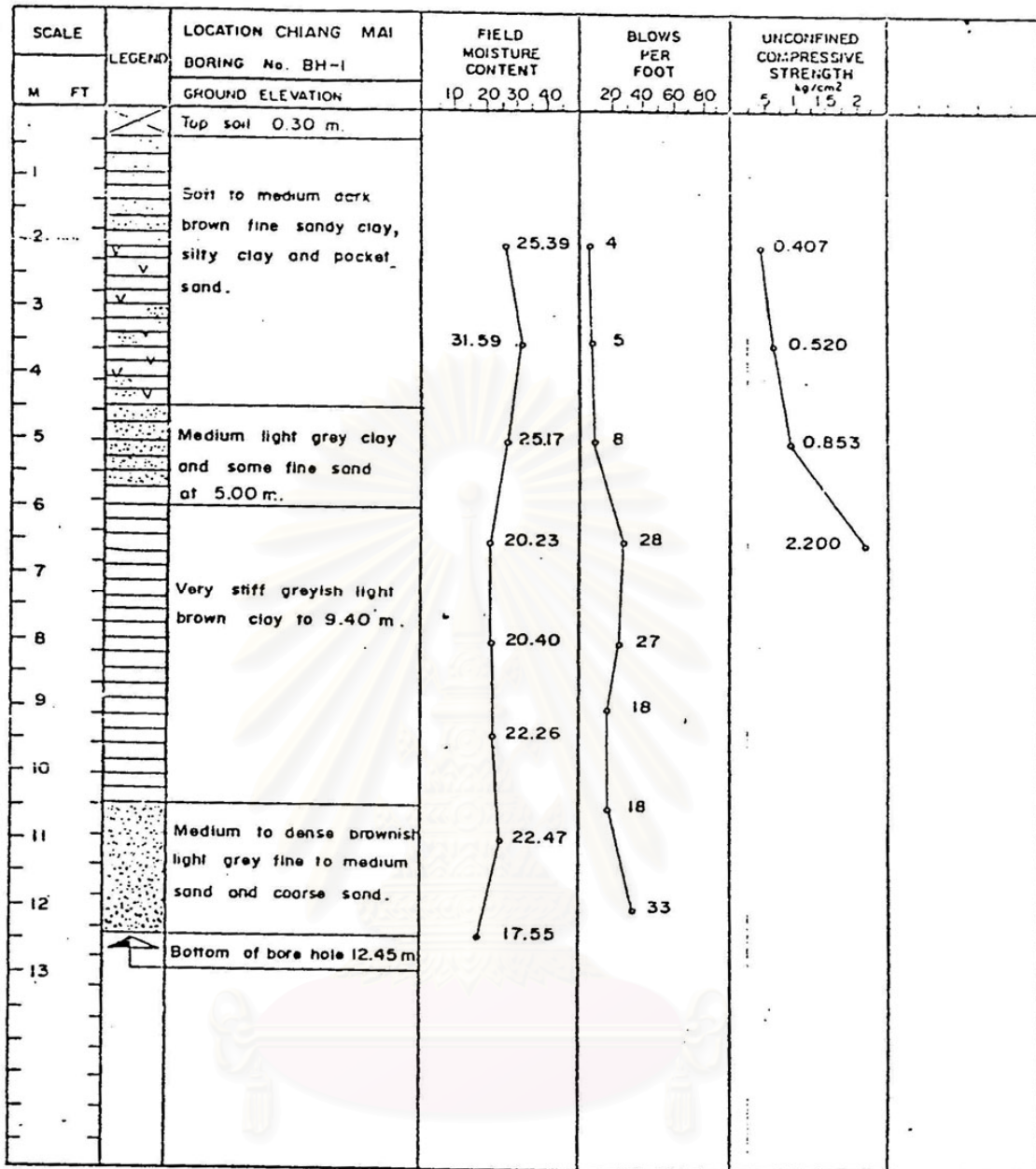
สถาบันวิทยบริการ  
จุฬาลงกรณ์มหาวิทยาลัย



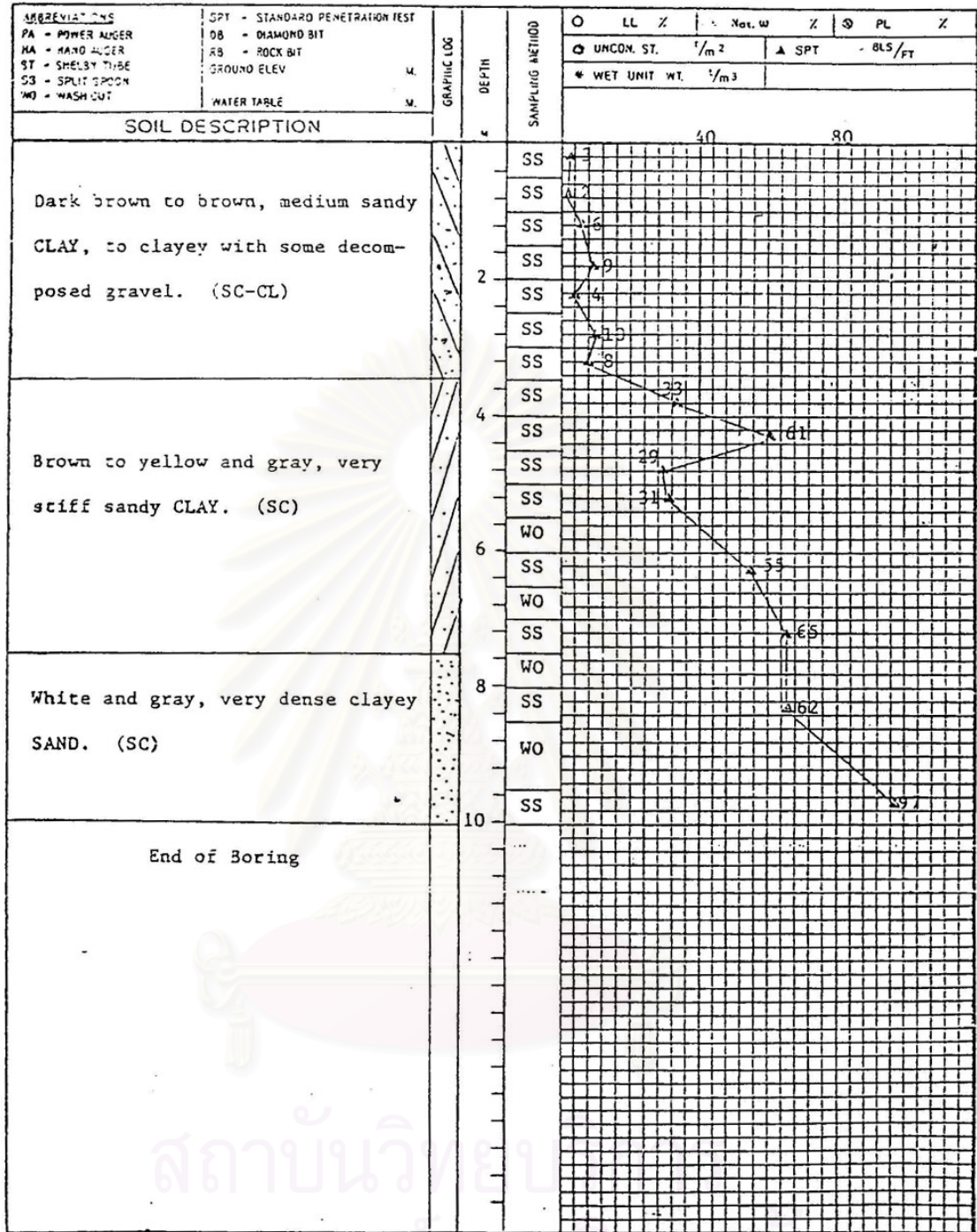
สถาบันวิทยบริการ  
จุฬาลงกรณ์มหาวิทยาลัย



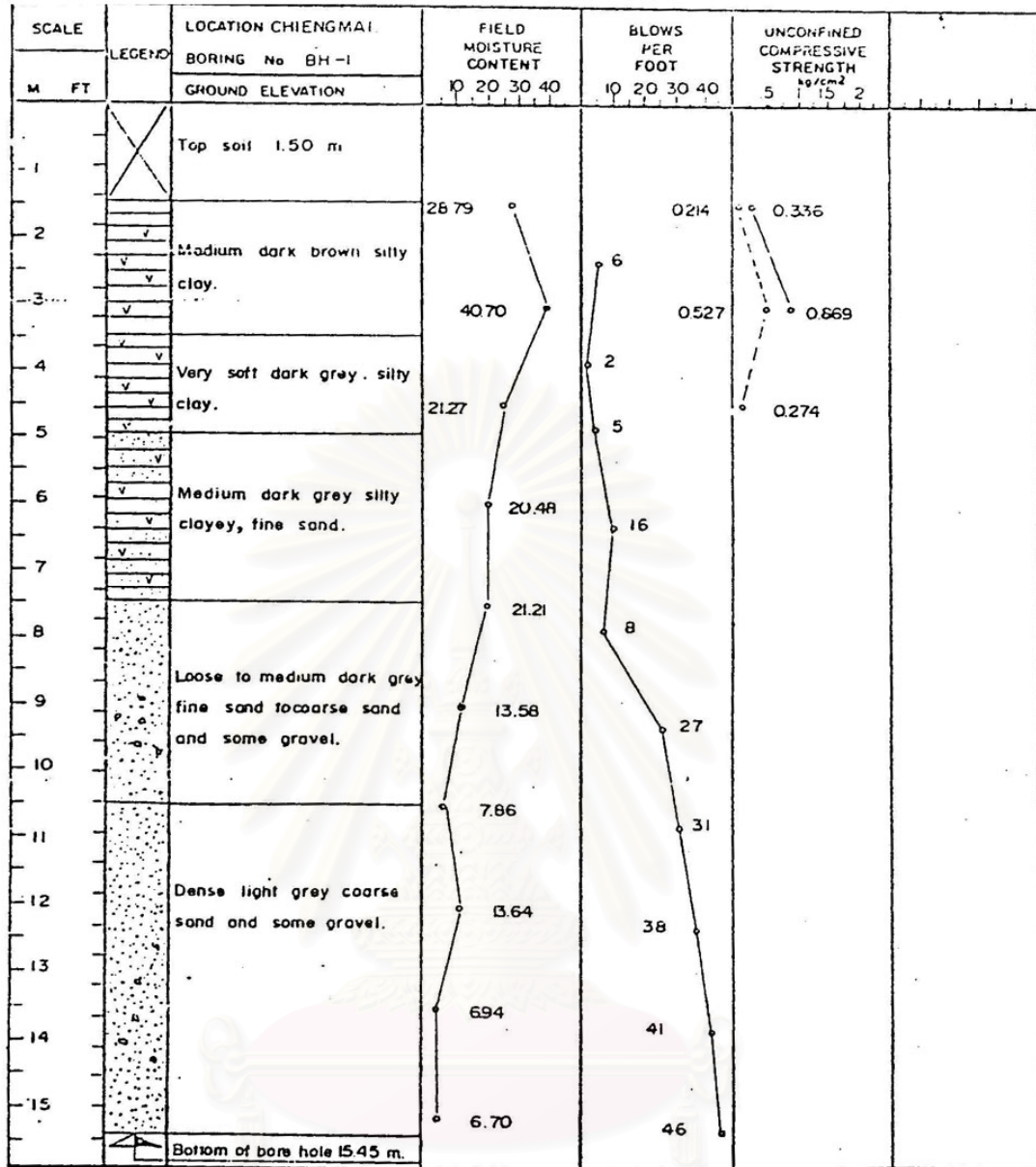
สถาบันวิทยบริการ  
จุฬาลงกรณ์มหาวิทยาลัย



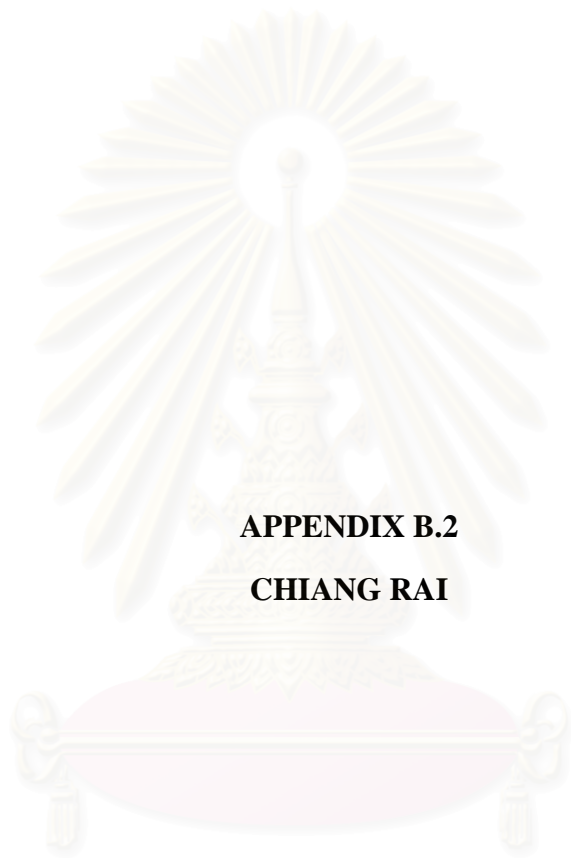
สถาบันวิทยบริการ  
 จุฬาลงกรณ์มหาวิทยาลัย



สถาบันวิจัย  
จุฬาลงกรณ์มหาวิทยาลัย



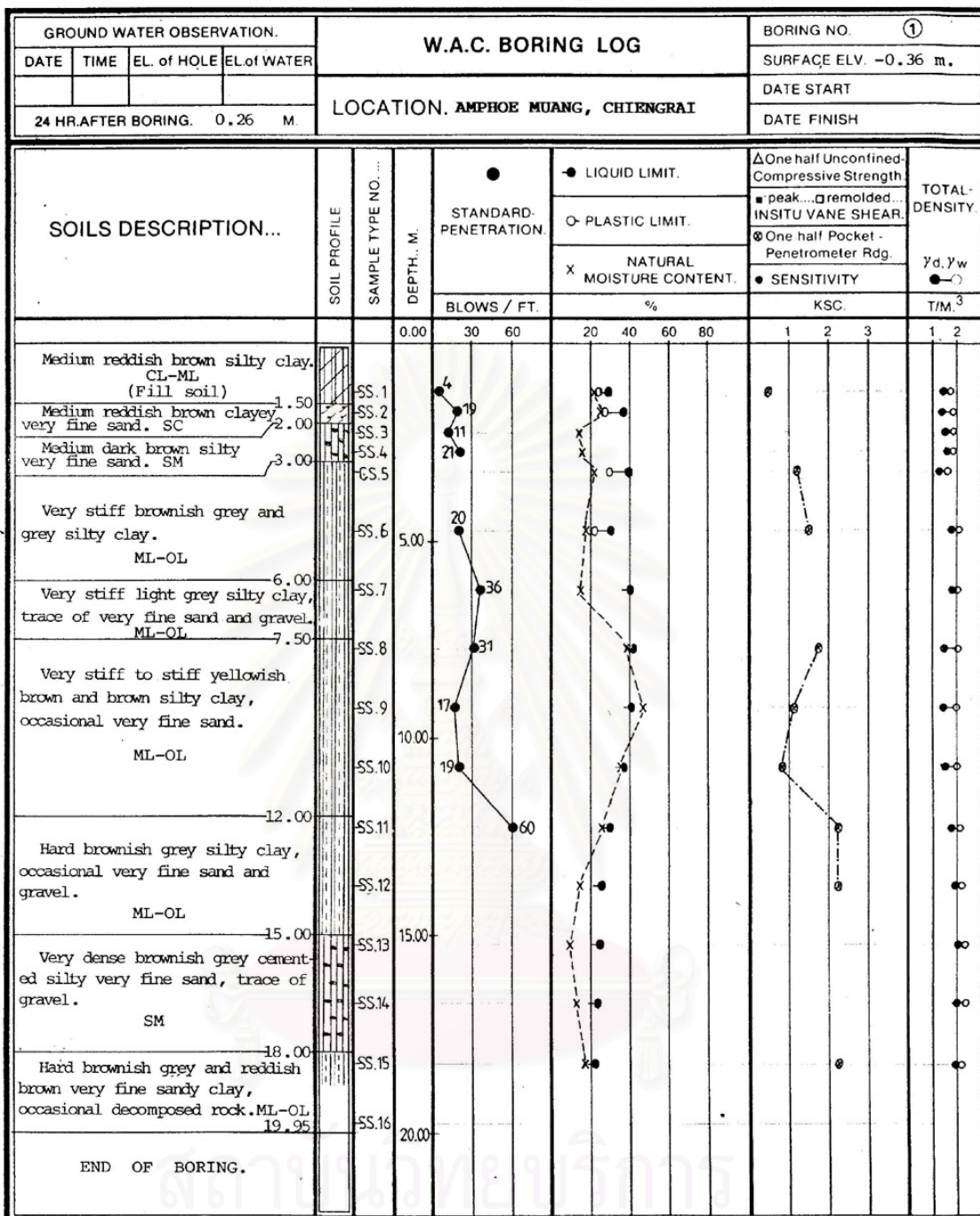
สถาบันวิทยบริการ  
จุฬาลงกรณ์มหาวิทยาลัย



**APPENDIX B.2**

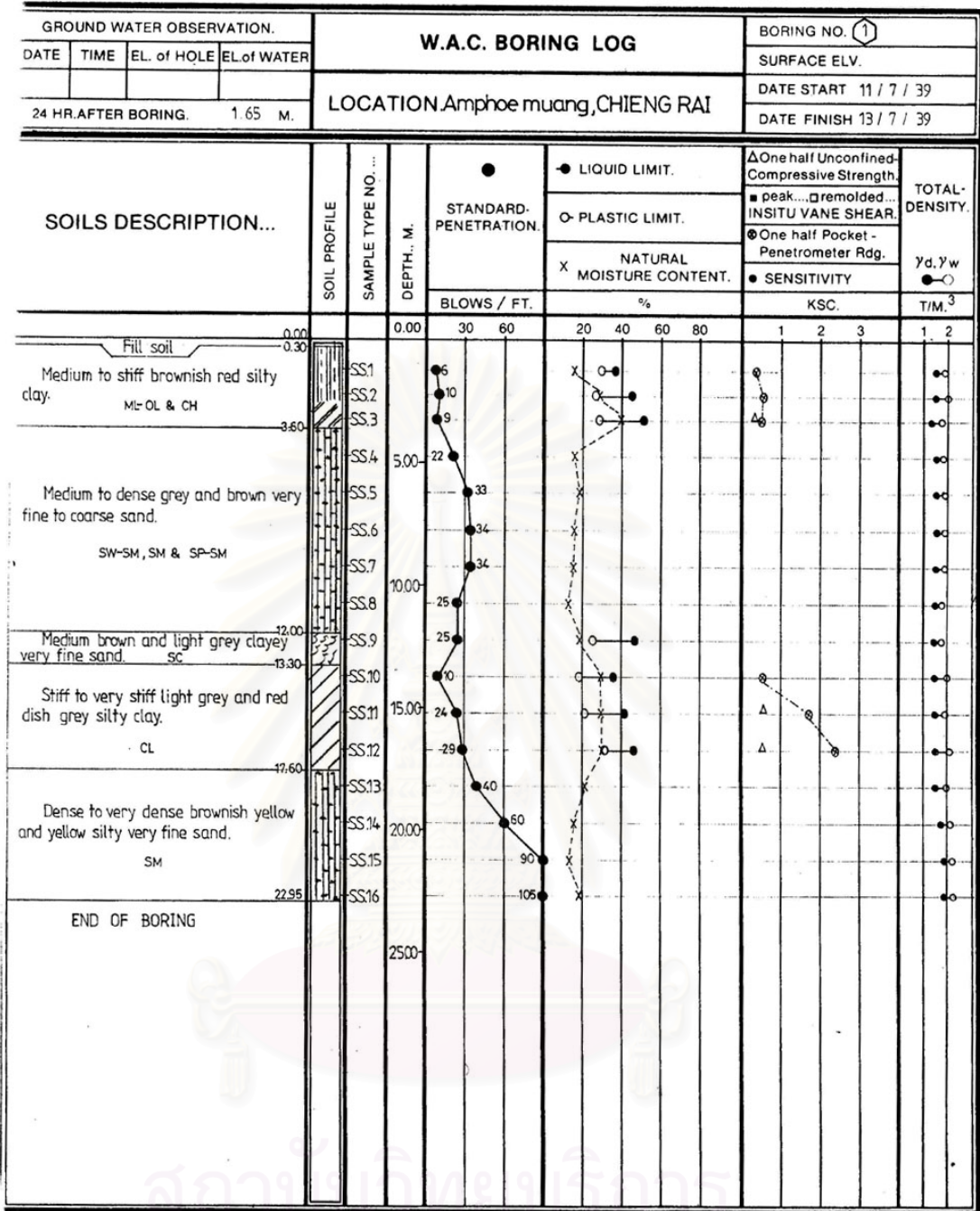
**CHIANG RAI**

สถาบันวิทยบริการ  
จุฬาลงกรณ์มหาวิทยาลัย

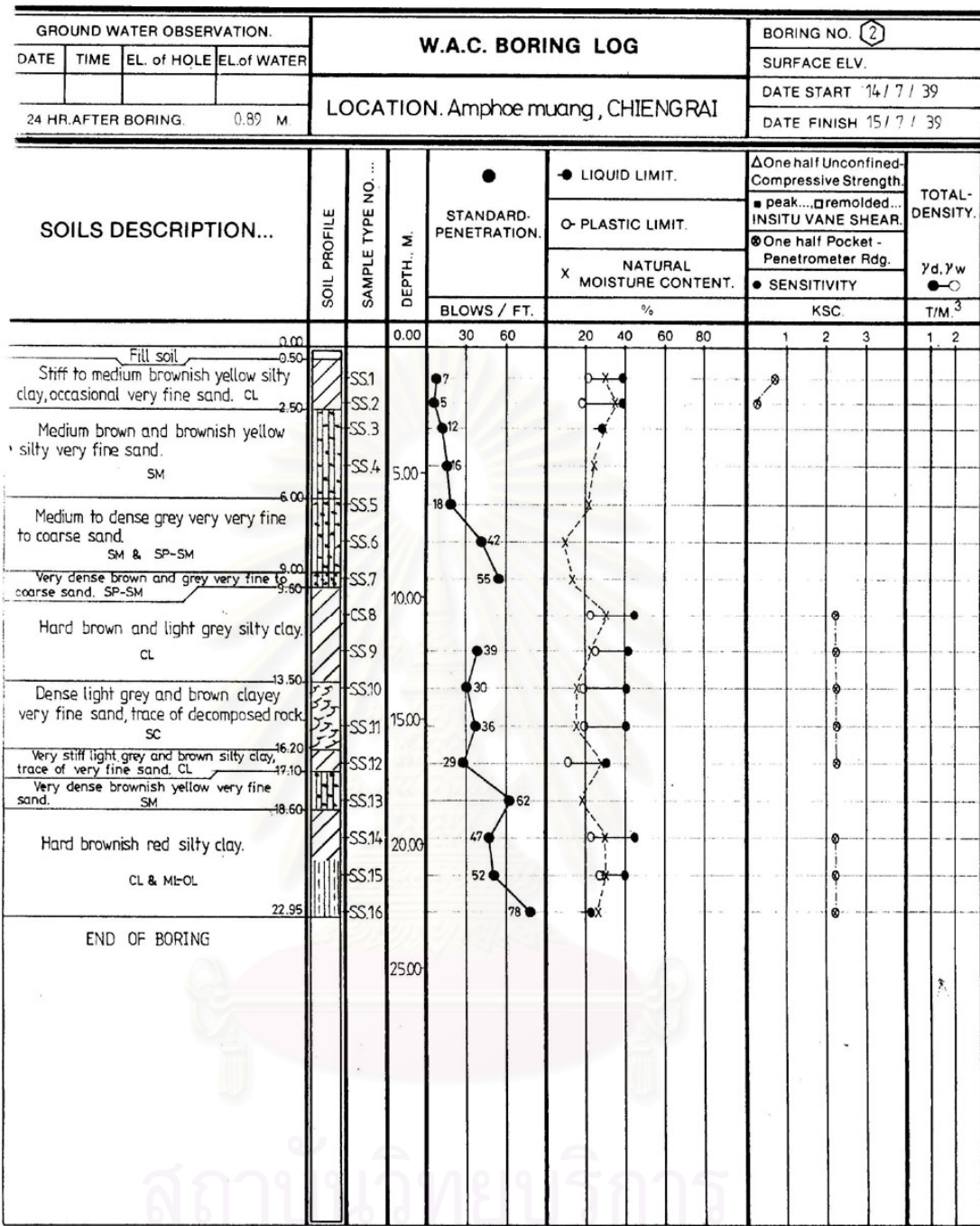


จุฬาลงกรณ์มหาวิทยาลัย





จุฬาลงกรณ์มหาวิทยาลัย



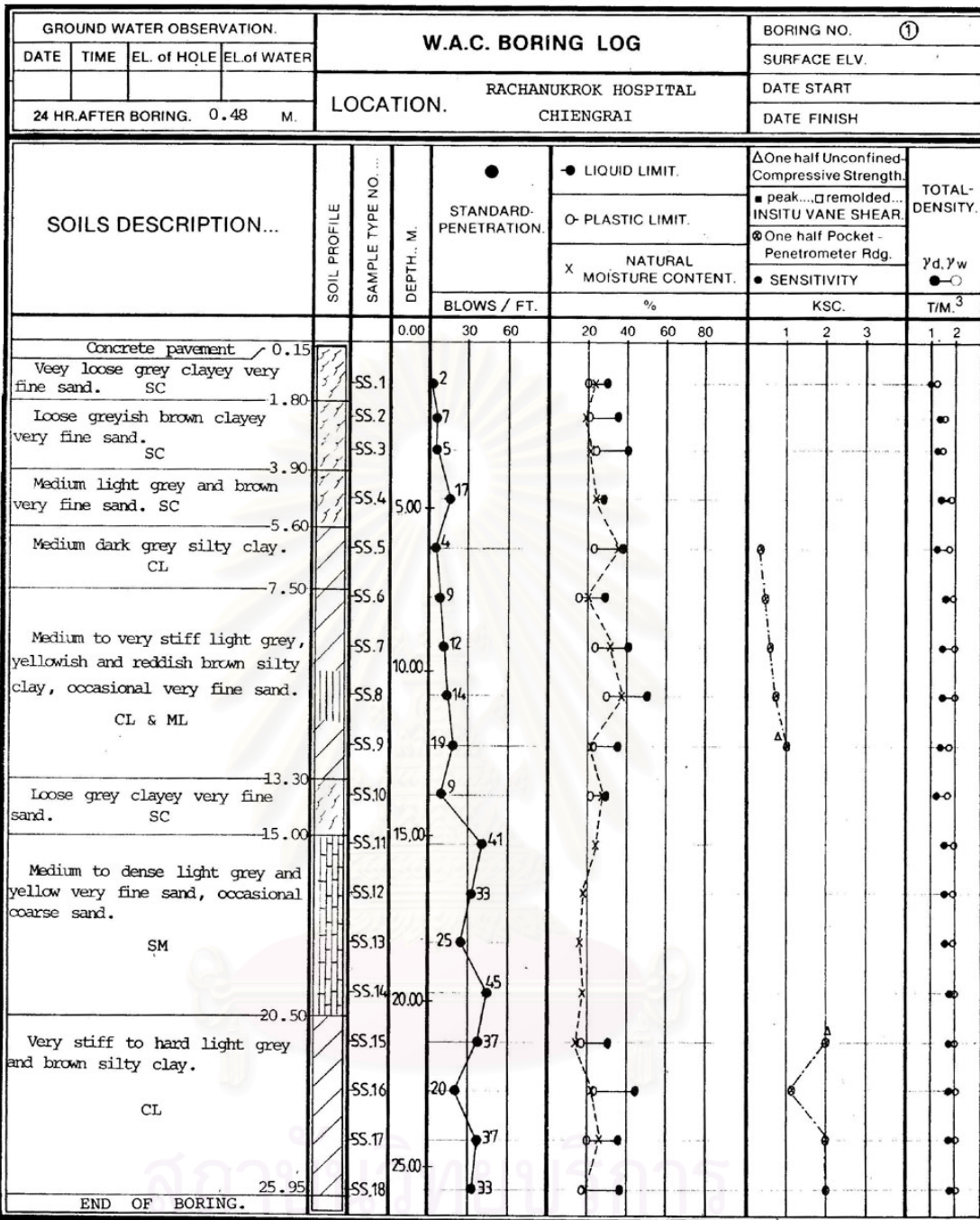
จุฬาลงกรณ์มหาวิทยาลัย

GROUND WATER OBSERVATION.				W.A.C. BORING LOG				BORING NO. 1									
DATE	TIME	EL. of HOLE	EL. of WATER	LOCATION. CHAINGRAI PRACHANUKROK CHAINGRAI				SURFACE ELV.									
								DATE START									
24 HR. AFTER BORING. 1.75 M.								DATE FINISH 31-OCT-43									
SOILS DESCRIPTION...								SOIL PROFILE		SAMPLE TYPE NO. ....		DEPTH... M.		STANDARD PENETRATION		LIQUID LIMIT.	
				BLOWS / FT.		PLASTIC LIMIT.								INSITU VANE SHEAR.		γ <sub>d</sub> , γ <sub>w</sub>	
								NATURAL MOISTURE CONTENT.		KSC.		T/M. <sup>3</sup>					
								%									
Filled Soil				0.35													
Medium dark brown silty very fine sand.				1.60		SS 1		11, 6, 7, 10, 12		20, 40, 60, 80		1, 2, 3		1, 2			
SM																	
Medium to stiff dark brown and reddish brown silty clay, trace of very fine sand.				3.60		SS 5		5									
ML-OL																	
Soft dark grey silty clay, trace of very fine sand.				7.00		SS 7		4									
ML-OL																	
Very stiff grey silty clay, trace of very fine sand.				8.90		SS 8		29									
ML-OL																	
Very stiff grey silty clay, trace of very fine sand.				12.00		SS 9		38									
ML-OL																	
Medium to very dense light grey silty very fine to fine sand, occasional coarse sand and pea gravel.				19.95		SS 10		53									
SM & SP-SM																	
Dense to very dense yellowish brown silty very fine sand, occasional pea gravel.						SS 11		13									
SM																	
						SS 12		46									
						SS 13		53									
						SS 14		71									
						SS 15		88									
						SS 16		77									
END OF BORING.																	

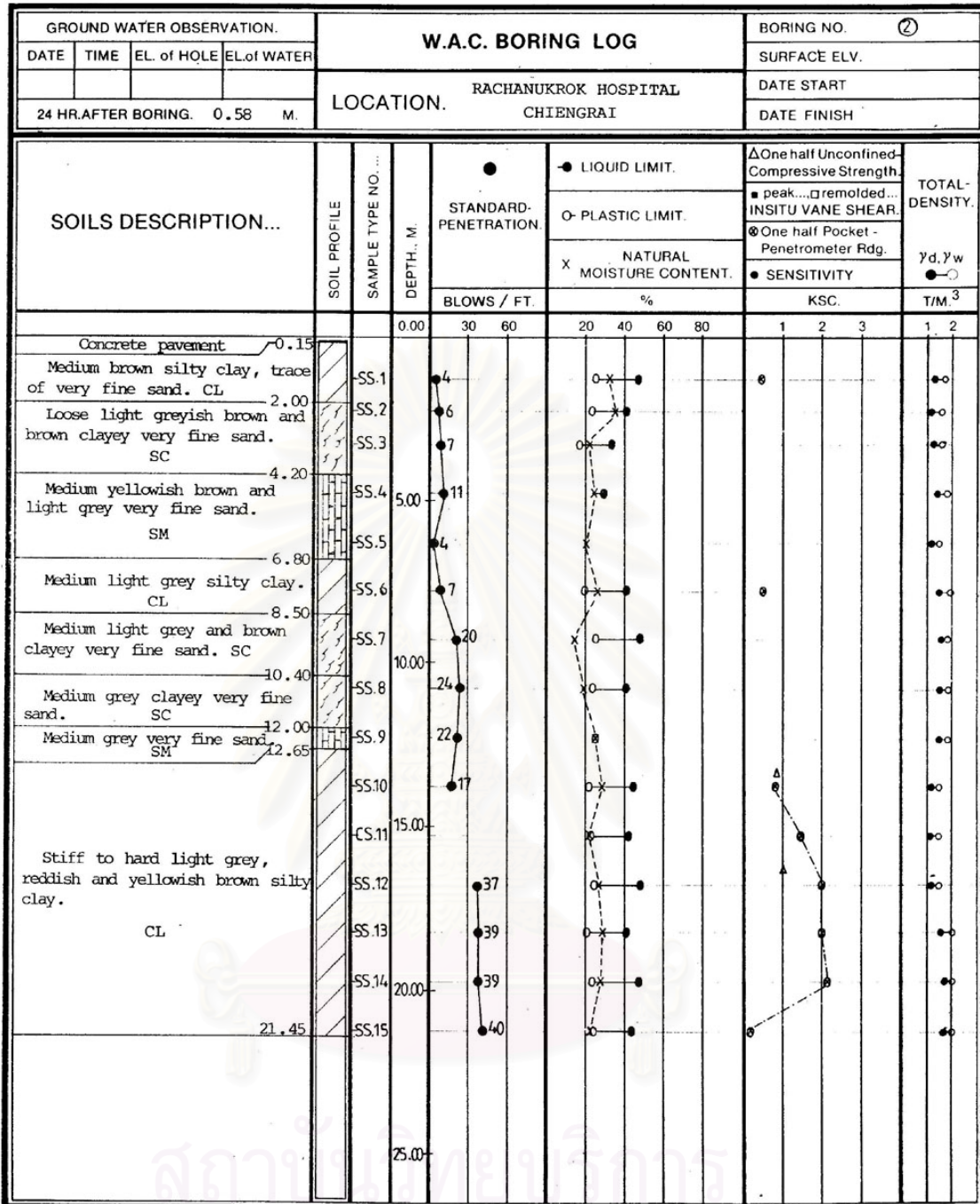
จุฬาลงกรณ์มหาวิทยาลัย

GROUND WATER OBSERVATION.				W.A.C. BORING LOG				BORING NO. 2	
DATE	TIME	EL. of HOLE	EL. of WATER	LOCATION. CHAINGRAI PRACHANUROK CHAINGRAI				SURFACE ELV.	
								DATE START	
24 HR.AFTER BORING. 1.75 M.				SOILS DESCRIPTION...				TOTAL DENSITY.	
SOIL PROFILE		SAMPLE TYPE NO. ...						DEPTH...M.	
								O- PLASTIC LIMIT.	
								X NATURAL MOISTURE CONTENT.	
								● SENSITIVITY	
				BLOWS / FT.		%		KSC.	
				0.00 30 60		20 40 60 80		1 2 3	
								1 2	
Filled Soil		0.35							
Soft to stiff light grey and brown silty clay, trace of very fine sand.		SS 1		4		●		●	
ML-OL		5.10		11		●		●	
Loose dark grey silty very fine sand.		SS 6		10		●		●	
SM & SP		11.50		17		●		●	
Medium to dense light grey very fine to fine sand, occasional coarse sand.		SS 10		52		●		●	
SM		19.95		66		●		●	
END OF BORING.				20.00					

สถาบันวิทยบริการ  
จุฬาลงกรณ์มหาวิทยาลัย



จุฬาลงกรณ์มหาวิทยาลัย



จุฬาลงกรณ์มหาวิทยาลัย







K. ENGINEERING CONSULTANTS CO., LTD.																	
BORING LOG					BORING NO. BH-1		GROUND ELEV.(m) -0.13										
PROJECT <u>แผนตนายทหารชั้นประทวนฯ ๘๐ ครอบคลุม</u>					DEPTH (m.) 9.28		OBSERVED WL (m) -2.80										
LOCATION <u>อ.เมือง เชียงราย</u>					COORD.		DATE STARTED 14/6/86										
							DATE FINISHED 14/6/86										
SOIL DESCRIPTION	DEPTH (m.)	GRAPHIC LOG	METHOD	SAMPLING & RECOVERY	SPT - N (blows/ft)				PL W <sub>n</sub> LL (%)			Su (t/m <sup>2</sup> )				γ <sub>t</sub> (t/m <sup>3</sup> )	
					10	20	30	40	20	40	60	80	5	10	15	20	1.6
LATERITIC CLAY (FILL), REDDISH BROWN	1.00		PA														
MEDIUM SILTY CLAY, BROWN (CL)	2.00		SS 1	X	8												
MEDIUM DENSE FINE TO COARSE SAND, BROWN (SP-SM)	3.00		PA														
	3.50		SS 2	X	11												
	4.50		WO														
	5.00		SS 3	X	15												
7.00	6.00		WO														
	6.50		SS 4	X	15												
HARD CLAY, DARK BROWN AND GREY (CL)	8.00		WO														
	8.50		SS 5	X	50/9"												
	9.00		WO														
9.28			SS	X	50/5"												
END OF BORING																	

สถานีวิทยุโทรทัศน์  
จุฬาลงกรณ์มหาวิทยาลัย





















SOIL DESCRIPTION		DEPTH (m.)	GRAPHIC LOG	METHOD	SAMPLING RECOVERY	SPT-N (blows/ft)	PL (%)	w (%)	LL (%)	Su (t/sq.m)				TOTAL UNIT WEIGHT (t/cu.m.)		
										1	2	3	4	1	2	
VERY SOFT SANDY CLAY TRACE GRAVEL, BROWN (CL)		1.00		PA	1	2	10	10	10							
LOOSE CLAYEY SAND WITH GRAVEL, BROWN (SC)		1.50		SS	2	9	10	10	10							
				SS	3	12	10	10	10							
				SS	4	6	10	10	10							
LOOSE AND MEDIUM DENSE CLAYEY SAND TRACE GRAVEL (SC)		4.50		FA	5	16	10	10	10							
				SS	6	19	10	10	10							
MEDIUM DENSE SILTY SAND, BROWN (SM)		5.20		WO	7	12	10	10	10							
				SS	8	17	10	10	10							
STIFF CLAY WITH SAND, BROWN (CL)		7.80		WO	9	5	10	10	10							
				SS	10	13	10	10	10							
				WO	11	13	10	10	10							
				SS	12	15	10	10	10							
MEDIUM DENSE CLAYEY FINE SAND, BROWN (SC)		8.60		WO	13	35	10	10	10							
SOFT CLAY, GREY (CL)		10.00		SS	14	44	10	10	10							
				WO	15	44	10	10	10							
				SS	16	47	10	10	10							
STIFF CLAY WITH SAND, GREY (CL)		12.80		WO	17		10	10	10							
				SS	18		10	10	10							
				WO	19		10	10	10							
DENSE SAND TRACE SILT AND GRAVEL, BROWN (SM)		16.95		SS	20		10	10	10							
END OF BORING																

**BORING LOG**

PROJECT : วิศวกรไทยพาณิชย์ สาขาแม่กรณ์  
 LOCATION : อ.เมือง จ.เชียงราย

BORING NO. : BH-1  
 DEPTH (m.) : 16.95  
 COORD. :  
 GROUND ELEV (m) :  
 WATER LEVEL (m) : -0.70  
 DATE STARTED : 20/6/95  
 DATE FINISHED : 20/6/95

PA = POWER AUGERING    HA = HAND AUGERING    WO = WASH OUT    ST = SHELBY TUBE    SS = SPLIT SPOON  
 PARTY CHIEF : SONGSAK S    DRILLER : BOONSONG C    GEOLOGIST : UB.    DRAFTMAN : SS    TYPIST : WS

<b>BORING LOG</b>		BORING NO. : BH-2		GROUND ELEV (m) : _____								
PROJECT : <u>ธนาคารไทยพาณิชย์ สาขาแม่กรณ์</u>		DEPTH (m.) : <u>16.95</u>		WATER LEVEL (m) : <u>-0.60</u>								
LOCATION : <u>อ.เมือง จ.เชียงราย</u>		COORD : _____		DATE STARTED : <u>21/6/95</u>								
				DATE FINISHED : <u>21/6/95</u>								
SOIL DESCRIPTION	DEPTH (m.)	GRAPHIC LOG	METHOD	SAMPLING	RECOVERY	SPT-N (blows/ft)	PL wn LL (%)	Su (Usq.m)				TOTAL UNIT WEIGHT γ <sub>t</sub> (t/cu.m.)
								O UCT	Δ PP	X FVT	□ TV	
						10 20 30 40	20 40 60 80	1 2 3 4	1.6 1.8 2.0			
LOOSE CLAYEY FINE TO MEDIUM SAND, BROWN (SC) 1.00	1	PA	SS 1	1	5	5	1					
VERY LOOSE CLAYEY SAND WITH GRAVEL, BROWN (SC) 2.00	2	SS 2	SS 3	3	4	4	1					
		SS 4	SS 5	5	8	8	1					
VERY LOOSE TO LOOSE CLAYEY SAND, BROWN (SC) 4.50	3	PA	SS 6	6	3	3	1					
	4	WO	SS 7	7	18	18	1					
MEDIUM DENSE SILTY SAND, BROWN (SM) 5.50	5	WO	SS 8	8	15	15	1					
	6	SS 9	SS 10	10	18	18	1					
VERY STIFF CLAY WITH SAND TRACE GRAVEL, BROWN (CL) 8.20	7	WO	SS 11	11	32	32	1					
	8	SS 12	SS 13	13	31	31	1					
MEDIUM DENSE TO DENSE SILTY FINE TO MEDIUM SAND, BROWN AND GREY (SM) 13.00	9	WO	SS 14	14	25	25	1					
	10	SS 15	SS 16	16	47	47	1					
	11	WO	SS 17	17	47	47	1					
DENSE TO VERY DENSE SILTY SAND TRACE GRAVEL, BROWN (SM) 16.95	12	SS 18	SS 19	19	54	54	1					
	13	WO	SS 20	20	54	54	1					
END OF BORING												

PA = POWER AUGERING	HA = HAND AUGERING	WO = WASH OUT	ST = SHELBY TUBE	SS = SPLIT SPOON
PARTY CHIEF : SONGSAK S	DRILLER : BOONSONG C	GEOLOGIST : UB	DRAFTMAN : SS	TYPIST : WS



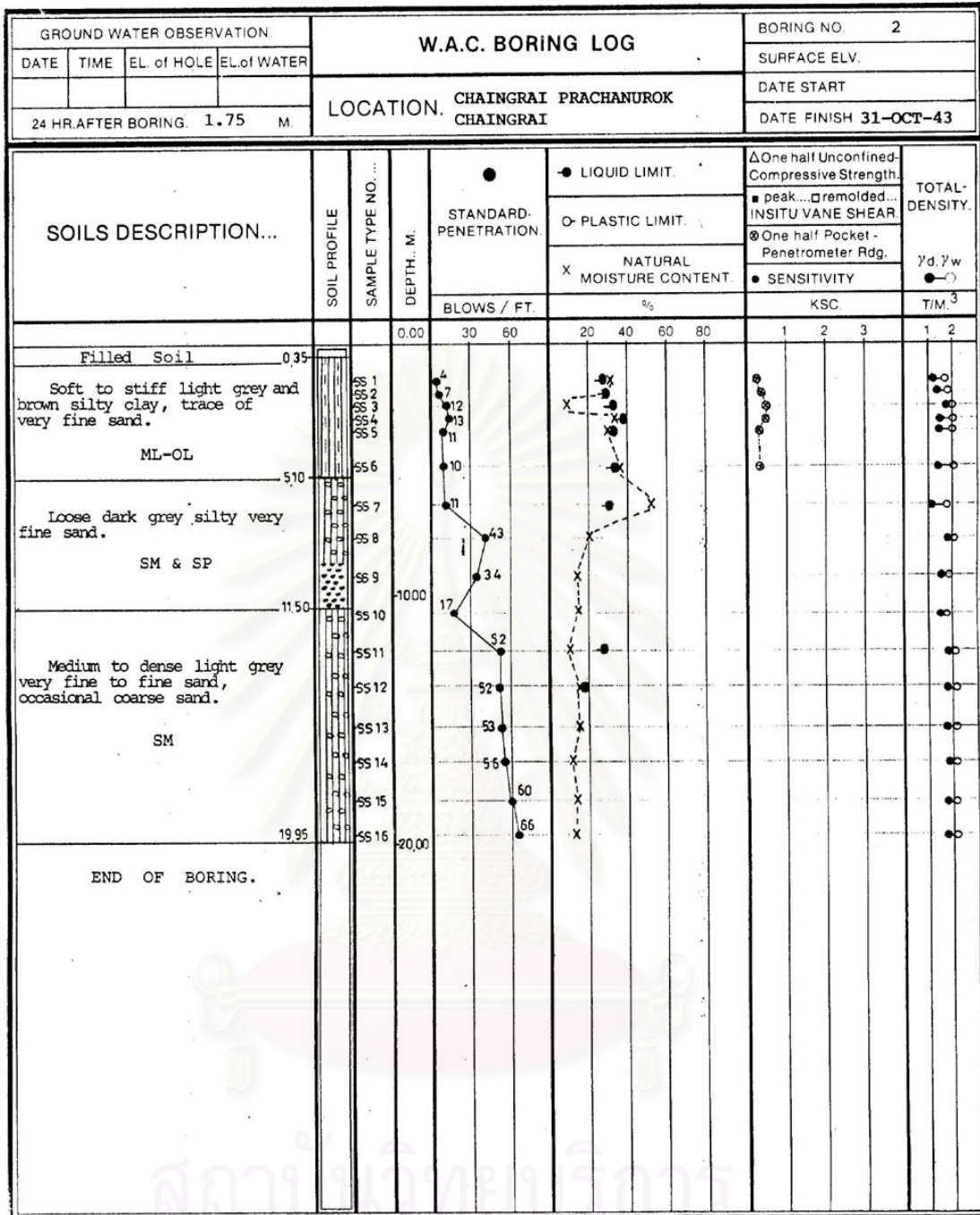
BORING LOG				BORING NO. : BH-2		ELEVATION (m) : -													
PROJECT : BCP ทอท. หัวสักปิโตรเลียม				DEPTH (m) : 10.65		GWL (m) : -3.40													
LOCATION : อ.เมือง จ.เชียงราย				COORD. N : -		DATE STARTED : 06/04/97													
				E : -		DATE FINISHED : 06/04/97													
SOIL DESCRIPTION	DEPTH (m)	GRAPHIC LOG	METHOD	SAMPLE NO.	RECOVERY (cm)	SPT-N VALUE (blows/ft)		NATURAL MOISTURE CONTENT (%)		Su (t/sq.m)				TOTAL UNIT WEIGHT (t/cu.m)					
						10	20	30	40	20	40	60	80	1	2	3	4	1.6	1.8
MEDIUM DENSE SILTY FINE SAND, BROWN (SM/ML)	1.00		PA	1	25														
STIFF FINE SANDY CLAY, BROWN (CL)	1.50		SS	2	24														
				3	30														
MEDIUM FINE SANDY CLAY, BROWN (CL,CL/SC)	3.00		PA	4	30														
				5	25														
MEDIUM DENSE SILTY FINE TO MEDIUM SAND, REDDISH BROWN AND LI-GREY (SM)	4.00		WO																
				6	35														
VERY DENSE SILTY SAND, LI-BROWN (SM)	6.00		WO																
	7.00		SS	7	20														
				8	15														
	8.00		WO																
				9	10														
	9.00		SS	9	10														
				10	10														
	10.00		WO																
				10	10														
	10.65			SS	10	10													
END OF BORING																			

PA = POWER AUGERING	HA = HAND AUGERING	WO = WASH OUT	ST = SHELBY TUBE	SS = SPLIT SPOON
PARTY CHIEF SURADECH CH	MADE BY PACHAREE C	GEOLOGIST NATTAPHON	FILE HUAYSAK2	DISK 10 CHAING RAI

จุฬาลงกรณ์มหาวิทยาลัย

GROUND WATER OBSERVATION.				W.A.C. BORING LOG				BORING NO. 1	
DATE	TIME	EL. of HQLE	EL. of WATER	LOCATION. CHAINGRAI PRACHANUKROK CHAINGRAI				SURFACE ELV.	
								DATE START	
24 HR. AFTER BORING. 1.75 M									
SOILS DESCRIPTION...	SOIL PROFILE	SAMPLE TYPE NO. ...	DEPTH, M.	STANDARD-PENETRATION. BLOWS / FT.	● LIQUID LIMIT. ○ PLASTIC LIMIT. X NATURAL MOISTURE CONTENT.	One half Unconfined-Compressive Strength.			TOTAL-DENSITY. $\gamma_d, \gamma_w$ T/M. <sup>3</sup>
						1	2	3	
0.35 Filled Soil			0.00						
1.60 Medium dark brown silty very fine sand. SM		SS 1-5	0.35-1.60	11, 6, 7, 10, 12	20-40				
3.60 Medium to stiff dark brown and reddish brown silty clay, trace of very fine sand. ML-OL		SS 6	1.60-3.60	5	20-40				
7.00 Soft dark grey silty clay, trace of very fine sand. ML-OL		SS 7-8	3.60-7.00	4, 29	20-40				
8.90 Very stiff grey silty clay, trace of very fine sand. ML-OL		SS 9-10	7.00-8.90	38, 53	20-40				
12.00 Medium to very dense light grey silty very fine to fine sand, occasional coarse sand and pea gravel. SM & SP-SM		SS 11-13	8.90-12.00	13, 46	20-40				
Dense to very dense yellowish brown silty very fine sand, occasional pea gravel. SM		SS 14-16	12.00-19.95	53, 71, 88, 77	20-40				
19.95 END OF BORING.			19.95-20.00						

จุฬาลงกรณ์มหาวิทยาลัย



จุฬาลงกรณ์มหาวิทยาลัย



<b>BORING LOG</b>				BORING NO. : <b>BH-1</b>		GROUND ELEV (m) : _____														
PROJECT : <b>อาคารศูนย์โทรศัพท์ค่ายเมืองราย</b>				DEPTH (m) : <b>12.35</b>		WATER LEVEL (m) : <b>NOT FOUND</b>														
LOCATION : <b>อำเภอเมือง จังหวัดเชียงราย</b>				COORD. : _____		DATE STARTED : <b>15/12/94</b>														
						DATE FINISHED : <b>15/12/94</b>														
SOIL DESCRIPTION	DEPTH (m)	GRAPHIC LOG	METHOD	SAMPLING	RECOVERY	SPT-N (blows/ft)	PL wn LL (%)		Su (t/sq.m)	TOTAL UNIT WEIGHT $\gamma_1$ (t/cu.m.)										
							10	20			30	40	20	40	60	80	1	2	3	4
STIFF CLAY WITH FINE TO MEDIUM SAND, LI-BROWN, REDDISH BROWN (CL)	2.00		PA	SS 1		10														
MEDIUM CLAY, LI-BROWN (CL)	3.00		PA	SS 2		11														
LOOSE TO MEDIUM DENSE SILT/FINE TO MEDIUM SANDY SILT, LI-BROWN, REDDISH BROWN (ML)	4.00		WO	SS 3		7														
	5.00		WO	SS 4		8														
	6.00		WO	SS 5		12														
	7.00		WO	SS 6		9														
	8.00		WO	SS 7		17														
	9.00		WO	SS 8		17														
	10.00		WO	SS 9		17														
	11.00		WO	SS 10		31														
	12.00		WO	SS 10		50/8														
	END OF BORING																			

PA = POWER AUGERING      HA = HAND AUGERING      WO = WASH OUT      ST = SHELBY TUBE      SS = SPLIT SPOON  
 PARTY CHIEF : KOBKIT T      DRILLER : SARAWUT Y      GEOLOGIST : PANYA . I      DRAFTMAN : SS      TYPIST : WS

K. ENGINEERING CONSULTANTS CO., LTD.																				
BORING LOG					BORING NO. BH-1		GROUND ELEV.(m.)													
PROJECT อาคาร บก. ศูนย์การศึกษา นศท. จหน. เชียงราย					DEPTH (m.) 13.15		OBSERVED WL (m.) -4.50													
LOCATION อําเภอเมือง จังหวัด เชียงราย					COORD.		DATE STARTED 24/7/93													
							DATE FINISHED 25/7/93													
SOIL DESCRIPTION	DEPTH (m.)	GRAPHIC LOG	METHOD	SAMPLING RECOVERY	SPT - N (blows / ft)				PL W <sub>n</sub> LL (%)			S <sub>u</sub> (t/m <sup>2</sup> )				γ <sub>t</sub> (t/m <sup>3</sup> )				
					10	20	30	40	20	40	60	80	1	2	3	4	1.6	1.8	2.0	
VERY LOOSE SILTY FINE TO MEDIUM SAND, DARK GREY (SM)	1	[Pattern]	PA	SS 1	3															
	2		PA	SS 2	3															
	3		PA	SS 3	4															
MEDIUM DENSE SILTY FINE TO MEDIUM SAND, BROWN (SM)	4.50		PA	SS 4	13															
LOOSE SILTY FINE TO MEDIUM SAND, GREY (SM)	7.00		WO	SS 5	5															
			WO	SS 6	10															
MEDIUM DENSE SILTY FINE TO MEDIUM SAND, GREY (SM)	8		WO	SS 7	20															
	9		WO	SS 8	21															
	10		WO	SS 9	27															
VERY DENSE SILTY GRAVEL, GREY (GP-GM)	13.15		WO	SS 10	26															
			WO	SS 11	50/6															
END OF BORING																				

สถาบันวิจัยและพัฒนา  
จุฬาลงกรณ์มหาวิทยาลัย







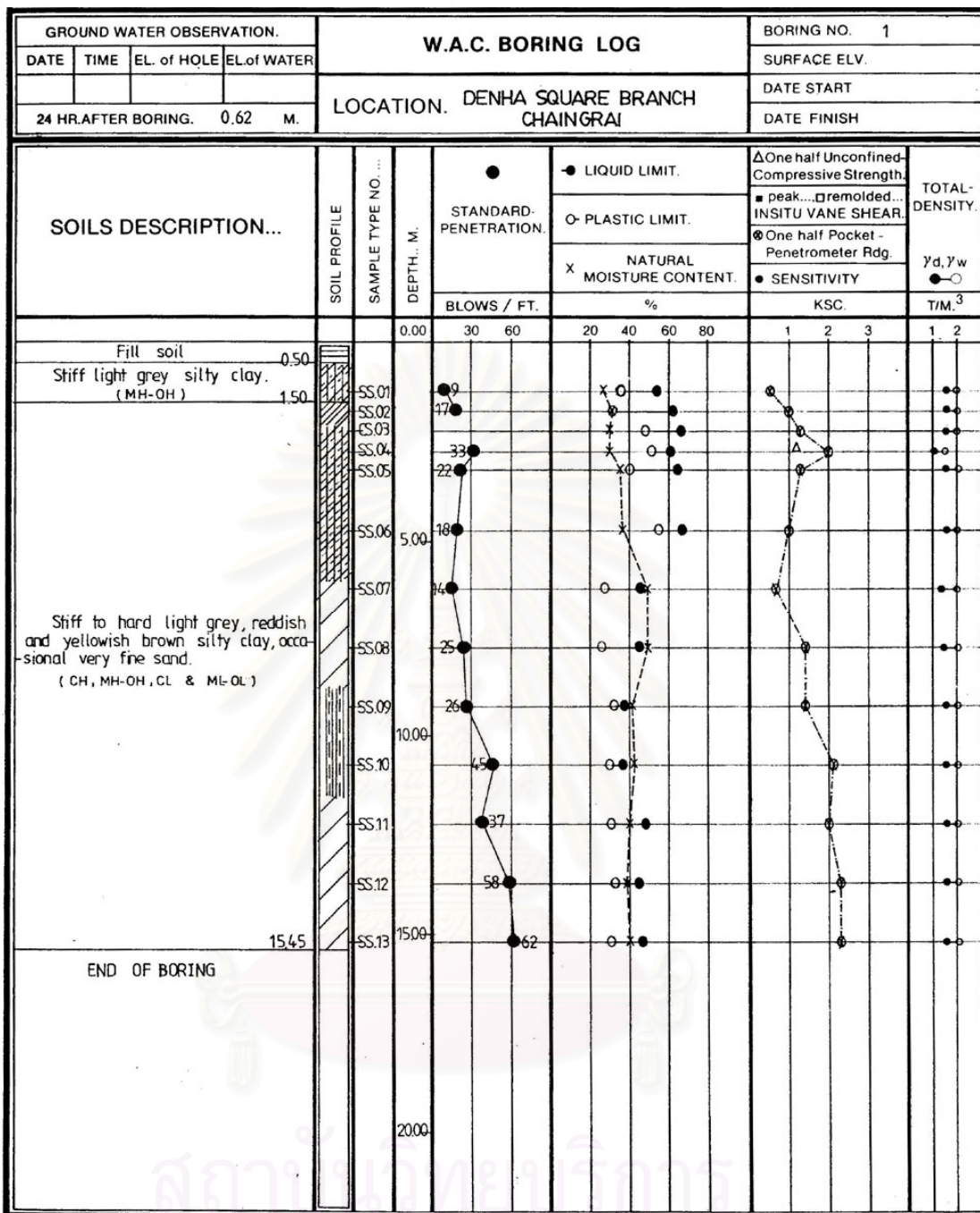
K. ENGINEERING CONSULTANTS CO., LTD.									
BORING LOG					BORING NO. <u>BH-1</u>		GROUND ELEV.(m.) _____		
PROJECT <u>ปรับปรุง รพ. จทบ. ช.ร.ป ๓๖</u>					DEPTH (m.) <u>23.45</u>		OBSERVED WL (m.) <u>-1.20</u>		
LOCATION <u>อำเภอเมือง จังหวัดเชียงราย</u>					COORD. _____		DATE STARTED <u>11/11/93</u>		
							DATE FINISHED <u>11/11/93</u>		
SOIL DESCRIPTION	DEPTH (m.)	GRAPHIC LOG	METHOD SAMPLING & RECOVERY	SPT - N (blows/ft)	PL (%)	W <sub>n</sub> (%)	LL (%)	S <sub>u</sub> (t/m <sup>2</sup> )	γ <sub>t</sub> (t/m <sup>3</sup> )
				10 20 30 40	20 40 60 80			1 2 3 4	1.6 1.8 2.0
LATERITIC COMPACTED SOIL (FILL)	1.00		PA						
VERY SOFT TO SOFT CLAY, GREY (CL)	2.50		SS 1 SS 2 SS 3	0 4 4					
STIFF TO VERY STIFF CLAY, BROWN, YELLOWISH BROWN, GREY AND LI-GREY (CL,CH)	3		PA						
	4		SS 4	15					
	5		PA						
	6		SS 5	21					
	7		PA						
	8		SS 6	13					
	9		WO						
	10		SS 7	12					
	11		WO						
	12		SS 8	11					
	13		WO						
	14		SS 9	13					
	15		WO						
	16		SS 10	13					
	17		WO						
18		SS 11	16						
19	19.00		WO						
HARD CLAY, LI-GREY (CL)			SS 12	18					
			SS 13	23					
			SS 14	29					
			SS 15	50/6"					
			WO						

K. ENGINEERING CONSULTANTS CO., LTD.																			
BORING LOG				BORING NO. BH-1			GROUND ELEV.(m.):												
PROJECT ปรับปรุง รพ. จทบ. ช.ร. ปี ๓๘				DEPTH (m.) 23.45			OBSERVED WL (m.) -1.20												
LOCATION อำเภอเมือง จังหวัดเชียงราย				COORD.			DATE STARTED 11/11/93												
							DATE FINISHED 11/11/93												
SOIL DESCRIPTION	DEPTH (m.)	GRAPHIC LOG	METHOD	SAMPLING & RECOVERY	SPT - N (blows/ft)				PL W <sub>n</sub> LL (%)			S <sub>u</sub> (t/m <sup>2</sup> )			T <sub>1</sub> (t/m <sup>3</sup> )				
					10	20	30	40	20	40	60	80	1	2	3	4	1.6	1.8	2.0
HARD CLAY, DARK GREY (CL)	21		WO																
	22.00		SS	16	50	10													
DENSE CLAYEY FINE TO MEDIUM SAND, GREY (SC/CL)	23		WO																
	23.45		SS	17	47														
END OF BORING																			

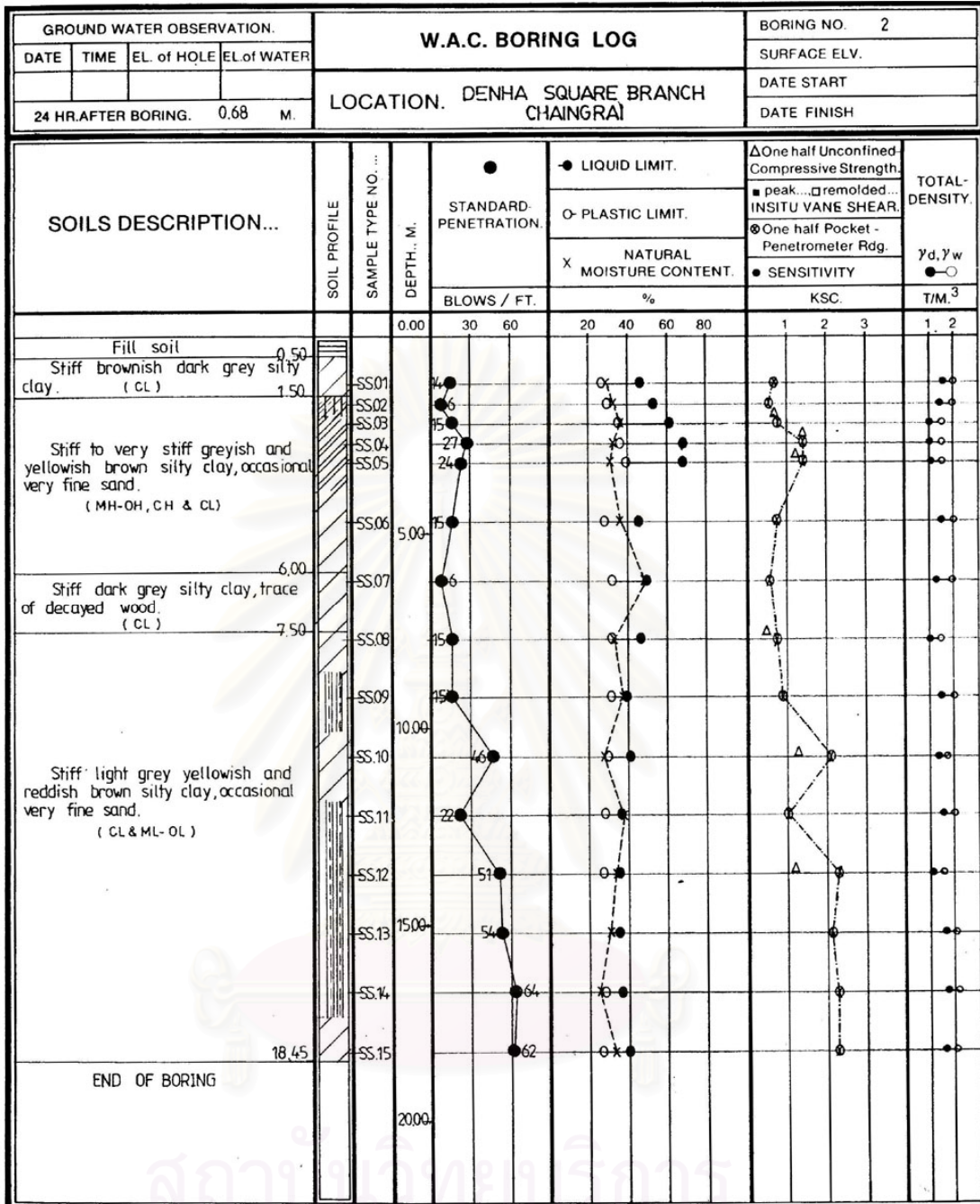
สถาบันวิจัยและพัฒนา  
จุฬาลงกรณ์มหาวิทยาลัย







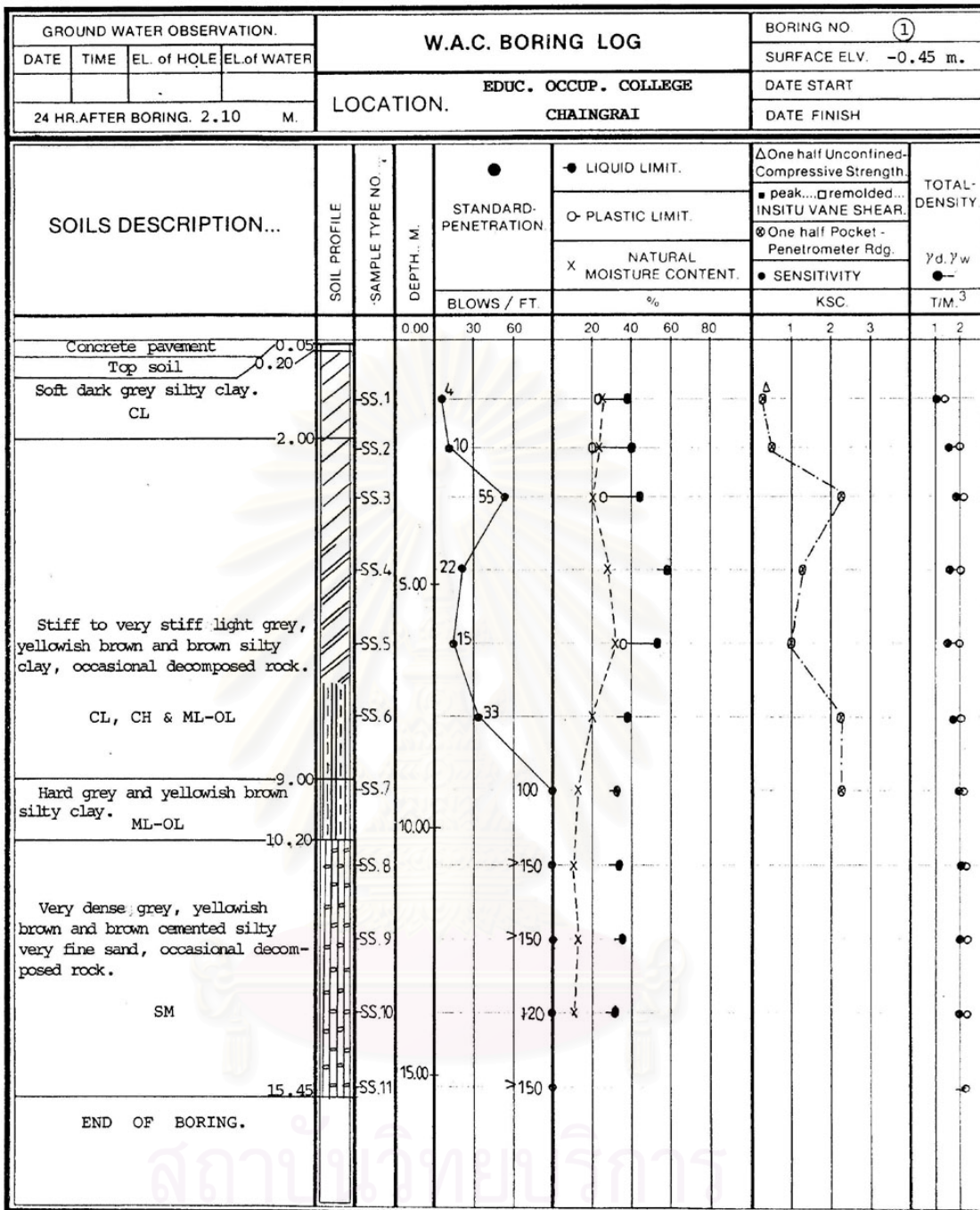
จุฬาลงกรณ์มหาวิทยาลัย



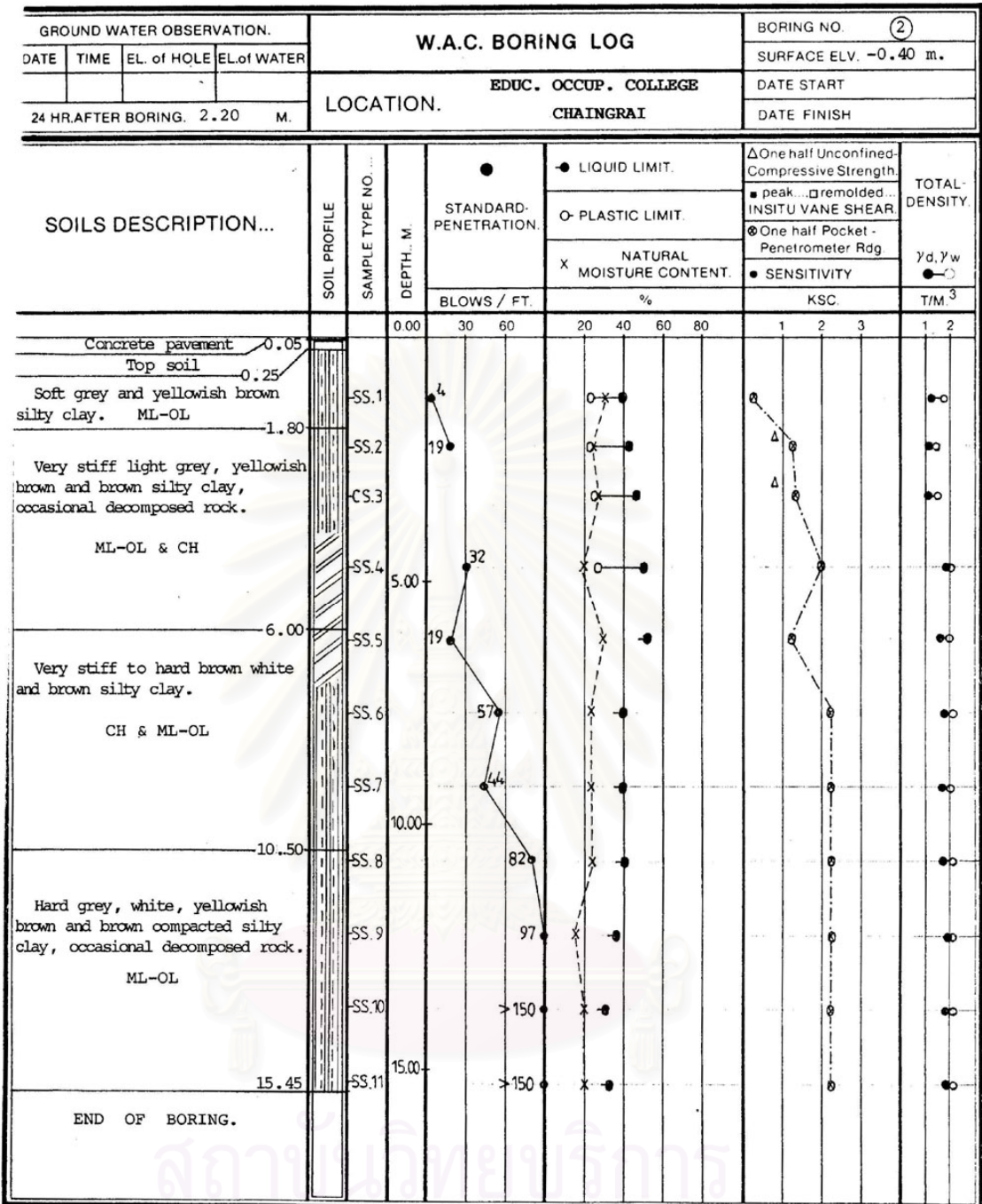
จุฬาลงกรณ์มหาวิทยาลัย

GROUND WATER OBSERVATION.				W.A.C. BORING LOG				BORING NO. 1				
DATE	TIME	EL. of HOLE	EL. of WATER	LOCATION. AMPHOE MUANG CHIANGRAI				SURFACE ELV.				
								DATE START		DATE FINISH		
24 HR. AFTER BORING. 1.26 M.												
SOILS DESCRIPTION...	SOIL PROFILE	SAMPLE TYPE NO. ...	DEPTH. M.	STANDARD-PENETRATION. BLOWS / FT.	● LIQUID LIMIT.			△ One half Unconfined-Compressive Strength.			TOTAL-DENSITY. γ <sub>d</sub> , γ <sub>w</sub> T/M <sup>3</sup>	
					○ PLASTIC LIMIT.			■ peak... □ remolded... INSITU VANE SHEAR.				γ <sub>d</sub> , γ <sub>w</sub> T/M <sup>3</sup>
					X NATURAL MOISTURE CONTENT. %			● SENSITIVITY				
Fill soil			0.00	30 60	20 40 60 80	1 2 3	1 2					
0.35												
Medium to hard grey and brown silty clay, occasional pea gravel and very fine sand. CL & ML-OL			5.00									
7.60												
Very stiff to hard brown and grey silty clay, trace of very fine sand and decomposed rock. ML-OL			10.00									
10.50												
Hard brown, light grey and brownish yellow silty clay, trace of very fine sand and decomposed rock. ML-OL			15.00									
15.45												
END OF BORING.			20.00									

สถาบันวิจัยวิศวกรรม  
จุฬาลงกรณ์มหาวิทยาลัย



สถาบันวิทยบริการ  
จุฬาลงกรณ์มหาวิทยาลัย



สถาบันวิทยบริการ  
จุฬาลงกรณ์มหาวิทยาลัย

## VITAE

Pichai Pattararattanakul was born in Trang, a southern province of Thailand, on April 3, 1974. He attended Prince of Songkla University, one of the most prestigious universities in southern Thailand, where he obtained a bachelor's degree in civil engineering in 1995. He received a master's degree from Chulalongkorn University with a major in structural engineering in 1998. His master's thesis title was "Effects of Different Shear Reinforcement Detailings on Behavior of Reinforced Concrete Shear Walls Subjected to Cyclic Loadings" and was published in the ACI Structural Journal in 2001. After graduation, he worked as a research assistant at the earthquake engineering and vibration research laboratory of Chulalongkorn University from 1998 to 1999, conducting the full-scale behavior of reinforced concrete columns subjected to cyclic loadings.

Pichai began his engineering career when he studied in the last year of master's degree with an engineering consulting firm. In 1999, he has started his Ph.D. in the area of geotechnical engineering at Chulalongkorn University, together with working as part time structural engineer with many consulting firms in Bangkok. He has been involved in design of various types of structure both concrete and steel structures, including low- and high-rise buildings, industrial buildings, water treatment tanks, machine foundations, and etc.

สถาบันวิทยบริการ  
จุฬาลงกรณ์มหาวิทยาลัย